Biomechanical Human Performance Metrics of Coordination and Balance for Operational Decision-Making

Richard A. Fineman

B.A., Columbia University (2013)

Submitted to the Harvard-MIT Program in Health Sciences & Technology
in partial fulfillment of the requirements for the degree of

Doctor of Philosophy
at the
MASSACHUSETTS INSTITUTE OF TECHNOLOGY
May 2019

Signature of Author .....
Richard A. Fineman
Harvard-MIT Program in Health Sciences & Technology
June 6, 2019

Certified by .....
Leia A. Stirling, PhD
Assistant Professor of Aeronautics and Astronautics
Institute for Medical Engineering and Science
Thesis Supervisor

Accepted by .....
Emery N. Brown, MD, PhD
Director, Harvard-MIT Program in Health Sciences and Technology
Professor of Computational Neuroscience and Health Sciences and Technology

Biomechanical Human Performance Metrics of Coordination and Balance for Operational Decision-Making

Richard A. Fineman

B.A., Columbia University (2013)

Submitted to the Harvard-MIT Program of Health Sciences & Technology
in partial fulfillment of the requirements for the degree of

Doctor of Philosophy

Abstract

The overall goal of this work is to develop a series of biomechanically-driven human performance metrics that aid operational decision-making. By quantifying inter-limb coordination and balance, we enable decoupling motor patterns without direct visual observation, providing objective feedback to decision-makers on the quality of human motion. To effectively develop and validate metrics for coordination and balance, we take a human-centered approach, contextualizing and evaluating in specific domains of interest. This work will focus on two: clinical geriatrics and aerospace spacesuit assembly (SSA) design. While these domains might seem distinct, both require a detailed understanding of nominal human motion and are interested in measuring deviation from desired motor patterns. To this end, we will test the hypothesis that we can augment decision-making in two domains of interest through the development and validation of biomechanically-driven human performance metrics for coordination and balance.

Thesis supervisor: Leia Stirling, PhD
Title: Assistant Professor of Aeronautics and Astronautics

Acknowledgements

The contents of this thesis highlight what I have been up to for the last 5 or so years of my doctorate. This process had some of the highest highs and lowest lows of my life so far. Needless to say, there are too many people to thank along the way... I just hope I can remember everyone.

First, I have to thank my parents and family. If you saw my father, Jeff Fineman, in person you would not believe he is as accomplished and well respected as he actually is. For one, he has a "rugged" sense of style that I unfortunately also inherited, but more importantly he is one of the most humble people I know. He is also one of the most selfless people I know and I couldn't ask for a more supportive dad. I strive for these qualities in life and work. I only hope I can be half the person he is. My mother, Sandra Luna-Fineman, is one of the hardest working people I know. Her stubbornness makes her one of the most career driven people ever and she does it all to set a good example for her kids and family. Thank you to her for showing me what real hard work looks like, while having some of the strongest family values I know. I really look up to my parents for different, but equally important reasons, so thank you for you examples and providing me with the opportunities to pursue whatever dreams I have. My siblings, Melissa and David Fineman, both inspire me everyday to be better and strive for more. To say we are not competitive is a lie, but I could not have done this without them.

Next, my girlfriend Taylor Ellis, who moved to Boston and left home for the first time right around when this whole PhD process was the most stressful and time consuming. I know your patience is always tested with me and that this whole PhD process has stretch it to its limit, but I am thankful that

you were here during this time to force me to take breaks on the weekends and to remind me that things will always be OK. I cannot wait where the adventure of life will take us next, but I know it will not be as bad as the last six months. Also, I have to thank your family who took me in as their own pretty quickly and has been cheering me on to finish ever since!

To the HSL (formally MVL), I could not think of a better group of lab mates. I was honestly sad at the beginning of the thesis process because that meant having to leave this group eventually. I have to give a special shout out to Aditi Gupta and Tim McGrath who have been my office mates for the past 4 years. Thanks for always listening to me complain and vent. This whole process would have not been possible without our awesome office squad. Thank you also to the other faculty in the HSL: Dava Newman, Jeff Hoffman, Larry Young, Alan Natapoff, Chuck Oman, and Andy Liu. Each and every one of you has always been supportive and looking out for me, so thank you for that.

To my HST classmates, we have been through hell together. Erica Mason, you and your dad taught me how to write good (pun intended). You also got me through a lot of hard times. This would not have been possible with your help! Roman Stolyarov, thanks for always being there to pull my head out of my ass and making me laugh. To the rest of the HST class of 2014, could not have done it without you! Fianlly, thank you to the HST administrator, Julie Greenberg, Laurie Ward, and Traci Anderson, who have always been supportive and flexible with my absent mindedness when it comes to the requirements of this program.

Next to my thesis committee members: Thomas Heldt, Jonathan Bean, and Andrew Abercromby. Each and everyone one of you made yourself always accessible despite your busy other jobs. I values each and every one of our one-on-one meetings and learned so much from each every one of you and I hope we can all continue to work together in the future.

Finally, I have to thank my advisor and mentor Leia Stirling. Everyday you teach me something new and your drive for teaching and mentoring is second to none. You inspire me to pursue academics and be at least half the professor and mentor that you are. The last few months have been a test for all of us, but I am more excited than ever for what is to come for you. I know

you will flourish.

This work supported in part by the National Science Foundation, Award IIS-1453141, NASA Space Technology Research Fellowship NNX16AM71H, the National Space Biomedical Research Institute through NASA NCC 9-58, and the NASA Robotics Institute Award NNX15AR20G.

Contents

1 Introduction: What Rehabilitation and Spacesuits Have in Common **12**
1.1 How physical medicine physicians make decisions 14
1.1.1 Telemedicine as a Lens for Metric Development 17
1.1.2 Human-Centered Metric Development 21
1.2 Understanding the Problems with Spacesuit Fit and Sizing . . 24
1.3 Wearable Sensors: Inertial Measurement Units 28
1.4 Research Objectives and Specific Aims 31

2 A Method for Quantifying Coordination during Non-Cyclic Motions **33**
2.1 Defining Coordination 33
2.2 Existing Coordination Measures 36
2.2.1 Continuous Relative Phase, γ^{12} 38
2.2.2 Vector Coding, τ^{12} 42
2.2.3 Beta Coordination Matrix, β_{ij} 43
2.2.4 Gaps and Limitations of Current Measures 45
2.3 The Relative Coordination Metrics ρ 48
2.3.1 Defining Coordination and the Goals of a new Metric ρ 48
2.3.2 A Numeric Definition of ρ 49
2.3.3 How to interpret ρ 50
2.3.4 The Need to Normalize Ω 56
2.3.5 Composite Measures of ρ 60
2.4 Application and Experimental Validation of ρ 61
2.4.1 Experimental Design 63
2.4.2 Data Analysis 64

2.4.3 Statistical Analysis 66
2.5 Results 67
2.5.1 Effect of normalization and trajectory stage on the Relative Coordination Metric (ρ) 71
2.5.2 Effect of normalization and object on $\hat{t}_{\pm Z_n}$ 75
2.5.3 Effect of normalization and trajectory on $\hat{t}_{\pm Z_n}$ 76
2.6 Discussion 81
2.7 Conclusion 85

3 Objective Means of Quantifying Spacesuit Fit: Applications in Aerospace Medicine 86
3.1 Defining Suit Fit 87
3.1.1 Previous Efforts at Quantifying Suit Mobility and Comfort 87
3.1.2 Cognitive Task Analysis of NASA JSC MKIII Fit Checks 89
3.1.3 Static vs. Dynamic Fit 96
3.1.4 Defining New Measures for Dynamic Fit: $\rho^n_{HS}$and $\Delta tRoM$ 98
3.2 Experimental Methods 101
3.2.1 Subjects 101
3.2.2 Equipment 102
3.2.3 Procedure 103
3.2.4 Data Analysis 104
3.2.5 Statistical Analysis 105
3.3 Experimental Results 107
3.3.1 Effect of Suit Configuration on Normalized Cadence . . 107
3.3.2 Effect of Suit Configuration on Task Knee Range of Motion 108
3.3.3 Effect of Suit Configuration on $\Delta tRoM$ 109
3.3.4 Effect of Subject and Configuration on $\rho^F_{HS}(t)$ and $\rho^T_{HS}(t)$109
3.4 Discussion 112
3.5 Conclusions and Future Work 119

4 Technique-based Measures for the Standing Balance Test 123
4.1 Gait Speed and Clinical Outcomes 124

4.1.1 Defining Dismobility . . . 124
4.1.2 Disambiguating Between Slow and Moderate Walkers . 127
4.2 Existing Balance Models and Metrics . . . 128
4.2.1 Existing Static Balance Metrics . . . 128
4.2.2 Limitations of the Inverted Pendulum Model . . . 129
4.2.3 Previous Efforts Using Multi-segmented Inverted Pendulum Models . . . 130
4.3 Frequency in Balance Region . . . 133
4.3.1 A numerical definition of $FBR_n^{P,LU}$ . . . 135
4.4 Assessing Participant Specific Balance Technique using $FBR_n^{P,LU}$ 141
4.4.1 Changes in Static Balance Technique Between Trials . 141
4.4.2 Changes in Static Balance Technique Between Participants . . . 143
4.4.3 Changes in Static Balance Technique Between Anatomical Planes . . . 146
4.5 Experimental Methods . . . 148
4.5.1 Statement of Hypotheses . . . 148
4.5.2 Participants Demographics . . . 149
4.5.3 Experimental Design . . . 150
4.5.4 Data Processing . . . 151
4.5.5 Statistical Analysis . . . 153
4.6 Results . . . 154
4.6.1 The Effect of Age and Gait Speed on Balance . . . 165
4.6.2 The Effect of Balance Region on $FBR^{P,UL}$ . . . 166
4.6.3 The Effect of Anatomical Plane on FBR_n^{UL} . . . 167
4.7 Discussion . . . 168
4.8 Conclusions . . . 176

5 Conclusions and Future Work 178
5.1 Summary of Results . . . 179
5.1.1 A Method for Quantifying Coordination during Non-Cyclic Motions . . . 179
5.1.2 Objective Means of Quantifying Spacesuit Fit . . . 180
5.1.3 Technique-based Measures for the Standing Balance Test 181

5.2 Contributions to Literature 181
5.3 Applications and Future Work 182
5.3.1 Computing Coordination Patterns for a Diverse Set of Tasks 183
5.3.2 Longitudinal Progression of Patient Progression 184
5.3.3 Development Goal-based Performance Metrics 185
5.3.4 Comprehensive Suit Fit Assessments 186
5.3.5 Suit Fit in Operationally Relevant Environments . . . 187
5.3.6 Assessing Balance Technique of Other Patient Populations 188
5.4 Concluding Remarks 188

Bibliography **190**

A Testing Material and Questionnaires **211**

B Supplemental Figures: Technique-based Measures for the Standing Balance Test **215**

List of Figures **223**

List of Tables **248**

Chapter 1

Introduction: What Rehabilitation and Spacesuits Have in Common

There is an overarching theme to this thesis: motion. More specifically, the theme is human motion, and how we can use the information provided by human motion to helps us make decisions. Often human motion is used to make decisions through a task and ***how*** the motion is performed provides the decision-maker with valuable insight to make a decision. There are many domains where qualitative assessments of human motion and performance are used to make decisions. Two such examples we will discuss in detail are rehabilitation and spacesuit sizing selection. For example, a rehabilitation physician might use a series of motion-based tasks to help them understand the current state of a patient and then make a decision regarding their plan-of-care. Meanwhile, a spacesuit engineer might use a different series of tasks to help them make a decision as to what size boot an astronaut should wear. Both these decisions are made from qualitative, often visual assessments of human motion [1, 2].

The overall goal of this thesis is to develop a series of biomechanically-driven human performance metrics that aid decision-making. We aim to test the hypothesis that we can provide quantitative feedback to augment decisions typically made subjectively and qualitatively regarding upper and lower

extremity human function. In order to develop usable and effective decision-making metrics, a thorough understanding of how the decision is made is required. Therefore, a human-systems approach is taken to better comprehend the information that end users (i.e. physical therapist or astronaut) gather and interpret human motion to make decisions [3, 4]. Operational relevance will often be used in this thesis to refer to the usefulness of a measure toward making a decision. In the context of rehabilitation, for example, the operational relevance of a biomechanical metric refers to whether a certain value might prompt a clinician to change the patient's plan-of-care. This thesis will also consider statistical significance. Achieving statistical significance does not mean that the measurable difference is operationally relevant. For example, in the context of rehabilitation, the effect size might be small and not require any formal intervention because intervention may not harm the patient, but also may not yield perceptible differences in performance affecting activities of daily living (ADLs). The opposite is also true: something that is operationally relevant might not achieve statistical significance. This could mean that our measure might not be sensitive enough to detect a difference or is just not appropriate for measuring the difference. Understanding operational relevance and decision-making methods helps streamline translatability of this work.

The inspiration for this thesis largely arose from working with physical therapists in outpatient clinics. Section 1.1 and 1.1.1 will highlight that experience and the need for more objective metrics of performance in rehabilitation settings. Section 1.1.2 will then highlight the human-systems approach taken to develop new metrics for not only rehabilitation, but other settings as well. Finally, Section 1.4 will outline the research questions and the specific aims of this thesis.

1.1 How physical medicine physicians make decisions

Day-to-day life requires constant interaction with the surrounding environment. In clinical environments, these actions are referred to as ADLs. ADLs include but are not limited to: using a fork, opening a cabinet, buttoning a shirt, walking, and drinking from a glass. While these tasks may seem simple, they require recruitment of thousands of neurons and muscle fibers in specific ordering. A reduction in someone's ability to move their body can have many causes. Henceforth, we will refer to the root cause of a patient's musculoskeletal injury or ailment as their "pathology," which can include strains, sprains, stroke, physical trauma, musculoskeletal disorder, aging, and more.

When a patient reports symptoms or is diagnosed with a musculoskeletal pathology, they often turn to physical medicine and rehabilitation (PMR) clinicians to intervene and help improve motor function. In general, there are three practitioners who might help with a patient's treatment: PMR physicians, physical therapists (PT), and occupational therapists (OT). PMR physicians, often called physiatrists, are in charge of a patient's medical diagnosis, plan-of-care, and prescribe their therapy. Meanwhile, the PTs are in charge of performing the prescribed treatment therapy [5]. While physiatrists and PTs help care for the root cause of a patient's pathology, OTs specialize in rehabilitating patients to independently perform their ADLs that are impaired due to the pathology. Henceforth, we will focus our efforts on OT because of how much it relies on visual feedback of human motion for decision-making. OT covers a wide range of applications with studies showing the efficacy of OT in the context of stroke [6, 7, 8], within the aging population [9], after amputation [10], and after injury or surgery [11]. The American Occupational Therapy Association describes the process of therapy as evaluation, intervention, and targeting of outcomes in various domains of interest,

including occupations (ADLs, work, leisure, etc.), performance skills (motor control), performance patterns (routines, habits, etc.) and the interrelated context and environment of the patient [12].

As part of this work, OTs were observed and questioned to better understand how they interact with patients and make clinical decisions. An OT's main goal is to help their patient gain more independence. OTs accomplish this through strength training, repetitive tasks meant to emulate ADLs, splinting, and more. How OTs and other physical medicine clinicians make decisions stems from a combination of qualitative measures and quantitative tests. Qualitative measures can be subjective and include, but are not limited to, patient feedback, and visual motion assessments. These subjective measures inherently contain variability between clinicians due to differences in training and opinion. While most clinical decisions made by therapists are based on visual observation of the patient, there are common functional state and outcome measurements used to quantify patient progression (Table 1.1). Despite these various clinical outcome measures, there is no consensus among researchers or clinicians as to which of them are best [13, 14, 15]. Beyond these measures, there are also general evaluations commonly used by therapists in the clinic related to the capabilities and pathology of a patients disease, such as active joint range of motion, passive joint range of motion, and compensatory motions. While these other measure are quantitative, variability exists between clinicians based on the tools they use, the training they have, and their experience [16, 17]. For example, Pomeroy et al. [17] found that the variance senior PTs gave a series of patients ranged from 18% for a task picking up a pencil to 38% for a sit to stand task. It is important to note that while measures listed above and in Table 1.1 are quantitative, subjective assessment of ***how*** patients complete the task is also

Measure	Description	Category
9-hole Peg Test [19]	Placing pegs in a peg board	IO
Barthel Index [20]	Grading of independence on 10 ADLs	IS
Disabilities of the Arm and Hand (DASH) [18]	Questionnaire on level of difficulty and pain to perform a set of tasks	D
Fugl-Meyer Upper Limb Test [21]	Grading of range of motion, motor function, and sensory function	IS
Manual Muscle Test (MMT) [22]	Grading of movement against examiner or gravity resistance	IS
Wolf Motor Function Test [23]	Combination of timed activities, functional activities, and strength measures	IO, IS
Box and Block Test [24]	Moving blocks across a barrier in a box	IO

Table 1.1: Sample of Common Clinical Outcome Measures. IO=Interactive Objective, IS=Interactive Subject, D=Descriptive

used to help make clinical decisions. For example, the Disabilities of the Arm and Hand (DASH) questionnaire is used to quantitatively assess the severity of upper extremity pathology [18]. The questionnaire asks patients to rate how difficult or painful it is to perform a series of tasks on a scale from $1-5$, 5 being extremely difficult or unable to perform the task. The higher the DASH score, the more severe the patient's pathology. While the DASH score helps the clinician understand the patient's general state and well-being, it does not help them formulate a plan-of-care. Watching ***how*** the patient performs some of the tasks in the DASH questionnaire better helps the clinician see what muscle groups might not be firing properly so they can formulate how to intervene and treat the patient's pathology.

OT plan-of-care is not homogeneous and is adapted for each patient based on their motor constraints [12, 6]. The frequency of OT visits varies depending on each patient's functional needs, but is also heavily influenced by insurance and ease of transport to a care facility. There is a need within physical medicine and rehabilitation to develop technologies and measures

that can assess human motion in an objective and quantitative way. Developing objective measures would reduce the variability that currently exists between provider assessment and could enable quicker and earlier diagnosis that current subjective measures cannot do.

1.1.1 Telemedicine as a Lens for Metric Development

Stirling and McLean [2] performed a series of observations of OTs to better understand the decision-making process in rehabilitative medicine. Their goal was to use these observations to provide a roadmap for developing telemedicine platforms in rehabilitation. Telemedicine enables the remote practice of certain aspects of medicine through advances in communication and health technology. Telemedicine improves patient outcomes at costs lower than those of traditional in-person visits to the clinic or hospital for such conditions as congestive heart failure, diabetes, chronic obstructive pulmonary disease, and chronic wound healing [25, 26]. Telemedicine also improved outcomes in depression [27, 28] and improved dermatology care [29] by providing support and screening services. The care provided by tele-rehabilitation includes diagnostic patient assessment, therapeutic intervention, monitoring of patient performance, education, and training. The driving factors for the development of tele-rehabilitation include, but are not limited to, providing access to rehabilitative services for individuals who are far from specialists or who are isolated due to physical impairment, and easing the financial burden of transportation costs and frequent clinical visits on the patient [30]. Figure 1.1 highlights the potential designs of a tele-rehabilitation system based on the work of Stirling and McLean [2], including the various methods of collecting patient motion data (optical cameras, wearable sensors, depth cameras), presenting the data to clinicians (video vs. summary

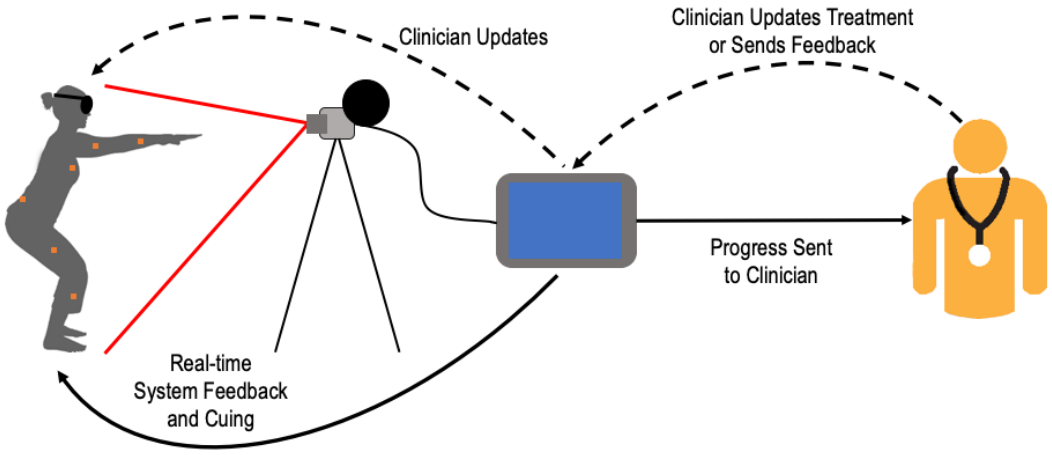

Figure 1.1: Graphical Representation of Tele-rehabilitation approaches. Technologies that could be used to collect patient data include: wearable sensors, optical cameras, depth sensing cameras. Information could be sent directly to the clinician for evaluation or the system could intelligently provide feedback to the patient in real-time via visual or auditory aids using a screen or virtual reality.

metrics), and providing feedback to the patient (clinician updates, real-time feedback, virtual reality).

According to Stirling and McLean [2], the biggest challenge in creating tele-monitoring systems is robustly quantifying features monitored by clinicians (e.g. coordination, fluidity, etc.) in ways that support decision-making. Outcome-based measures provide a summary of the task, for example how long it took to complete the task, and do not provide information of ***how*** the task was completed. Many current tele-monitoring systems and all the clinical measures listed above (Table 1.1) focus on outcome-based metrics for task completion. For example, the 9-hole peg test and Box and Block tests listed in Table 1.1 only evaluate patients based on how long it takes them to complete the task, but there is relevant information to clinicians in how they complete the task regardless of the time it takes. For example, when completing 9-hole peg test, some patients grasp the objects with their fingertips, while others with decreased fine motor control use the sides of their

fingers. The time it took the patient to complete the 9-hole peg test does not tell the clinician how the patient grasped the objects. Some patients compensate and can complete the task rather quickly using the sides of their fingers when the therapist wants them to use the tips. This detail is missed if a tele-rehabilitation system only sent a clinician how long it took the patient to finish the task. Therefore, there is a need for performance-based metrics that enable deeper insight by disambiguating desired and undesired motor patterns used to complete the task [31]. These desired motor patterns may change due to the heterogeneity of treatment protocols and pathologies between patients. Measures that quantify how a patient performs a motion or technique used to complete a task shall be called performance-based metrics. As highlighted by Stirling and McLean [2], any new performance-based metrics must be developed and presented intuitively in ways that decrease the workload necessary for decision-making [32, 33, 34].

Tele-rehabilitation also aims to disambiguate differences in patient progression between clinical visits. Typically, similarities or differences between clinical visits are due to the patient 1) not participating in prescribed home exercises, 2) participating in home exercises incorrectly, or 3) participating in home exercises correctly [2]. While the implementation of tele-rehabilitation has not been well studied, the technology is extremely promising [35, 36, 30].

Most difficulties in effectively providing tele-rehabilitation lie in the importance of direct observation and interaction of the patient with the provider, something we noted as very important in Section 1.1. In addition, many subtleties and complexities exist in human three-dimensional motion and motor control [30]. In other words, it is very difficult to effectively represent 3D information on a 2D screen or paper. Russel [30] classifies tele-rehabilitation into three categories: 1) video images, 2) virtual reality (VR), and 3) sensors.

Fig. 1.1 also highlights these three technologies. Video only provides a two-dimensional viewpoint of subtle three-dimensional motions that can become occluded from view. The clinician must therefore rely solely on visual cues while reviewing these videos in real-time or at a later time, still creating a large time burden on the therapist. VR systems could provide quantitative outcome measures based on games designed for the patient. These games can encourage certain movement patterns to aid in improving motor skills, which are hypothesized to carry over to ADLs. Nonetheless, pure VR systems only have the capability of quantifying outcomes and cannot quantify the motor patterns used to achieve those outcomes. This could lead to patients using compensatory mechanisms to reach a desired outcome, while not achieving the desired motor pattern. Rizzo et. al [37] highlighted some of these technical, practical and human factors challenges associated with VR and tele-rehabilitation. Rizzo [37] suggested that coupling video images with environmental sensing or wearable sensors could improved observability and quantification of motor patterns, but we still do not understand the variability associated with bringing some of these technology into non-laboratory, natural environments. Laboratory settings are far more controlled environments and at times can cause measurable differences in the way technology and patients perform [38]. It is therefore important to investigate what kinds of changes might occur when using these technologies in different environments.

Holden et al. [39] addressed the challenges of tele-rehabilitation using real-time video conferencing with a therapist, VR, and motion tracking sensors. While travel burden was relieved for the patient, the time burden for the therapist remained as they interacted with the home system in real-time. Additional studies reduced the time burden on therapists by decreasing the number of video conferences and relying on patients to directly interact with

the home system. While these studies found improvements in selected clinical performance metrics, it is unclear which metrics are the most valuable to the clinician in between clinical visits. In other words, the therapist was unsure which metrics were most useful in assessing patient progress, and the determining factors of patient progression remained ambiguous [40, 41]. Thus, the therapist could not use the system to inform treatment progression between clinical visits. Similar outcomes were observed by Veltra et al. [15] who was able to summarize outcome measures using sensors to categorize patients with upper extremity disabilities, but these parameters were not useful in clinical decision-making. Thus, while the literature shows a need for tele-rehabilitation, especially with regards to OT [42], there are no systems that effectively inform clinical decision-making.

1.1.2 Human-Centered Metric Development

Stirling and McLean [2] provide a framework for how to effectively develop performance-based measure using a human-centered approach and cognitive task analysis (CTA, Fig. 1.2). CTA aims to understand information required, thinking processes, and goals of an environment requiring some form of decision-making [43, 44]. CTA is a broad field, and includes a variety of methods and techniques used to analyze the underlying mental tasks for particular situations. A modified CTA was performed by Stirling and McLean [2] to reveal important factors within therapy sessions. Figure 1.2 highlights the methodology that can be applied for the development of relevant performance metrics. The modified CTA is composed of three segments: characterizing the subject matter, defining the relevant information, and formalizing system requirements (Fig. 1.2).

Characterization of subject matter requires observation of the domain of

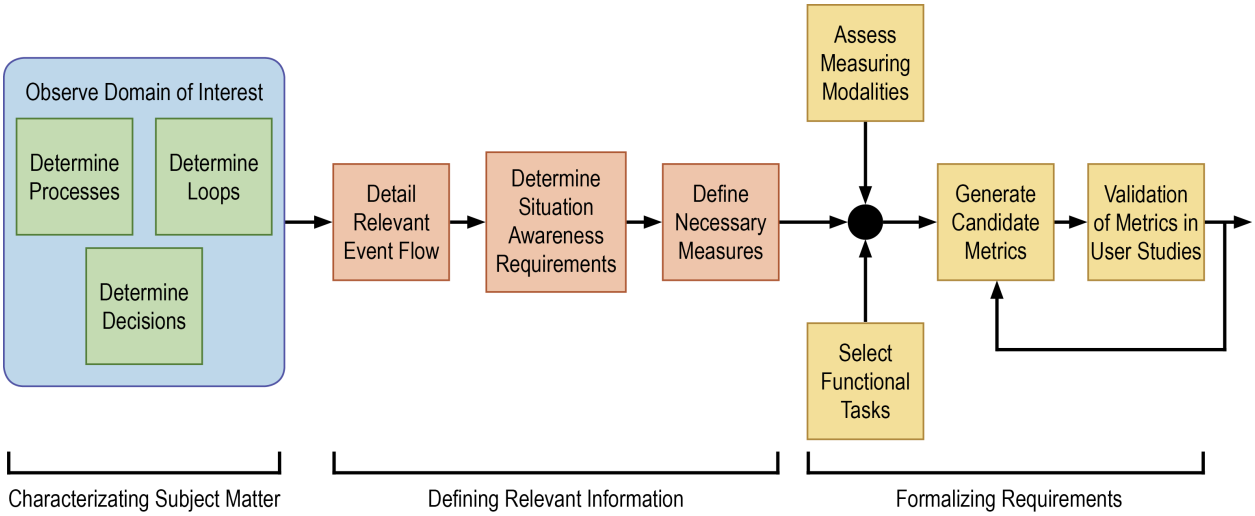

Figure 1.2: Modified Cognitive Task Analysis methodology developed to generate performance metrics for occupational therapy decision-making aids.

interest, in this case occupational therapy clinical rehabilitation sessions. Each domain of interest observed is unique due to patient-specific needs. Within each of these observable domains, we can determine the processes, loops, and decisions aligned with decision making [45]. Processes require a direct or indirect interaction between the clinician and patient. For example, in order to help a patient achieve the desired motion, an OT might provide vocal cues to remind them of what limbs or joints to use. Loops are defined as processes that are repeated until predetermined events occur, such as a certain amount of time passes or an observation is made that requires a decision. Finally, decisions are defined as the processes that require a clinician to make a rule- or knowledge-based judgment. Observations of these processes, loops, and decisions allow the development of event workflow diagrams for therapy sessions that aid in visualizing how clinicians make decisions and the information they need to do so. Figure 1.3 provides a sample workflow diagram from Stirling and McLean [2]. Fig. 1.3 highlights how an OT might regulate their time with a patient and how they might decide whether a cer-

tain task needs to be repeated, needs to be increased in difficulty, or is no longer necessary.

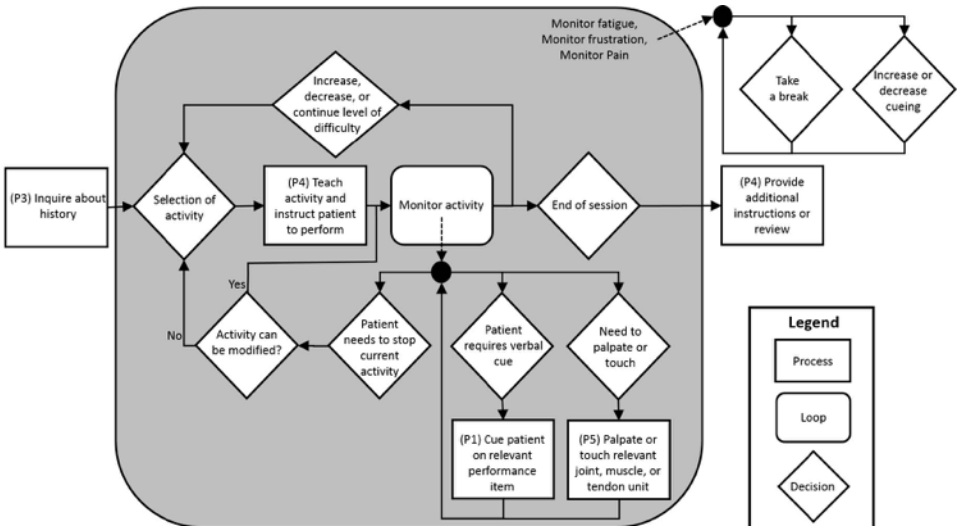

Figure 1.3: A sample workflow diagram for a physical therapy session containing various activities and patient evaluations borrowed from Stirling and McLean [2]

With an understanding of the subject matter we mean to quantify, the relevant information and their corresponding situation awareness (SA) requirements can be defined (Fig. 1.2). SA is the human's ability to thoroughly understand their surroundings. SA can be decomposed into three levels: perception of the elements, comprehension of the current situation, and projection of future states [46]. In the context of OT, perception of the elements involves the OT monitoring a patient perform a task (see the center of Fig. 1.3). During this stage, the OT is observing how the patient moves and how the patient interacts with the environment. The next phase, comprehension, involves taking information of how the patient is performing the task and determining if they are doing the task appropriately. If they are not doing it appropriately, the OT might decide to intervene with a verbal cue or perhaps physical manipulation (see Fig. 1.3). The final level of SA, projection into the future, involves the OT predicting what future plan-of-care the patient

requires.

Finally, the third segment of this methodology formalizes the requirements of the tele-rehabilitation system by integrating the measures required for the selected activity to define a series of design requirements for the system, and to generate a series of candidate metrics that will all eventually be tested in user studies to validate their efficacy. As part of the CTA, Stirling and McLean [2] provide a long and comprehensive list of features physical medicine clinicians use to evaluate motion. These terms are good candidates for performance-based metric development because clinicians already use them to describe the pathologies and motions they observe in their patients. This work focused on two: coordination and balance. Their definitions and SA requirements related to rehabilitation medicine are displayed in Table 1.2 and serve as a template for metric development in future chapters of this thesis. Coordination was selected as part of this thesis due to the lack of appropriate measures from the literature that could be used by clinicians [47, 48]. While various measures exist to quantify balance, there are very few balance metrics that quantify balance strategy, something that is relevant for certain patient populations (i.e. aging populations). In Chapter 2 and Chapter 4, we will discuss the limitation of current measures of coordination and balance, respectively, and address these limitations by defining new measures for each.

1.2 Understanding the Problems with Spacesuit Fit and Sizing

As mentioned earlier in this chapter, similar to rehabilitation physicians, spacesuit engineers also use tasks and how the tasks are performed to provide

Feature	Description	SA Level 1: Perception	SA Level 2: Comprehension	Current Methods
Balance	How does the patient hold themselves? Are joints well positioned? Will current position affect balance?	Observation of joint orientation and center or mass	Assess orientation in the context of task and patient pathology	Visual assessment by clinician
Coordination	Are the appropriate motor patterns present within and across limbs?	Observations of joint and hand motions	Assessment of joint and hand derivatives	Visual assessment by clinician

Table 1.2: Motion features being quantified for this thesis and their respective situation awareness requirements

valuable insight into spacesuit sizing and fit. Human spaceflight and exploration beyond low-earth orbit requires providing astronauts with life support systems in the form of not just space vehicles, but also extravehicular activity (EVA) spacesuit assemblies (SSA). These SSAs allow astronauts to perform tasks outside the space vehicle necessitating an appropriate amount of mobility to perform the task and protecting them from the extreme environment of space. Critical to mission success is the ability for users to effectively accomplish such mission-related operational tasks while reducing risks to health and injury [49, 50]. Human performance during mission-related tasks is limited by the ability of the user and the restrictions due to the SSA being worn. Newer SSA designs aim to increase astronaut mobility and reduce changes in their motor patterns from when they are unsuited. This aims to reduce injury risk and the metabolic cost of using the suit [51, 52]. However, these designs still tend to limit mobility and increase the amount of torque joints need to move compared to unsuited. These extra torques arise from bearing resistances, torques added by soft goods and rolling convolute joints, and inertial changes of heavy components [53]. SSAs can also be considered passive exo-systems that have various open human factors research questions in the

physical and cognitive domains [54].

Knowing that spacesuits add extra torques and increase the energy required to move, there is a need to understand how different SSA designs can impact human kinematics and whether these changes could lead to astronaut injury. This research goal becomes even more complex when considering the environments in which these systems are designed to operate. SSAs are designed for specific kinds of environments (microgravity vs. planetary) and specific kinds of tasks. Fig. 1.4 highlights three kinds of SSAs that are either actively being used by NASA astronauts or that are regularly used for research and development of future generations of suits. The Extravehicular Mobility Unit (EMU, Fig. 1.4A) is currently being operated by astronauts aboard the International Space Station (ISS). In microgravity, astronauts move around using handrails attached to the ISS or they are positioned around the station by having their feet attached by a giant robotic arm. Astronauts therefore rarely use their legs and predominantly perform tasks using their arms and hands. Since the EMU is used in microgravity environments and astronauts do not really use their legs in microgravity, there is little need to design for extra leg mobility. For this reason, the lower extremities of the EMU are fairly restricted in their mobility and it would not make sense to use this suit for any sort of walking task. Meanwhile, the Mark III (MKIII, Fig. 1.4B) is designed to operate in planetary environments that would require walking and geological exploration. For this reason, it is designed with greater mobility at the hips to enable more fluid gait movements and to enable crouching motions. Finally, the Z-2 SSA (Fig. 1.4C) was designed for use in both microgravity and planetary environments, with inter-changeable legs that are either rigid for microgravity or more mobile for planetary exploration. Therefore, not only do spacesuits alter the natural

way the astronaut moves, but different suit designs alter astronaut kinematics in distinct manners and need to be evaluated using the specific tasks the suit was designed to perform [55].

A. EMU **B. Mark III** **C. Z-2**

Figure 1.4: Existing Spacesuit Assembly Designs. A) The Extravehicular Mobility Unit (EMU) is designed for use in microgravity environment, while B) the Mark III is designed for planetary exploration. C) The Z-2 advanced suit concept is meant for use in both environments.

A common theme between all suit design is that getting a suit to fit and perform properly is challenging. Even dating back to the Apollo era when suits were custom built for astronauts, problems existed with the way astronauts interacted with different components of the suit leading to difficulty performing their assigned tasks [56]. To further complicate the problem, human motion within the suit is extremely difficult to quantify and observe because the human is completely occluded and there is little spacing available between the human and suit. To address the problems associated with fit, suit engineers perform a series of fit checks to properly exchange different sizing components and fit the astronaut as best they can to the suit.

If we create an analogy between physical medicine and spacesuit designers, the astronaut is like the patient and the suit engineer is like the OT. When evaluating an astronauts ability to perform in a suit, suit engineers, like OTs, rely on their experience to observe how the suit moves to diagnose any fit issues. Similar to OTs, there is a need for more objective measures of suit fit to help suit engineers decide the optimal way to design spacesuits that are versatile and fit well. For example, if suit fit measures reveal that the torso size does not affect an astronauts ability to walk, suit engineers could create a universally-sized torso and not need to customize this piece for every astronaut. Decreasing the degree of customization is important because it implies that future mission to the moon and Mars would require fewer suits, saving on the weight of material they need to bring with them on their journey.

Similar to OTs in Section 1.1, in order to define objective measures of suit fit, we must first understand what exactly suit fit is and how suit engineers currently make decisions about suit fit. In Chapter 3 of this thesis, we use a similar CTA used to understand how OTs make decisions (Section 1.1.2) to understand how suit engineers make decisions. From here, we are able to provide a comprehensive definition of suit fit and outline new techniques and metrics for quantifying suit fit.

1.3 Wearable Sensors: Inertial Measurement Units

As highlighted in Section 1.1 and Fig. 1.1, it is important to consider what technologies you might use to collect data on patients. For applications in OT, it is important that the technologies we use to collect our data do not alter the natural motion of our patients. Similarly, for our applications in suit fit and sizing, we need a technology that is low profile and can used inside the spacesuit. While we highlighted in Section 1.1 technologies such

as VR and video, this thesis focuses primarily on using wearable sensors, specifically inertial measurement units (IMUs), because of their portability and new methods for computing human kinematics.

Low-power wireless communication and microelectromechanical systems (MEMS) for sensing have rapidly matured into comfortable wearable motion sensors that enable real-time measurement of human kinematics. The most common is the IMU, which is composed of embedded accelerometers, gyroscopes, and magnetometers. The combination of these three sensors allows for rigid-body kinematic characterization of objects using outputted three-axis accelerations, three-axis angular velocities, and an estimation of the sensor's 3D orientation in space (either in Euler or quaternion representation). IMUs have been integrated into biomechanics research studies for the upper and lower extremities to assess feasibility, algorithm development, and the ability to characterize and classify motion patterns [57, 58, 59]. It is important to note that most methods rely on the assumption of rigid-body dynamics, meaning we assume that the segment is inflexible and all points along the segment have the same motion behavior. Rigid-body dynamics allows for a full description of an object's motion with just information regarding its linear displacement, rotational properties, and orientation relative to a fixed frame of reference. IMUs allow us to do this by outputting accelerations (linear displacement), angular velocity (rotational properties), and an estimation of orientation. The rigid-body assumption of each segment permits one IMU to be placed on each segment to estimate the entire segment's orientation . However, since human tissue is not perfectly rigid, current models are sensitive to sensor placement, initial calibration, and applied loads.

Many have tackled the issues associated with measuring human motion using IMUs. Mayagoitia et al. [60], for example, precisely aligned accelerom-

eters and gyroscopes with the femur and tibia body segments to measure knee angle to an accuracy of at most $2.73deg$ RMSE (5.2% of gait task range of motion). Precise placement of these sensors, however, can be cumbersome, difficult, and inaccurate for non-expert users. Vanegas and Stirling [61] also showed there is significant variability in IMU data when they are repeatedly removed and put back on due to differences in sensor placement on the body. To address some of the issues associated with sensor placement, functional calibration motions are implemented to estimate the alignment of the IMU reference frame with the body segment frame. For example, Cutti et al. [62], Favre et al. [63, 64], and Vitali et al. [65] each used a functional calibration procedure to calculate a rotation matrix that aligns the sensor frame to the segment frame. These methods offer powerful estimation tools over human-aligned techniques, especially in the presence of noisy sensors, but the need to calibrate the sensors does take time. Stirling and McLean [2] argue that it is important to minimize the time it takes to set up these kinds of sensors because clinical time is very valuable and clinicians do not want to waste time setting up technology when they could be using it to be with their patient. Recent work by Seel et al. [66, 67] and Muller et al. [68] implemented optimization-based methods to auto-calibrate and align IMUs with segment reference frames. McGrath et al. [69] used a PCA method to auto-calibrate and estimate the human knee axis. These methods allow for less precise placement of the IMU on the body segment and quicker set up time, making them more ideal candidates for our application here. Beyond estimating human kinematics, IMUs have already been implemented to measure other aspects of human performance, such as agility [70, 71], balance [72], stair climbing [73], and fall risk [74]. The recent advances in auto-calibrating joint angle estimation and low profile nature of these devices make IMUs ideal

candidates for the applications in this thesis.

1.4 Research Objectives and Specific Aims

The aim of this work is to provide ways to make the jobs of these clinicians easier by providing them with data that can help better disambiguate pathologies, identify decrements in function, and quantify rehabilitation progression (Section 1.1). Similarly, this work aims to help suit engineers better understand the complexities of spacesuit fit (Section 1.2). Both the domains of rehabilitation and suit fit need performance-based measures of human motion that can help individuals in their respective fields make more informed decisions.

In summary, the research objective of this work is to develop a series of biomechanically-driven human performance metrics compiled to aid operational decision-making, testing the hypothesis that we can provide quantitative feedback typically made subjectively and qualitatively regarding upper and lower extremity human function. In order to achieve this objective the following research questions must be answered:

1. Can we provide information on ***how*** motions are performed not just the outcomes of the motions being performed?
2. Are these metrics sensitive enough to detect operationally relevant differences that might influence decision making?

Furthermore, these research questions will more specifically be tackled through the following Specific Aims:

1. **Develop and determine whether a new metric for coordination can detect operationally relevant differences in motor control.** Current measures for coordination are difficult to interpret and limited

to cyclic tasks. We will define a new metric for coordination that is not restricted to cyclic motion and test the hypothesis that we can detect differences in coordination during a grasp and release task.

2. **Adaptation and validation of this new measure for coordination to the field of bioastronautics, specifically detecting operationally relevant changes in suit fit.** Motion coordination between the human and suit will be used to quantify suit fit. We will evaluate how changing the sizing components of the Mark III SSA (MIII) affects a modified RCM and outcome measures of a simple walking task. We will evaluate the hypotheses that changes in foam padding between the human and hip brief assembly of the MIII would affect measures of (a) gait performance and (b) dynamic fit.
3. **Develop and determine how differences in balance technique can detect operationally relevant differences in postural control.** Various clinical measures and tasks are associated with poor clinical outcomes in older clinical populations. We will test the hypotheses that we can detect differences in balance technique between different aging populations.

Chapter 2 of this thesis will go more into the background of coordination and a candidate metric for rehabilitation. Chapter 3 will discuss using this metric for decisions regarding spacesuit fit. Finally, Chapter 4 will discuss balance and a new metric created to better quantify balance technique.

Chapter 2

A Method for Quantifying Coordination during Non-Cyclic Motions

Chapter 1 of this thesis highlighted the motivation of this work stemming from rehabilitative medicine. This chapter will explicitly explore coordination, providing a detailed background and literature review (Section 2.1), presenting a new metric for coordination based on clinical needs and literature gaps (Section 2.3), and applies this new metric to a series of upper extremity tasks (Sections 2.4 - 2.6).

2.1 Defining Coordination

Human movement involves manipulating many human joints. Each joint also has multiple directions about which they rotate and move called their respective degrees of freedom (DoF). In human motion models, each joint is typically simplified to have between one to three DoF. For example, the shoulder is simplified in the global to have three DoF (flexion/extension, abduction/adduction, and internal/external rotation), meanwhile, the knee

joint is simplified to be one DoF. In reality, both the shoulder and knee within the joint reference frame have more directions about which they can move and rotate, but simplifying them in the global frame makes motion easier to describe and measure. The differences between motion in the global frame and joint motion are important to consider in some clinical scenarios. For example, some patient with partial paralysis of the arm might use their scapula more to compensate for weakness in the glenmoral-humorous joint. In this context, OTs might cue their patients to try and use their arm more to begin to rehabilitate those muscle groups affected.

When humans manipulate their joints in the appropriate manner, an elegant motion is produced that often allows us to perform a variety of tasks, such as walking or other ADLs. In rehabilitation medicine, certain motions and tasks are often described "coordinated" or "uncoordinated." While a motion being "uncoordinated" might have a negative connotation, the degree to which a motion is "uncoordinated" or "coordinated" is dependent on the context in which the motion is being performed. For example, human walking is a repeated pattern of trunk, hip, knee, and ankle motions that produce forward movement. Meanwhile, a clam-shell motion is a glute strengthening exercise that involves lying on one side with the knees bent and repeatedly drawing them apart, sometimes with a resistance band between the thighs. To the naked eye, this exercise might appear awkward or uncoordinated because it looks silly and there is no resulting forward motion or manipulation of weights, but this exercise does have a specific purpose when being performed in the context of physical therapy. Both motions (walking and clam-shells) in the wrong contexts might be considered uncoordinated, but in the appropriate context, these particular motor patterns are indeed coordinated. In other words, if someone tried to walk in a swimming pool,

the motions associated with walking would look rather uncoordinated, but on land and over ground, the joint motion we often affiliate with walking are quiet coordinated. Therefore, coordination must be defined in a context-specific manner.

This chapter defines a new measure for coordination, but first it must be defined. Since coordination is context dependant, we draw from multiple sources of literature to explicitly define what what we mean by coordination. Bernstein [75] was one of the first to define coordination; he defined it as the following:

"[Coordination is] the organizational mastery of human joint degrees of freedom, with complexity arising from the multiple kinematic solutions available in human dynamics" [75]

Turvey [76] built on Berstein's definition by decomposing coordination into two categories: (1) kinematic patterns and (2) neural control. Turvey also explains that task and environment lead to small differences in how humans move their joints despite the same end goal. For example, someone might reach for a cup differently than when reaching for a pen, despite being in the same starting position and having the same goal of grasping an object in front of them. Turvey's definition further strengthens the idea that coordination should be interpreted in a context-dependent manner. A more clinical definition of coordination was made by Stirling and McLean [77], who describe coordinated movements as motions with appropriate, non-pathologic motor patterns across multiple limbs, again implicating the importance of context. Definitions by Turvey [76] and Stirling [77] align in that they discuss (1) kinematic and neurological contributions of coordination and (2) the importance of context. From the definitions and descriptions of coordina-

tion acquired from the literature it is clear that human coordination involves context-dependent and planned out manipulation of human joints. To further explore the definition of coordination, Section 2.2 explores existing quantitative measures of coordination and what these measures imply about the underlying motion.

2.2 Existing Coordination Measures

Current measures that represent coordination are 1) continuous relative phase (CRP), 2) vector coding (VC), and 3) beta coordination matrix (BCM, $\beta_i j$). CRP and VC differ from BCM in that they are readily applied to a variety of cyclic tasks. BCM was created exclusively to evaluate the coordination of a crawling task [78]. First, we will focus on CRP and VC. It is important to note that both CRP and VC are represented using the greek symbol θ, however, this symbol is also used to represent joint angles. For simplicity and to avoid confusion in this thesis, the symbols γ and τ will to used to represent CRP and VC, respectively. Additionally, in order to better understand these metrics for coordination and their potential limitations, we will refer to Fig. 2.1 that provides reference hip and knee joint angles (Fig. 2.1a) and respective joint angular velocities (Fig. 2.1b) for a single step during a walking task. All 3 DoF of the hip (flexion, adduction, and rotation) and single DoF of the knee are plotted. These reference data will be used to visualize and compute coordination during walking using the metrics CRP and VC in the Sections 2.2.1 and 2.2.2.

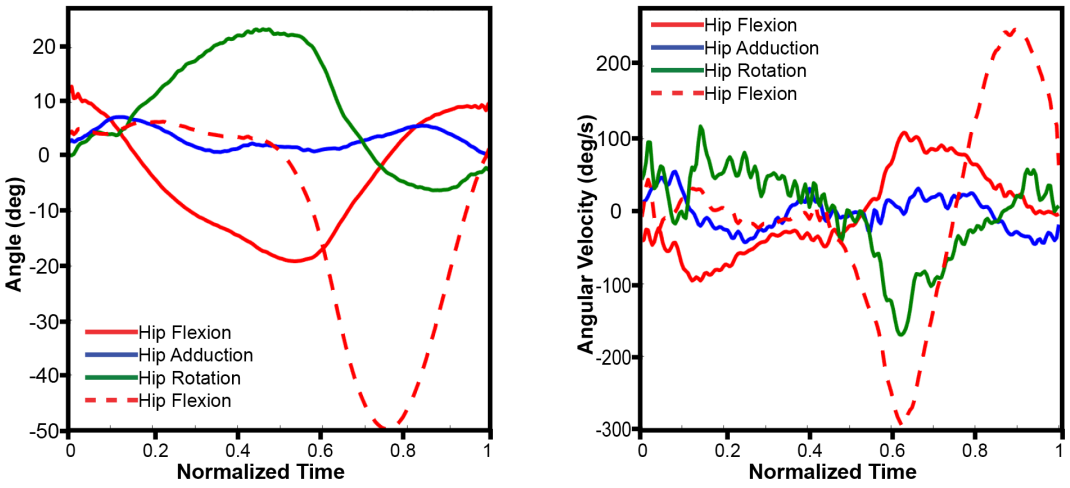

(a) Joint Angles

(b) Joint Angular Velocities

Figure 2.1: Sample hip and knee joint angle and angular velocity data from a single step. Joint coordinate systems are defined based on International Society of Biomechanics recommendation [79]. Hip **flexion/extension** is positive when in the anterior plane and negative when in the posterior plane. Hip **adduction** is positive when moving towards the midline and negative when moving away. Hip **rotation** is positive when rotating towards the rotating and negative when moving away. Knee **flexion** is defined as 0° when straight and negative when bent.

2.2.1 Continuous Relative Phase, γ^{12}

Phase space is a series of coordinates meant to represent all possible states of a system. CRP (γ^{12}) relies on the position and velocity signals of joints 1 and 2. A total of 4 data points are used to compute $\gamma^{12}(t)$ between joints 1 and 2 at time t. In order to compute γ^{12}, position (θ) and velocity (ω) are first normalized based on the constraints and kinematics to the task ($\tilde{\theta}$ and $\tilde{\omega}$, respectively). Position is normalized based on the maximum and minimum angular position values of joint n:

$$\tilde{\theta}_n(t) = 2 * \left[\frac{\theta_n(t) - min(\theta_n)}{max(\theta_n) - min(\theta_n)}\right] - 1 \tag{2.1}$$

where $\theta(i)_n(t)$ is the angular position at time t and $\tilde{\theta}_n(t)$ is the normalized angular position at time t, computed for each joint n. The normalization scheme in Eq. 2.1 results in the the normalized angular position of each joint n ranging between and including -1 to 1. Angular velocity is normalized based on the maximum absolute value of angular velocity for joint n:

$$\tilde{\omega}_n(t) = \frac{\omega(t)}{max(|\omega|)} \tag{2.2}$$

where $\omega(t)$ is the angular velocity at time point t and $\tilde{\omega}_n(t)$ is the normalized angular velocity at time point t, computed for each joint n. The normalization scheme in Eq. 2.2 results in the normalized angular velocity of each joint n lying between -1 and 1, but might not fully cover the range of -1 and 1 based on whether joint n has more negative or positive angular velocity.

Once normalized, a position-velocity phase space is created for each joint by plotting $\tilde{\theta}_n$ versus $\tilde{\omega}_n$ for all time, as shown in Fig. 2.2 with the reference data in Fig. 2.1. It is important to note that Fig. 2.2a is a position-velocity phase space representation of only the hip flexion/extension axis because

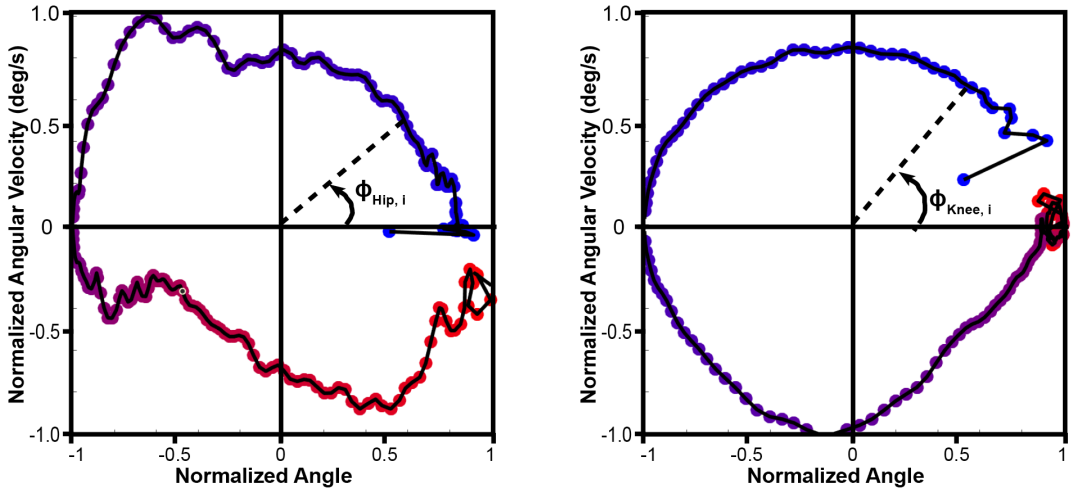

(a) $\tilde{\theta}_{Hip}$ vs. $\tilde{\omega}_{Hip}$ (b) $\tilde{\theta}_{Knee}$ vs. $\tilde{\omega}_{Knee}$

Figure 2.2: Position-Velocity phase space representations of hip flexion axis and knee using data found in Fig. 2.1a and Fig. 2.1b, respectively. The start of the step ($t = 0$) is represented by the red markers that slowly transition to blue markers, representing the end of the step ($t = 1$).

CRP only allows us to compare two joint axes as a time. In this case, we are comparing the hip flexion/extension axis with the knee axis. The joint "phase" in position-velocity phase space, termed ϕ, is computed for time point t as the angle from the positive x-axis, as displayed in Fig. 2.2a and 2.2b for ϕ_{Hip} and ϕ_{Knee}, respectively. Mathematically, ϕ_n for joint n is defined using the following equation:

$$\phi_n(t) = tan^{-1}\left[\frac{\tilde{\omega}_n(t)}{\tilde{\theta}_n(t)}\right] \tag{2.3}$$

where $\tilde{\omega}_n(t)$ is the normalized angular velocity of joint n at time t and $\tilde{\theta}_n(t)$ is the normalized angle of joint n at time t. The respective values of ϕ_{Hip} and ϕ_{Knee} based on the reference joint data in Fig. 2.1 are found in Fig. 2.3a. As seen in Fig. 2.3a, discontinuities can exist in ϕ based on the version of in the inverse tangent used.

The coordination between of the two joint system is then computed using CRP. The CRP between joints 1 and 2, γ^{12} is mathematically computed as the absolute difference in ϕ_1 and ϕ_2. $\gamma^12(t)$ is defined as:

$$\gamma^{12}(t) = |\phi_1(t) - \phi_2(t)| \tag{2.4}$$

where $\phi_1(t)$ and $\phi_2(t)$ are the ϕ_n of joints 1 and 2, respectively, for time t. Fig. 2.3b illustrates the γ^{HK} of the reference data in Fig. 2.1. γ^{12} is typically applied to cyclic task, such as gait [80, 81], running [82], and swimming [83], which is why we chose gait as the example task. It is important to note that the normalization scheme implemented using Eqs. 2.1 and 2.2 are performed for each repetition of the task. In other words, for our example, a new normalization would be applied to raw forms of θ and ω for each step performed, however, in our example we are only looking at one step to simplify the example. Part of the reason that CRP is typically applied to cyclic tasks is because in a cyclic task the values of θ and ω start and stop around similar values. This leads to ϕ having a full 360° range. With this in mind, the value of γ^{12} represents the difference in ϕ_1 and ϕ_2 at each time point of the cyclic task. For our example, it is convenient that both position-velocity plots of the hip extension axis and knee axis both start around the coordinates $(1, 0)$. If both these joint axes traveled through their respective phase spaces in a similar manner, then $\gamma^{12} = 0°$. However, as seen in Fig. 2.1a, the knee actually does not bend much at the beginning of the step cycle. This region is during stance phase when the knee is fairly rigid as the hip extends to shift the center of mass over the angle. Quantitatively, this results in ϕ_{Knee} hovering around zero, while ϕ_{Hip} get more negative and γ^{HK} grows in value. During the latter half of the step (i.e. swing phase), the knee bends and extends forward, while the hip flexes and the value of ϕ_{Knee} travels

through phase space rather quickly to catch up to ϕ_{Hip}, decreasing the value of γ^{HK}.

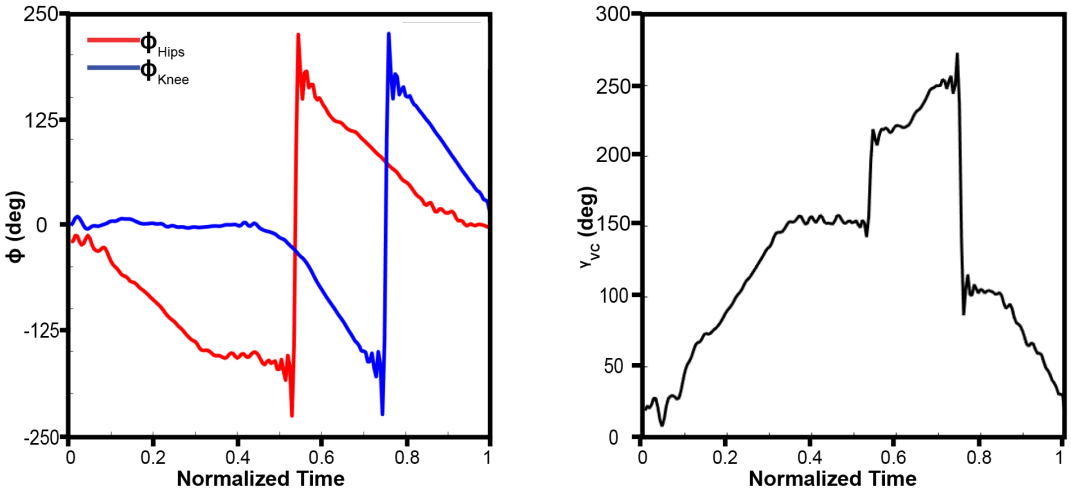

(a) ϕ_{Hip} and ϕ_{Knee} (b) γ^{HK}

Figure 2.3: Hip Flexion ϕ_{Hips} and Knee ϕ_{Hips} with corresponding γ^{HK} over a single representative step

As seen in Fig. 2.3, discontinuities exist when computing both ϕ and γ due to unwrapping issues present when using the inverse tangent. Fig. 2.3a uses a version of the inverse tangent ranging from $-180°$ to $180°$, leading to some of the sharp changes and discontinuities observed when $\tilde{\theta}$ and $\tilde{\omega}$ hover around the coordinates $(-1, 0)$ (see Fig. 2.2). Unwrapping problems associated with the inverse tangent can make interpreting the γ_{HK} more difficult because there can be sudden jumps in the value of γ_{HK} that stem from actual changes in the joint kinematics or from unwrapping problems when computing the metric, as seen in Fig. 2.3b at $t \approx 0.55$ and $t \approx 0.75$. Disambiguating the origins of these jumps is difficult when interpreting γ. Another difficulty in interpreting γ is it can be difficult to relate the value of γ back to the underlying kinematics [48]. The two transformations the joint kinematics undergo in Eqs. 2.3 and 2.4 create added layers of complexity that need to be disambiguated to try

and understand the underlying joint motion from the pattern observed in γ alone. In other words, if someone had one the representation of a motion from γ, it would be difficult to back out what the original joint angles were doing without prior knowledge of the underlying task and kinematics. In the paragraph above, we were able to fully understand and interpret γ^{HK} only because we had the raw joint angle data to help us. Interpretation are far more difficult without the raw data. In addition, without extra knowledge of the task being performed, there are many solutions that could be come up with when trying to guess the kinematics that lead to a value of γ.

This section presented one methods for normalizing γ^{12} but for cyclic tasks other methods of normalization do exist to account for changes in the motion period, such as Mean Period Normalized Continuous Phase and Half Period Normalized Continuous Phase [84, 85]. While predominately applied to cyclic tasks, there is justification to use CRP to analyze discrete tasks as it can assess coordination variability between trials of tasks that necessitate low variability (e.g. basketball shooting [86]), but discrete motions preclude the estimation of time continuous measures [48]. Time continuous measures refer to metrics that can be extracted from cyclic tasks that end where they started, giving the impression that the time-series is continuous over time. One example is the damping coefficient used to describe the time it takes to return to normal after a perturbation is introduced.

2.2.2 Vector Coding, τ^{12}

While CRP relies on position and velocity signals, vector coding (τ^{12}) relies only on position signals of joints 1 and 2 [87]. An angular position-angular position phase space is created between joint axes 1 and 2. Fig. 2.4a displays the position-position phase space representation of the hip flexion and knee

flexion axes the in Fig. 2.1 reference data. The coordination "state" of the two joint system is then computed for time point t as the angle of the slope between time points $t+1$ and t from the horizontal, as displayed visually in Fig. 2.4a. Mathematically, $\tau^{12}(i)$ is defined as follows:

$$\tau^{12}(t) = tan^{-1}\Big[\frac{\theta_2(t+1) - \theta_2(t)}{\theta_1(t+1) - \theta_1(t)}\Big], t = 1, 2, ..., T-1 \tag{2.5}$$

where θ_1 and θ_2 are the angular positions of joints 1 and 2 respectively, t is the time index, and T is the total number of time points within the trail. τ^{HK} is computed between the hip flexion axis and knee flexion axis in Fig. 2.4b. Similar to γ^{HK}, τ^{HK} can only be computed between single axes of joints. In addition, based on the form on inverse tangent used to compute τ^{12}, some discontinuities exist. Fig. 2.4b using a version of the inverse tangent ranging from $-180°$ to $180°$, leading to some of the discontinuities observed. This problem is very apparent when exploring our example here. Towards the beginning of this walking task, the knee is fairly rigid, while the hip extends backwards. In Fig. 2.4a, this leads to a fairly flat line as the hip becomes more negative and the knee does not change. Slight oscillations here leads to the value of τ^{HK} shifting from negative to positive fairly rapidly. In general, values of τ^{HK} are a numeric representation of how quickly the task is moving through position-position phase space.

2.2.3 Beta Coordination Matrix, β_{ij}

While γ_{12} and τ_{12} can be applied to a variety of cyclic tasks, Vitali et al. [78] created a coordination metric specific to a crawling task: the Beta Coordination Matrix (BCM, $\beta_{i,j}$). BCM is a 2×2 matrix where each component, $\beta_{i,j}$, corresponds to the coordination between a participants i^{th} arm and j^{th} leg. Vitali et al. [78] evaluated the specific hypothesis faster forward crawl-

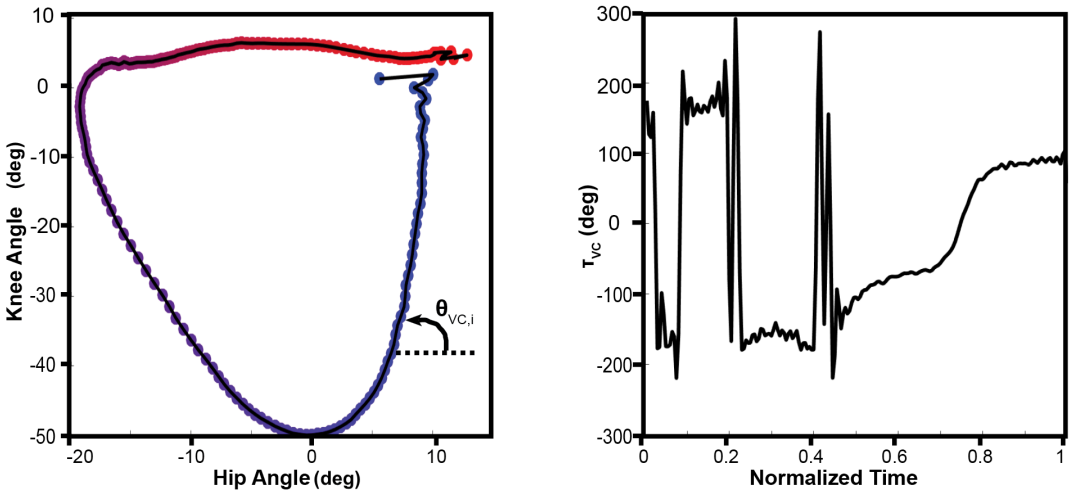

(a) θ_{Hip} vs. θ_{Knee} (b) τ^{HK}

Figure 2.4: Hip Flexion θ_{Hips} and Knee θ_{Knee} with corresponding τ^{HK} over a single representative step

ing speed was associated with greater limb coordination as computed using the BCM. BCM relies on the angular velocity reading from an IMU (Section 1.3) and computes limb coordination between different elbow strikes. Fig. 2.5 provides sample acceleration magnitude data from a participant performing a crawling task used to parse out different elbow strikes [78]. BCM is calculated using the following equation:

$$\beta_{ij} = \frac{\int_{t_1}^{t_2} \omega_{arm,i}(t)\omega_{leg,j}(t)dt}{\sqrt{\int_{t_1}^{t_2} \omega_{arm,i}(t)^2 dt}\sqrt{\int_{t_1}^{t_2} \omega_{leg,j}(t)^2 dt}} \tag{2.6}$$

where the time integral limits are the first elbow strike (t_1) to the last elbow strike (t_2) of the i^{th} upper arm. Each component β_{ij} is a measure of the phase between the principal angular velocities of the i^{th} upper arm and the j^{th} thigh, where again i, j = left (l) or right (r). Each component ranges $-1 \leq \beta_{ij} \leq 1$, where $\beta_{ij} = 1$ denotes the arm and thigh moving completely in phase (i.e. same speed and direction) and $\beta_{ij} = -1$ denotes the arm and

thigh moving out of phase (i.e. equal speed, but opposite direction). Fig. 2.5b provides sample angular velocity data between elbow strikes occurring between $4 - 5sec$ and the computed β_{ij}.

Work by Vitali et al. [78] supported their hypothesis that faster forward crawling speeds were associated with in-phase ($\beta_{ij} = 1$) motion between opposite-sided arms and legs and with out-of-phase (β_{ij}) motion between same-sided arms and legs. It is still unclear if BCM could also be applied to other tasks such as gait. This work by Vitali et al. [78] demonstrates how creating a metric to quantify performance of a specific task can be informative and effective at quantifying human performance. The heterogeneous nature of rehabilitative plan-of-care, prescribed tasks, and patient pathologies makes creating unique metrics for every task challenging.

2.2.4 Gaps and Limitations of Current Measures

Sections 2.2.1-2.2.2 and previous work highlight the non-intuitive results generated by VC and CRP, making it difficult to infer the original motor patterns [48, 88, 89]. Peters et al. [89] highlights that CRP should be used to understand relationships in phase-space and should not be used to make interpretations regarding the original time-series. Lamb and Stockl [48] also mention this drawback in a review of CRP highlighting space for a new form of dynamic coordination analysis that is more descriptive and easier to interpret. Finally, Miller et al. [88] advised caution when using CRP or VC to assess movement variability due to the inconsistent results based on how the data is normalized and averaged across cycles. Variability assessment during walking studies, for example, is important because it provides researchers and physicians with an understanding of how participants are able to compensate for small fluctuations in the way we walk [90]. Therefore, if CRP

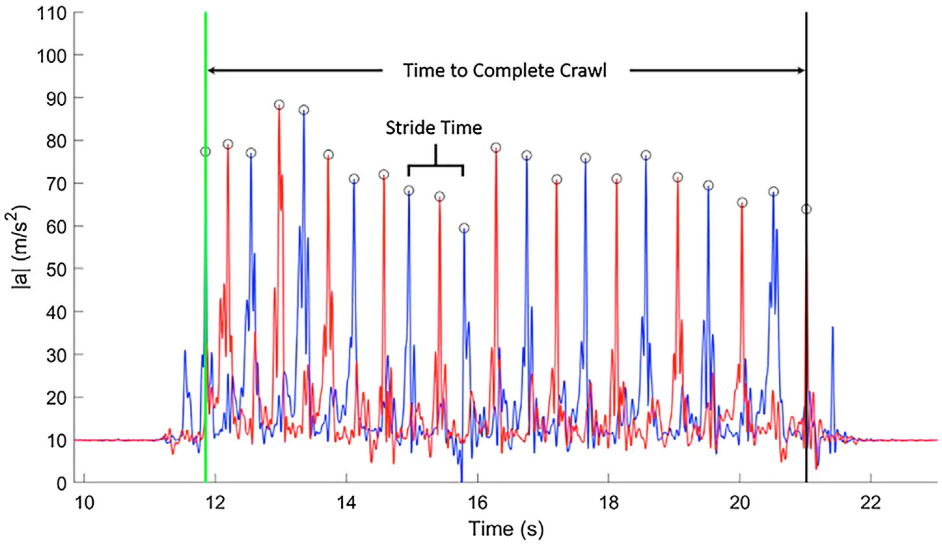

(a) Acceleration magnitudes (including superimposed gravity) of IMUs attached to left and right upper arm. Circles are the beak acceleration values correlated with elbow strikes for each arm. A single "stride" time is illustrated for the left arm. Data from a single stride is used to compute β_{ij} below.

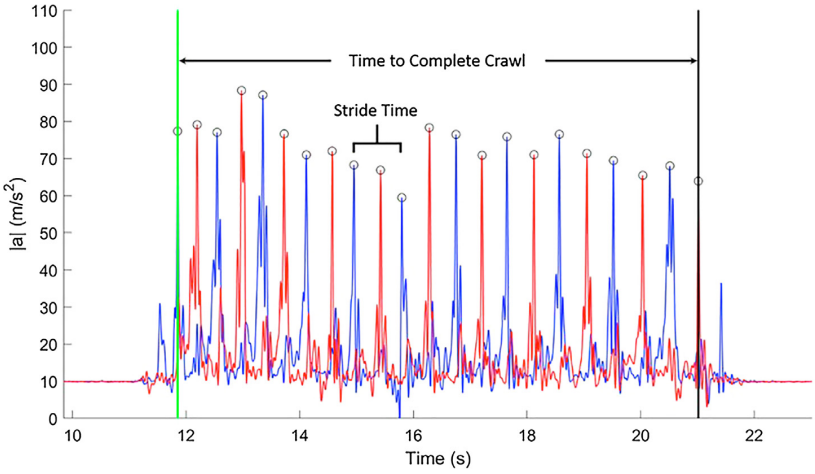

(b) Sample angular velocities of the upper arms and thighs over a single stride. If, for example, the right upper arm is rotating counterclockwise, the principal angular velocity is positive. The resulting components of the beta coordination matrix β_{ij} are highlight above each figure.

Figure 2.5: Example data and values of BCM borrowed from Vitali et al. [78]

and VC provide differing and inconsistent trends in coordination variability, participant data could be interpreted inappropriately.

For more clinical applications, interpretability back to the original motion is important because the original motor pattern is the thing that clinicians observe visually. As stated in Section 1.1.1, if these metrics are meant to substitute or augment visual observation made by clinicians, the measures should try to align as best they can with the way clinicians already think. The difficulty involved in relating CRP or VC could relate to the multiple transformations away from the underlying motion. CRP, for example, creates a phase angle in position-velocity space, ϕ, and then compares the two joints by subtracting these phase angles. For one, the relationship between velocity and position can often be counter-intuitive in the context of biomechanics as position planes are not defined the same between joints [91, 79, 92]. For example, knee angles are often not defined with negative values, while hip flexion/extension angles can [91, 79, 92]). The knee angle is normalized according to Eq. 2.1, forcing the normalized value of θ_{Knee} to be negative (see Fig. 2.2b) when in reality it is never actually negative. Without a deep understanding of the way we compute these metrics, it would appear odd to see the knee angle containing negative values. Therefore, fewer transformations of the original data might be easier to interpret. The drawback of CRP interpretabilty was also mentioned by Lamb et al. [48], highlighting space for a new form of dynamic coordination analysis that is more descriptive and easier to interpret, specifically even velocity-based.

Finally, CRP and VC do not have methodology for comparing entire joints to one another, just single DoFs. Again in more clinical settings, it might be valuable to compare coupled DoF joint motion since all DoFs contribute to end-effector motion. It can also be difficult to decouple some of the DoFs in

clinical settings when you are relying solely on observation and not on more technological approaches. Therefore, there is a need to evaluate multi-joint coordination.

2.3 The Relative Coordination Metrics ρ

2.3.1 Defining Coordination and the Goals of a new Metric ρ

Considering these limitations presented in Section 2.2.4, there is a need for a new coordination metric that is: a) easier to interpret, b) velocity-based, and c) translatable to non-cyclic motions. Therefore, we present a new, velocity-based coordination metric and accompanying normalization scheme for non-constrained, non-cyclic motion to quantify coordination between body segments, called the Relative Coordination Metric (ρ).

To start, we define coordination as the degree of relative motion between two body segments, specifically the relative velocity. In Section 2.1, coordination as defined by Bernstein [75], "the organizational mastery of human joint degrees of freedom." We define coordination as the degree of relative motion between two joints because relative motion provides an idea of how joints are "organizing" or moving in conjunction with one another. Certain tasks require two joint to move in unison, while others to not, and the relative motion between them can quantify this phenomenon.

From here, we define the relative coordination metric, where ρ_{12} is the relative velocity between body segment 1 and 2. The aim of the ρ is to quantify the level of coordination and relative motion between two body segments using velocity-based measures that inform on the underlying kinematics. ρ_{12} is defined with units of degrees over the range $-90^\circ \leq \rho_{12} \leq 90^\circ$, such that $\rho_{12} = 0^\circ$ represents a movement in which both segments are moving syn-

chronously. $\rho_{12} = 90°$ represents motion in which only segment 1 is moving, while $\rho_{12} = -90°$ represents motion of only segment 2. Values in between represent motions with varying degrees of segment domination. When neither segment is moving, ρ_{12} is undefined and represents no motion. While this metric quantifies relative coordination, a value of $\pm 90°$ or $0°$ does not imply bad or good coordination. To determine overall task coordination, ρ and the underlying task are considered in the context of what motor patterns are desired before any conclusion can be made regarding overall performance.

2.3.2 A Numeric Definition of ρ

To start, we consider the angular velocity of each body segment about its proximal joint. Human kinematic models assume that each body segment has its own number of rotation axes analogous to each DoF of the proximal joint. In other words, these rotational axes also correspond to the different directions each joint can rotate. For example, the thigh only has one DoF and rotation axis because its proximal joint, the knee, is a hinge joint, while the hip has three DoF because its proximal joint, the hip, is a ball joint. The total angular velocity for each segment is calculated by taking the L^2-norm of the measured components about these axes. To appropriately compare joints with varying DoF, we modify the L^2-norm angular velocity of body segment i at time t as follows:

$$\Omega_i(t) = \frac{\sqrt{\sum_{n=1}^{N} (\frac{\omega_n(t)}{j_n})^2}}{N * J_T} \tag{2.7}$$

where N is the number of joint DoF, $\omega_n(t)$ is the angular velocity component of segment i about joint axis n at time t, j_n is an axis-specific normalization parameter, and J_T is a normalization parameter encompassing all joint axes.

In other words, the normalized angular norm ($\Omega_i(t)$), is a weighted average of each of its n DoF.

Using Eq. 2.7, the relative coordination metrics (ρ_{ij}) is defined as:

$$\rho_{ij}(t) = 2tan^{-1}\left(\frac{\Omega_i(t)}{\Omega_j(t)}\right) - 90^\circ \tag{2.8}$$

where $\rho_{ij}(t)$ represents the relative motion between body segments i and j at time t, and $\Omega_i(t)$ and $\Omega_j(t)$ are the normalized L^2 angular velocity norms of body segments i and j, respectively. To achieve a range between 90° and -90°, the inverse tangent is scaled and a phase shift applied. This definition of ρ_{12} therefore achieves the previously stated goals for this metric: ρ_{12} approaches 0° when $\Omega_1 \approx \Omega_2$, approaches $+90^\circ$ for $\Omega_1 \gg \Omega_2$ and approaches -90° for $\Omega_1 \ll \Omega_2$. At small Ω_n, ρ_{12} can amplify measurement noise, which results in inaccurately favoring one segment over another. Therefore, it is necessary to set a minimum velocity threshold to avoid this effect. Using a weighted angular magnitude (Ω_i) in Eq. 2.7, grants ρ_{12} the ability to evaluate the coordination of single or multiple DoF across joints with different underlying joint characteristics.

2.3.3 How to interpret ρ

Equations 2.7-2.8 defined a new velocity-based metric for coordination ρ. In order to better understand how to interpret ρ, this section presents a series of simulated angular velocity data and the corresponding values of ρ.

Let us consider body segments A moving with angular velocity ω_A and body segment B moving with ω_B resulting in a motion that produces ρ_{AB}. The goals of this new metric are that $\rho_{AB} = 90^\circ$ represents motion in which only segment A is moving, while $\rho_{AB} = -90^\circ$ represents motion of only segment B. In order to evaluate this requirement, Fig. 2.6 displays simulated

angular position (Fig. 2.6a) and velocity (Fig. 2.6b) data in which segment A (blue, $|\omega_A| > 0$) has one DoF and moves from $\theta_A = 0°$ to $75°$, pauses, and then moves back, while segment B (red, $\omega_B \approx 0$) also has one DoF and has a constant position values of $\theta_B = 0°$. The x-axis of these plots is meant to be representative of normalized time $0 - 1$, where 0 is the beginning of the simulated motion and 1 the end. Random noise was added with a max amplitude of $0.1rad$ to both motions in order to simulate measurement from real-world devices, such as IMUs.

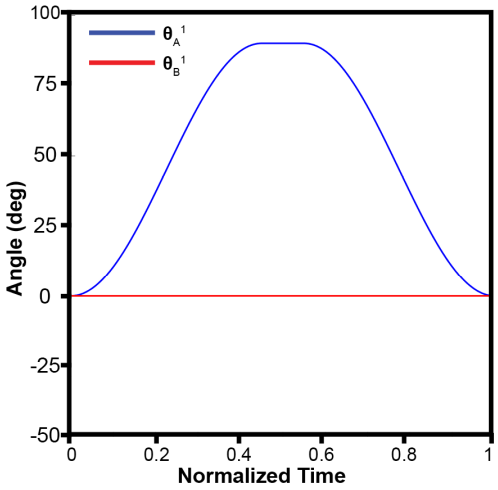

(a) Simulated Angular Position ($\theta_B = 0$)

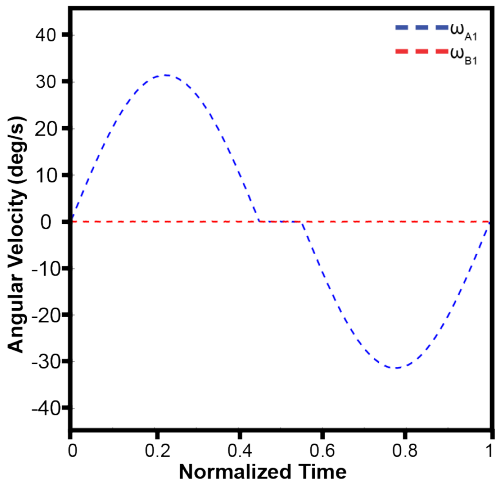

(b) Simulated Angular Velocities ($\omega_A > 0, \omega_B = 0$)

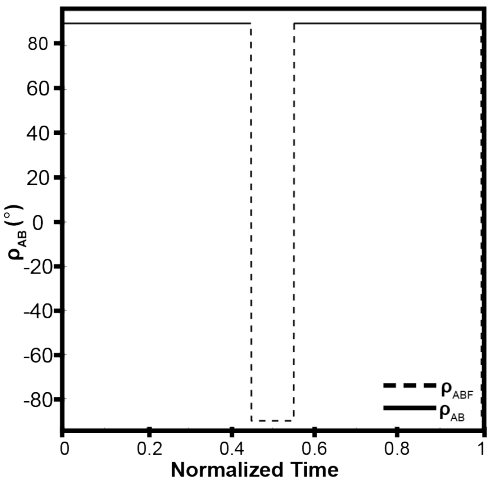

(c) Computed ρ_{AB} ($\omega_A > 0, \omega_B = 0$)

Figure 2.6: Simulated Data and Corresponding ρ_{AB} for Independent Segment A motion. Solid black line treats ρ_{AB} as undefined when Segment A and B are not moving, while the dashed black line does not remove noise when both segments are stationary.

Based on the goals of ρ and the simulated data in Fig. 2.6a and 2.6b, we expect that $\rho_{AB} \approx 90°$. As seen in Fig. 2.6c, the resulting ρ_{AB} matches what we would expect ($\rho_{AB} \approx 90°$), except around $t \approx 0.5$ when both segment A and B are not moving ($\omega_A = \omega_B \approx 0 deg/s$) and ρ_{AB} becomes undefined. The dashed version of ρ_{AB} represents what happens to the signal when ρ_{AB} is not undefined when both Ω_A and Ω_B are not moving beyond some measurement noise. In other words, when we do not set limits for when $\Omega = 0$, random noise in the signal can fluctuate the signal uncontrollably, as stated in Section 2.3.2.

Fig. 2.7 represents inverted simulated data to Fig. 2.6 in which segment B is moving (Fig. 2.7a, $0° \leq \theta_B \leq 75°$, and Fig. 2.7b, $|\omega_B| > 0$) while segment A is not (Fig. 2.7a, $\theta_A \approx 0°$, and Fig. 2.7b, $\omega_A \approx 0$). Fig. 2.7c shows the opposite pattern of Fig. 2.6c, which aligns both with the definition of ρ (Section 2.3.1) and the opposing simulated data in Fig. 2.6a compared to Fig. 2.7a.

As per Section 2.3.1, instances in which both body segments A and B are moving in a coordinated, synchronous fashion results in $\rho_{AB} \approx 0°$. Fig. 2.8a and 2.8b show simulated data in which ω_A and ω_B could be considered coordinated due to their nearly identical, inverted angular position and velocity patterns. Based on this simulated data and Eqs. 2.7 and 2.8, we would expect that $\rho_{AB} \approx 0°$. Fig. 2.8c plots the resulting ρ_{AB} which matches our prediction expect around $t \approx 0.5$ where both segments are not moving and the metric is undefined. This behavior is expected as discussed in Section 2.3.2. It is important to note that for Fig. 2.6-2.8, no normalization schemes are implemented when computing Ω_A and Ω_B (Eq. 2.8).

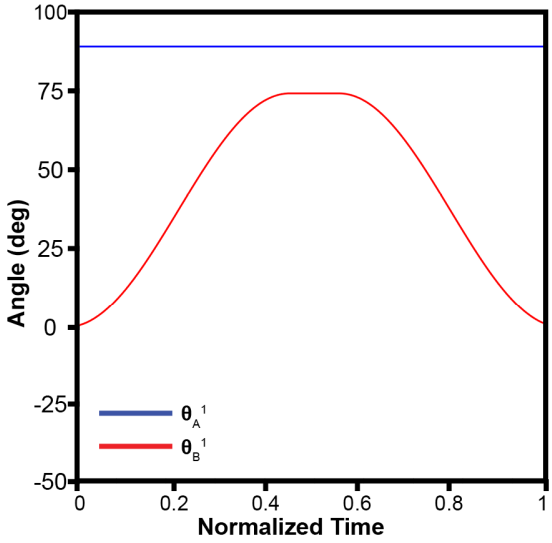

(a) Simulated Angular Position ($\theta_A = 0$)

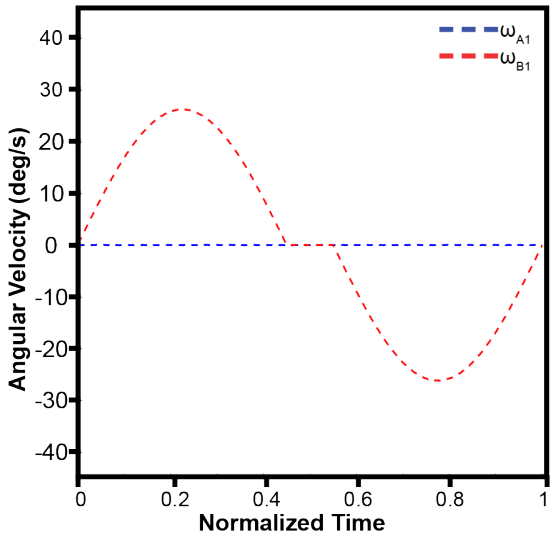

(b) Simulated Angular Velocity $\omega_B > 0$

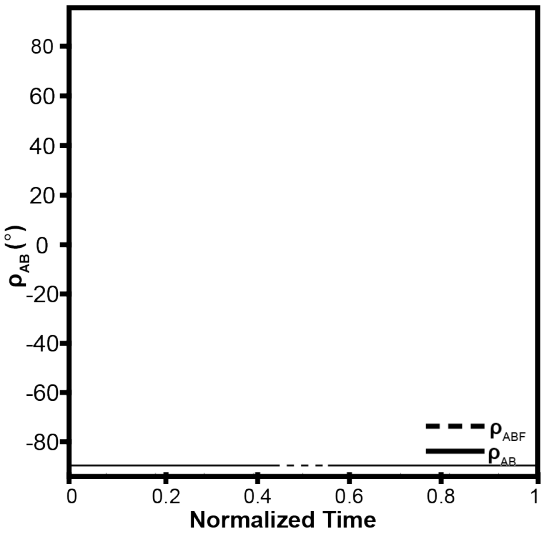

(c) Computed ρ_{AB} ($\omega_A = 0, \omega_B > 0$)

Figure 2.7: Simulated Data and Corresponding ρ_{AB} for Independent Segment B motion

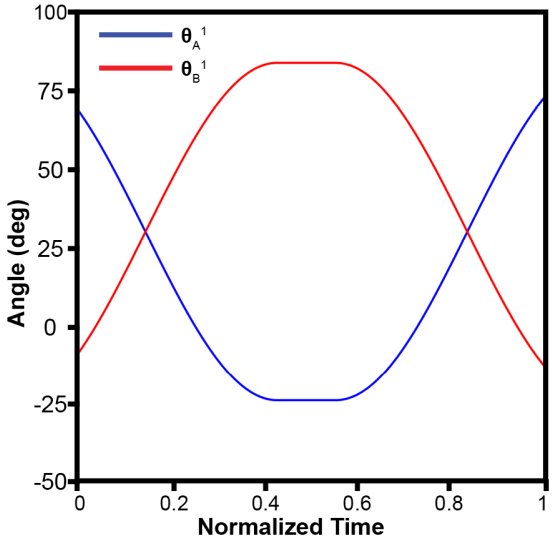

(a) Simulated Angles $\theta_A > 0, \theta_B > 0$

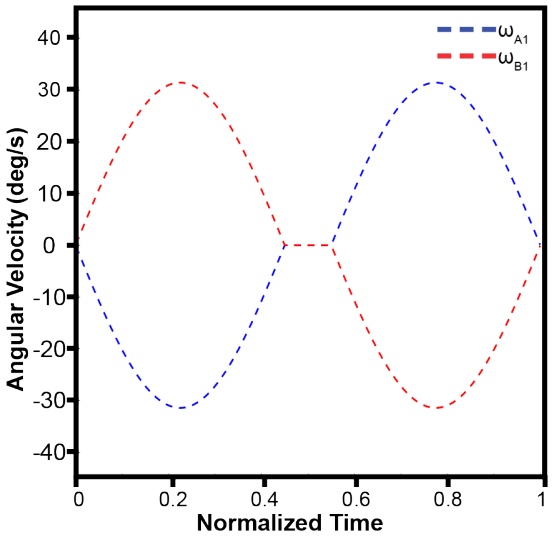

(b) Simulated ω ($\omega_A > 0, \omega_B > 0$)

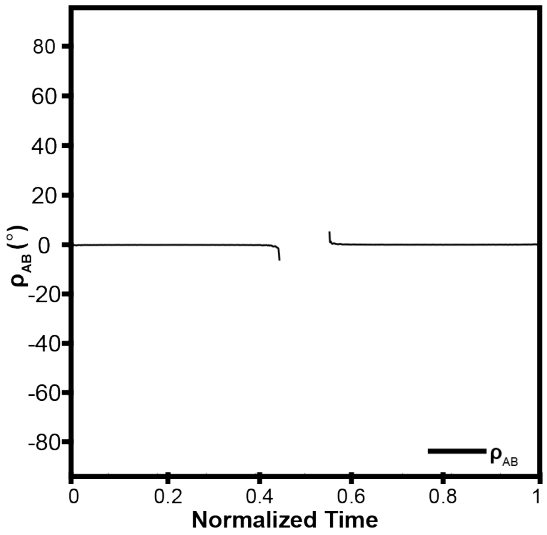

(c) Computed ρ_{AB} ($\omega_A > 0, \omega_B > 0$)

Figure 2.8: Simulated Data and Corresponding ρ_{AB} for Dual Joint motion

2.3.4 The Need to Normalize Ω

As discussed in Section 2.2, different human joints have varying DoF, ranges of motion (RoM), and coordinate systems [79, 91, 92]. In order to effectively compare joints with different underlying characteristics (for example, the shoulder can be modeled with 3DoF, elbow with 2DoF, and both these joints have different RoM), there is a need to appropriately normalize these joints because additional DoF or greater RoM could artificially increase Ω_i making it appear as if motion is "uncoordinated" when the joints are actually moving in a synchronous, coordinated fashion. To demonstrate the need to normalize and how normalization can affect ρ_{AB}, more simulated data is presented here.

To start, Fig. 2.9a presents simulated data for body segment A with two DoF (ω_A^1, ω_A^2) and body segment B also with two DoF (ω_B^1, ω_B^2). This example is meant to mimic the elbow joint in blue (2DoF, flexion/extension and pronation/supination) and the wrist joint in red (2DoF, flexion/extension and radial/ulnar deviation) during a reaching task over a table. Typically during this task, the elbow has a much higher RoM than the wrist as the participant extends their arm across the table to reach and uses the wrist for more fine tuned motions to interact with objects. While both segments have the same number of DoF and have the same phase, the max amplitudes of ω_A^1, ω_A^2, ω_B^1, and ω_B^2 are not the same value and neither are max angular magnitudes Ω_A and Ω_B, similar to how the elbow has more RoM than the wrist during a reaching task. When ρ_{AB} is computed in Fig. 2.9c, it would appear that these motions are not coordinated ($\rho_{AB} \approx 58°$) due to the disparity in maximum values of ω_A^1 and ω_A^2 being much greater than the maximum values of ω_B^1 and ω_B^2, shifting the value of ρ_{AB} to be very positive. Reaching tasks require finely tuned and coordinated manipulation between the elbow and wrist joints. For this reason, ρ_{AB} is also computed in Fig. 2.9c by using

a normalization scheme where each joint axis is normalized by its maximum angular velocity ($j_n = max[\omega_n]$ in Eq. 2.7, light grey line). As a result of this normalization scheme, $\rho_{AB} \approx 0$, which would be more indicative of a coordinated movement, which we would expect of the example reaching task.

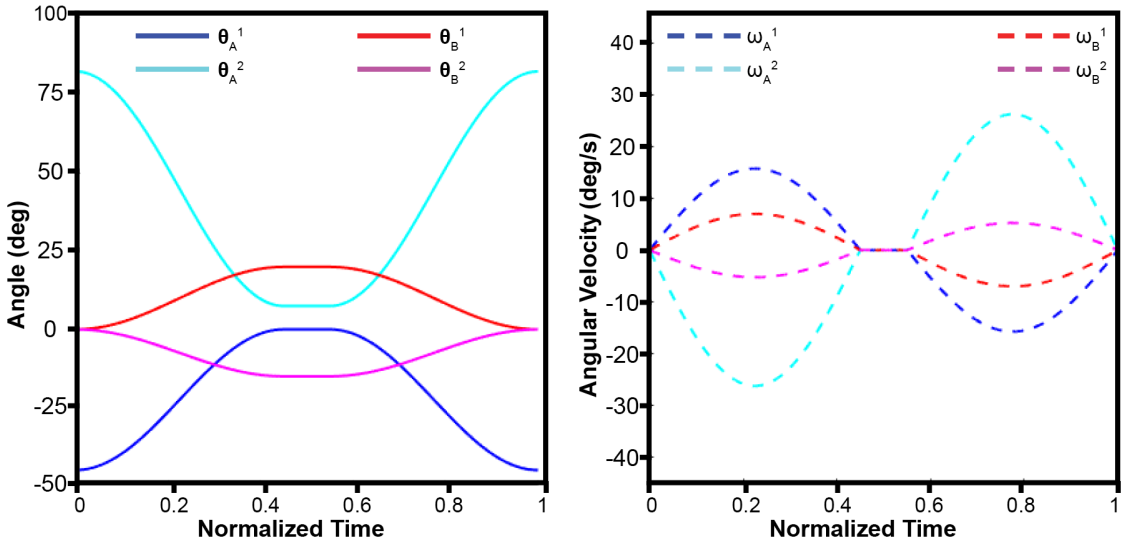

(a) Simulated Angles $\omega_A > 0, \omega_B > 0$ (b) Simulated $\omega_A > 0, \omega_B > 0$

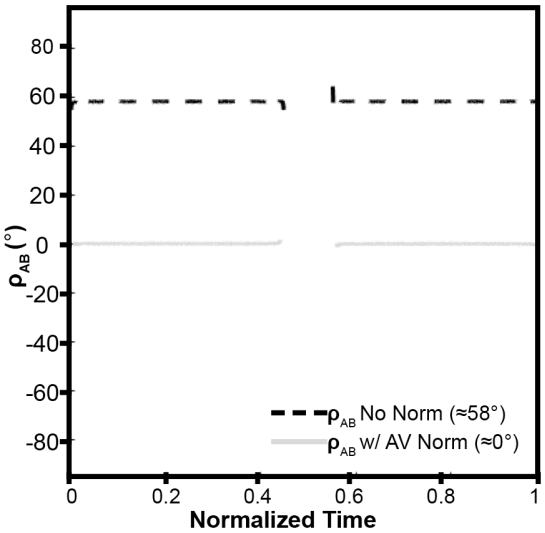

(c) Computed ρ_{AB} $(\omega_A > 0, \omega_B > 0)$

Figure 2.9: Simulated Data and Corresponding ρ_{AB} for Dual Joint motion

In order to illustrate the necessity for normalization when joints have dif-

fering DoF, Fig. 2.10 simulates motion for body segment A with 3DoF (ω_A^1, ω_A^2, ω_A^3) and body segment B with 2DoF (ω_B^1, ω_B^2). This example is meant to also mimic a reaching task over the table, but this time comparing the shoulder joint in red (3DoF, flexion/extension, abduction/adduction, and internal/external rotation) and the elbow joint in blue (2DoF, flexion/extension and pronation/supination). During these tasks, both joints might have similar RoM depending on how far up or across the table participants reach, but the main factor is that the shoulder has more DoF that make the effective angular magnitude higher than the elbow in most cases. In this simulated data, all individual joint axes carry reach, pause around $t \approx 0.5$, and then return to their starting position; however, they each possess differing amplitudes (Fig. 2.10a). Similar to the example in Fig. 2.9, we expect these sort of planar tasks to be coordinated tasks. However, due of the differing DoF and angular velocities of each joint, it might appear that this motion is coordinated, but without appropriate normalization when computing ρ_{AB}. Fig. 2.10c displays ρ_{AB} with varying normalizations. ρ_{AB} in the dash black line displays no normalization with $\rho \approx 58$ due to differing maximum angular velocities, angular magnitudes (Ω_A and Ω_B), and differing DoF. When normalizing just by joint axis max angular velocity (Eq. 2.7, $j_n = max[\omega_n]$), $\rho_{AB} \approx 10^\circ$ as shown in Fig. 2.10c with the large, lighter grey line. This is due to the differing DoF still artificially increasing Ω_A. Therefore, there is also a need to normalize by the number of DoF as shown with the darker grey line in Fig. 2.10c. This metric, ρ, therefore provides methodology for computing the coordination between entire joints with differing DoF.

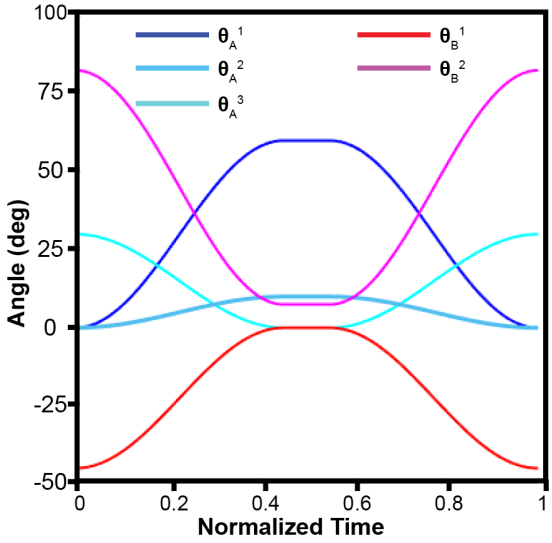

(a) Simulated Angles ($\omega_A > 0, \omega_B > 0$)

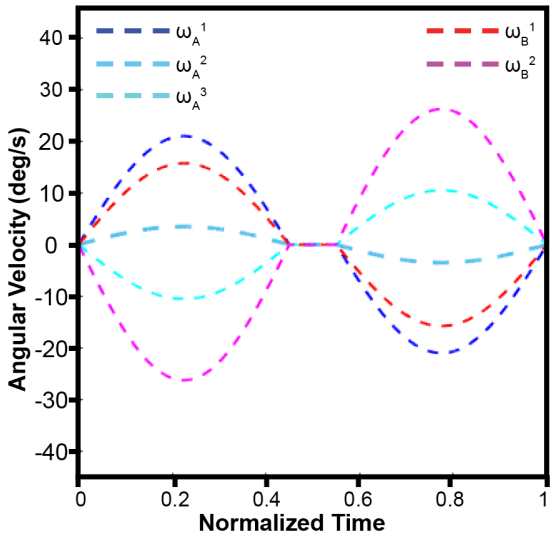

(b) Simulated Velocity ($\omega_A > 0, \omega_B > 0$)

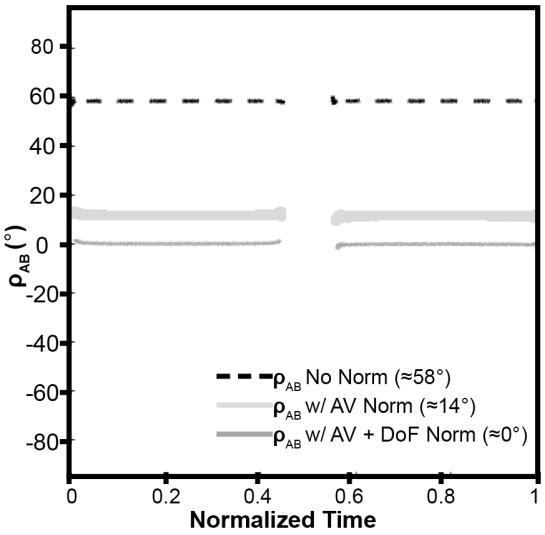

(c) Computed ρ_{AB} ($\omega_A > 0, \omega_B > 0$)

Figure 2.10: Simulated Data and Corresponding ρ_{AB} for Dual Joint motion

Certain applications might not warrant any normalization. For certain patient pathologies, OTs use splitting as a technique to restrict certain muscle groups and encourage their patients to use other muscle groups. For example, if a patient has upper extremity muscle weakness, OTs might restrain the patients chest to avoid them from leaning forward and encouraging them to

reach with their arms. In this scenario, if you were evaluating the coordination between the torso and upper arm, it might be desirable not to normalize the motion data so you can explicitly see an undesired torso motion. Normalizing could make any torso motion seem coordinated (like in Fig. 2.9c), but in reality you want to see behavior like that demonstrated in Fig. 2.6c where one segment is moving and the other is not, which might be more easily observed without any normalization. In the case that a normalization scheme is desired, sample, nominal data population could aid in determining what normalization scheme is the most appropriate.

2.3.5 Composite Measures of ρ

Both CRP and VC are used to evaluate motions using descriptive statistics, specifically variability, in addition to their time-series representations as a way to summarize the time-series result [88, 82]. Additionally, since there is desire to reduce the time burden on clinicians [2], it might be easier to observe a series of summary measures for coordination instead of time-series that might take more time to process.

As the ρ is a time-series metric, we define the percent time in a coordination zone ($\hat{t}_{\pm Z_n}$) to provide a composite overview on the ρ during the task (Fig. 2.11). Here we define seven zones. Zone 1 (Z_1) ranges from $-20^\circ \leq \rho_{12} \leq 20^\circ$, corresponding to motions with the highest relative coordination (i.e. neither segment is dominant in the motion). Zones $+Z_2$, $+Z_3$, $+Z_4$ represent progressively less coordinated movements in which segment 1 dominates, with ranges $20^\circ < \rho_{12} \leq 40^\circ$, $40^\circ < \rho_{12} \leq 60^\circ$, and $60^\circ < \rho_{12} \leq 90^\circ$, respectively. Meanwhile, zones $-Z_2$, $-Z_3$, $-Z_4$ represent motion dominated by segment 2, with ranges $-40^\circ < \rho_{12} \leq -20^\circ$, $-60^\circ < \rho_{12} \leq -40^\circ$, and $-90^\circ < \rho_{12} \leq -60^\circ$, respectively. These zones are represented graphically in Fig. 2.11.

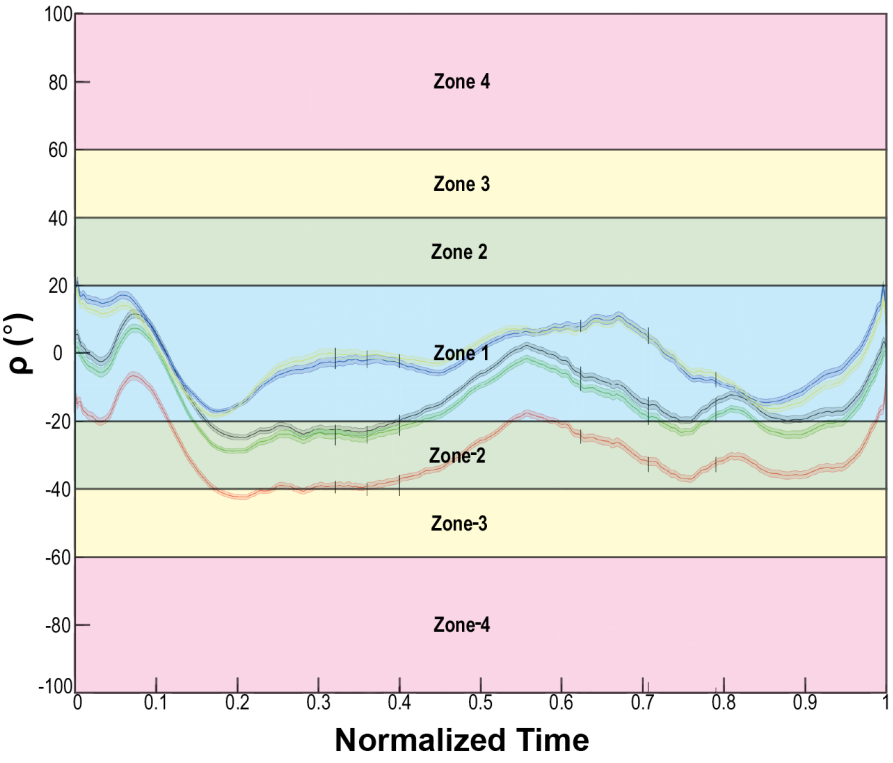

Figure 2.11: Graphical description Frequency in Coordination Zone ($\hat{t}_{\pm Z_n}$)

2.4 Application and Experimental Validation of ρ

Section 2.3.2 defined a new metric for quantifying coordination (ρ, Eq. 2.7 and 2.8) that is velocity-based and easier to interpret than existing measures. Section 2.3.3 uses simulated data to describe how to interpret ρ. Kurtz et al. [85] provides evidence that normalization significantly alters the interpretation of CRP. Section 2.3.4 illustrates both the need to normalize ρ and how normalization can affect the way ρ is interpreted. Therefore, there is a need to understand the effect of normalization in an experimental setting. In addition, it is necessary to assess the sensitivity of ρ to detect operationally relevant differences or differences that are significant enough for clinical intervention.

In this initial work, upper extremity coordination patterns during a grasp, transport, and release task in a healthy population were used to assess the effect of various normalization schemes, as well as specific variations of the task on ρ interpretation. Previous work [93, 94, 95, 96] demonstrated varying kinematic relationships between the shoulder, elbow, and wrist joints during reach, transport, and grasping tasks because they each had their participants reach different distances, interact with different objects, and transport to different locations. Therefore, the trajectory and objects selected for these reaching tasks is likely to have an effect on upper limb coordination. In order to observe these changes in coordination and to examine task and environmental effects on coordination as expressed by Turvey [76], two objects and two reach, transport, and grasp trajectories were evaluated to assess if ρ was sensitive to these variations. As ρ is a velocity-based metric, it is important to consider how underlying differences in joint RoM and DoFs affect the estimation. Thus, we consider normalizing ρ using joint-specific parameters to compare between body segments. As ρ is expected to naturally vary during different stages within grasp, transport, and release task, we considered how ρ changes during five predefined stages (50% reach, grasp, 50% transport, release, and 50% return). In addition to considering the ρ time-profile, we consider the time-independent composite measure of the percent time in a coordination zone ($\hat{t}_{\pm Z_n}$) defined in Section 2.3.5.

We evaluated the hypotheses that there was a difference in ρ within the grasping task when (1) different normalization schemes were implemented and (2) during the five task stages; and that there was a difference in $\hat{t}_{\pm Z_n}$ (3) when grasping a cup vs. a pen, and (4) when the task involved different motion trajectories (moving towards or away from the torso).

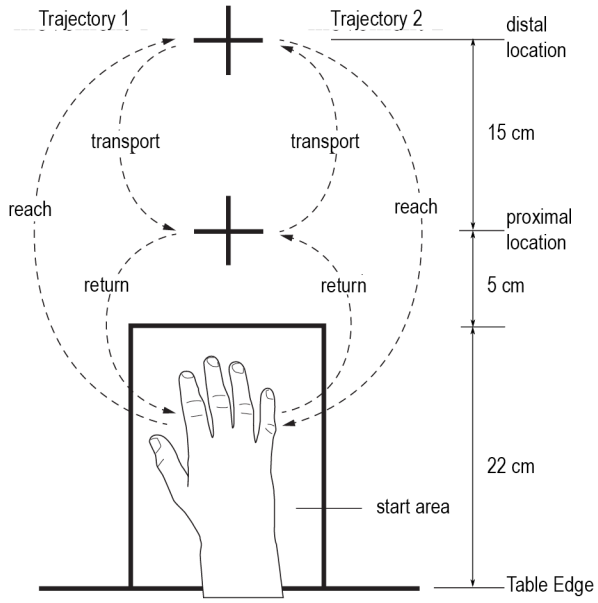

Figure 2.12: Task Description: participants, seated behind a table, moved an object from the distal location to the proximal location on the table and back. Each trial was divided into two trajectories while interacting with each object. Each trajectory included 5 stages: reach, grasp, transport, release, and return.

2.4.1 Experimental Design

A secondary analysis was performed on data acquired from 15 right-handed healthy participants who performed reach/grasp tasks (Fig. 2.12, [93]). Participants were 23-26 years old ($M = 24.4$, $SD = 1.2$), 5 females/10 males, arm lengths 29.2-37.8cm ($M = 33.9cm$, $SD = 2.4cm$), and forearm lengths 19.9-29.6cm ($M = 25.7cm$, $SD = 2.5cm$). Participants gave written informed consent and the protocol was approved by the MIT Committee on the Use of Humans as Experimental Subjects.

While seated behind a table, participants moved an object from one location to another using their right hand, Fig. 2.12. In each trial, participants made two movements with distinct trajectories: moving the object from the distal to the proximal location (trajectory 1) and moving the object from the

	Normalization Scheme	N	j_n	J_T
A.	None	# Joint axes	1	1
B.	Degrees of freedom	# Joint axes	1	1
C.	Angular Velocity	# Joint axes	$\max[\lvert\omega_n\rvert]$	1
D.	Range of Motion	# Joint axes	RoM$[\omega_n]$	1
E.	Angular Magnitude	# Joint axes	1	$\max[\sum_{m=1}^{N} \omega_n]$

Table 2.1: Definitions of Normalization Parameters

proximal to distal location (trajectory 2). Each trajectory was sub-divided into 5 stages: reach, grasp, transport, release, and return. Kinematics were recorded using a 10-camera motion capture system (Bonita, VICON Inc., USA) at 100Hz. Eighteen reflective markers were placed unilaterally on the right shoulder, arm, forearm, and hand.

Participants performed the task with two objects: a cup (diameter: 6 cm, height: 9 cm, mass: 0.2 kg) and a rod (dimensions and mass like a ballpoint pen). Participants were asked to place the objects on specific marks in one smooth, continuous movement. The pen was placed perpendicularly to the transport direction. Participants grasped one object per trial. A total of four tasks (trajectory 1 and 2 for both the cup and pen) were performed, each with 50 trails (200 total).

2.4.2 Data Analysis

Marker data were processed using Nexus (v. 1.8.5, VICON Inc., USA). The marker position data were filtered using a 6th-order Butterworth low-pass filter (corner frequency at 30Hz to remove high frequency noise). Joint rotations and translations were determined using inverse kinematics with OpenSim 3.0 [97] and the Stanford upper extremity model [98]. Marker and joint kinematic data were used to determine the start, grasp, release, and end of

each trajectory using the movement segmentation methodology in Schot et al. [99]. The start of each trajectory and minimum angular velocity was defined based on Beckers et al. [93]; each trajectory started once the wrist velocity exceeded 3cm/s (as calculated from a marker on the wrist) and was finished when the hand was completely inside the start area and the wrist velocity was less than 3cm/s. The grasp event was defined as the moment when the thumb and index fingertip were within 2cm of the object, the wrist velocity was minimum, and the grip aperture (i.e. closing the thumb and index finger) rate was at a minimum. The moment of release was determined using the same parameters as grasping, but when grip aperture was increasing.

We implemented a 7DoF model of the upper extremity with 3DoF at the shoulder (flexion/extension, abduction/adduction, internal/external rotation), 2DoF at the elbow (flexion/extension, forearm pronation/supination), and 2DoF at the wrist (flexion/extension, radial/ulnar deviation). The RCM was calculated between shoulder-elbow (ρ_{se}), shoulder-wrist (ρ_{sw}), and elbow-wrist (ρ_{ew}) (3 total). ρ_{se}, ρ_{sw}, and ρ_{ew} for each trial were time-normalized from 0 (movement initiation) to 1 (movement completion). Each normalization parameter in Eq. 2.7 and Table 2.1 were calculated individually for each participant and all 200 trials. The normalization parameters of maximum angular velocity and RoM for each joint axis, as well as the maximum angular velocity magnitude were determined using the OpenSim results for each individual and trial.

For this study, a minimum velocity of the wrist was used as an indication that motion had begun (see Section 2.4). This work considers five normalization schemes (Table 2.1) accounting for the DoFs, maximum angular velocities, RoM, and maximum angular magnitudes, while comparing to a baseline of no normalization.

To analyze the effect of normalization scheme and trajectory stage, the ρ for all three joint pairings (ρ_{se}, ρ_{sw}, ρ_{ew}) and five normalization schemes (Table 2.1A-E) was extracted at discrete time points associated with the 5 trajectory stages: A) 50% reach, B) grasp, C) 50% transport, D) release, E) 50% return all extracted by detecting of grasp and release events using methodology in Beckers et al. [93].

2.4.3 Statistical Analysis

Statistical analysis was performed using SYSTAT 13.1 (Systat Software Inc., USA). Due to the non-normal distribution of the data set, non-parametric Kruskal-Wallis (KW) tests were performed to assess main effects of our hypotheses. To evaluate the effect of normalization scheme (hypotheses 1) and the effect of trajectory stage (hypothesis 2), 5 values of ρ corresponding to stages A-E (listed above) were selected from the time-series data for each of the 5 normalization schemes (Table 2.1). A new independent variable, termed the "norm-stage," was created for each combination of stage within the task and normalization scheme for a total of 25 norm-stage groups. The effect of norm-stage on ρ was evaluated by performing a separate KW test for each combination of object (2 levels, cup/pen), trajectory (2 levels, trajectory 1/2), and joint comparisons (3 levels), for a total of 12 tests.

To evaluate the effect of the object grasped (hypothesis 3), $\hat{t}_{\pm Z_n}$ for the 7 coordination zones was considered for both objects (cup and pen). A new independent variable comprised of all combinations of objects and coordination zones was created and termed "object-zone." A total of 14 object-zones were created, pooling both trajectories together. The effect of object-zone on $\hat{t}_{\pm Z_n}$ was assessed using a KW test for 3 of the 5 normalization schemes (Table 2.1A-C) for each of the 3 joint comparisons, resulting in 9 total tests.

The same tests were performed to assess the effect of trajectory (hypothesis 4), however, $\hat{t}_{\pm Z_n}$ was considered for both trajectories 1 and 2. We created the independent variable called "trajectory-zones" comprised of all 14 total combinations of trajectory and coordination zone, pooling objects instead of trajectories as done for the object-zones.

The False Detection Rate controlling procedure [100] was implemented to address the multiple omnibus tests performed ($p_i < \frac{m_o}{m} * 0.05$), where m is the total number of tests performed and m_0 is the number of false null hypotheses prior to the correction. When significant main effects were observed, the Dwass-Steel-Critchlow-Fligner post-hoc test containing embedded correction methods [101] was performed.

2.5 Results

A time-series representation of ρ_{se}, ρ_{sw}, and ρ_{ew} during the four tasks performed with each of the five normalization schemes is shown in Fig. 2.13-2.15. Shifts in ρ between negative and positive values during the time-series are indicative of switching between limb segments that have higher relative motion. Henceforth, we refer to the limb segment with greater relative motion the dominant limb. For example, in Fig. 2.14 all four types of reach, transport, and grasp task start with a large upward, positive shift in the value of ρ_{SW} that is representative of the shoulder joint having a higher amount of motion relative to the wrist or this is shoulder dominated motion. Around the grasp portion of the task (the vertical blue region in Fig. 2.14), there is a sharp, negative decline in ρ_{SW}, which is indicative of more wrist dominated motion and the wrist having more relative motion than the shoulder.

Prior to discussing the results of the statistics performed, there are some notable general trends within Figs. 2.13-2.15. Most notable is that during the

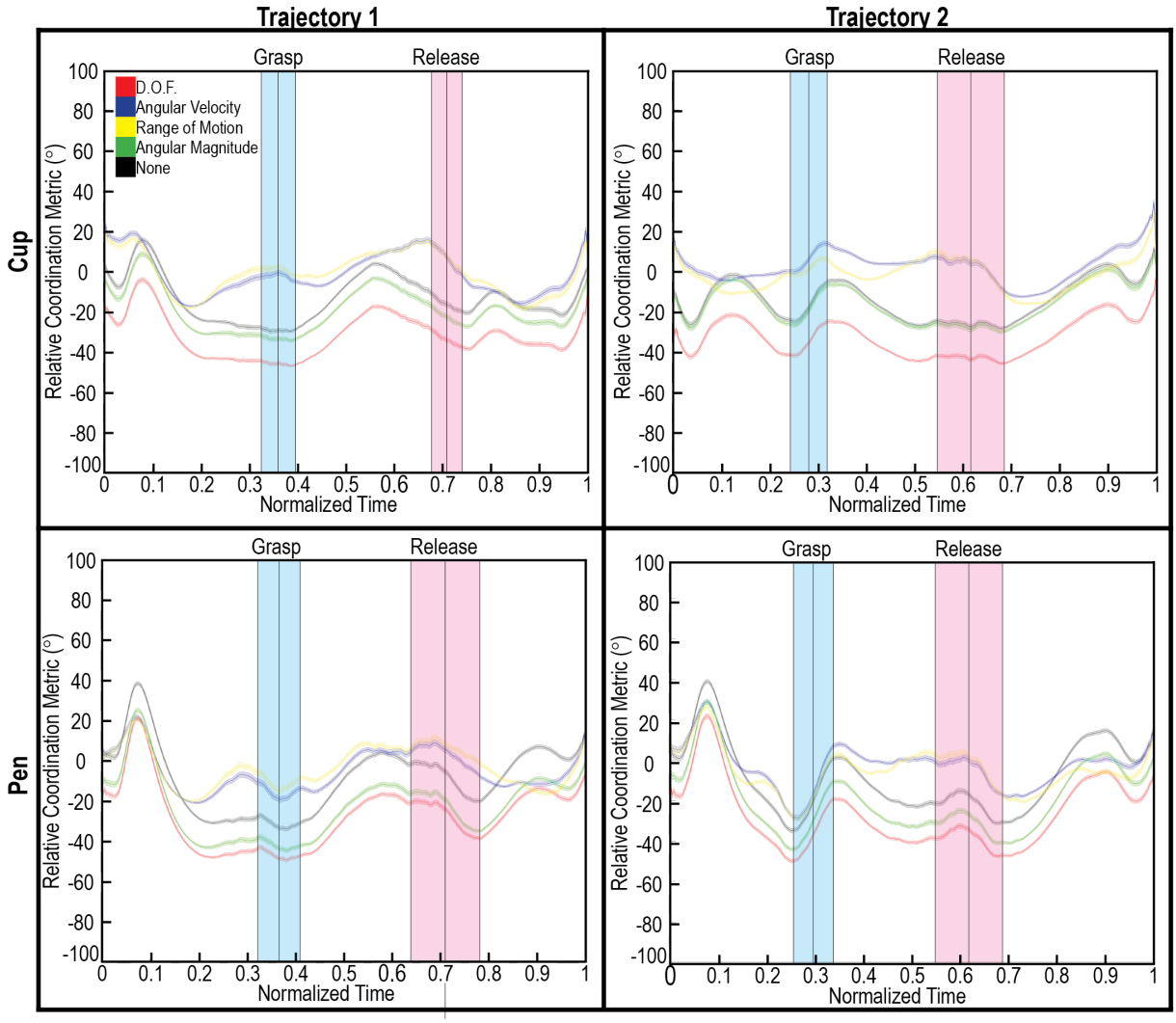

Figure 2.13: Time-series Shoulder-Elbow Relative Coordination Metric (ρ_{se}): A time-series representation of the ρ_{se} between the shoulder and elbow using all five normalization schemes presented in Table 2.1. $+\rho_{se}$ is representative of shoulder dominated motion, while $-\rho_{se}$ is representative of elbow dominated motion. Shaded regions represent the locations of grasp (blue) and release (red) ±standard deviation. Shaded regions represent the locations of grasp (blue) and release (red) ±standard deviation. Shaded regions around each normalization scheme represent ±standard error.

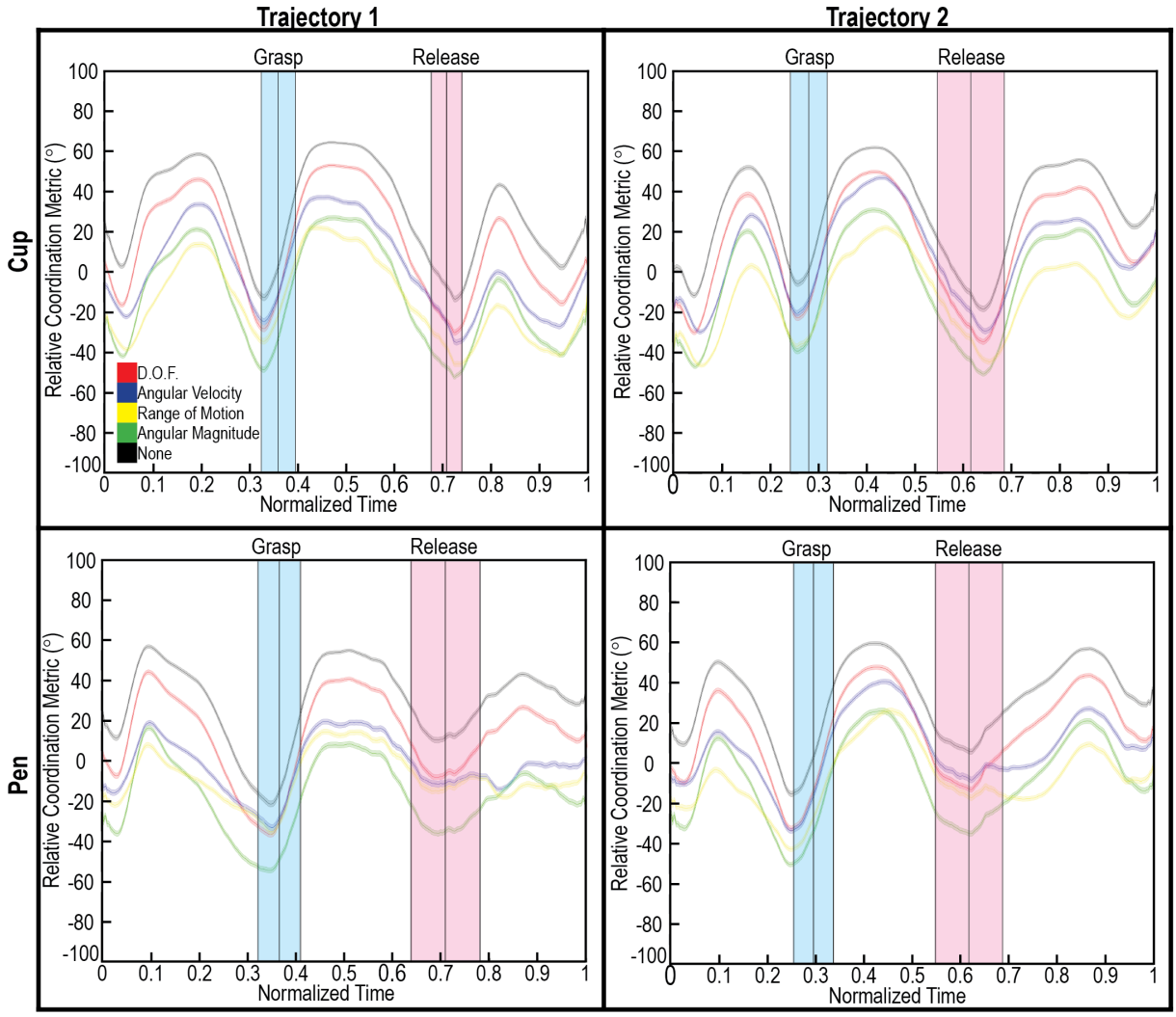

Figure 2.14: Time-series Shoulder-Wrist Relative Coordination Metric (ρ_{sw}): A time-series representation of the ρ_{sw} between the shoulder and wrist using all five normalization schemes presented in Table 2.1. $+\rho_{sw}$ is representative of shoulder dominated motion, while $-\rho_{sw}$ is representative of wrist dominated motion. Shaded regions represent the locations of grasp (blue) and release (red) ±standard deviation. Shaded regions around each normalization scheme represent ±standard error.

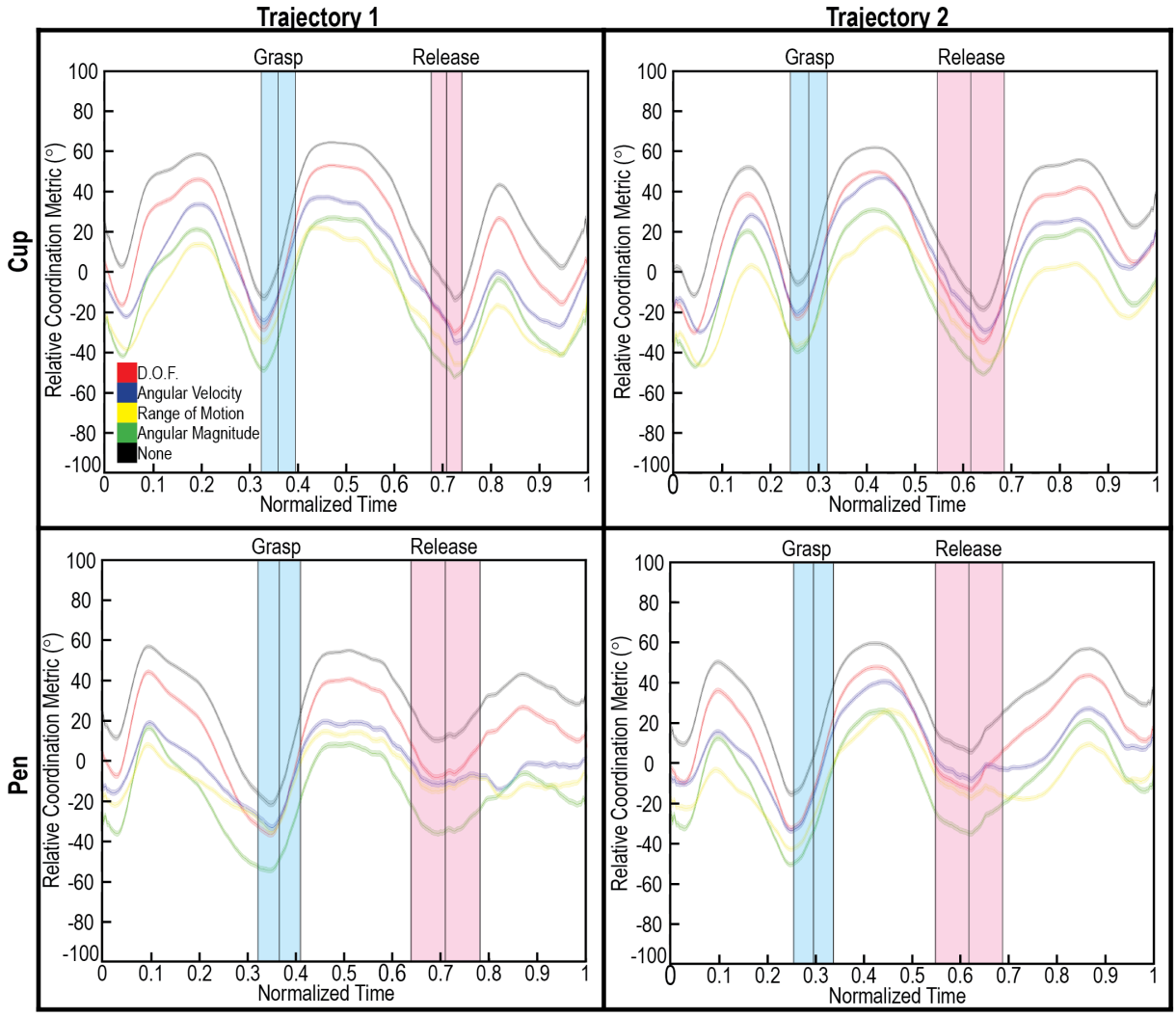

Figure 2.15: Time-series Elbow-Wrist Relative Coordination Metric (ρ_{ew}): A time-series representation of the ρ_{ew} between the elbow and wrist using all five normalization schemes presented in Table 2.1. $+\rho_{sw}$ is representative of elbow dominated motion, while $-\rho_{sw}$ is representative of wrist dominated motion. Shaded regions represent the locations of grasp (blue) and release (red) ±standard deviation. Shaded regions around each normalization scheme represent ±standard error.

reach, transport, and return phases of the task (Fig. 2.12), the more proximal body segment has greater relative motion than the more distal segment. The opposite is true during grasp and release phases of the task. The proximal segment refers to the segment closer to the midline of the body, while the distal segment is the segment further away from the body. For example, in Fig. 2.15, there are sharp, positive spikes in $\rho_e w$ during the reach, transport, and return phases of the task. This is indicative of elbow dominated motion, the more proximal body segment. Meanwhile, ρ_{ew} becomes negative around the grasp and release parts of the task, meaning the wrist is dominating the motion, the more distal segment. These trends are fairly consistent for all time-series data (ρ_{se}, Fig. 2.13 and ρ_{sw} Fig. 2.14).

2.5.1 Effect of normalization and trajectory stage on the Relative Coordination Metric (ρ)

Norm-stage had a significant effect on ρ in all twelve test cases. Fig. 2.16-2.19 highlight shifts in ρ_{se}, ρ_{sw}, and ρ_{ew} based on the selected stage and normalization during trajectories 1 and 2 while grasping a cup and pen.

Post-hoc tests revealed several significant differences between norm-stage groupings. For a given normalization scheme there were significant differences in ρ between stages for ρ_{se}, ρ_{sw}, and ρ_{ew}. As mentioned earlier, values of ρ_{sw} and ρ_{ew} at 50% reach, 50% transport, and 50% return were significantly greater than values at grasp and release. This trend was consistent for all motion trajectories and objects. For a given stage there were significant differences in ρ based on the normalization scheme implemented. When considering ρ_{sw} and ρ_{se}, normalizing by joint RoM and max angular magnitude, resulted in the lowest values of ρ, while no normalization and DoF normalization had the higher values of ρ for a given task stage. These trends were

fairly consistent for each motion trajectory. ρ_{se} had very inconsistent trends when comparing normalization schemes at particular stages.

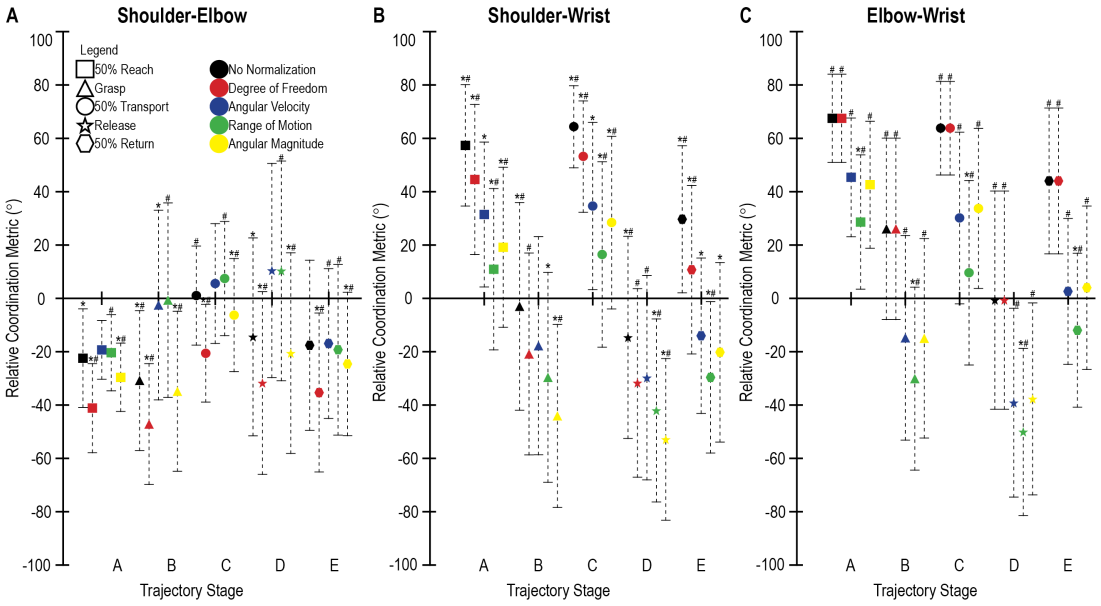

Figure 2.16: ρ by Normalization Scheme and Trajectory Stage during Trajectory 1 when grasping a cup. The five stages tested were A) 50% of reach, B) grasp, C) 50% of transport, D) release, E) 50% of return. *Indicates that the selected ρ norm-stage was significantly different from all other normalization schemes at that stage. #Indicates that the selected ρ norm-stage was significantly different across stages for that normalization scheme. More significant differences were present, but not shown here for simplicity.

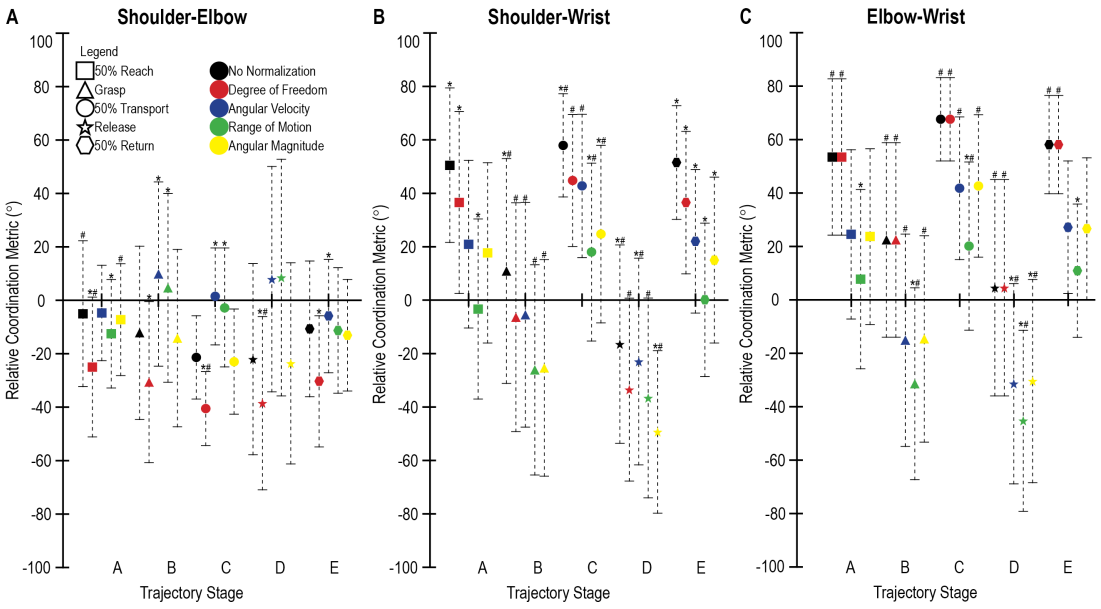

Figure 2.17: ρ by Normalization Scheme and Trajectory Stage during Trajectory 2 when grasping a cup. The five stages tested were A) 50% of reach, B) grasp, C) 50% of transport, D) release, E) 50% of return. *Indicates that the selected ρ norm-stage was significantly different from all other normalization schemes at that stage. #Indicates that the selected ρ norm-stage was significantly different across stages for that normalization scheme. More significant differences were present, but not shown here for simplicity.

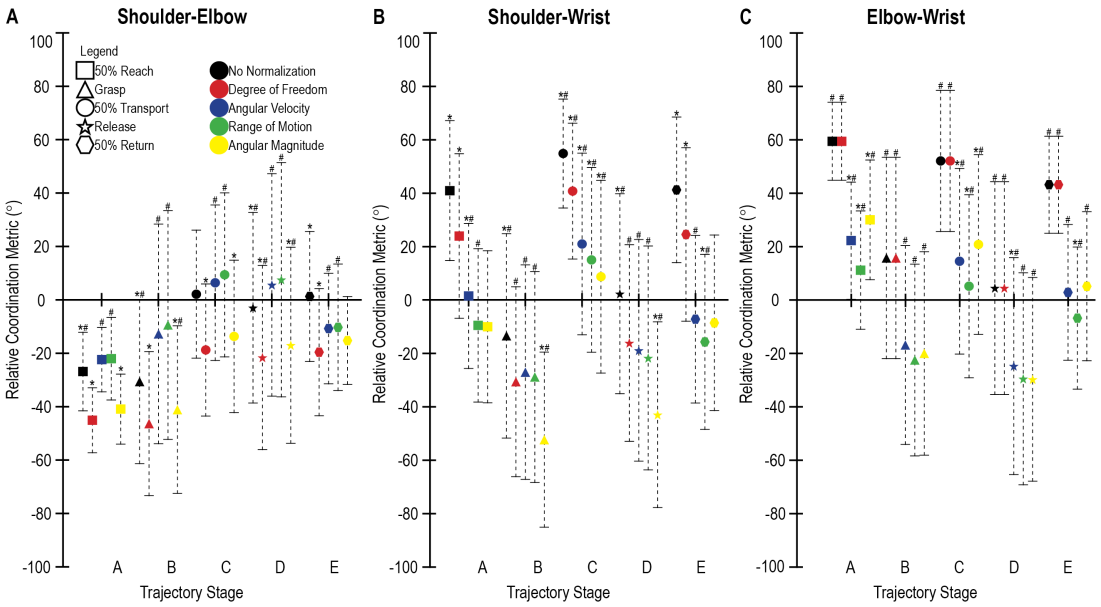

Figure 2.18: ρ by Normalization Scheme and Trajectory Stage during Trajectory 1 when grasping a pen. The five stages tested were A) 50% of reach, B) grasp, C) 50% of transport, D) release, E) 50% of return. *Indicates that the selected ρ norm-stage was significantly different from all other normalization schemes at that stage. #Indicates that the selected ρ norm-stage was significantly different across stages for that normalization scheme. More significant differences were present, but not shown here for simplicity.

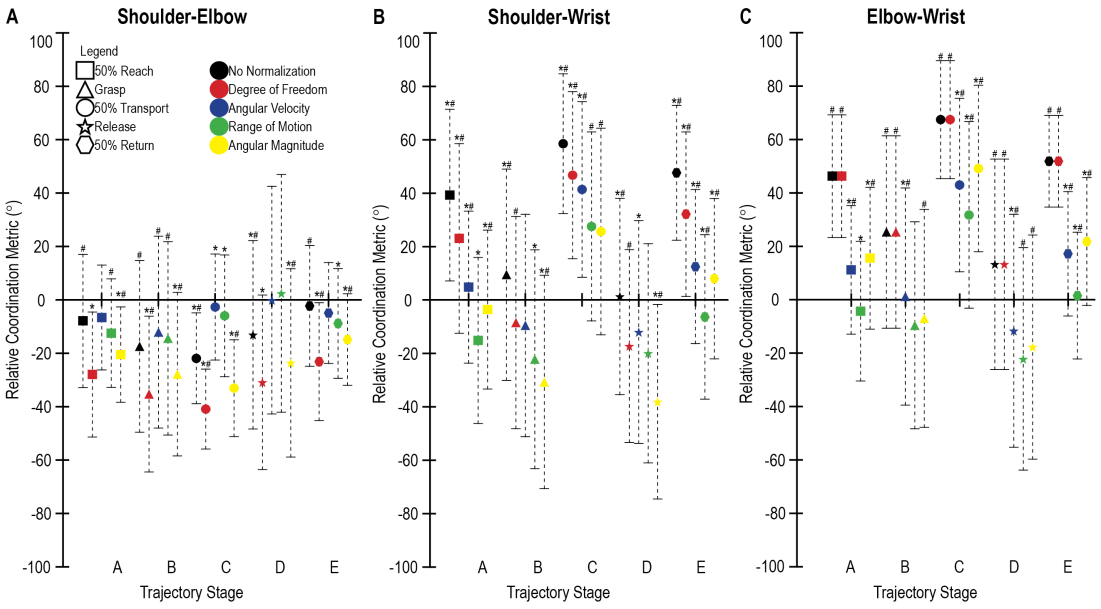

Figure 2.19: ρ by Normalization Scheme and Trajectory Stage during Trajectory 2 when grasping a pen. The five stages tested were A) 50% of reach, B) grasp, C) 50% of transport, D) release, E) 50% of return. *Indicates that the selected ρ norm-stage was significantly different from all other normalization schemes at that stage. #Indicates that the selected ρ norm-stage was significantly different across stages for that normalization scheme. More significant differences were present, but not shown here for simplicity.

2.5.2 Effect of normalization and object on $\hat{t}_{\pm Z_n}$

Object-zone had a significant effect on $\hat{t}_{\pm Z_n}$ in all nine test cases, Fig. 2.20 and Fig. 2.21. When normalizing by angular velocity, Fig. 2.20G-I and Fig. 2.21G-I, post-hoc tests revealed less time spent in each successive zone ($\hat{t}_{Z_1} > \hat{t}_{\pm Z_2} > \hat{t}_{\pm Z_3} > \hat{t}_{\pm Z_4}$) for both objects and all three joints evaluated. $\hat{t}_{Z_1}$ was greater for the pen than the cup for both shoulder-wrist and elbow-wrist RCMs, opposite for the shoulder-elbow. $\hat{t}_{-Z_2} > \hat{t}_{+Z_2}$ when comparing the shoulder-elbow while grasping both objects and shoulder-wrist while grasping the pen. Meanwhile, $\hat{t}_{+Z_2} > \hat{t}_{-Z_2}$ for both elbow-wrist comparisons and shoulder-wrist when grasping the cup. The other two normalizations revealed inconsistent trends between joint comparisons.

2.5.3 Effect of normalization and trajectory on $\hat{t}_{\pm Z_n}$

Trajectory-zone had a significant effect on $\hat{t}_{\pm Z_n}$ in all nine test cases, Fig. 2.22 and Fig. 2.23. When normalizing by angular velocity, Fig. 2.22G-I and Fig. 2.23G-I, post-hoc tests also revealed less time spent in each successive zone ($\hat{t}_{Z_1} > \hat{t}_{\pm Z_2} > \hat{t}_{\pm Z_3} > \hat{t}_{\pm Z_4}$) during both trajectories; these results were consistent for all three joint comparisons. There was no difference in $\hat{t}_{Z_1}$ between trajectories 1 and 2 when comparing the shoulder-wrist and elbow-wrist. Shoulder-elbow $\hat{t}_{Z_1}$ was significantly greater during trajectory 2 than 1. The other two normalizations examined revealed inconsistent trends between joint comparisons.

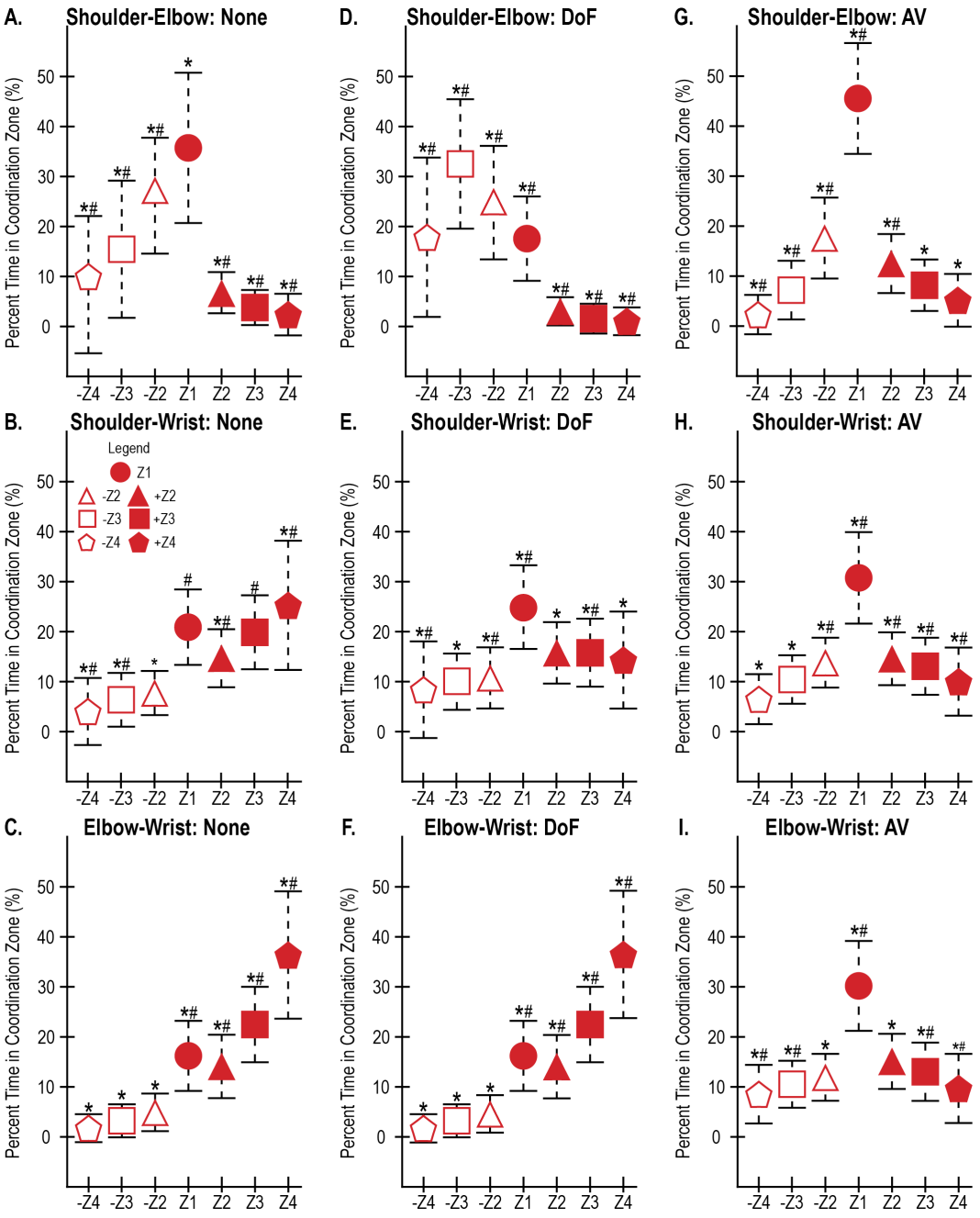

Figure 2.20: Percent Time in Coordination Zone When Grasping Cup by Normalization Scheme. *Indicates that the selected value was significantly different from all other $\hat{t}_{\pm Z_n}$ computed for the cup. #Indicates that the selected value was significantly different from the corresponding $\hat{t}_{\pm Z_n}$ of the pen. More significant differences were present, but not shown here for simplicity.

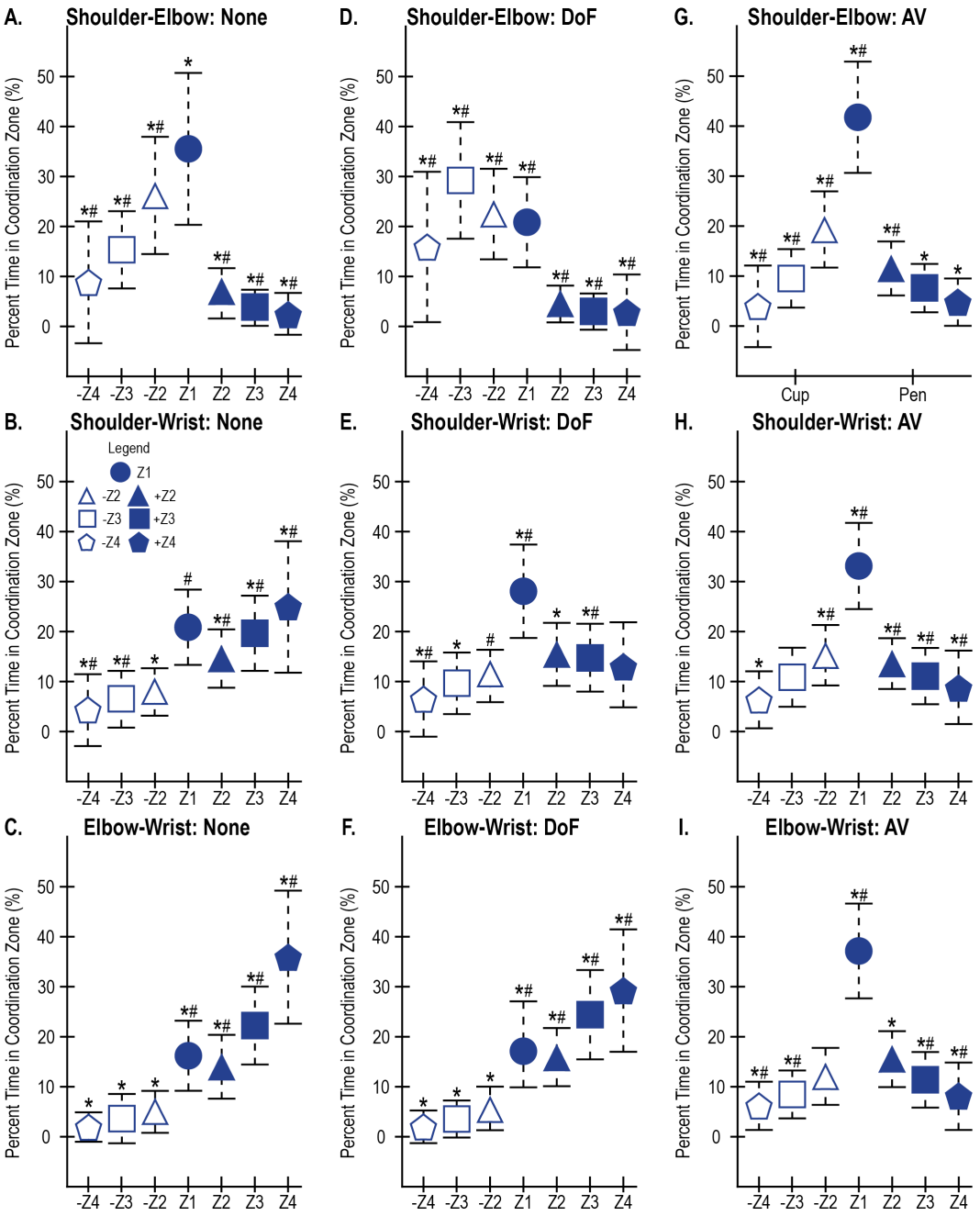

Figure 2.21: Percent Time in Coordination Zone When Grasping Cup by Normalization Scheme. *Indicates that the selected value was significantly different from all other $\hat{t}_{\pm Z_n}$ computed for the pen. #Indicates that the selected value was significantly different from the corresponding $\hat{t}_{\pm Z_n}$ of the cup. More significant differences were present, but not shown here for simplicity.

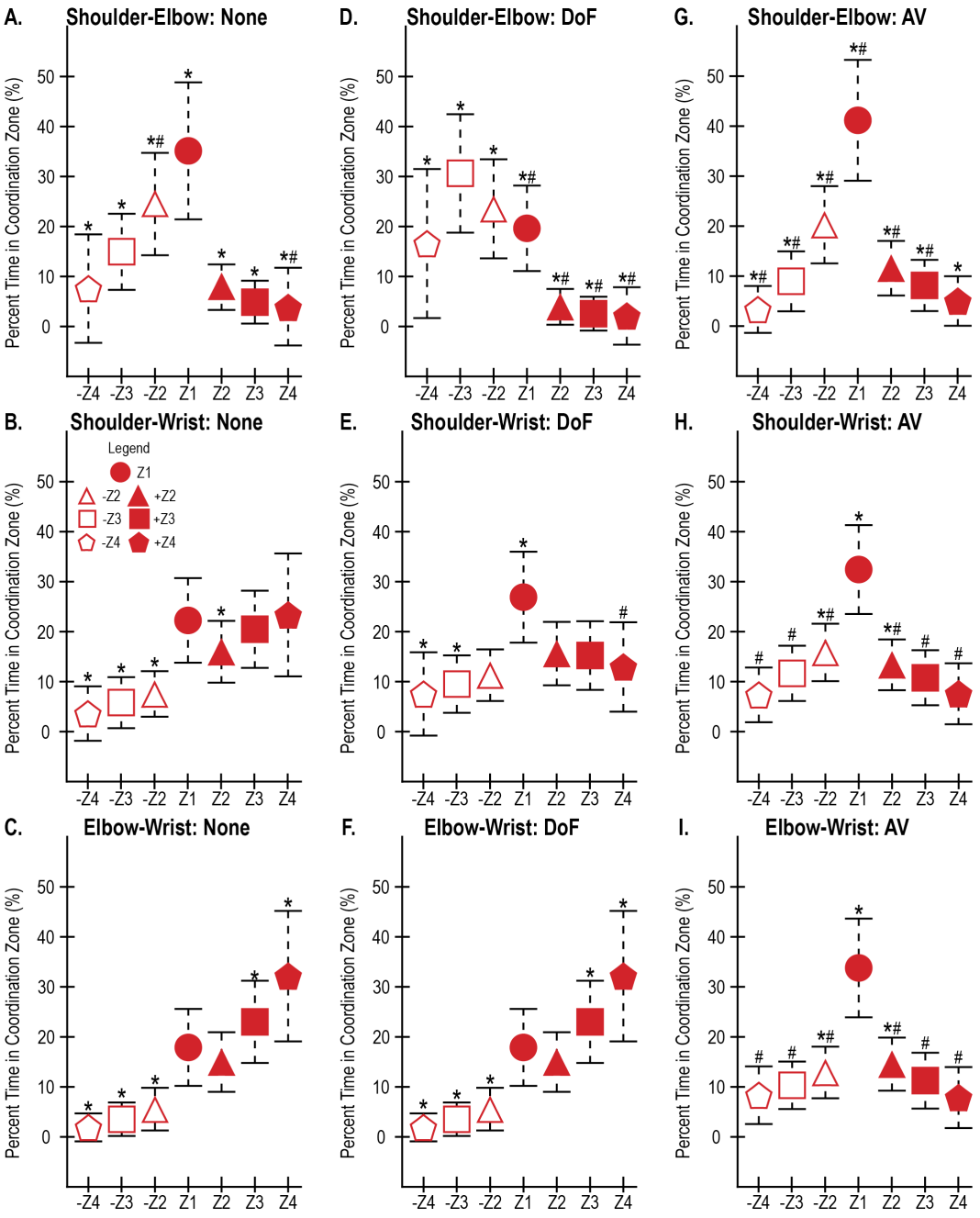

Figure 2.22: Percent Time in Coordination Zone During Trajectory 1 by Normalization Scheme. *Indicates that the selected value was significantly different from all other $\hat{t}_{\pm Z_n}$ computed for Trajectory 1. #Indicates that the selected value was significantly different for the $\hat{t}_{\pm Z_n}$ of the opposing Trajectory 2. More significant differences were present, but not shown here for simplicity.

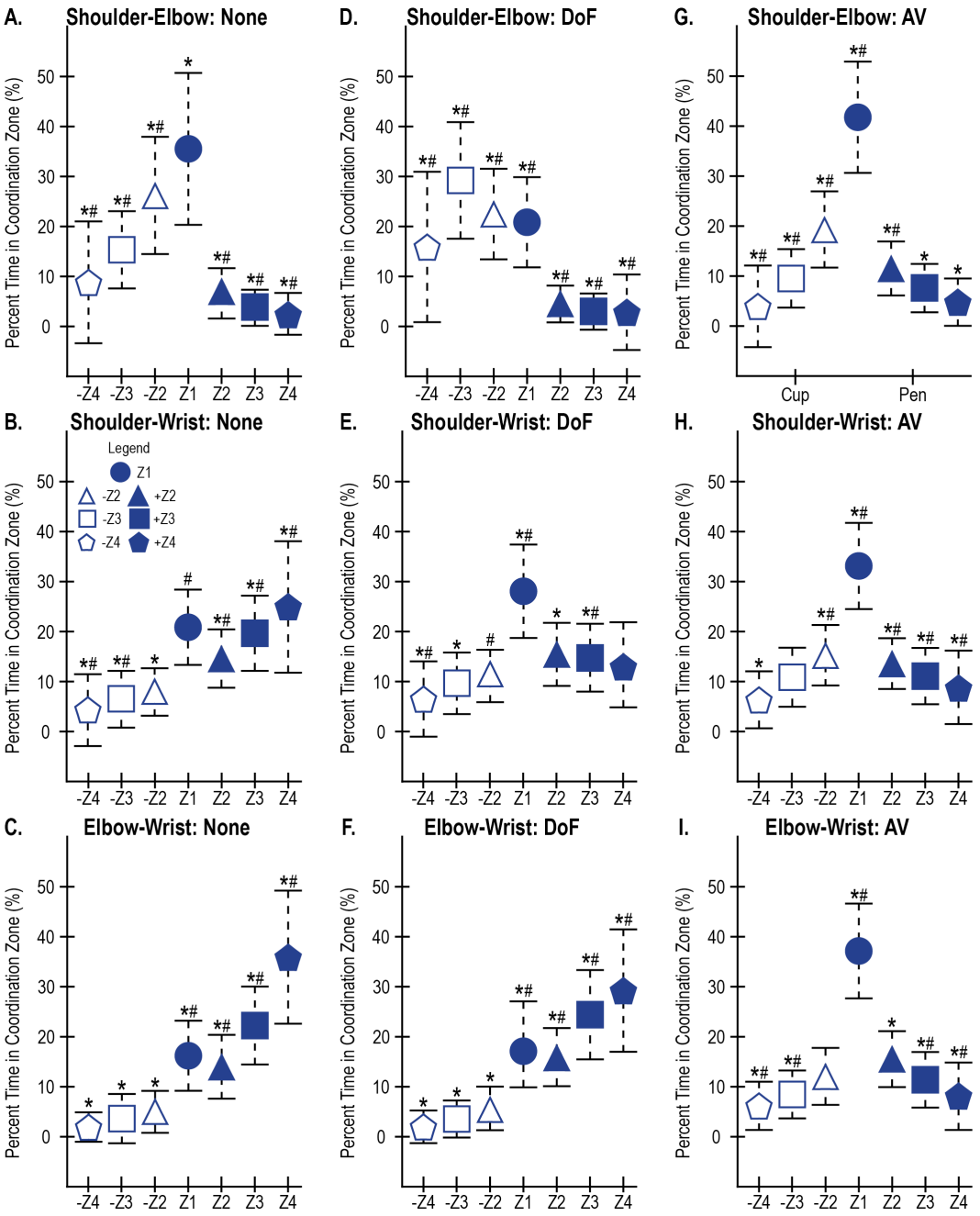

Figure 2.23: Percent Time in Coordination Zone During Trajectory 2 by Normalization Scheme. *Indicates that the selected value was significantly different from all other $\hat{t}_{\pm Z_n}$ computed for Trajectory 2. #Indicates that the selected value was significantly different for the $\hat{t}_{\pm Z_n}$ of the opposing Trajectory 1. More significant differences were present, but not shown here for simplicity.

2.6 Discussion

This study introduces and assesses a new metric, the relative coordination metric (ρ), for quantifying non-cyclic, non-constrained coordination based on body segment angular velocity. Qualitative, visual observation of gross motions might categorize certain motions as coordinated, but differences in joint characteristics (DoF, RoM, etc.) might imply that motions are quantitatively uncoordinated when not normalized appropriately. For example, let joint 1 have more DoF than joint 2. With more DoF, joint 1 can move across greater RoM than joint 2; therefore, it can potentially accelerate to higher maximum angular velocities than joint 2. However, joint 1s higher angular velocities compared to joint 2 do not imply that the overall motion is uncoordinated. Therefore, biomechanical differences require normalization when evaluating this metric to prevent favoring certain joints. In addition, joint RoMs and angular velocity profiles are also task-specific [75, 76]. For example, a planar reaching task requires less shoulder flexion than an overhead reaching task. Thus, comparisons of intra-participant coordination patterns should be normalized in a joint- and task-specific manner. Similar to other motion metrics (i.e. joint angles), ρ should be interpreted with a particular task in mind and normative datasets will be required for clinical usage. While this work finds statistical differences when varying a planar grasp/release task, it is necessary to determine what differences are clinically or operationally relevant.

θ_{VC} and θ_{CRP}, other metrics for coordination assessment, can be difficult to interpret, especially when trying to make conclusions concerning motor patterns in the time-series domain. ρ is a velocity-based methodology that provides a tool that indicates which body segment is dominant and contributes more to the overall motion at any point in time. While the intuitive understanding of this metric needs to be assessed in user studies, we

hypothesize that this velocity-based measure will be more straightforward to interpret. Studies on human manual control show that humans typically have an easier time interpreting and controlling velocity and rate-based methods as the human is required to make fewer mental calculations to predict how actions would affect the position time-series [32]. While ρ also transforms the original signal, there are fewer mental calculations required to relate to the original time-series. Therefore, this methodology has potential to more intuitively represent the underlying gross motor patterns. However, additional work is necessary to understand ρ interpretability in clinical settings and during different tasks. While no formal survey or data was obtained, preliminary discussions with rehabilitation physicians found that ρ is fairly easy to understand and interpret. They also found the time-series graph more useful than the composite measures ($\hat{t}_{\pm Z_n}$). Currently ρ does not provide direct knowledge of whether the underlying joint is in flexion or extension, knowledge of the selected task can aid in this disambiguation. Future work will also explore expanding the signal processing to directly provide information on whether the joint is flexing or extending. Relying solely on angular velocity also enables ρ evaluation using wearable sensors, such as IMUs, as the method does not require integration, which can lead to errors over time [102].

These data support Hypothesis 1, which assessed whether the normalization scheme affected ρ, Fig. 2.16-2.19. These data also support Hypothesis 2, finding for a given normalization, the ρ changed across task stage, Fig. 2.16-2.19. The implications of these differences on clinical interpretation can be considered by examining Fig. 2.13-2.15. When normalizing by DoF, it would appear this motion is elbow dominated ($\rho_{se} < 0^\circ$) throughout the task. When normalizing by angular velocity or RoM, the shoulder and elbow ap-

pear to be moving synchronously ($\rho_{se} \approx 0^{\circ}$), slightly oscillating between $+\rho_{se}$ and $-\rho_{se}$ depending on the time within the task. These results are similar to those discussed in Section 2.3.4 and those found by Kurz and Stergiou [85] when assessing the effect of normalization on θ_{CRP}. It is important to understand how different normalizations might affect the interpretation of task performance for conflicting interpretations could generate different clinical assessments and could affect follow up decision-making on plan-of-care.

Conflicting interpretation of task coordination based on the normalization used also arose when considering composite measures of ρ, $\hat{t}_{\pm Z_n}$, Fig. 2.20-2.23. Consistent with the time-series interpretation of the data, $\hat{t}_{\pm Z_n}$ differed based on the choice of normalization scheme. When interpreting Fig. 2.20C and Fig. 2.21C (no normalization), $\hat{t}_{Z_1} < \hat{t}_{\pm Z_2} < \hat{t}_{\pm Z_3} < \hat{t}_{\pm Z_4}$, indicating that motion was dominated more by the elbow than the wrist. When normalizing by angular velocity, $\hat{t}_{Z_1} > \hat{t}_{\pm Z_2} > \hat{t}_{\pm Z_3} > \hat{t}_{\pm Z_4}$, indicating even dominance of both joints. In a healthy population, we would expect that this motion is not dominated by any single joint for this could be evidence of a compensatory mechanism [103, 104]. Therefore, we would expect $\hat{t}_{\pm Z_n}$ is greatest in either Z_1 or Z_2; an ideal metric should align with this interpretation. Here we find the most appropriate normalization for this task and population is the angular velocity normalization (Table 2.1C).

Hypotheses 3 and 4 were assessed to determine how sensitive ρ was to kinematic changes arising from the task and environment. Significant differences in $\hat{t}_{\pm Z_n}$ were found when interacting with different objects and movement trajectories when using normalizations A-C (Table 2.1). Interpretation of this task using the angular velocity normalization shows coordinated motions between the shoulder and elbow as $\rho_{se} \approx 0^{\circ}$ within the time-series profiles, Fig.2.13, and $\hat{t}_{Z_1} > \hat{t}_{\pm Z_2} > \hat{t}_{\pm Z_3} > \hat{t}_{\pm Z_4}$, Fig. 2.20G and Fig. 2.21G. These

results are consistent with previous work that showed linear, coordinated relationships between joint angular velocities during reach/grasp tasks [95, 96]. While there were statistical differences between both objects and movements, the effect size was small. General trends remain consistent, and these small differences might not be clinically relevant. Therefore, while results from hypotheses 3 and 4 show sensitivity to distinguish between tasks, more work is necessary to understand the effects of different tasks and environmental constraints on ρ, and to define clinically relevant differences for decision-making.

While normalization by the angular velocity was appropriate for this task and population, it remains to be determined if in other contexts there are normalizations that are more suitable. If specific motion patterns are desired, normalizing by the desired motor behavior instead of normalizing by parameters recorded during the task might be more clinically relevant. A strategy-based normalization could allow clinicians to visualize how patients move relative to these preferred motions. While the current work presents a method that could be used directly for a planar reaching task, more work is necessary to understand which normalization schemes are applicable to a wider range of scenarios, which would enable increased applicability across clinical protocols. As stated previously, ρ value does not infer good or bad coordination; this conclusion arises from synthesizing the ρ, patients abilities, task performed, and clinician needs. Further, this metric is limited in that it does not inform on the neural control mechanisms that drive the musculoskeletal response, but quantifies the kinematic patterns.

Future work will apply ρ to evaluate upper extremity coordination in a broader set of tasks and patient populations. The usability of this metric will need to be validated with clinicians to understand practical implications when integrated into both tele-rehabilitation systems and clinical settings for

assessing patient performance and disease progression. ρ will also need to be validated against ρ_{CRP} and vector coding to understand its applicability to cyclic motions. ρ also shows potential applications in other fields, such as coordination analysis in athletics and performance evaluation of prosthetic devices.

2.7 Conclusion

We define a new metric to help quantify coordination for clinical application in rehabilitation. ρ addresses some limitations of current coordination measures as it is applicable to discrete motions and uses velocity-based measures. Using ρ to evaluate the coordination patterns of a grasping task in a healthy population, we demonstrate that ρ can discern between different planar reaching tasks. We also show that the interpretation of ρ results can be affected by the implemented normalization. Future work will expand analysis of ρ to different tasks and patient populations to further validate ρ in clinical applications. While there was a clear clinical need for new measures, such as ρ, in clinical settings, we also found use for ρ in other settings requiring biomechanical decision-making aids. Chapter 3 of this thesis will explore applying ρ in the field of aerospace medicine as a test bed for further application in quantifying the human-machine interaction.

Chapter 3

Objective Means of Quantifying Spacesuit Fit: Applications in Aerospace Medicine

The overall goal of this thesis is to develop performance-based metrics derived from biomechanics to aid in decision-making. This chapter will specifically expand the work in in Chapters 1 and 2 to aerospace medicine and specifically the areas of spacesuit fit and sizing. This chapter first more thoroughly defines aspects of spacesuit fit from a modified CTA, similar to that described in Section 1.1.2. Chapter 2 of this thesis discussed the development (Section 2.3.1 and 2.3.2), interpretation (Section 2.3.3) and application (Section 2.4-2.5) of a new performance metric intended to quantify coordination (ρ). Results of the CTA performed in this chapter found that a modified version of ρ could be applied to quantifying aspects of suit fit as well. This chapter will evaluate how changing the sizing components of the Mark III (MKIII) spacesuit affects a modified ρ and other outcome measures of a walking task. We will explicitly evaluate the hypotheses that changes in foam padding between the human and hip brief assembly of the MKIII affect measures of (a) gait performance and (b) dynamic fit. These measure of gait

performance and suit fit are more thoroughly defined in Section 3.1.3.

3.1 Defining Suit Fit

3.1.1 Previous Efforts at Quantifying Suit Mobility and Comfort

As discussed in Section 1.2, open research areas regarding spacesuit design are potential injury risk while an astronaut operates the suit and how suits impacts physical and cognitive performance [55]. Injury risk and operator performance, however, are not just dependent on SSA design, but also how the human operator interacts and fits within the system as a whole. Ross et al. [51] describe how designing SSAs with joint-specific mobility and range of motion does not necessarily guarantee the ability to perform specific mission-related tasks. Inappropriate fit can lead to misalignment between the human and suited joint, thereby decreasing overall mobility. Discomfort can also arise due to human-suit interaction pressures and can result in reduced mobility [51]. Therefore, mobility, fit, and comfort of the suited operator are all related to overall task performance and mission success. Suit mobility has been quantified by evaluating suit joint ranges in motion and gait parameters. Cullinane et al. [53] compared unsuited to suited gait kinematics using the Mark III (MKIII) planetary SSA and showed that the MKIII system-imposed gait characteristics that significantly deviated from unsuited gait properties. Meyen et al.[105] used a representative robotic system to test SSA mobility and demonstrated that pressurized SSAs add resistive joint torques that would increase the effort necessary to actuate SSA joints. Di Capua and Akin [106] first proposed using inertial measurement units (IMUs) to evaluate human positioning inside of SSAs. Bertrand et al.[107] expanded on this work and used IMUs to measure upper extremity human and suit kinematics as

a means of understanding suit mobility and how humans move inside SSAs. IMUs were also implemented to measure other aspects of human biomechanical performance, such as agility [72, 71], balance [70], and stair climbing [73]. Comfort is typically evaluated subjectively from user feedback. However, Anderson et al. [108] built pressure sensors to measure the interaction forces between the shoulder, arm, and forearm of suited subjects and the shoulder bearings in the MKIII. The human-suit interaction has also been modeled using computer-aided design (CAD). The Anthropometry and Biomechanics Facility at NASA Johnson Space Center created a digital model of the suit and human manikins to observe how different human anthropometries affect the alignment with suit joints and components [55, 109].

While these efforts examined suit mobility and comfort, suit fit is an area of the human-suit interaction that is not well understood and has not been objectively measured in experimental settings. Apollo era SSAs were custom built based on individual crewmember anthropometry. Despite these custom fit suits, fit issues still existed in flight [56]. Some of the Apollo program fit issues arose from using the suits for the first time in the altered gravity environment on the moon ($1/6^{th}$ that of Earth) and other problems arose from an incomplete understand of proper fit. For example, it was believed that in order to achieve maximum mobility, the suit needed to be a tight as possible. However, one astronaut in particular had issues with the shoulder of the suit because of his large biceps [56].

Newer SSA designs, such as the EMU and MKIII, have components of different sizes that can be interchanged to fit individual subjects. Next-generation suit designs have also explored greater degrees of customization, such as the PXS prototype with the ability to adjust shoulder bearing angles [55]. However, it is unclear how changing the suit component sizes affects

operational performance. NASA internal documentation suggests that suit operators can notice changes in arm length greater than 6mm (0.25in) [55]. In addition, suit operators with large gaps between the human and suit report difficulty in performing certain mission-related tasks [55, 51]. SSAs also add mass and resistive torques to the human operator, which can fundamentally change natural operator kinematics [53, 105]. However, it is unclear how the operator will handle these changes in mass and resistive torques based on the task they are performing and the environment in which they are being performed (i.e. microgravity vs. planetary environments). A better understanding of the relationship between suit component size, overall suit fit, and mission-related performance will aid design requirements for the degree of customization necessary for SSAs. Therefore, while there is evidence that spacing within the suit (indexing) and sizing of soft goods (arm and leg length) play a role in perceived suit fit, quantified methods for evaluating fit are warranted to aid in the evaluation of different design solutions on operational performance. This question helps drive some of the main hypotheses of this chapter trying to relate aspects of suit fit to task performance. Prior to testing this hypothesis, however, we need a more thorough and updated definition of suit fit so we know what metrics might be useful to answering this research question. Section 3.1.2 will use a modified CTA to define suit fit.

3.1.2 Cognitive Task Analysis of NASA JSC MKIII Fit Checks

A key challenge in creating measures of suit fit is that it is not obvious what characteristics define acceptable fit in a task and environment-specific manner. In other words, we need to understand how decisions regarding fit are make currently so we can design metrics that will aid in suit fit decision-

(a) Part I: Glove Fit and Crotch Height

(b) Part II: Upper Extremity Fit

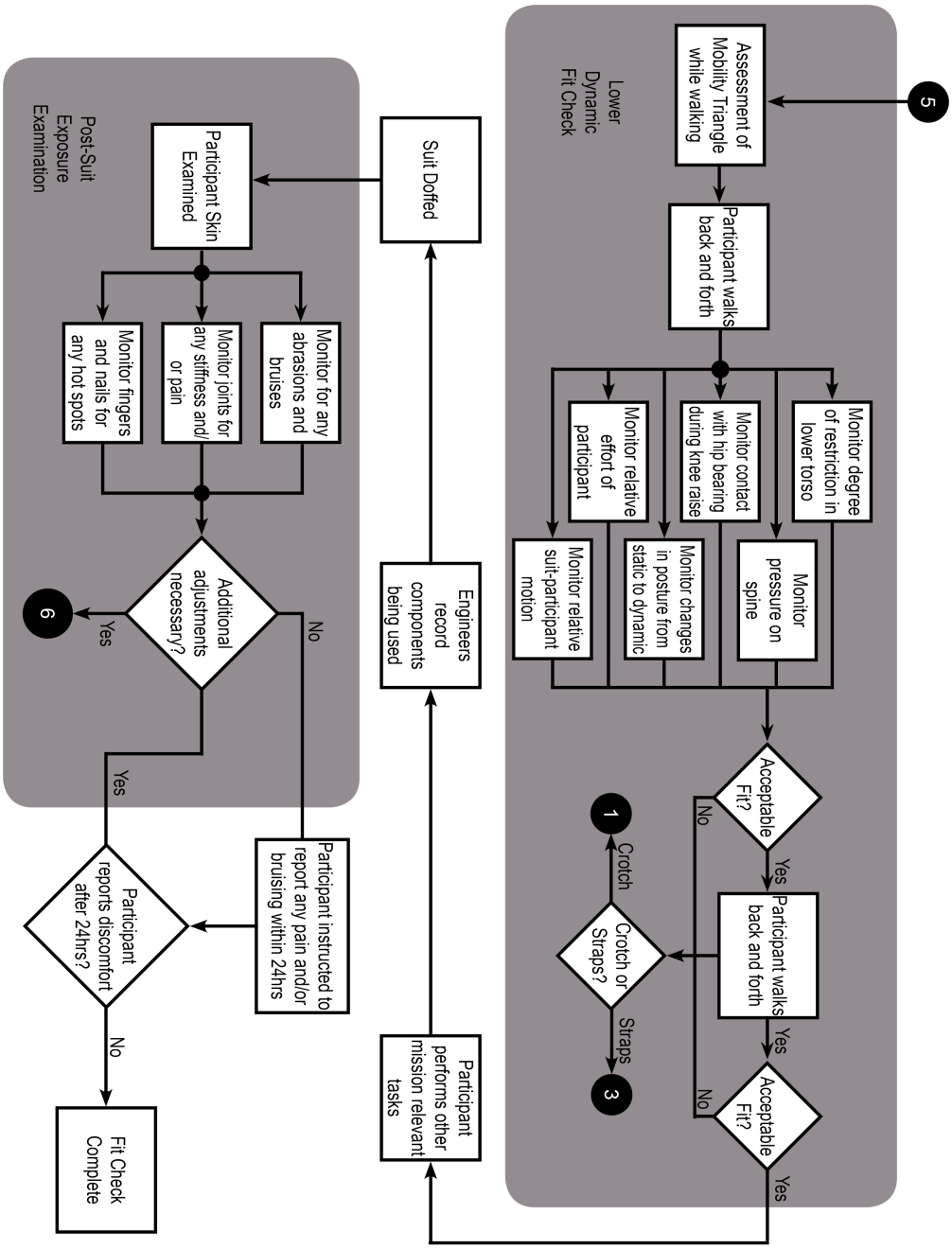

(c) Part III: Lower Extremity Fit and Post-Fit Assessment

Figure 3.1: Cognitive Task Analysis Decision Workflow Diagram MKIII Fit Checks

making. Just like with OTs in Section 1.1.2, we use a modified Cognitive Task Analysis (CTA) (adapted from Stirling and McLean [2]) to define characteristics relevant to suit fit. CTA aims to understand information required, thinking processes, and goals used to make decisions within observable environments. Current decisions regarding fit are made qualitatively by astronauts and engineer experts during fit-checks and familiarization runs. We used this human-centered approach through observations of MKIII fit checks and discussion with engineers at NASA Johnson Space Center to generate suit fit decision workflow diagrams.

Fig. 3.1 highlights the general structure of a MKIII fit check. This workflow diagram for a MKIII fit check follows the same structure as the OT workflow diagram in Fig. 1.3 with processes, decisions, and loops. Processes (represented as rectangles) require direct or indirect interaction with the participant getting fit into the suit and allows the engineer making fit decisions gather information regarding the participant's fit. All the information gathered during a process is used to make a decision (represented with diamonds). Typically, processes are repeated in loops until a favorable outcome of a decision is achieved. Loops are represented using dark shaded rectangles with curved edges. In this case, a favorable decision outcome means that an acceptable fit is achieved. To start, it is important to know that the MKIII spacesuit contains the following components: hard upper torso, hard lower torso, soft arm components, soft leg components, boots, gloves, and a helmet. Hard components are made of composite materials with smooth bearing joints at specific angles to allow shoulder and hip motion for the upper torso and lower torso respectively. The soft goods are made of spring-like flexible material that serves as elbow and knee joints. Participants inside the suit have shoulder straps that are attached to the hard lower torso of the MKIII

that helps to keep the hard lower torso and human crotch at distances apart. Fig. 1.4a has a picture of the MKIII suit with these different design aspects.

As seen in Fig. 3.1a, fit checks for the MKIII generally start with measuring the participant's anthropometry so suit engineers can make a first approximation of what size suit components the participant will need. Next come a series of loops: (1) glove fit check, (2) crotch height check, (3) strap adjustment, (4) upper body dynamic fit check, (5) lower body dynamic fit check, and (6) a post-fit check examination. The first three loops performed (glove fit, crotch height, and strap adjustment) are typically done while the participant is standing still and when the suit is not pressurized. Meanwhile, the upper and lower body dynamic fit checks are performed while the participant wearing the suit performs a series of tasks. Two of the loops performed statically (shoulder strap tension and crotch height) are often repeated when there are undesirable fit outcomes during the upper and lower body fit check loops because small adjustments to the shoulder strap tension and the height of the crotch can have undesirable fit outcomes that can only be observed when the participant is moving. In other words, when the shoulder strap tension and crotch height might feel as though they are appropriate when standing quietly, but once the suited participant starts moving, they might be uncomfortable or might have inappropriate fit in the lower or upper body due to postural changes or new human-suit interactions.

To better understand how fit decisions are made, we consider the lower body dynamic fit check (Fig. 3.1c). This loop of processes and decisions typically involved with suited participant walking back and forth while the engineers observe how the participants moves and interacts with the suit. The engineers are monitoring things such as relative motion between the human and suit, posture changes, and effort levels required to move. Engineers also

will ask the participant directly if they feel any pressure on the spine, if they felt any rubbing on their legs, and ask how hard it was to move. As stated earlier, comfort is an aspect of fit; therefore, if the participant reports pressure on their spine, engineers might reduce the tension in the shoulder straps. Alternatively, if engineers see relative motion between the human and suit, such as the heel lifting out of the boot, engineers might first try to increase the shoulder tension. To get at the root cause of some of these fit issues, however, might take multiple iterations of adjustments. Similar to the OT CTA in Fig. 1.3, multiple features that are observed visually inform a decision. For example, as described earlier, the heel lifting out of the boot can have multiple causes, such as the height of the hip brief crotch, the tension in the shoulder harness, the length of the legs, and how well the boots fit. All or some of these particular aspects of fit could be changed when engineers observe thus phenomenon and the lower body fit check loop is often repeated multiple times until all fit issues are resolved.

Fit checks are currently done almost entirely qualitatively with suit fit experts and we can therefore leverage this diagram to generate candidate quantified suit fit metrics. Specifically, any process within Fig. 3.1 is a candidate for a suit fit metric. Most decisions regarding suit fit are made qualitatively; there exist no objective, quantitative metrics of suit fit that aid in sizing subjects to these SSAs. Quantitative measures could augment subjective feedback currently provided when SSAs are fitted to new subjects and aid in understanding how tasks and environments affect performance as a function of the selected fit parameters.

It is important to note that this general structure might not hold for all suits because of different design characteristics. For example, the EMU (Fig. 1.4a) is designed so astronauts enter at the hips, while the MKIII and Z-2

(Fig. 1.4b and c, respectively) are designed so astronauts can enter from the rear. These different ways of putting the suit on affect how the suit fit process is carried out. It is also important to note that because these spacesuits are designed for exploration on other planets, like the moon and mars, or in microgravity, it difficult to test them in realistic, lower gravity environments. Therefore, testing the impact of spacesuits on human kinematics on Earth might not be 100% accurate due to changes in the weight and inertial properties of the suit in space exploration environments [55, 56]. Despite this drawback, the workflow diagrams in Fig. 3.1 depict a lot the information currently used to make fit decisions and these diagrams can help inform quantitative metrics for fit.

3.1.3 Static vs. Dynamic Fit

From the workflow diagrams, two categories of suit fit are observed: static and dynamic (Fig. 3.2). Static fit (Fig. 3.2a) refers to how the suited subject sits within the suit in a neutral posture. One of the most relevant measures for static fit is indexing, which is the amount of space the subject has between certain anatomical landmarks and components of the suit architecture. Indexing is affected by human antropometry, padding added between the human and suit, and the size of the suit components. Other relevant considerations of static fit include the length of soft goods and locations where the human rubs against the suit when not moving. The indexing can be altered by adding layers of padding between the human and suit component. Dynamic fit (Fig. 3.2b) refers to how the human and suit move and interact with each other in dynamic settings. Relevant measures for dynamic fit include differences in human and suit joint angles while moving and the relative motion between the suit and human. The human-suit interaction,

when and where the human and suit come into contact, is also an important consideration when evaluating dynamic fit. Examples used in Section 3.1.2 regarding relative human-suit motion and the heel lifting out of the boot all are contributing factors to dynamic fit. No literature currently provides a quantitative relationship between static fit and dynamic fit. Furthermore, it is unclear how static and dynamic fit might affect suited performance in operationally relevant conditions and what injury risks (if any) might be associated with changes in these two categories of fit. For this reason, in Section 3.2, we design and conduct an experiment to test how changing static fit, specifically adding padding between the human and suit, affects measures of dynamic fit. Dynamic fit is measured using new metrics derived from the CTA in Fig. 3.1 and defined in Section 3.1.4.

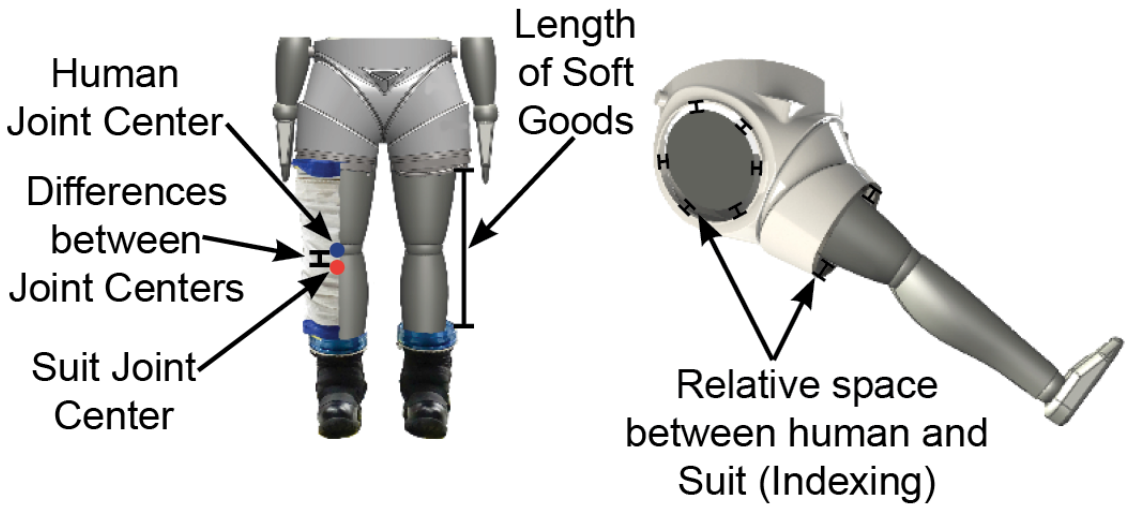

(a) Static Fit

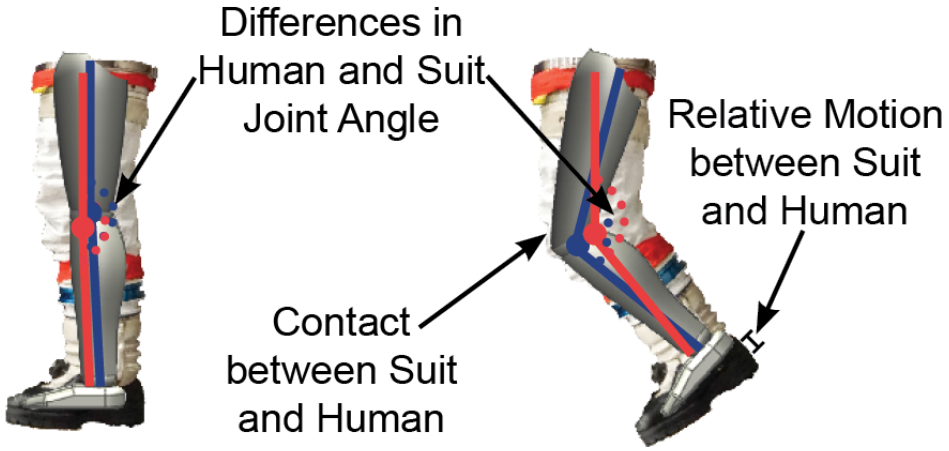

(b) Dynamic Fit

Figure 3.2: Schematics highlighting aspects of: a) Static Fit, and b) Dynamic Fit extracted from a CTA of MKIII fit checks (Fig. 3.1)

3.1.4 Defining New Measures for Dynamic Fit: $\rho^n_{HS}$and $\Delta tRoM$

This section provides the physics-based rationale behind the selection of new metrics for suit fit. Fig. 3.2b highlights three aspects of dynamic fit, with more aspects presented in Fig. 3.1, but here we focus on quantifying the two aspects of fit that are the most motion and kinematic driven:

1. the difference in suit and human knee angle ($\Delta tRoM$) and

2. relative motion between the suit and the knee ($\rho^n_{HS}(t)$)

Different tasks and joints will carry out different range of motions (RoM) and joint trajectories. The difference in the suit and human angles is therefore computed by comparing task-specific joint range of motion (tRoM). $\Delta tRoM$ is defined by:

$$\Delta tRoM = tRoM_S - tRoM_H \tag{3.1}$$

where $tRoM_S$ is the task RoM of the suit and $tRoM_H$ is the task RoM of the human. Positive values of $\Delta tRoM$ are indicative of tasks during which the suit had a greater $tRoM$, while negative values of $\Delta tRoM$ represent tasks when the human had a greater $tRoM$. $\Delta tRoM$ should be computed and interpreted in a task- and joint-specific context because certain tasks and joints have different values of $\Delta tRoM$ that are operationally relevant. In other words, some tasks have a low tolerance for $\Delta tRoM$ before injuries occur, while other tasks have a much larger tolerance in $\Delta tRoM$ before injuries are observed [110]. More work is necessary to understand what these tolerances might be for specific suit designs. Relating back to the workflow diagrams in Fig. 3.1c, $\Delta tRoM$ could help the suit engineers make decisions during the lower body dynamic fit check. Specifically, positive or negative values of $\Delta tRoM$ could be related to the crotch height, leg length, or even shoulder strap tension.

Relative motion between the suit and human can be quantified by adapting the methodology from Equations 2.7 and 2.8. In Section 2.3.2, RCM was used to compare the relative angular velocity of one body segment to another. In this Chapter, we consider a comparison between the the human and spacesuit for the same rigid body segment. We modify Eq. 2.7 and 2.8 as follows:

$$\rho^n_{HS}(t) = 2tan^{-1}\Big(\frac{\Omega_H(t)}{\Omega_S(t)}\Big) - 90^\circ \tag{3.2}$$

where $\rho^n_{HS}(t)$ represents the relative motion between the human and suit body segment n at time t. Since it is extremely difficult to measure human kinematics inside the suit, $\Omega_H(t)$ and $\Omega_S(t)$ are defined assuming the use of wearable inertial measurement units (IMUs). The angular velocity magnitude of the human and suit are defined as:

$$\Omega_{H/S}(t) = \sqrt{\omega^2_x(t) + \omega^2_y(t) + \omega^2_z(t)} \tag{3.3}$$

where $\omega_{x/y/z}$ are the angular velocity readings from IMU x, y, and z axes. By definition, $\rho^n_{HS}(t)$ ranges between 90° and -90°, where $\rho^n_{HS}(t) = 0^\circ$ represents motion in which both the human and suit are moving completely synchronously, $\rho^n_{HS}(t) = +90^\circ$ represents a movement in which the human is moving while the suit is not, $\rho^n_{HS}(t) = -90^\circ$ represents a movement in which the suit is moving while the human is not, and values in between represent motions with varying degrees of coordination between the human and suit. The time-series nature of $\rho^n_{HS}(t)$ allows for the observation of how relative motion between the human and suit evolves over time and at various phases of a task.

Relating back to Fig.3.1c, $\rho^n_{HS}(t)$ could aid suit engineers better quantify relative human-suit motion during the lower body dynamic fit check and could help them quantify phenomenon such as the heel lifting out of the boot. Now that dynamic fit metrics are defined, we can test our hypothesis that changes in static fit will alter our measures of dynamic fit, specifically $\Delta tRoM$ and ρ^n_{HS}. Section 3.2 presents the experimental methods used to test this hypothesis.

Table 3.1: Subject Data and Testing Order

Subject #	Age (yrs)	Height (in)	Crotch Height (in)	Knee Height (in)	Hip Breadth (in)	Thigh Breadth (in)	Suit Leg Length	Boot Size (Type)*	Testing Order**	C1 (in)	C2 (in)
2	26	66	29	18.5	14.5	22	Large	8-10 (S)	US-C0-C1-C2	0.375	0.75
3	25	69	31	19.5	14.5	22.5	Large	11-13 (B)	C2-C1-C0-US	0.375	0.75
4	27	68	32	20	16	23	Large	8-10 (S)	C2-C1-C0-US	0.25	0.50

*S=strap-based boot design; B=boa-based boot design.
**US=unsuited, C0=Configuration 0 (no padding), C1=Configuration 1(one layer of padding), C2=Configuration 2 (two layers of padding).

3.2 Experimental Methods

A pilot study was performed to evaluate the sensitivity of these proposed new metrics to changes in nominal fit. Specifically, we assess the sensitivity of our metrics to detect how changes from nominal static fit cause potential changes in dynamic fit in the lower extremities during a simple gait task. The sensitivity analysis was accomplished by evaluating the hypotheses that adding padding between the human and hip brief assembly of the MKIII spacesuit would affect measures of (a) gait performance and (b) dynamic fit.

3.2.1 Subjects

A pilot study was performed with three male subjects. Due to time constraints and SSA availability, an incomplete dataset was collected on a fourth male subject. Thus, here we present results from three subjects (Table I). All three subjects were novice suit operators and performed a fit check with the MKIII spacesuit on a separate day prior to this study. All subjects were cleared with a Class I medical exam to participate as a suit operator. The study protocol was approved by the NASA Johnson Space Center IRB and the MIT Committee on the Use of Humans as Experimental Subjects. Subjects provided written informed consent prior to performing the experiment.

3.2.2 Equipment

This study was performed in the Anthropometry and Biomechanics Facility (ABF) at the NASA Johnson Space Center. Subjects wore a long-sleeve compression shirt and pant below the liquid cooling garment (LCG). Five strap-on IMUs (Opal IMU, APDM, Inc. Portland, OR, USA), with embedded accelerometers, gyroscopes, and magnetometers (sampling rate of 128Hz) were placed above the LCG on the left/right tibia, left/right femur, and sacrum of each subject (Fig. 3.3). Five IMUs were also secured to the MKIII spacesuit with tape and co-flex to the left/right upper leg, left/right lower leg, and hip brief. Custom sleeves at the hips and thighs were stitched into the LCG to add padding between the suited subject and MKIII spacesuit. Foam padding (Viton) was inserted into these sleeves to alter the indexing between the subjects and MKIII at these two locations (Fig. 3.3B and C). Volumetric scans were obtained at the U.S. Army Natick Army Center and ABF to obtain subject anthropometry. A combination of these anthropometric scans and a CAD model of the MKIII hip brief was used to determine the level of padding added to the LCG between the subject hips/thighs and MKIII hip briefs (Table 3.1).

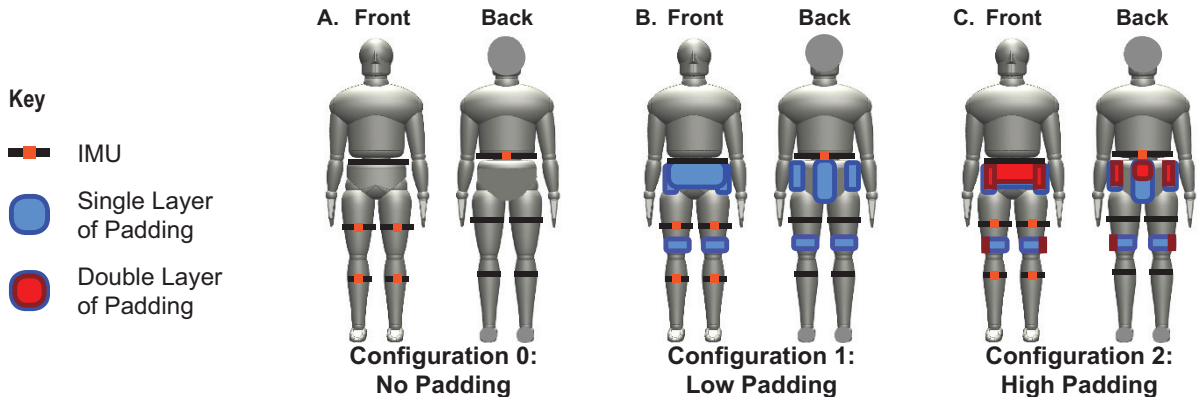

Figure 3.3: Locations of padding and inertial measurement unit sensors on humans for Configuration 0 (C0), Configuration 1 (C1), and Configuration 2 (C2).

3.2.3 Procedure

Subjects performed a series of walking tasks on an elevated walkway (10m long and 1m wide). For the unsuited condition, subjects donned the compression shirt, pant, LCG and human IMUs and performed 12 walking trials. For the suited condition, the MKIII was pressurized to nominal suit pressure (4.3psi) in a tethered configuration (i.e. no closed-loop portable life support system (PLSS) was used). Subjects donned the MKIII with all 10 IMUs three times, each with different padding configurations at the hips and thighs: no (C0), single (C1), and double (C2) layer of padding (Fig. 3.3, Table 3.1). The C0, no padding, configuration served as a control and was the nominal component sizing fit configuration for each subject acquired from fit checks performed prior to this experiment. The approximate weight of the MKIII without a human inside or PLSS attached is 59kg [49]; the actual total weight of the human and MKIII varied based on the subject and configuration. For each suited condition, subjects performed 24 walking trials, resting as needed in between all trials. All 10 IMU sensors were wirelessly synchronized using manufacturers software at the beginning and end of each walking trial. In addition to walking tasks, participants performed single and double leg balance tasks while unsuited and suited, but these data were not analyzed within the scope of this paper. Following each suited configuration, subjects were asked to subjectively evaluate their perceived fit compared to the other padding configurations. Subjective feedback was recorded by the test conductors. The order in which unsuited and suited trials were performed was counterbalanced between all subjects (Table 3.1).

3.2.4 Data Analysis

Task performance for the gait task was examined through 1) cadence and 2) human knee range of motion. These metrics can be computed and compared between suited and unsuited trials to understand how the MKIII affects nominal task performance. An ideal SSA design and fit should minimize deviation from unsuited kinematics [53, 51]. Unsuited data can also be compared to the literature so it is understood in a broader context.

Walking trials were parsed using recorded UNIX timecode stamps. For each trial, a wavelet analysis was performed using the human tibia accelerometer and gyroscope data to identify the following gait phases: stance (ST), heel-off (HO), toe-off (TO), swing (SW), and heel strike (HS) [111, 112]. Steps were parsed from heel strike to heel strike and compiled for each subject. A total of 72 steps were recorded for each subject. The final 20 steps in each of the conditions were used for the remainder of the analysis to aid in minimizing learning effects from adapting to the MKIII suit. Strides per minutes was computed by dividing the number of samples from heel-strike to heel-strike by the IMU sampling rate. Since strides per minute only accounts for one leg, participant cadence (steps per minute with both legs) was approximated by doubling the computed strides per minute. For each subject, all unsuited and suited (C0-C2) cadence values were normalized by their mean unsuited cadence. Knee angles of the human and suit were estimated using a Principal Component Analysis (PCA) method to estimate the knee hinge axis and Davenport algorithm to estimate the angle with respect to the axis [69, 113]. This method requires a static period with straight legs to define the zero-degree flexion datum. Since this static offset was not incorporated into the original study design, absolute values for the angles could not be shifted to the standard datum. However, task-specific range of motion ($tRoM$) was

possible to assess. Thus, human and suit knee $tRoM$ were computed for each unsuited/suited configuration and step. This measure does not reflect the full range of motion of the human and suit knee, it represents the range of the knee specific to the task performed. For every suited step, Eq. 3.1 was used to compute $\Delta tRoM$.

Raw angular velocities from IMU 3-axis gyroscopes were mean subtracted based on individual sensor static noise offsets obtained every day prior to testing and were then filtered using a 6th order Butterworth 30Hz low-pass filter. $\rho^n_{HS}(t)$ was then computed between the human femur-suit upper leg ($\rho^F_{HS}(t)$) and human tibia-suit lower leg ($\rho^T_{HS}(t)$) using Eq. 3.2 and 3.3. Small values of $\Omega(t)$ can amplify measurement noise, which can represent inaccurate favoring of one segment over another. Therefore, for differences between $\Omega_H(t)$ and $\Omega(t)_S$ less than $0.05 rad/s$, $\rho^n_{HS}(t)$ was set to 0. This value was determined based on the maximum static noise offset of the gyroscope magnitude for all ten IMU sensors. Values of $\rho^F_{HS}(t)$ and $\rho^T_{HS}(t)$ were extracted at all five gait phases (ST, HO, TO, SW, HS) and all twenty steps for statistical analysis. For the present analysis, right-sided sensors and body segments are presented due to an incomplete left-sided dataset.

In summary, for each step taken while the user was wearing the spacesuit, the following metrics were obtained: 1) normalized step cadence, 2) human knee $tRoM$ ($tRoM_H$), 3) $\Delta tRoM$, 4) $\rho^F_{HS}(t)$, and 5) $\rho^T_{HS}(t)$.

3.2.5 Statistical Analysis

To assess sensitivity of the fit metrics, we evaluated the hypotheses that the addition of padding between the human and hip brief assembly of the MKIII SSA would affect:

1. gait performance, specifically:

(a) normalized cadence (H1)

(b) $tROM$ (H2)

2. measures of dynamic fit, specifically

   (a) differences in human and suit knee $tRoM$ ($\Delta tRoM$, H3)

   (b) relative motion between the human and suit at various phases of the gait cycle as measured using $\rho^{n}_{HS}(t)$ (H4)

Three mixed-effect analysis of variance (ANOVA) models were fit to assess hypotheses 1-3. For the model with dependent variable of normalized cadence (H1) and the model with the dependent variable of tRoMH (H2), the indpendent variables were subject (3 levels, modeled as a random effect) and unsuited/suited configuration (4 levels, modeled as a fixed effect). To evaluate differences in $\Delta tROM$ between subject and degree of padding (H3), a two-factor ANOVA was implemented with subject (3 levels) as a random-effect and suited configuration (3 levels) modeled as a fixed effect. Post-hoc comparisons were performed using Tukey's honesty criterion when significant main and/or interaction effects were found. Significance was set at $p < 0.05$ for all tests. Cohen's d effect sizes were computed for all significant post-hoc comparisons [114]. All ANOVA statistical tests were performed using MATLAB 2017b (The Mathworks, Inc., Natick, MA).

The effect of gait phase and padding on femur ρ $[\rho^{F}_{HS}(t)]$ and tibia ρ $[\rho^{T}_{HS}(t)]$ (H4) was evaluated using mixed-effect regression models due to their temporal nature. The data were modeled by fitting a random-effect intercept for each subject-by-configuration and, for the random-effect slope, fitting the RCM trajectory across gait phase. The inclusion of this random-effect slope improved model fit, $p < .0001$. The fixed effects included the higher-order interactions Gait Phase x Step Number and Configuration x Segment x Gait Phase, modeling Segment (femur and tibia), and modeling Gait Phase and

Step Number in terms of 4th-order orthogonal polynomials. All lower-order interactions and main effects were included. The 4th-order orthogonal polynomials for Gait Phase was selected as Gait Phase was an ordinal variable whose five values required all four polynomial terms to properly account for nonlinearity. The 4th-order polynomials interaction with Gait Phase significantly improved model fit, $p < .05$. There were a total of 33 observations per number of predictors, which is above the 10 observations per predictor heuristic observed in the literature [115, 116, 117]. A post-hoc bootstrap power analysis revealed that this model had adequate power (i.e. $> 80\%$) for all significant effects [118]. These models were created using the statistical software package R (Release 3.4.3, The R Foundation).

3.3 Experimental Results

3.3.1 Effect of Suit Configuration on Normalized Cadence

An ANOVA for the dependent variable normalized cadence supports significant main effects of Configuration ($F(3,228) = 266.839$, $p < 0.0001$) (Table IV). Post-hoc comparisons of the Configuration revealed that all subjects had significantly greater normalized cadences when unsuited than when suited (20.4% reduction when suited compared to all padding configurations pooled with all subjects pooled, Cohen's $d = 3.87$). C2 had significantly greater normalized cadence than both C0 and C1 (Cohen's $d = 0.97$ and 0.45, respectively). There was no significant difference in normalized cadence between C0 and C1.

Table 3.2: Knee RoM and Cadence by Subject and Configuration

Subject and Configuration	**Human Knee** (RoM°)	$\Delta RoM(^{\circ})$	**Cadence (spm)**	**Normalized Cadence**
2				
US	65.8 (2.4)	N/A	106.0 (6.3)	1.00 (0.06)
C0	46.8 (5.5)*	1.9 (1.8)†	79.6 (3.7)	0.75 (0.04)‡
C1	50.1 (5.8)*	9.9 (2.0)†	83.8 (4.2)	0.79 (0.04)‡
C2	49.7 (6.4)*	24.7 (5.5)†	88.0 (4.6)	0.83 (0.04)‡
3				
US	61.4 (2.4)	N/A	84.7 (3.8)	1.00 (0.04)
C0	54.9 (10.5)*	49.0 (6.2)†	68.7 (3.9)	0.79 (0.04)‡
C1	45.6 (6.3)*	2.0 (2.7)†	67.8 (4.6)	0.80 (0.05)‡
C2	50.5 (8.9)*	12.4 (5.7)†	71.4 (3.8)	0.84 (0.05)‡
4				
US	53.2 (2.7)	N/A	99.1 (5.7)	1.00 (0.06)
C0	54.0 (5.6)	4.4 (6.4)	77.2 (5.3)	0.78 (0.05)‡
C1	52.7 (7.0)	3.1 (8.2)	78.1 (4.0)	0.79 (0.04)‡
C2	47.2 (5.9)	4.2 (6.3)	79.4 (6.3)	0.80 (0.06)‡

All values are presented as MEAN (STD), US = unsuited, C0 = Configuration, C1 = Configuration 1 (one layer of padding), C2 = Configuration 2 (two layers of padding).
*Indicates significant difference from unsuited condition for that subject.
†Indicates a significant difference from the other two suited configurations.
‡Indicates significant difference between subject pooled suited condition and unsuited condition.

3.3.2 Effect of Suit Configuration on Task Knee Range of Motion

An ANOVA for the dependent variable $tRoM_H$ supports that there was a significant main effect of Configuration ($F(3,228) = 40.24$, $p < 0.0001$) and a significant interaction effect of Subject-Configuration ($F(8,228) = 9.662$, $p < 0.0001$) (Table 3.2). Post-hoc tests for the effect of Configuration revealed that suited trials significantly reduced $tRoM_H$ compared to unsuited (16.5% reduction when suited compared to all padding configurations pooled with all subjects pooled, Cohen's $d = 1.39$). Post-hoc pairwise comparisons were performed to examine configuration within subject. Subject 2 unsuited $tRoM_H$ was significantly greater than $tROM_H$ in all suited configurations

C0-C2 (Cohen's d = 3.14, pooled for all suited and padded configurations); there were no significant differences in $tRoM_H$ between C0-C2. Subject 3 also had significantly higher $tROM_H$ when unsuited than C0-C2 (Cohen's d = 1.34, pooled for all suited and padded configurations); however, C0 was significantly greater than C1 and C2 (Cohen's d = 1.06 and 0.45, respectively). Subject 4 had significantly greater $tRoM_H$ during C0 than C2 (Cohen's d = 1.18); no other significant differences were observed.

3.3.3 Effect of Suit Configuration on $\Delta tRoM$

An ANOVA for the dependent variable $\Delta tRoM$ supports significant main effect of Configuration ($F(2,171) = 27.7$, $p < 0.0001$), and a significant interaction effect between Subject-Configuration ($F(6,171) = 35.3$, $p < 0.0001$). Post-hoc pairwise comparisons of the Subject-Configuration interaction effect revealed specific trends for each subject. Subject 2 had significantly greater tRoM with more layers of padding ($\Delta tRoM_{C2} > \Delta tRoM_{C1}$, Cohen's d = 3.58, $\Delta tRoM_{C1} > \Delta tRoM_{C0}$, Cohen's d = 4.59, and $\Delta tRoM_{C2} > \Delta tRoM_{C0}$, Cohen's d = 5.75) indicating that $tRoM_S$ was progressively larger than $tRoM_H$ with increased layers of padding. Subject 3 had significant differences in $\Delta tRoM$ for all three suited configurations with the trend $\Delta tRoM_{C0} > \Delta tRoM_{C2}$ (Cohen's d = 0.71), $\Delta tRoM_{C2} > \Delta tRoM_{C1}$ (Cohen's d = 2.10), and $\Delta tRoM_{C0} > \Delta tRoM_{C1}$ (Cohen's d = 2.26). Subject 4 had no significant differences in $\Delta tRoM$ with changes in padding.

3.3.4 Effect of Subject and Configuration on $\rho^F_{HS}(t)$ and $\rho^T_{HS}(t)$

A mixed-effects model (Table 3.3 and 3.4) was fit for $\rho^n_{HS}(t)$ (Fig. 3.4). Table IV highlights all significant fixed-effect intercepts. In general, fixed-effect intercepts indicate that $\rho^T_{HS}(t)$ was negative and significantly less than $\rho^F_{HS}(t)$

during all configurations. A slightly positive cubic component of $\rho^n_{HS}(t)$ across gait phase indicates increases in $\rho^n_{HS}(t)$ over phases of gait. $\rho^T_{HS}(t)$ also showed a negative linear and cubic change across gait phase that femur did not; this negative linear relationship was also present in C2. Finally, there was a significant positive interaction between the quartic change in $\rho^n_{HS}(t)$ over gait phases and the quartic change in $\rho^n_{HS}(t)$ over step number.

In general, random-effect intercept predictions support that subject 4 had the highest values of $\rho^n_{HS}(t)$ (Fig. 3.4c and f), while subject 3 had the lowest (Fig. 3.4b and e). Linear terms reveal that subject 3 had the fastest positive growth of $\rho^n_{HS}(t)$ over gait phase (ST to HS), while subject 2 (Fig. 3.4a and d) had negative decline in $\rho^n_{HS}(t)$ over gait phase. Quadratic terms demonstrate that subject 2 had the highest $\rho^n_{HS}(t)$ over the middle of gait phase (HO, TO, SW), as seen in the large peaks in the middle of Fig. Fig. 3.4a, while subject 3 has the lowest $\rho^n_{HS}(t)$ over the middle of gait phase, as seen by the flatter nature of Fig. 3.4b and e.

Table 3.3: $\rho^n_{HS}(t)$ Significant Fixed Effect Model Predictions and Coefficients

Predictor	**Coefficient**	**Standard Error**	***t***	***P*-Value**
Intercept	9.37	1.85	5.06	0.0004
Gait Phase (Cubic)	19.26	3.65	5.27	0.0003
Segment	-15.69	1.01	15.54	< 0.0001
Gait Phase (Quartic) X Step Number Quartic	60.83	27.66	2.20	0.0280
Segment X Step Number Quartic	52.78	24.74	2.13	0.0331
Configuration (2) X Segment	6.40	1.43	4.48	< 0.0001
Gait Phase (Linear) X Segment	-5.83	2.26	-2.58	0.0099
Gait Phase (Cubic) X Segment	-16.49	2.26	-7.30	< 0.0001
Configuration (2) X Gait Phase (Linear) X Segment	-6.29	3.19	-1.97	0.0490

Table 3.4: $\rho^n_{HS}(t)$ Random-Effect Model Predictions for Subject-Configurations

Subject and Configuration	**Intercept**	**Linear**	**Quadratic**	**Cubic**	**Quartic**
2					
C0	0.781	-9.947	-3.9514	5.414	-9.546
C1	-1.730	-10.338	-2.250	6.269	-12.067
C2	3.025	-3.438	-0.861	10.004	-10.529
3					
C0	-4.248	5.465	4.035	-5.258	5.539
C1	-2.600	6.692	3.518	-5.420	7.164
C2	-1.268	3.152	1.152	-4.424	5.377
4					
C0	3.467	4.483	-0.083	-0.156	4.007
C1	4.330	3.646	-1.268	-0.849	4.903
C2	-1.757	0.286	-0.291	-5.581	5.162

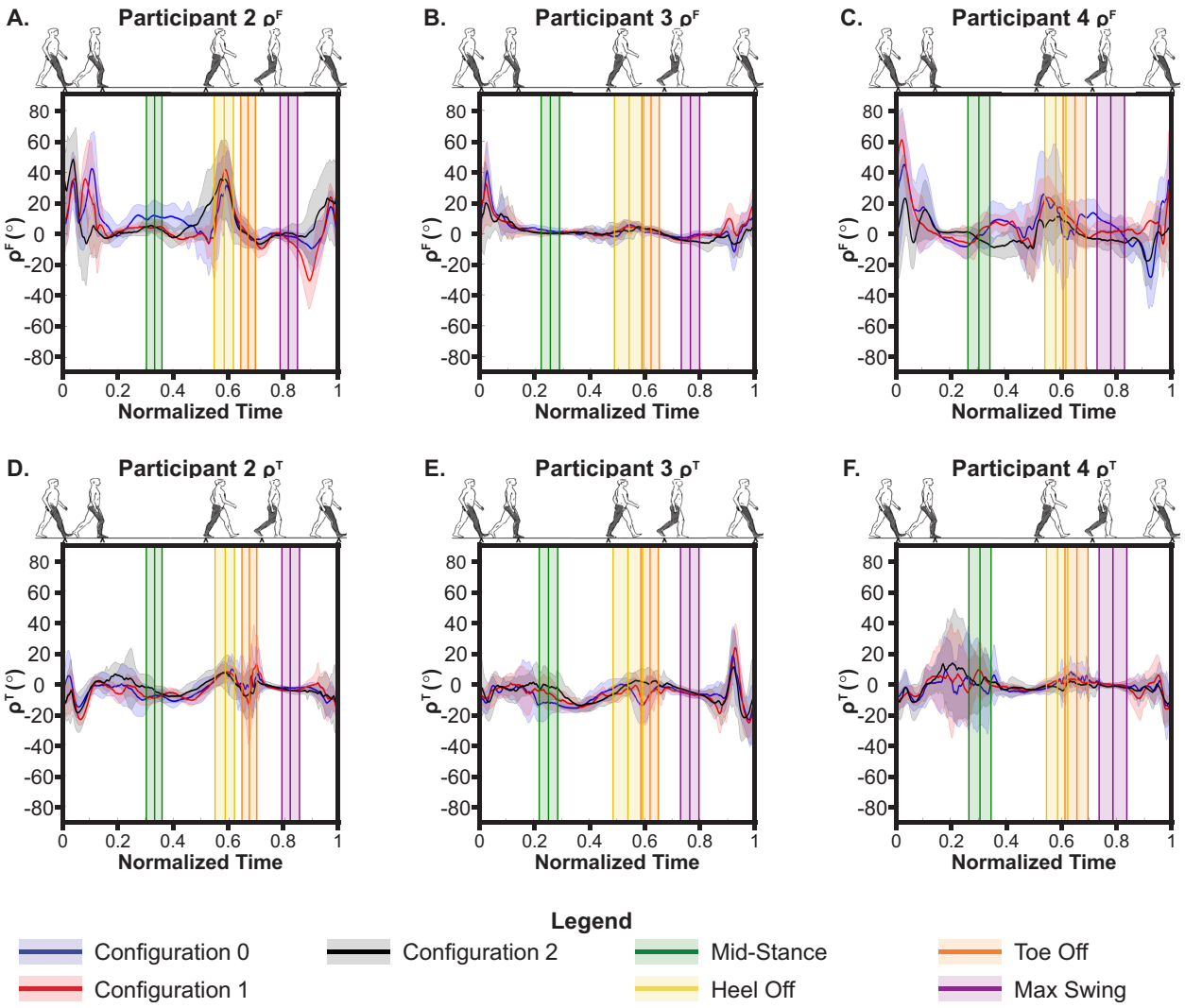

Figure 3.4: Time-series representations of ρ^F_{HS}[A-C] and ρ^T_{HS}[D-F] for each configuration: US (light green), C0 (blue), C1 (red), and C2 (black). Vertical lines represent the gait phases stance (green), heel off (yellow), toe off (orange), and max swing (purple). Solid lines represent means across all 20 steps and shaded regions represent 1 SD. For these plots, time-series were normalized and resampled to be the same length based on the trial with the most samples (250 samples, i.e., $\sim 1.95s$).

3.4 Discussion

This study aimed to develop quantitative measures of suit fit based on observed suit fit checks. In this study, static fit (how the human sits and is

indexed within the suit in a neutral static position) was altered while we quantified task performance (cadence, knee RoM) and dynamic fit (how the human and suit move and interact relative to each other during dynamic tasks). We hypothesized that changes in lower extremity static suit fit as altered through padding around the hips and thighs would affect parameters associated with dynamic fit during a walking task. The specific hypotheses we evaluated were that changes in padding between the human thigh and MKIII spacesuit hip brief assembly would affect measures of (a) gait performance (H1 normalized user cadence and H2 - the $tRoM$ of the human knee) and (b) dynamic fit (H3 - the differences in human and suit knee $tRoM$ ($\Delta tRoM$) and H4 - the relative motion between the human and suit at various phases of the gait cycle as measured using $\rho^n_{HS}(t)$). Statistical analysis of these hypotheses showed that the MKIII SSA 1) reduced user cadence despite changes in padding, 2) reduced human knee tRoM compared to unsuited kinematics with subject-dependent changes due to the added levels of padding, 3) $\Delta tRoM$ was typically positive and varied in a subject-specific manner with padding, and 4) that $\rho^n_{HS}(t)$ varied throughout the gait phase and could potentially be affected by suit components (i.e., boot fit and soft goods length). Changes in $\Delta tRoM$ and $\rho^n_{HS}(t)$ between subjects and levels of padding illustrate the sensitivity of these metrics to potential changes in fit. While these metrics are sensitive to donning the suit and adjusting a component of fit, it is still unclear if these changes in quantitative metrics are relevant in operational settings (i.e. a Cohen's d effect size of 3.68 comparing unsuited $tRoM_H$ to suited versus Cohen's d effect sizes of 0.4-1.0 between suited configurations). The results presented here, in combination with subjective feedback from participants, highlight that boot fit and soft goods lengths might influence fit more than padding at the hips for during a

walking task.

User cadence and $tRoM_H$ were used as measures of task performance. Brinkmann and Perry [119] found that the human knee has a $60 \pm 7°$ $tRoM$ during normative gait, while Kadaba et al.[120] found a self-paced cadence of 111.6 ± 8.3 steps/min. When not normalized, all three subjects in this study fell within the one standard deviation of the reported $tRoM$ during unsuited trials (Table 3.2). While Subject 2 appeared to fall within the cadence ranges also reported by Kadaba et al. [120], Subjects 3 and 4 appeared to have lower than reported cadences. Slower cadence could be explained by the equipment subjects were wearing during unsuited trials (LCG, TCG, etc.) and precautions taken to stay within the elevated platform. In addition, subjects were instructed to strike a force plate with a specific foot during each trial; the addition of this cognitive element to the study may have created a decrease in cadence. Subjects 3 and 4 also performed all unsuited trials after the suited portion of this study (Table I). The lower cadences observed for these subjects could be lingering effects of donning the MKIII SSA as all subjects had a lower cadence suited than when unsuited. When assessing differences in $tRoM_H$ between unsuited and suited configurations, subjects 2 and 3 had significantly lower knee $tRoM_H$ during all three suited configurations (C0-C2) than when unsuited. Meanwhile Subject 4 had no significant difference in $tRoM_H$ between all conditions (US-C0-C1-C2). It is possible that these changes in stride parameters and knee $tRoM$ could be due to the extra weight and inertial effects of the SSA; however, previous literature found increases in cadence and knee range of motion due to increased load carrying [121]. The results presented here are consistent with Cullinane et al. [53] that found similar deviations in operator walking kinematics while donning the MKIII spacesuit. They proposed that these changes may be due to degree of free-

dom limitations within the MKIII hip brief assembly. While Cullinane et al. [53] discussed these restrictions at the hip, torques are required to flex the knee as well; therefore, restrictions of the MKIII could have decreased the ability of Subjects 2 and 3 to fully flex and extend their knees during gait. Subject 4 only had a significant decrease in operator knee $tRoM$ during C2 (highest level of padding), but also had the lowest knee $tRoM$ during unsuited trials and had the lowest values of $\Delta tRoM$. Since Subject 4 had lower unsuited $tRoM_H$, this subject might have had fewer restrictions than Subjects 2 and 3 leading to lower values of tRoM and similar $tRoM_H$ when suited and unsuited.

In general, the level of padding at the hip brief had a subject-dependent effects on task performance as measured using cadence and $tRoM_H$, with large effect sizes observed comparing unsuited to suited measures (Cohen's $d = 1.34 - 3.87$) and smaller effect sizes between suited and padded configurations (Cohen's $d = 0.45 - 1.34$). In general, Subject 2 had no significant changes in these metrics with different levels of padding, indicating no observable change in performance due to adding padding. However, Subject 2 subjectively reported the suit being more responsive with high levels of padding. Subject 3 had significantly greater $tRoM_H$ when walking with no added padding, which could be indicative of better task performance, and potentially a better fit without added padding, aligning with this subject subjectively reporting not enjoying having greater levels of padding at the hip brief. Finally, Subject 4 had reduced $tRoM_H$ when fully padded, which could indicate poorer task performance and poorer fit with greater levels of padding. Subject 4 did not subjectively notice any differences due to levels of padding. These mixed results using gait performance metrics and $tRoM_H$ alone could imply that there are other factors affecting the fit of these subjects beyond just static

fit, especially when compared to the subjective feedback provided. These results highlight how fit is an integrated task and a few static and dynamic fit measures alone might not be sufficient for explaining all the variability within a population. Therefore, additional measures of dynamic fit could help broaden a quantitative interpretation of fit in the context of this task and better augment subjective measures, which naturally incorporate these varied factors.

This work introduced a new measure, $\rho^n_{HS}(t)$, to quantify the relative motion between human body segments and suit components. Positive values of $\rho^n_{HS}(t)$ are indicative of human-dominated motion, while negative values of $\rho^n_{HS}(t)$ represent instances where the MKIII has a higher degree of relative motion. With this in mind, $\rho^F_{HS}(t) > \rho^T_{HS}$ and $\rho^T_{HS} < 0$ is indicative that above the knee, the human moved relatively more than the suit and dominated the motion, while below the knee, the suit moved more relative to the human. The quartic change in $\rho^n_{HS}(t)$ across gait phase and step number indicated values of $\rho^n_{HS}(t)$ fluctuated, with more steps taken over the course of the study. This increase could be a learning effect as all subjects were novice suit operators, with only one prior experience within the MKIII SSA and thus were still learning how to properly perform the required programmed motions required by the suit. General changes in $\rho^n_{HS}(t)$ over the course of the last twenty steps analyzed here could also be due fatigue effects. Future work could further examine how fatigue and experience influence the $\rho^n_{HS}(t)$. More experience and training with these SSAs could aid human operators in changing $\rho^n_{HS}(t)$ in a way that is optimized for the desired task performance outcomes and in ways that synergize with the pre-programmed motions the SSA was designed to execute. In this instance, some relative motion might be appropriate ($\rho^n_{HS}(t) > 0$), but too much relative motion ($\rho^n_{HS}(t) >> 0$)

may indicate a need to change component sizing or add padding at a different location. It is important to consider that relative space (or certain amount of indexing) at one location may be required dynamically to enable appropriate spacing at another joint for a particular task [56]. Training to execute certain motion strategies could encourage human kinematics that would be more in line with that of the suit for the specified dynamic task.

Subject-specific random intercepts revealed that Subject 2 had the highest changes of $\rho^n_{HS}(t)$ over the middle of gait phase (i.e. around HO to SW), while Subject 3 had the smallest changes at these locations within the gait cycle. As shown in Fig. 3.4A and 3.4C, Subject 2 and 4 had very large spikes in $\rho^F_{HS}(t)$ right before HO during all three configuration that are absent for Subject 2 (Fig. 3.4B). Due to availability of suit sizing components, Subject 3 was wearing a different size and design of boot. During suit fit observations, suit engineers discussed a common occurrence in which the operator heel pops out of the boot during gait. If this were the case during HO, the femur would move freely within the suit prior to coming into contact with the leg of the suit and providing an interaction force that swings the suit leg forward. We hypothesize that different fits of boot could be contributing to the different behaviors $\rho^n_{HS}(t)$ exhibited during HO for Subjects 2 and 4 that were not present for Subject 3. Subjectively, Subject 2 did report the occurrence of this phenomenon during C0 and C1, while Subjects 3 and 4 never reported issues with their boots. Follow-on studies controlling for boot design and fit are necessary to assess this hypothesis. Data here suggest that improper boot fit at the heel could lead to greater values of $\rho^F_{HS}(t)$ and affect task performance.

While looking into these fit metrics individually provides insight into the effect of padding on dynamic fit, synthesizing these results from $\rho^n_{HS}(t)$,

$tRoM_H$, and $\Delta tRoM$ provide a clearer picture of overall task performance and subject fit. Subject 3 had lower values of $\rho^n_{HS}(t)$ and Subject 4 had higher values, which could suggest that Subject 3 had a more acceptable fit than Subject 4. However, $tRoM_H$ and $\Delta tRoM$ might suggest the opposite since Subject 3 had the highest values of tRoM and had a greater deviation of $tRoM_H$ from unsuited kinematics. These phenomena could be explained by the different boots these two subjects were wearing. The soft components of the suit act as a spring. When the foot is in contact with the ground, a ground reaction force aids in keeping the soft components of the leg compressed. When contact with the ground is removed, a force would be required to keep the suit from extending. If the soft components are able to be sized exactly, the extension force would be smaller than if the soft components are larger than desired. (This sizing condition may be the case as there are a fixed number of soft goods sizes.) The extension force may be a cause of the heel lifting out of the boot during HO. The tighter fitting boot of Subject 3 in combination with the sizing of the soft components, may have reduced the motion of the heel, thereby enabling increased fluency between the human and suit. If the heel stays within the boot throughout the entire gait cycle, the suit knee might reach higher degrees of flexion as the soft components of the legs buckle and bend around the knee (as opposed to the expansion when the heel slips). From this point of view, small, positive values of $\Delta tRoM$ close to 0 might be indicative of good suit fit so long as $\rho^n_{HS}(t)$ remains close to 0.

The trend for the tibia to have more negative ρ_{HS} values between HO and TO is consistent with the heel lifting. In general, $tRoM_S > tRoM_H$ ($\Delta tRoM > 0$) and $\rho^T_{HS}(t) < \rho^F_{HS}(t)$. If there is some degree of the heel slipping out of the boot and motion is driven from the contact point of the

femur with the suit upper leg, expansion of the suit leg soft goods allows any extra soft material in the legs to swing freely around the human foot, resulting in lower values of $\rho_{HS}^{T}(t)$ (more suit dominated motion) and more $tRoM$ in the suit knee. Synthesizing observations made about $\rho_{HS}^{F}(t)$ and $\rho_{HS}^{T}(t)$, a less constrained boot fit can result in the heel slipping out, creating high values of $\rho_{HS}^{F}(t)$ during HO. Meanwhile, the length of soft goods affected the degree of suit dominated motion between HO and TO ($\rho_{HS}^{T}(t) < 0$). Subject 3 had a boa boot design enabling a tighter fit, consistent with the lower values of $\rho_{HS}^{F}(t)$. Meanwhile, all subjects had the same length of leg soft goods, although they had different anthropomorphic crotch heights ($S4 > S3 > S2$). Subject 4 had the largest crotch height and therefore the smallest difference between soft goods length and crotch height. Greater differences between crotch height and soft goods length permits allows more room for the soft goods to expand during SW. We hypothesize that this would then lead to values of $\rho_{HS}^{T}(t)$ closer to 0, as observed for Subject 4. Despite tighter boots, Subject 3 still had slightly negative values of $\rho_{HS}^{T}(t)$ at HO and TO, which may be due to the extra length in the leg soft goods based on his anthropometry and soft goods size. Finally, Subject 2 had both looser boots and the shortest crotch height and it is consistent that there were high values of $\rho_{HS}^{F}(t)$ during HO and negative values of $\rho_{HS}^{T}(t)$ between HO and TO.

3.5 Conclusions and Future Work

This work aimed to examine how changing the level of static fit around the hip brief assembly using padding affected metrics of dynamic fit and task performance. Emergent in the analysis were underlying differences in the subject objective measures that may be explained by alternate components of suit fit, including boot design and soft goods lengths. The data showed

that the effect of padding on objective measures of gait performance (H1-H2) and performance-based measures of dynamic fit (H3-H4) was mixed and subject-specific. While Subject 3 had differences in tRoM with configuration, there were small changes in $\rho^n_{HS}(t)$. Subject 4 showed minimal changes in all metrics due to changes in padding level. It is possible that the level of padding changed how Subject 3 was sitting within the suit (i.e. higher or lower within the hip brief), creating a modified boot fit, altered static alignment, and different slack within the soft goods. Subjects in this study had different boots and underlying anthropometry measures, but were fitted with a constant lower leg length of soft goods. The addition of padding had a small effect size compared to donning the suit (Cohen's $d = 0.45 - 1.18$ for padding vs. $d = 1.69 - 3.87$ for the suit, for normalized cadence, $tROM$, and $\Delta tROM$ metrics); however, it might be the case that boot design and length of soft goods played a greater role in reducing $\rho^n_{HS}(t)$ than did padding and that these smaller effect sizes might not be operationally relevant. It would appear that the kind and fit of the boot might be more important during a walking task due to the larger differences of $\rho^n_{HS}(t)$ observed between Subjects 2 and 4 compared to Subject 3, who had an upgraded boot design. While there were inconsistencies in the effect of padding between subjects, this work demonstrates that candidate quantitative metrics for suit fit presented here are sensitive to small changes in fit and provide information that aligns with decisions made by suit technicians. These measures of dynamic fit directly related to specific decisions made during the lower body dynamic fit check of the MKIII spacesuit in Fig. 3.1c. Integrating techniques used here into all fit checks could help suit engineers detect fit anomalies, such as heel lift, leading to a decision to possible alter the suit boot.

Suit fit is an integrative process and multiple metrics are necessary to

appropriately interpret how well subjects fit within the suit, including the subjective feedback provided from subjects wearing the SSA. This work does not attempt to assess goodness of fit, simply the sensitivity of new candidate metrics to changes in performance due to components of fit. As fit is a function of multiple factors, multiple metrics are required to quantify this complex term. This work does not attempt to limit the importance of subjective feedback. The relationship between subjective feedback and quantitative metrics will be important to consider during the development of these new metrics. Quantitative metrics are an additional tool that can be used to objectively compare the different performances achieved when components of fit are changed and may be useful to better understand subjective preferences. Objective metrics, like those presented here, do not eliminate the need to subjective feedback.

This work was limited in the metrics that could be defined describing the knee angle as the study did not include a formal calibration period. The implementation of more robust joint angle estimation methods, including methods that can decompose joints with higher degrees of freedom, could also allow for deeper insight into how suit fit affects the kinematics of human gait at other joints, such as the hip or ankle. This work was limited in the generalizations that were possible due to the low number of subjects and the varying sizes of suit worn. This limitation is common in studies with space suits due to the limited number and availability of the suits. However, future work should have higher numbers of subjects and control for different anthropometric values across subjects cleared to wear the suit. Future work will also explore the hypotheses of how boot fit and soft goods length affect both $\rho^n_{HS}(t)$ and human kinematics by controlling for the boot design subjects wear and the length of the suit leg soft goods. These studies should be

performed with a greater variety of tasks where operationally relevant differences in performance can be assessed. While we examined a walking task here, the changes in static fit (through padding at the hips) may have more implications on performance in other operational tasks, such as kneeling, digging, or climbing through a hatch. The operationally relevant effects sizes for these tasks will be important to define, and could be determined based on mission success criteria or injury risk mechanisms. Further, padding was only used around the HBA in this study. Padding in alternate locations with alternate tasks may have a greater effect on performance. Finally, subjective feedback is still an integral part of evaluating fit and users may have different preferences; therefore, future studies should incorporate subjective ratings of fit in a more comprehensive manner.

Chapters 2 and 3 of this thesis adapted a metric for coordination to clinical and aerospace applications. It is possible that these measures could be generalized to other areas as well, such as robotics and mechatronics. In order to do so, we must first understand open research questions in these fields and see if there is need to quantify relative motion. For example, these measures could also be applied to exo-skeleton performance evaluation by measuring the relative motion between the human and exo. These chapters also only evaluated two tasks. In order to generalize these metrics in their respective fields, it is important to test other relevant tasks. Future work will apply ρ to evaluate inter-joint coordination in a clinical settings and will also apply ρ to quantify upper extremity suit fit.

Chapter 4

Technique-based Measures for the Standing Balance Test

Chapter's 2 and 3 of this thesis highlighted the development and application of a new metric for coordination to both clinical and aerospace medicine fields. As discussed in Chapter 1, this work also aims to develop technique-based measures for balance. This chapter reviews existing measures of balance and demonstrates the need for methods that quantify balance technique. Balance is a complex task that fuses sensory information from the vestibular, visual, and musculoskeletal systems. Quantifying balance technique permits comparing interventions across various clinical populations and could inform the selected plan-of-care. For example, as further described in Section 4.1, slower gait speed is attributed to higher rates of falls and other mortalities in older adults. Quantifying and understanding balance deficits associated with mediolateral stability could lead to a selected plan-of-care that includes strengthening and recruitment of hip abductor/adductor muscle groups commonly associated with mediolateral stability [122].

This chapter will define a new metric for balance that we call Frequency in Balance Region (FBR, Section 4.3.1) that helps to answer the question ***how*** people balance. Static balance is typically described using an inverted

pendulum model (see Section 4.2) that assumes joints are rigid when humans balance on two feet. Our approach to quantifying balance technique (FBR) involves measuring deviations from this model at different body segments, thereby quantifying balance strategy. After defining this new metric, this chapter moves on to quantify technique-based differences in balance associated with different gait speeds.

4.1 Gait Speed and Clinical Outcomes

4.1.1 Defining Dismobility

By 2040, an estimated 81 million adults in the United States are expected to be older than 65 [123]. Of these, an estimated 15.4 million will be unable to walk 2-3 blocks without assistance, adding an estimated $42 billion to annual health costs [124, 125]. Slower gait speeds are common in older adults and a part of the aging process [126, 127]. It is hypothesized that gait speed slows with aging as a means of increasing gait stability; however, studies also show that gait speeds below certain thresholds reverse this effect and decrease stability [128, 129, 130, 131]. Self-selected gait speed is shown to be a predictive factor of overall physical function, fall risk, and cognitive ability ([127, 132]). Figs. 4.1a and 4.1b show predicted life expectancy for both males and females. At age 65, individuals who walk less than $0.6m/s$ have a median survival of only 10 and 17 years for males and females, respectively. Meanwhile, individuals who walk $> 1.2m/s$ are expected to live on average 20 and 30 years longer for males and females, respectively. While slowing gait speed is common during aging, variability still exists within older patient populations and gait is still highly predictive of overall mortality [125, 131]. In addition, Fig. 4.1c shows how slower gait speeds is associated with a higher

rates of disability.

Dismobility is an arising clinical diagnosis defined as a gait speed $< 0.8m/s$ that is attributed to higher levels of disability and lower 5- and 10-year survival rates, Fig. 4.1 [124]. A diagnosis of dismobility can prompt clinical action in the form of physical therapy, provision of assistive device, or adjustment of perscription medications to improve physical performance and reduce the risk of negative outcomes, such as falling or other forms of disability. However, gait and gait speed are complex movements requiring the manipulation of multiple degrees of freedom and various decrements could contribute to a decreased gait speed (i.e. static balance, dynamic balance, proprioception, cognition, cardiac output, etc.). Physical ability and mental cognition are large contributors to older quality of life and decrements to either are associated with higher mortality [133, 134, 135, 136]. It is possible that these higher physical disability rates seen among slow older walkers could be contributing factors to higher rates of mortality, but a simple gait speed test can make it difficult to distinguish what underlying mechanism might stratify which patients need clinical intervention. Despite the complex mechanics underlying gait and gait speed, improvements in gait speed are shown to predict 8-year survival in older adults [123]. Targeted physiotherapy for specific impairments that contribute to decreased gait speed could then potentially better improve survival and quality of life in older adults.

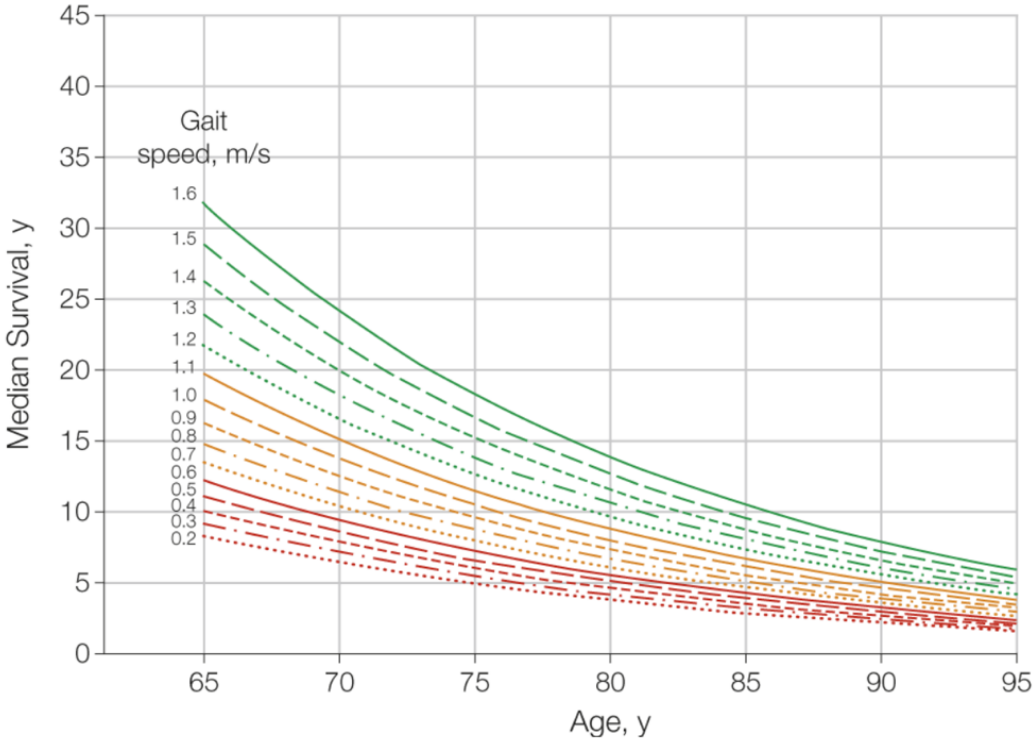

(a) Predicted Life Expectancy By Age and Gait Speed: Men

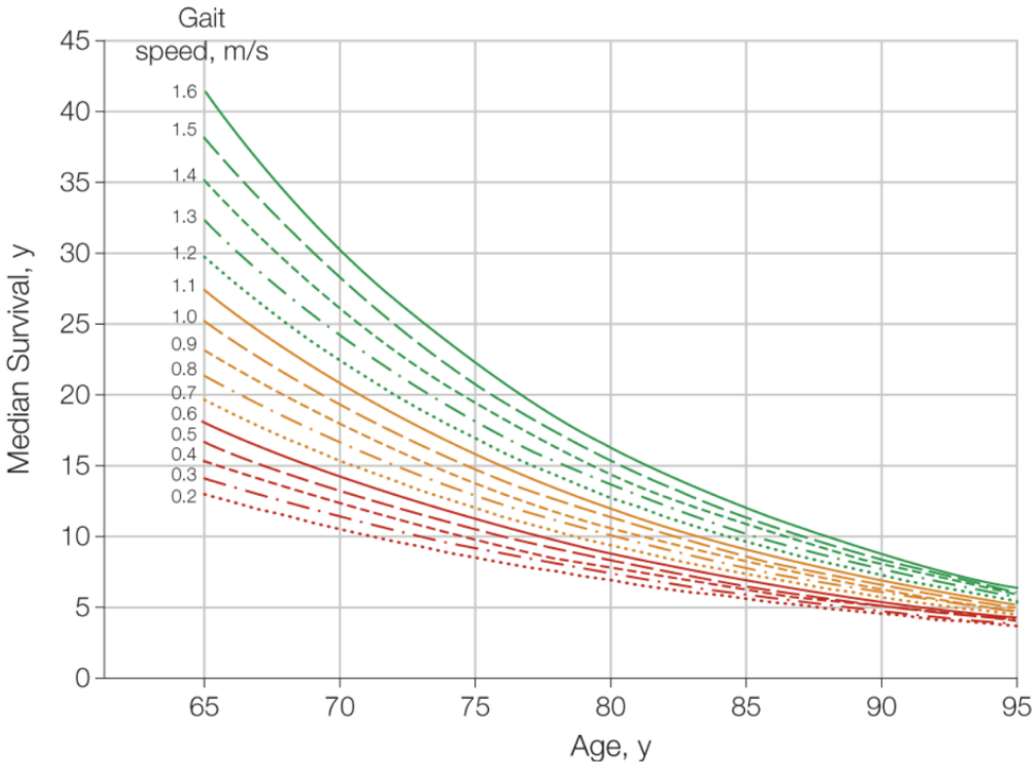

(b) Predicted Life Expectancy by Age and Gait Speed: Women

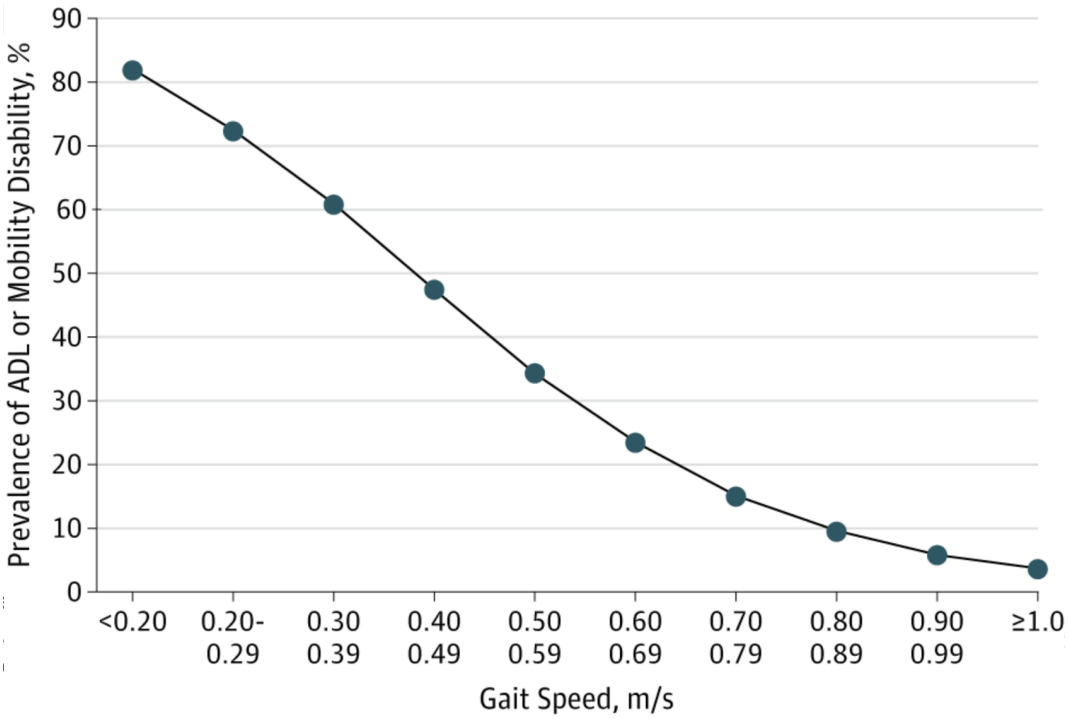

(c) Mobility and Activity of Daily Living Prevalences by Gait Speed

Figure 4.1: Life Expectancy and Disability Rate in Older Adults by Gait Speed (Source: Castranova et al. [124] and Studenski et al. [125])

4.1.2 Disambiguating Between Slow and Moderate Walkers

The kinematic changes and decrements that occur for higher-risk dismobile adults is not well understood. Other clinical measures do exist that are correlated with fall risk, disability, and mortality in older adults. Examples of these tests include 400m walk test [123, 137], short physical performance battery (SPPB) [137, 138, 139, 140], timed-up-and-go task (TUGT) [141, 142], and 10meter walk test (10MWT) [126, 143]. The 10m and 400m walk test measure the time to complete their respective distances. The TUGT task asks participants to start seated, stand, walk 3m out-and-back, and then sit back down; the main outcome measure of this task is also time to completion. Finally, the SPPB involves a gait speed measure, a series of

sit-to-stand tasks, and static balance test. A composite score is assigned to each patient following the SPPB based on their ability to complete each task. These measures evaluate task outcomes (i.e. time to completion) as opposed to task performance. Evidence still exists that improving the scores of these tests can reduce mortality and improve quality of life [123, 139], other more longitudinal studies show mixed results due to an inability to distinguish between task outcomes (i.e. can participants perform a task) versus physical function (i.e. methods and frequency of performing the tasks) [140, 77]. In other words, short-term improvements that focused on task outcomes might are due to the introduction of compensatory mechanisms that in the long-term did not improve overall quality of life. Therefore, there is a need to understand and quantify the potentially subtle biomechanical differences between healthy and dismobile adult populations as a means of creating diagnostic tools and informing potential rehabilitation and treatment regimens.

4.2 Existing Balance Models and Metrics

4.2.1 Existing Static Balance Metrics

Static balance tests are commonly used to assess postural stability and fall risk in older adults [144, 145, 146, 147, 148]. Decrements in muscle strength, mobility, and endurance are thought to negatively impact postural control and balance, which could then lead to a higher risk of falling and dismobility [131, 144, 149]. Various efforts have been made to improve balance performance in the older adult population, ranging from strength training [150] to tactile feedback [151, 152], but there is limited evidence these interventions improve mobility or decrease mortality. In the case of Seinko et al.

[153], continuous vibrotactile feedback around torso did decrease short-term medio-laterial trunk tilt and increased dynamic stability during a walking task. Static balance is currently evaluated using standing balance tests (i.e. double leg support [145], single leg support [148], eyes open vs. eyes closed [154]) that result in subject balance scores. Biomechanical metrics, such as media-lateral sway, center of pressure (COP) path, and COP velocity, are extracted from stabilograms generated using motion capture or force plates [144, 151, 154].

Previous work assessing static balance in older and young population show mixed results. Priplata et al. [151] showed a small differences between younger and older adult when computing sway area, but there was no difference in other static balance metrics, such as Antero-posterior (AP) and mediolateral (ML) Range. Melzer et al. [144] looked into differences in static balance for older faller and non-fallers, but only found small differences between groups in ML Range, and no other metrics such as AP Range, or COP path. While the authors of these works both address potential sample size issues, it is possible that standard outcome static balance measures alone are not sensitive enough to differentiate these group. It is possible to achieve similar sway patterns and COP when using different a balance technique. Therefore, there is a need for measure of static balance technique on top of existing outcome measures.

4.2.2 Limitations of the Inverted Pendulum Model

Many current metrics are outcome-based and do not quantify the underlying motor patterns used to achieve postural stability. Therefore, there is a need to expand the capability of current measures to include a more thorough understanding of balance technique. Current balance measures inherently make an

assumption of the person behaving as an inverted pendulum [155, 156, 157], meaning that all body segments above the ankles are rigid and keep their alignment between the upper and lower body, Fig. 4.2a. Gage et al. [155] validated the inverted pendulum model in younger participants by demonstrating that COP measures correlated with body segment center of mass (COM) paths indicating that you can collect static balance measure values (i.e. ML/AP sway) at various parts of the body with similar results. Additionally, Gage et al. [155] showed that displacement of each body segment COM increased linearly with height above the ankle joint despite there being some movement of joints above the ankle, such as knee and hip. While this behavior was shown in younger adults, aging reduces muscle strength and joint flexibility thereby shifting the COM posterior to the heels, which is not the case for younger adults [145, 158]. Manchester et al. [159] also described that older adults flexed and extended the hips (hip strategy) compared to younger adults who used more of an ankle strategy. With these considerations, a single inverted pendulum may no longer hold for different populations. Measuring deviations from an inverted pendulum may provide a way to assess static balance technique.

4.2.3 Previous Efforts Using Multi-segmented Inverted Pendulum Models

There have been a few attempts to quantify balance as a double pendulum, adding an additional hinge about the hips similar to Fig. 4.2b. Aramaki et al. [160] explored a double pendulum model by approximating the ankle and hip displacement in the sagittal plane using a laser displacement system. Participants had their spine and knee restrained to focus analysis on the hip and ankle joints. A simple inverse kinematics method was used to to

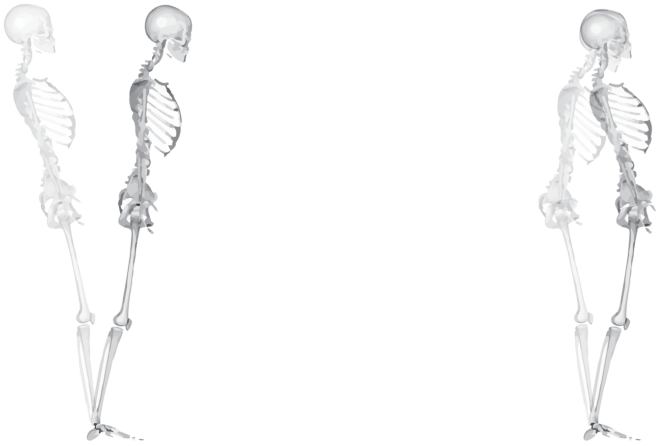

(a) (b)

Figure 4.2: Possible Models and Mechanisms to Maintain Static Balance: a) is representative of a single inverted pendulum model where all segments above the ankles are rigid and do not move relative to one another while b) is representative of a double pendulum model in which static balance can be achieved through additional joint motion, such as the hip (shown), knee (not shown, or torso (not shown).

measure ankle and hip angular displacement during a series of 30s standing balance trials. Aramaki et al. [160] observed how hip and ankle motion had reciprocal joint angular velocities to maintain balance and concluded that angular displacement of the hip and ankle joints were not meant to keep the COM in a constant position, but to minimize its acceleration. This behavior was seen artificially, however, by restraining the spine and knee joints.

Crenna et al [161] used a double pendulum when studying balance strategy for controlled forward and backward movements of the torso. In this study, sagittal plane trajectories of the head, torso, hips, knee, and ankle were tracked using passive markers and a single camera. Muscle EMG was also collected. Young participants voluntarily moved their head and torso forward or backward either at fast or slow speeds. Crenna et al. [161] reported the hips and knee tended to move in the opposite direction of the head and torso. However, during fast displacements of the torso, all segments moved together

in the same direction at first, followed by a quick switch of lower segments moving in the opposite direction of upper segments. Despite similar results to Aramaki et al. [160], these were voluntary motions and not static balance tasks.

Accorcero et al. [162] also used a double pendulum model with a joint at the hips, but this time compared the rigidity between younger and older adults. Accorcero et al. [162] described measuring this double pendulum using an electromagnetic tracking device with single markers on the head and hips without decoupling motion from the torso, hip, knee. Velocity vectors from these two trackers were used to quantify how "rigid" or "flexible" the double pendulum was during a quiet standing task. Accorcero et al. [162] referred to the double pendulum as "rigid" when the head and torso velocity vectors traveled in the same direction and "flexible" when they traveled in opposite directions. Similar to the previous two works, Accorcero et al. [162] showed that both older and young participants had double pendulum behavior with hip motion relative to head motion, but this work did not examine the influence of the knee and did not decouple torso and hip motion; it is possible that torso, hip, and knee motion still existed that the two sensors alone could not decouple. Accorcero et al. [162] also found that young and older adults had different double pendulum behavior, concluding that older adults appeared more rigid that younger adults, in particular with eyes open. In other words, the head and hip markers in older adults appeared to travel in the same direction more often than younger adults.

Finally, Kim et al. [163] quantified knee stability during a single leg balance task by measuring relative motion of the shank and thigh (Fig. 4.3). As shown in Fig. 4.3a and 4.3b, IMU estimated maximum displacement of the shank and thigh in the AP and ML directions were used to compute

the region of limb stability (ROLS). ROLS is computed as the rectangular area created when plotting maximum AP and ML displacement for the thigh and shank (Fig. 4.3c). Kim et al. [163] did find differences in the thigh and shank trajectories that could be indicative of knee movement, with good correlation between IMU and marker-based datasets. Kim et al. [163] also computed ROLS between healthy and injured participants and found that ROLS is sensitive to knee impairment. ROLS is limited, however, in that it is a summary outcome metric that does not intuitively describe how these two segments move relative to each other.

These previous efforts using double pendulum assumptions highlight that there are motions in joints above the ankle. Many of these efforts assess a single plane of motion and do not provide a thorough understanding of balance technique. For example, it is possible that some participants use their torso, hips, and knees to make slight adjustments to their center of mass that might not be captured using the above methods. It is also not clear how the postural strategies change due to aging across the multiple relevant joints. Current measures are therefore limited in that they do not address all joints that could contribute to balance and do not decompose balance into all axes of rotation. Section 4.3 will attempt to address these shortcomings by creating a multi-joint, multi-axis model for static balance that will allow us to deduce the underlying balance strategy.

4.3 Frequency in Balance Region

We assume a multi-segmented, three-dimensional, inverted pendulum and define a new series of angular velocity-based metrics that quantify the directionality with which body segments move relative to one another, thereby categorizing and quantifying balance technique. We call this new balance

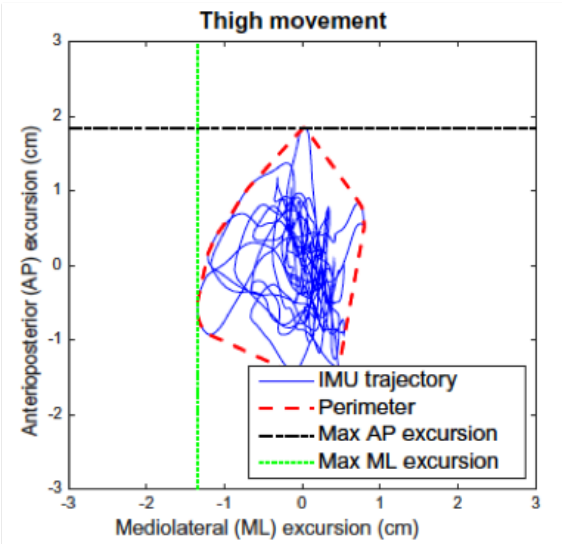

(a) IMU Trajectory and maximum AP and ML excursion of thigh

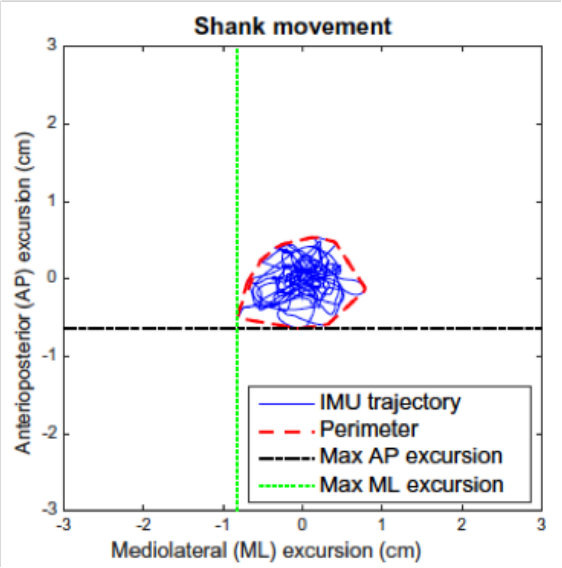

(b) IMU Trajectory and maximum AP and ML excursion of shank

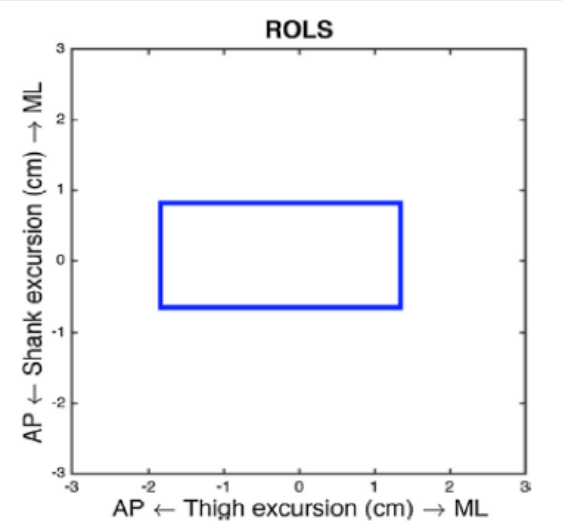

(c) IMU Trajectory and maximum AP and ML excursion of thigh

Figure 4.3: IMU movement trajectories in the horizontal plane (blue solid line, perimeter (red dashed line, and maximum excursions in the ML and AP directions of the (a) thigh and (b) shank during single leg stance (a green dotted line and a black dash-dot line). (c) ROLS excursion diagram. Adapted from Kim et al. [163]

metric the Frequency in Balance Regions ($FBR_n^{P,LU}$, Section 4.3.1). Here we choose an angular velocity-based metric due to it being more easily and accurately extracted from IMUs and gyroscopes and can still provide information on the relative motion between rigid body segments [164, 47].

4.3.1 A numerical definition of $FBR_n^{P,LU}$

The rigid body assumption of the inverted pendulum model was assessed by implementing a three-dimensional, multi-segmented inverted pendulum model for static balance, Fig.4.4. We consider a rigid body model with the body sub-divided into six body segments: torso (T), pelvis (P), R/L femur (RF, LF), and R/L shank (RS, LS). This model contains multiple relevant reference frame, such as the global inertial reference frame, in which the participant is moving, and the reference frames associated with each of the individual body segments listed above, Fig. 4.4. Quaternions are used to describe a rotation that aligns a vector in one reference frame to a vector in another reference frame. The orientation of each body segment relative to the global frame was computed via a rotation quaternion from the global frame to the segment frame (q_T^G, q_P^G, q_{RF}^G, q_{LF}^G, q_{RS}^G, q_{LS}^G). The angular velocity of these segment reference frames is then computed from changes in the rotation quaternion from the global frame to segment frame ($\vec{\omega}_T$, $\vec{\omega}_P$, $\vec{\omega}_{RF}$, $\vec{\omega}_{LF}$, $\vec{\omega}_{RS}$), $\vec{\omega}_{LS}$). If two segments behaved like a pure inverted pendulum with no joint in between them, there would be no relative motion. In the context of the inverted pendulum model, there would be no relative motion between the femur and shank, pelvis and femur, or torso and pelvis.

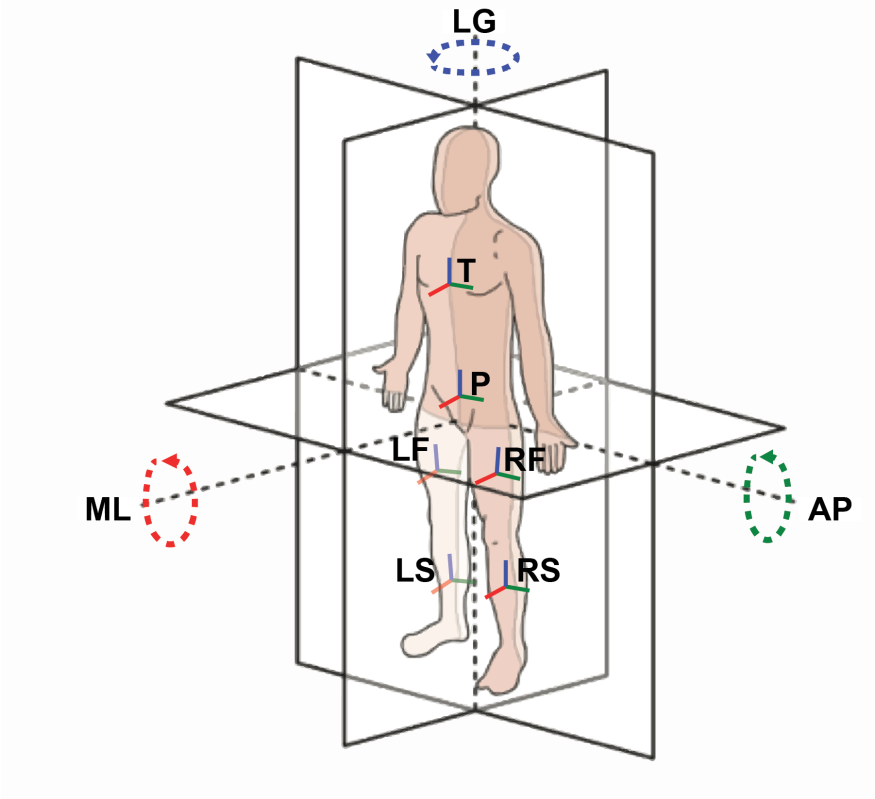

Figure 4.4: A multi-segmented inverted pendulum Model for static balance in which the body is divided into seven segments: torso (T), pelvis (p), right femur (RF), left femur (LF), right shank (RS), and left shank (LS). Each segment contains its own reference frame and coordinate system where each axis corresponds with its underlying anatomical axes: anteroposterior (AP), mediolateral (ML), and longitudinal (LG).

When comparing two segments, we refer to the segment more distal from the ankle as the upper segment and the segment proximal to the ankle as lower segment. If segments behave like single pendulums, upper segments will not have any relative motion to the lower segment. These relative motions can be examined by expressing the angular velocity of the upper segment in the reference frame of the lower segment and subtracting out the lower segment angular velocity. The relative angular velocity of upper segments in the reference frame of the lower body segment ($\vec{\omega}_T^P$, $\vec{\omega}_P^{RF}$, $\vec{\omega}_P^{LF}$, $\vec{\omega}_F^{RS}$, $\vec{\omega}_F^{LS}$) was then is therefore computed as follows:

$$q_L^U = q_L^G \times (q_U^G)^{-1} \tag{4.1}$$

$$\vec{\omega}_U^L = q_L^U \vec{\omega}_U (q_L^U)^{-1} - \vec{\omega}_L \tag{4.2}$$

where q_L^G, q_U^G are the rotation quaternions from the lower segment to the global frame and from the upper segment to the global frame, respectively, q_L^U is the rotation quaternion from the lower body segment frame to the upper body segment frame, $\vec{\omega_L}$, $\vec{\omega_U}$ are the angular velocities of the lower and upper body segment, respectively, and $\vec{\omega}_U^L$ is the relative angular velocity of the upper body segment in the lower body segment frame. Each component of these vectors corresponded to the angular velocity in different anatomical directions (AP, ML, and Longitudinal (LG)) because we define the biomechanical angular velocities directly. Should this method be computed using IMUs, an additional reference frame rotation is necessary to align the IMU frame and the rigid body biomechanical reference frame as in done by McGrath et al. [69] and Seel et al. [67].

In the inverted pendulum model, the six segments listed above (T, P, RF, LF, RS, LS) would not have an angular velocity relative to one another ($\vec{\omega}_T^P = 0$, $\vec{\omega}_P^{RF} = 0$, $\vec{\omega}_P^{LF} = 0$, $\vec{\omega}_F^{RS} = 0$, $\vec{\omega}_F^{LS} = 0$). Therefore, deviation from the single inverted pendulum model can be assessed by plotting $\vec{\omega}_P$ versus $\vec{\omega}_T^P$, $\vec{\omega}_F$ versus $\vec{\omega}_P^F$, and $\vec{\omega}_S$ versus $\vec{\omega}_F^S$ for each of the anatomical directions (AP, ML, LG). Fig. 4.5 plots $\vec{\omega}_P$ versus $\vec{\omega}_T^P$ for a single individual who performed six 30s SBT. The Cartesian coordinate system is divided into five regions each representing a different balance technique. Small values in relative angular velocity ($\vec{\omega}_T^P$, Fig. 4.5) could be representative of measurement error and actually be representative of participants behaving as a single pendulum. For this reason, five balance regions were defined. The frequency in balance

region 5 ($FBR_5^{P,LU}$) was computed as the percent time during the SBT spent behaving as a single pendulum. In other words, $\vec{\omega}_U^L \approx 0$. The frequency in balance region 1-4 ($FBR_{1-4}^{P,LU}$) was then defined as the percent time spent in each of the Cartesian quadrants and outside the $FBR_5^{P,LU}$ (Fig. 4.5). The sum of $FBR_{1-5}^{P,LU}$ is therefore equal to 1. The five balance regions can be written as follows:

$$t_{FBR_1}^P = \sum_{n=1}^{T} t_n \; where \; \omega_L^P > 0, \; \omega_U^{L,P} > R \tag{4.3}$$

$$t_{FBR_2}^P = \sum_{n=1}^{T} t_n \; where \; \omega_L^P < 0, \; \omega_U^{L,P} > R \tag{4.4}$$

$$t_{FBR_3}^P = \sum_{n=1}^{T} t_n \; where \; \omega_L^P < 0, \; \omega_U^{L,P} < -R \tag{4.5}$$

$$t_{FBR_4}^P = \sum_{n=1}^{T} t_n \; where \; \omega_L^P < 0, \; \omega_U^{L,P} < -R \tag{4.6}$$

$$t_{FBR_5}^P = \sum_{n=1}^{T} t_n \; where \; |\omega_U^{L,P}| < R \tag{4.7}$$

$$FBR_n^{P,LU} = \frac{t_{FBR_n}}{t_T} \tag{4.8}$$

where $\vec{\omega}_U^L$ and $\vec{\omega}_L$ are the angular velocities of the lower body segment and relative angular velocity of the upper body segment being compared, P is the anatomical direction, n is the balance region, t_{FBR_n} time spent in the nth region, t_T is the total time of the balance trial, and R is the threshold relative angular velocity for behaving as a single pendulum. In Fig. 4.5, this value R was set at $0.03 rad/s$ for it is representative of the measurement error of

various IMUs and gyroscopes, technologies that could be used to extract this metric.

Time spent in regions FBR_2 and FBR_4 is representative of an adaptive balance technique in which body segments rotate in opposite directions of one another. This strategy could be used to maintain the COM within a desired region and in some instances could be considered an adaptive strategy. Time spent in $FBR_{1,3}^{P,LU}$ is representative of a balance strategy where the upper segment is rotating at a faster rate than the lower segment. This strategy could occur to bring the COM quickly back to a desired region or potentially a maladaptive balance perturbation that moves the COM rapidly away from a desired region. For the proposed model described in Fig. 4.4 and Fig. 4.5, values for $FBR_n^{P,LU}$ can be computed from three anatomical directions and five body segment comparisons (left shank-left femur, right shank-right femur, left femur-pelvis, right femur-pelvis and pelvis-torso); therefore, for each SBT, a total of 75 values of $FBR_n^{P,LU}$ can be extracted. Each segment comparison is also indicative of different joint motions where pelvis-torso correlates with spinal motion, femur-pelvis to hip motion, and shank-femur to knee motion. A graphical representation of $FBR_n^{P,LU}$ can be found in Fig. 4.5 with color legends corresponding to the five regions and schematics of the balance techniques $FBR_{1-4}^{P,LU}$ represent. While this participant shows motion in all five regions, it is important to understand the percentage of time in each of these regions.

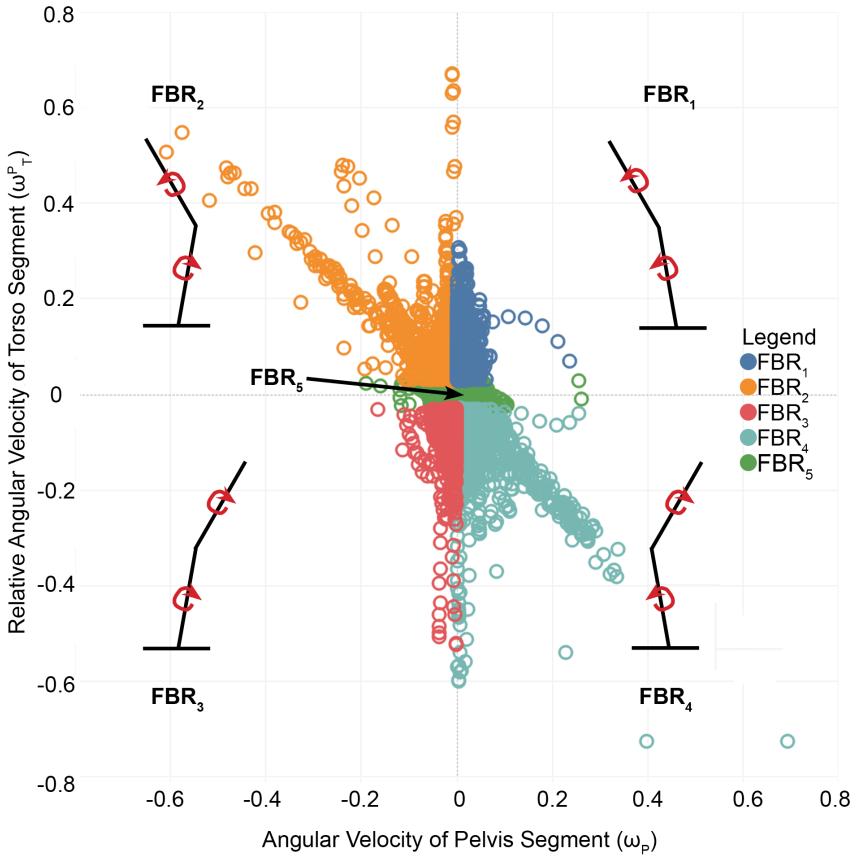

Figure 4.5: Definition and derivation of Frequency in Balance Region and corresponding balance strategies. Time spent in $FBR_{2,4}^{P,LU}$ is representative of a balance strategy in which the upper segment is rotating faster and in the opposite direction of the lower segment . Time spent in $FBR_{1,3}^{P,LU}$ is representative of a balance strategy where the upper segment is rotating at faster rate and same direction as the lower segment. Time spent in $FBR_{5}^{P,LU}$ is representative of balance strategies in which the upper segment has no relative motion to the lower segment. The above example represents six 30s static balance trails of a single participant comparing the angular velocity of the pelvis with the angular velocity of the torso relative to the pelvis in the AP axis. The corresponding values of FBR for this case are: $FBR_1^{AP,PT} = 0.08$, $FBR_2^{AP,PT} = 0.13$, $FBR_3^{AP,PT} = 0.07$, $FBR_1^{AP,PT} = 0.14$, and $FBR_5^{AP,PT} = 0.58$.

4.4 Assessing Participant Specific Balance Technique using $FBR_n^{P,LU}$

Prior to assessing balance technique in larger populations, it is important to assess the variability that might exist both within and between subjects. Additionally, we must assess whether or not $FBR_n^{P,LU}$ is capable of quantifying balance technique in a way that makes it easier to interpret the underlying kinematics and postural control, similar to ρ in Section 2.3.1. This section initially assesses $FBR_n^{P,LU}$ and figures similar to Fig. 4.5 in a qualitative manner. Example data from older and younger participants are used for this discussion.

4.4.1 Changes in Static Balance Technique Between Trials

Fig. 4.6 highlights two different 30s two-legged standing balance tests. Figs. 4.6a-4.6b highlight $FBR_n^{AP,RSF}$ (FBR for the AP plane comparing the right shank to the right femur, which is indicative of right knee motion), $FBR_n^{AP,RFP}$ (FBR for the AP plane comparing the right femur to the pelvis, which is indicative of right hip motion), $FBR_n^{AP,RPT}$ (FBR for the AP plane comparing the pelvis to the torso, which is indicative of spine motion) for one trial and 4.6c-4.6d highlight $FBR_n^{AP,RSF}$, $FBR_n^{AP,RFP}$, $FBR_n^{AP,RPT}$ for a second trial. First and foremost, it is clear that there are instances in both trials where the participant deviates from an inverted pendulum model (any area that is not green). Trial 5 for this particular participant (Fig. 4.6a-4.6b) appears more stable with fewer perturbations that cause segments to deviate from single pendulum behavior. There is one instance here in which the participant deviates heavily from a single pendulum (Fig. 4.6a, orange points in upper left quadrant). Fig. 4.6a comparing the right shank-femur imply that the

shank rotates in the anterior direction while the femur reacted by shifting in the opposite direction; this is indicative of knee joint flexion. A similar large region deviating from FBR_5 is also present in the pelvis-torso (Fig. 4.6b) during which the pelvis rotates in the posterior direction, while the torso flexes in the anterior direction to counteract this motion. In both cases, it would appear that the relative motion of the upper segment is greater than the angular velocity of the lower segment. Greater and opposite angular velocity of the upper region could be evidence of the upper region attempting to quickly correct motion of lower segments deviating the COM away from a desired region.

Meanwhile, Fig. 4.6c-4.6d demonstrate a different trial in which we can see various different balance strategies and behavior. At first glance, it is clear that both comparisons (right shank-femur and pelvis-torso) quantitatively deviate more from a single pendulum than they did in Trial 5 (Fig. 4.6a-4.6b). From observing these two different sets of trials, differences in balance strategy exist from trial to trial. This variability within a single subject demonstrates the need to collect more than one trial for a greater, more comprehensive review of balance strategies used and the natural variability that exists within subjects.

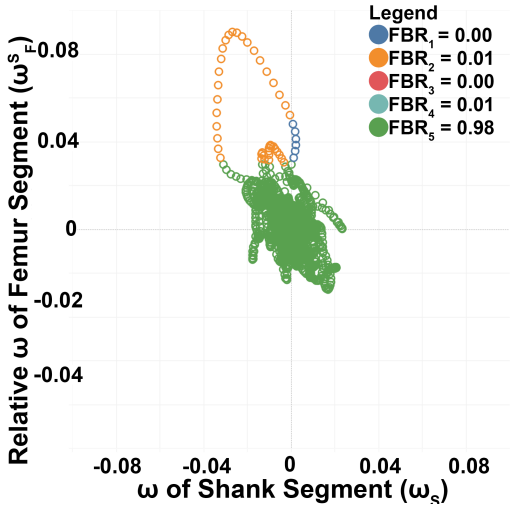

(a) Y8 Trial 5 $FBR_n^{AP,RSF}$

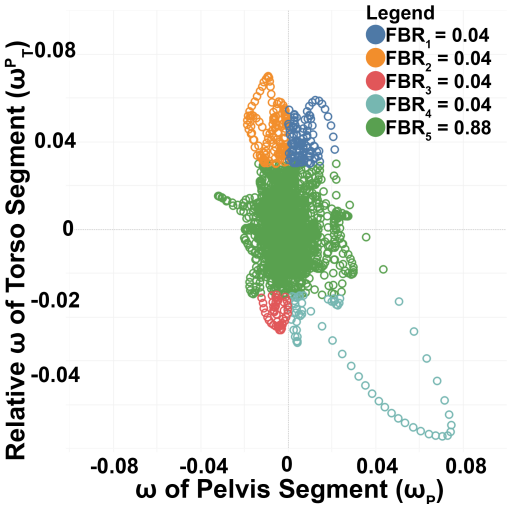

(b) Y8 Trial 5 $FBR_n^{AP,PT}$

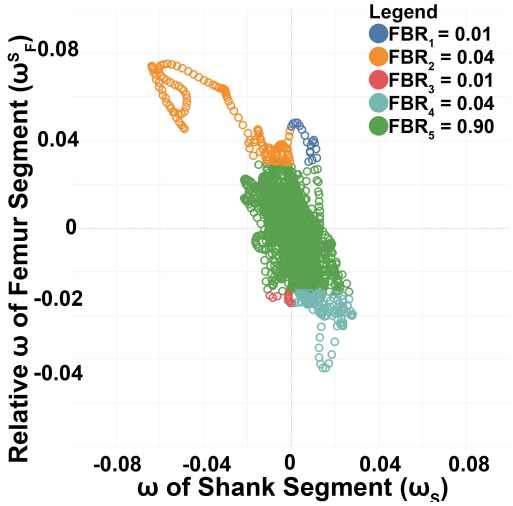

(c) Y8 Trial 1 $FBR_n^{AP,RSF}$

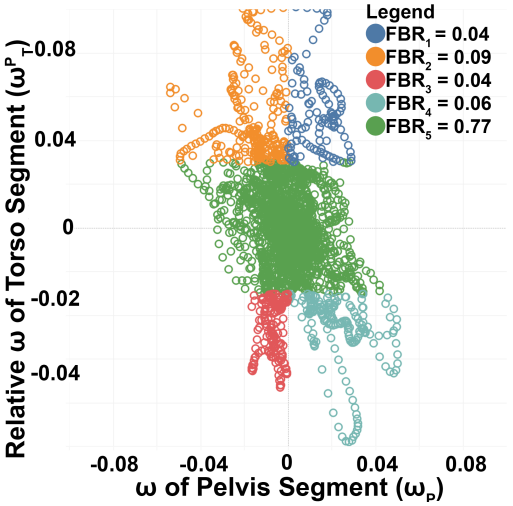

(d) Y8 Trial 1 $FBR_n^{AP,PT}$

Figure 4.6: Individual Balance Strategy for Two Trials of Single Young Participants in AP Plane. Green regions represents time points where the segments behave as rigid, single pendulums. Any other areas represents double-pendulum behaviors with different balance strategies.

4.4.2 Changes in Static Balance Technique Between Participants

Fig. 4.7 highlights one 30s two-legged standing balance tests for two different participants. Figs. 4.7a-4.7e highlight $FBR_n^{AP,RSF}$, $FBR_n^{AP,RFP}$, $FBR_n^{AP,RPT}$ for one participant (O25) and 4.7b-4.7f highlight $FBR_n^{AP,RSF}$, $FBR_n^{AP,RFP}$,

$FBR_n^{AP,RPT}$ for a second participant (O16), all in the AP anatomical axis. While we know there is variability in balance strategy within a single participant, these qualitative examples demonstrate differences in balance strategy between participants. Participant O25's knee (Fig. 4.7a and 4.7c) appear to rotate a relatively small amount compared to their hips and torso (Fig. 4.7e). In addition, the tall and narrow nature of the balance strategy seen for the pelvis-torso in Fig. 4.7e would imply that the torso is rotating a much greater amount than the hips, possible due to a weakened core strength or lower range of motion for the ankles and hips.

Meanwhile, participant O16 appears to use their hips and femur far more than participant O25. The tall and narrow nature of the angular velocities in Fig. 4.7b suggest the femur is rotating at much higher rates than the shank, indicative of knee joint motion. Similarly, the pelvis appears to be moving more than the femur (Fig. 4.7d), suggesting more hip and knee balance strategies being employed than ankle-based ones. Fig. 4.7f shows that similar to participant O25, there is torso rotation, but this time it counteracts the rotation of the pelvis. Therefore, participant O25 appears to use more of a torso-based strategy to balance while O16 uses both the hips and torso. While Section 4.4.1 highlighted variability between trials, this section demonstrated an ability for the newly proposed FBR metric to infer different balance strategies.

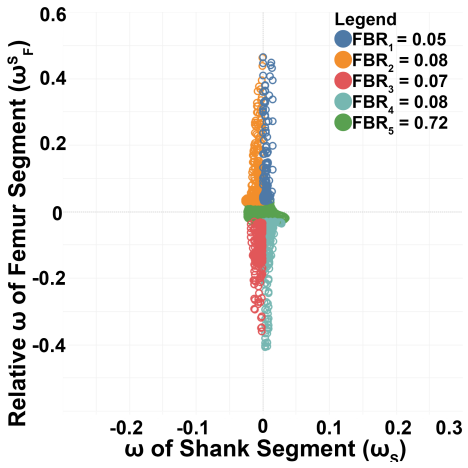

(a) O16 $FBR_n^{AP,RSF}$

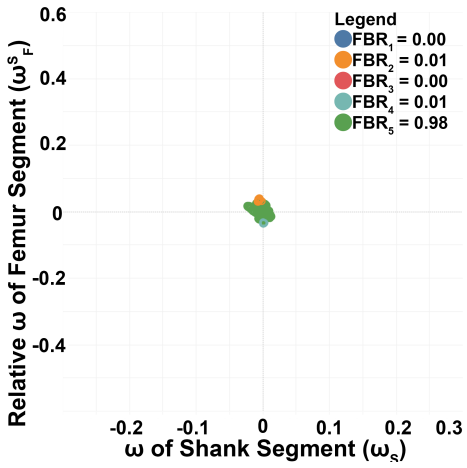

(b) O25 $FBR_n^{AP,RSF}$

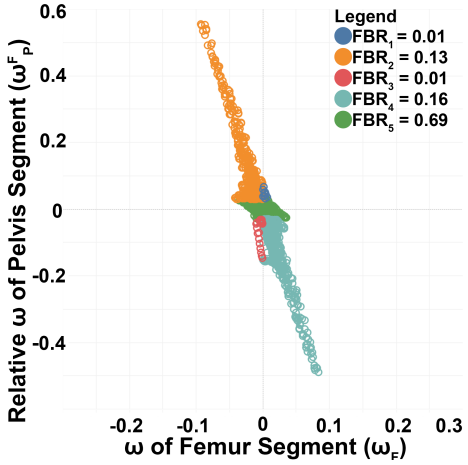

(c) O16 $FBR_n^{AP,RFP}$

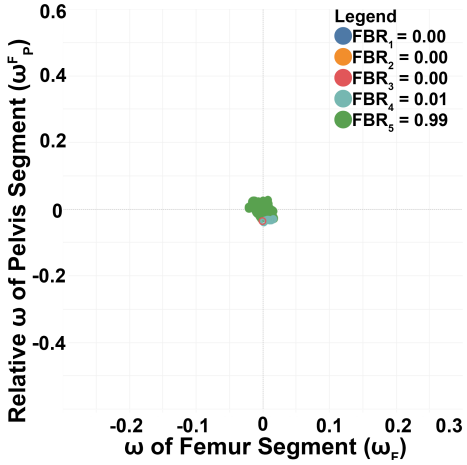

(d) O25 $FBR_n^{AP,RFP}$

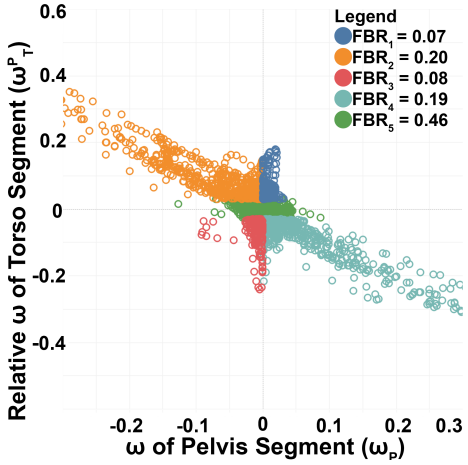

(e) O16 $FBR_n^{AP,PT}$

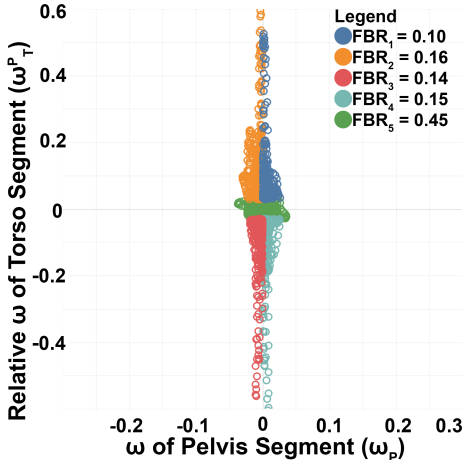

(f) O25 $FBR_n^{AP,PT}$

Figure 4.7: Individual Balance Strategy for Two Older Participants in AP Plane. Green regions represents time points where the segments behave as rigid, single pendulums. Any other areas represents double-pendulum behaviors with different balance strategies.

4.4.3 Changes in Static Balance Technique Between Anatomical Planes

Fig. 4.8 highlights one 30s two-legged standing balance tests for one participant (O16) but in the ML and LG axes. Figs. 4.8b-4.8f highlight $FBR_n^{LG,RSF}$, $FBR_n^{LG,RFP}$, $FBR_n^{LG,RPT}$ for the LG axis and 4.8a-4.8e highlight $FBR_n^{ML,RSF}$, $FBR_n^{ML,RFP}$, $FBR_n^{ML,RPT}$ for the ML axes. The AP axis for this same participant was highlighted in Fig. 4.7b-4.7f. Qualitatively, it is clear that this participant achieves greater rotational velocities in the AP axis than both the ML and LG axis. The lower angular velocities in the ML direction may arise from the greater base of support supplied by the feet, increasing the stability of the ML direction with respect to the AP direction.

Less motion exists in the ML direction for the right shank-femur (Fig. 4.8a) compared to the AP and LG directions due most likely to the little rotation and ML range of motion achievable by the knee. Rotation in the ML direction for the right shank-femur comparison could be evidence, however, of varus-valgus knee motion or internal/external rotation of the femur as a compensatory mechanism to achieve good balance. Examining all three axes can help quantify three dimensional nature of balance technique.

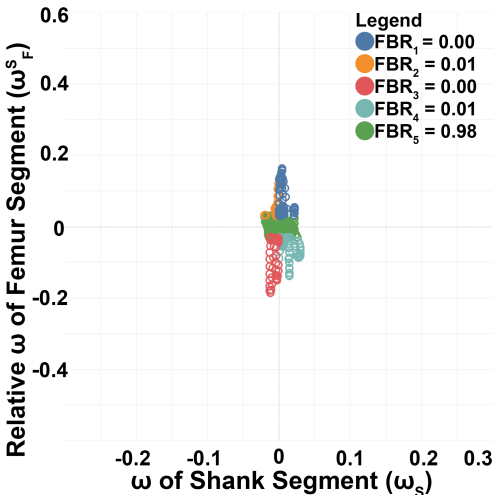

(a) O16 $FBR_n^{ML,RSF}$

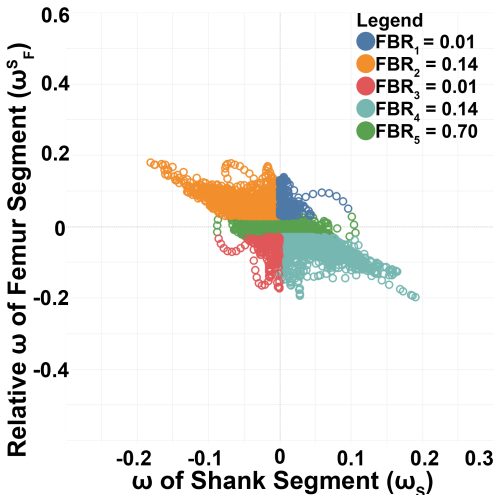

(b) O16 $FBR_n^{LG,RSF}$

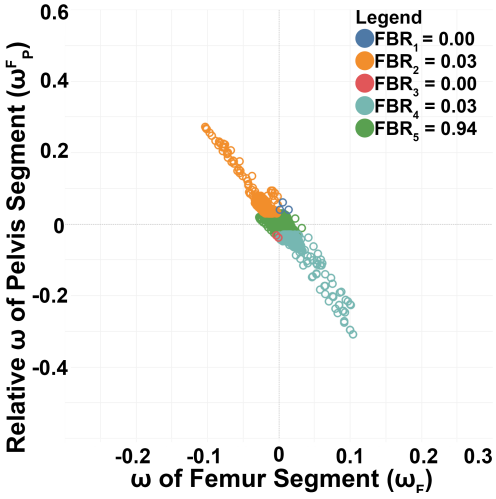

(c) O16 $FBR_n^{ML,RFP}$

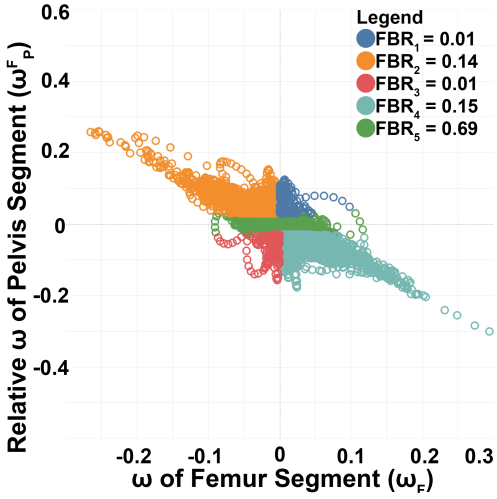

(d) O16 $FBR_n^{LG,RFP}$

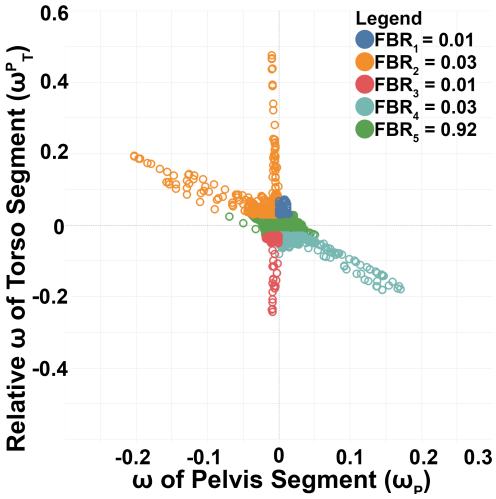

(e) O16 $FBR_n^{ML,PT}$

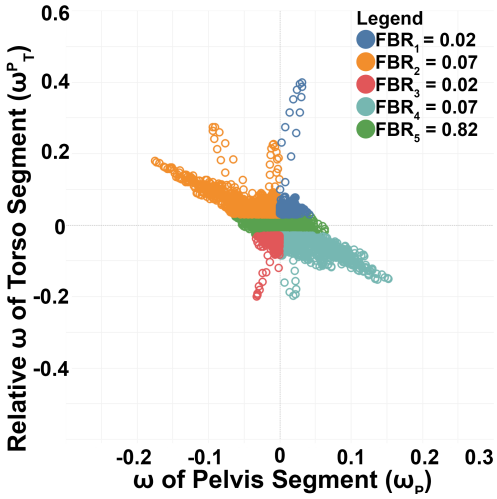

(f) O16 $FBR_n^{LG,PT}$

Figure 4.8: Individual Balance Strategy for One Older Participants in the ML and LG Planes

The qualitative observations made in Sections 4.4.1-4.4.3 illustrate the complex nature of three dimensional postural control. For a more thorough quantification of balance technique, it is therefore necessary to employ this more complex model. Using this metric, we can examine differences between clinical populations, such as dismobile and mobile older adults.

4.5 Experimental Methods

Section 4.2 revealed the limitation in the inverted pendulum model and Section 4.3.1 defined methodology for quantifying balance technique and deviations from the inverted pendulum model. Section 4.4 demonstrated the differing balance techniques used by young and older adults. As a means to evaluate our hypotheses regarding $FBR_n^{P,UL}$ (Section 4.5.1) and demonstrate its ability to quantify clinically relevant differences in static balance, we designed an experiment to evaluate differences in balance technique between three populations: young (Y) and older slow speed walkers (O_S) and older moderate speed walkers (O_M) based on diagnostic criteria for dismobility ($< 0.8m/s$, Section 4.1). This section will discuss the experimental design, data processing, and statistical methods used for this effort.

4.5.1 Statement of Hypotheses

This dataset was used to evaluate the hypotheses that during the SBT there are differences when:

1. comparing ML sway, AP sway and swept area static balance metrics between younger, older slow, and older moderate adults (H1),
2. comparing $FBR_n^{P,LU}$ between younger, older slow, and older moderate adults (H2),

3. comparing $FBR_n^{P,LU}$ in each balance region (H3), and
4. comparing $FBR_n^{P,LU}$ in each anatomical direction (H4).

Since $FBR_n^{P,LU}$ can be used to compare various body segments, hypotheses H2-H5 were explicitly evaluated for five body segment comparisons: pelvis-torso, right femur-pelvis, left femur-pelvis, right shank-femur, and left shank femur. While there are mixed results regarding balance changes due to aging [151, 162, 144], these hypotheses (H1-H2) will allow us to assess whether metrics quantifying static balance technique are sensitive to static balance deficits due to aging. Since there also is evidence of multi-segmented pendulum behavior during static balance tasks [155, 160, 162, 161], H3 and H4 allow us to better understand the extent to which static balance technique deviates from an inverted pendulum model by expanding upon existing models in the literature to include multiple joints (torso, hip, and knee) and to include additional axes of rotation (AP, ML, and LG).

4.5.2 Participants Demographics

Forty-five participants were recruited for this study (15 participants 18-30 years old and 30 above the age 60). Older participants were subdivided into two groups based on gait speed with 16 participants $> 0.8m/s$ and 14 participants $< 0.8m/s$. Full demographics of all three study groups can be found in Table 4.1. The protocol was approved by the Committee on the Use of Humans as Experimental Subjects at MIT. Exclusion criteria included:

1. Atypical neurological conditions or diagnosis including, but not limited to, stroke, Parkinsons Disease, and Multiple Sclerosis that could cause decrements in musculoskeletal function

2. Lower extremity fractures or surgeries performed within the previous six months
3. Any lower extremity joint replacements
4. Physical limitations which would require walking with an assistive device
5. Lower extremity neuropathy from diabetes or other ailments
6. Inability to speak English as a primary language

The full Health Screening Questionaire for this experiment can be found in Appendix A.

Table 4.1: Experimental Group and Participant Demographics

Exp. Group	**Total Subjects**	**Age (yrs)***	**Gender**	**Height (cm)***	**Shoulder Height (cm)***	**Leg Length (cm)***	**Gait Speed (m/s)***
Young (Y)	15	20.7 (2.8)	7 Male 8 Female	166.1 (7.9)	137.1 (7.2)	88.4 (6.4)	0.92 (0.14)
Eld. Slow (O_S)	16	74.3 (7.1)	8 Male 8 Female	163.7 (12.0)	136.9 (11.3)	87.3 (6.1)	0.67 (0.07)
Eld. Mod. (O_M)	14	73.4 (7.7)	8 Male 6 Female	166.0 (8.1)	139.7 (7.8)	87.5 (5.0)	0.86 (0.05)

∗All values are presented as MEAN (STD)

4.5.3 Experimental Design

Each participant was outfitted with 48 reflective markers and 8 strap-on IMUs (Opal IMU, APDM, Inc. Portland OR, USA, Fig. 4.9a). Reflective markers were placed on bony landmarks according to a modified Cleveland Clinic lower body marker set with secondary markers placed on IMUs. IMUs were placed on the sternum, sacrum, femur, shank, and feet. Marker data was collected using 14 Bonita Vicon motion capture cameras (Vicon Motion

Systems, Inc., Los Angeles, CA, USA). Each participant completed three evaluation tasks: the 10m walk test (10MWT), Standing Balance Test, and Timed-Up-And-Go task (TUGT). Tasks were completed in the following configuration for each participant: 1 x 10MWT, 3 x SBT, 15 x TUGT, 3 x SBT, and 1 x 10MWT. Participants were provided with as much rest as needed in between trials and tasks. For this analysis, only marker data was considered from the 10MWT and SBT.

During the SBT, participants were instructed to stand on two feet with eyes open and balance to the best of their ability for 40sec. Participants were instructed not to talk during this time. The first and last 5s of each trial were excluded from analysis to eliminate any effects of the experimenters call outs. Three of 270 SBT trials were excluded from this analysis due to missing pelvis markers that did not make it possible to proceed with data analysis.

4.5.4 Data Processing

Marker data were processed using the Nexus v2.6 software package (Vicon Motion Systems, Inc., Los Angeles, CA, USA). Balance metrics were further processed using Matlab 2018a (The Mathworks, Inc., Natick, MA). Marker position data were filtered using a 6^{th}-order Butterworth 10Hz low-pass filter. Two virtual markers were added for the right/left hip joint center using methods presented by Seidel et al. [165]. Marker data was then used to create three-dimensional coordinate systems for the upper torso (3 markers at C7, left acromion, right acromion), pelvis (4 markers at the R/L ASIS and PSIS), R/L femur (3 markers at the hip joint center, medial and lateral knee), and R/L shank (4 markers at the medial and lateral knee, medial and lateral ankle) (Fig. 4.9b). Angular velocities ($\vec{\omega_U}$ and $\vec{\omega_L}$) and relative angular velocities ($\vec{\omega_U^L}$) were extracted in the antero-posterior (AP), medio-

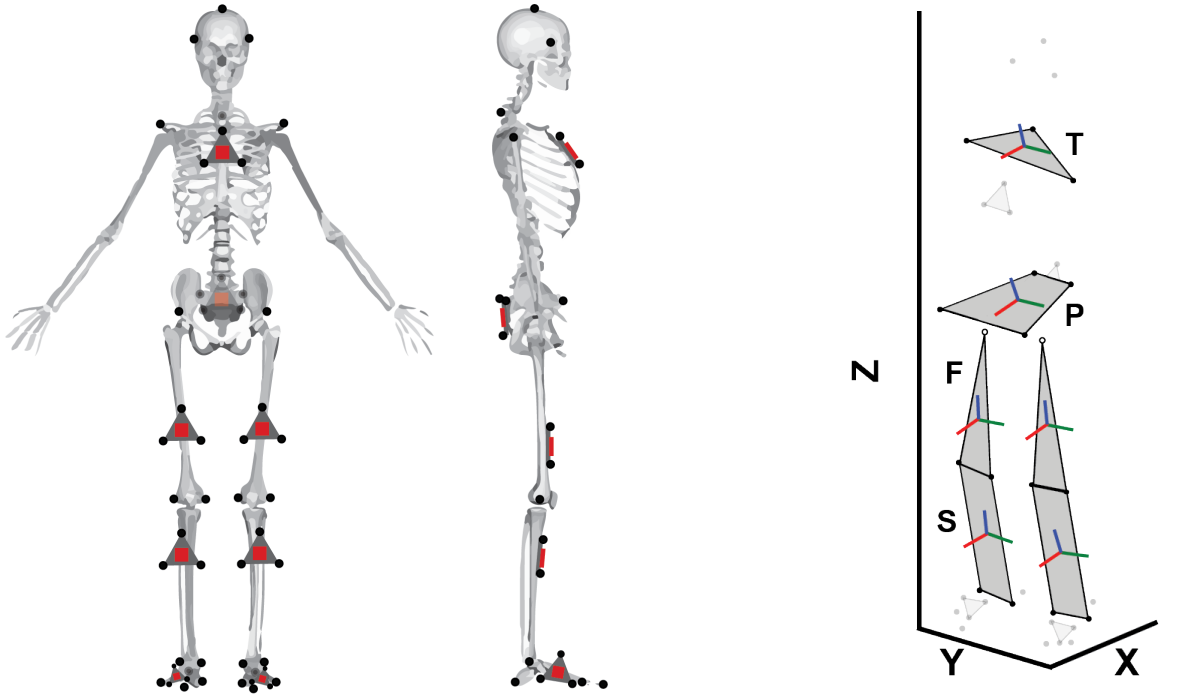

(a)

(b) $FBR_n^{P,LU}$ Body Segments and Coordinate Systems

Figure 4.9: Motion Capture Marker and IMU Locations: a) Approximate reflective marker and IMU locations on corresponding anatomical landmarks. b) Reflective Markers used to define segments of balance model: Shank (S), Femur (F), pelvis (P), and Torso (T). Markers not used for this balance model present with greater opacity. Solid, filled, black markers represent physical markers while markers with white center were virtually created during data processing.

lateral (ML), and longitudinal (LG) directions. This analysis focuses solely on Vicon marker positions and not IMU data. In order to enable their use, additional rotations of the IMU data from the IMU frame to the anatomical body frames is necessary. Since IMU output includes a measure of angular velocity, relative angular velocities would then need to be computed.

In order to compute $FBR_n^{P,LU}$, R is used to define the region in which segments are behaving like an inverted pendulum (Fig. 4.2b, FBR_5) instead of a double pendulum (Fig. 4.2c, FBR_{1-4}), as further described in Section 4.3.1. The nominal region R is defined based on the measurement noise

of the IMUs used for this study ($R = 0.03 rad/s$, Opal IMU, APDM, Inc. Portland OR, USA) as this value sets a higher threshold of noise and allows for appropriate comaprison of marker-based data to IMU-based data in the future. $FBR_n^{P,LU}$ was computed comparing the left shank-femur, right shank-femur, left femur-pelvis, right femur-pelvis, and pelvis-torso (Fig. 4.9b).

Similar to Priplata et al. [151], standard balance metrics were also extracted from right acromion marker at the shoulder: max AP Range, max ML Range, and swept area (product of AP and ML Range). AP Range and ML range were normalized for each participant by dividing the variable by the shoulder marker height ($\times 10^{-3}$). Meanwhile, swept area was normalized by the division of the shoulder marker height squared ($\times 10^{-6}$) [151].

4.5.5 Statistical Analysis

Statistical analysis was performed using SYSTAT 13.1 (Systat Software Inc., USA). To compare with previous literature, standard balance metrics were compared between younger participants (Y) and older adults, subdivided into slow- and moderate- gait speed (O_S and O_M). Three one-factor ANOVA tests were performed assessing the main effect of group (Y, O_S and O_M) on each of the three standard balance metrics extracted (AP Range, ML Range, Swept Area). To conform with model residual normality assumptions, logarithmic transformations were applied to the standard balance metrics. Post-hoc pairwise comparisons using the Tukey procedure were performed when significant main effects were observed.

Dependent measures of FBR could not be fit to a model that met normality residual assumptions. Therefore, non-parametric Kruskal-Wallis (KW) tests were performed to assess main effects of the hypotheses. To evaluate the effect of group on FBR (hypotheses 1-4), using a KW model, a grouping

variable was defined that included the five balance regions, three anatomical axes (AP, ML and LG), and three age groups, resulting in a total of 45 region-plane-group levels. The effect of region-plane-group on FBR value was evaluated by performing a separate KW test for each body segment comparison (5 tests, left shank-femur, right shank-femur, left femur-pelvis, right femur-pelvis, and pelvis-torso). When significant main effects were observed, the Conover-Inman post-hoc test was performed. The 45 total region-plane-groups resulted in a total of 990 post-hoc comparisons. The False Detection Rate controlling procedure [100] was implemented to address the multiple omnibus tests performed ($p_i < \frac{m_0}{m*0.05}$), where m is the total number of tests performed and m_0 is the number of false null hypotheses prior to the correction. Results from the separate right shank-femur, left shank-femur, right femur-pelvis, left femur-pelvis, and pelvis-torso KW tests resulted in an adjusted $\alpha_{RSF} = 0.0407$ ($m_0 = 805$), $\alpha_{LSF} = 0.0411$ ($m_0 = 811$), $\alpha_{RFP} = 0.0443$ ($m_0 = 877$), $\alpha_{LFP} = 0.0440$ ($m_0 = 871$), and $\alpha_{PT} = 0.0436$ ($m_0 = 864$), respectively.

4.6 Results

Mean value and statistics for the standard balance metrics computed can be found in Table 4.2. A significant main effect of experimental group (Y, O_S, and O_M) was found on all three standard balance metrics ($p < 0.05$). Post-hoc analysis revealed a significant difference in ML Range and Swept Area between O_S and O_M (Cohen‘s D = 0.54 and 0.41, respectively) and a significant difference in AP Range between Y and O_S (Cohen‘s D = 0.37).

Region-plane-age group had a significant main effect on FBR value for all segment comparisons, for example, pelvis-torso (PT, Fig. 4.10-4.12), right femur-pelvis (RFP, Fig. 4.13-4.15), right shank-femur (RSF, Fig. 4.16-4.18).

A significant main effect of region-plane-age group on FBR was also found on left femur-pelvis and left shank-femur. Since left sided segments had similar results to right sided segment, discussion will primarily focus on right sided segments and left sided segments are included in the Appendix B. The following sub-sections present additional details on the effects of age (H2), region (H3), and plane (H4) on FBR. In Fig. 4.10-4.18,

Table 4.2: Effect of Experimental Group on Conventional Balance Metrics

	Young*	**older Slow***	**older Mod.***	**p-Value****
AP Range	19.5 (0.8)†	23.1 (1.0)	21.8 (1.0)	0.048
ML Range	10.1 (1.0)	10.4 (0.7)	7.8 (0.6)†	0.003
Swept Area	234.7 (37.8)	286.9 (34.3)	198.7 (21.7)†	0.017

*All values are presented as MEAN (SE)
**Results for individual one-factor ANOVA tests assessing main effect of experiment group on metric
†Indicates significant different from older Slow Group

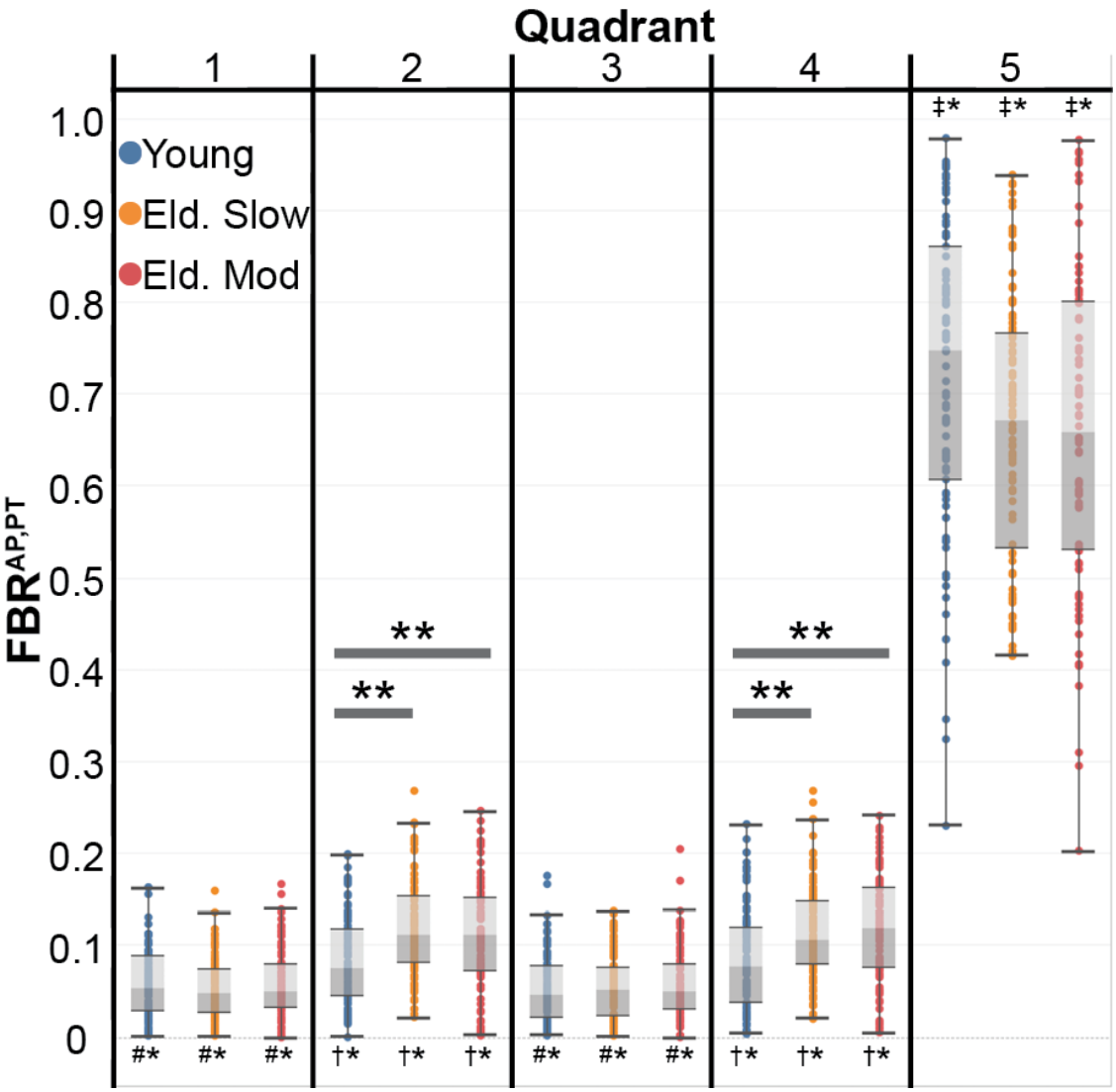

Figure 4.10: $FBR_n^{AP,PT}$ for the AP pelvis-torso comparison. **Indicates for a particular anatomical axis (AP, ML, or LG) and balance region (FBR_{1-5}), a significant difference in experimental group (Y, O_S, or O_M) was detected. *Indicates the particular experimental group and quadrant was significantly different from the other two anatomical planes. #Signifies that for the particular experimental group and anatomical plane the labeled $FBR_{1/3}$ was significantly different from $FBR_{2,4,5}$ in that same experimental group and anatomical plane. †Signifies that for the particular experimental group and anatomical plane the labeled $FBR_{2/4}$ was significantly different from $FBR_{1,3,5}$ in that same experimental group and anatomical plane. ‡Signifies that for the particular experimental group and anatomical plane, FBR_5 was significantly different from FBR_{1-4} in that same experimental group and anatomical plane. More differences were detected but are not listed for simplicity.

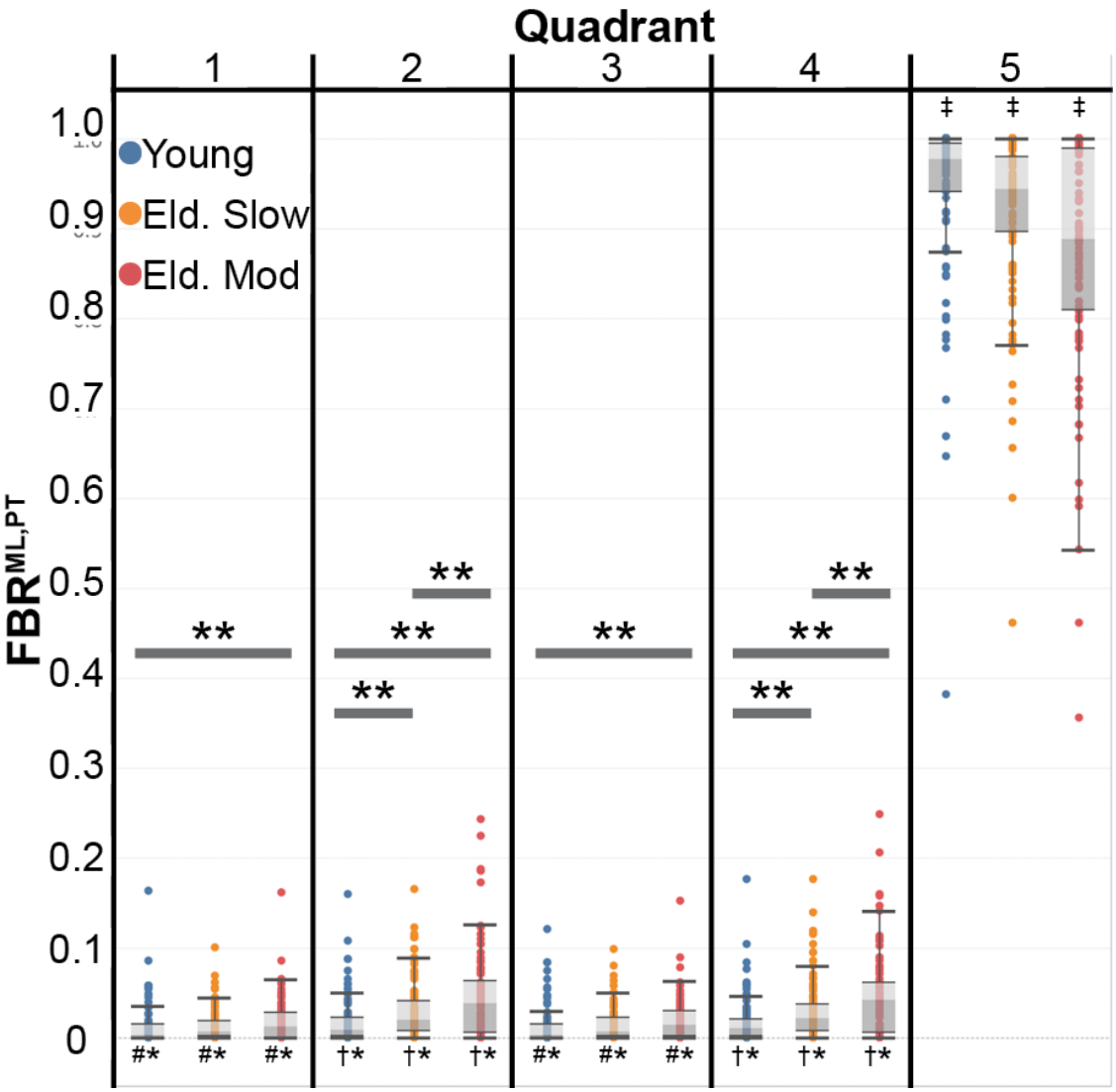

Figure 4.11: $FBR_n^{ML,PT}$ for the ML pelvis-torso comparison. **Indicates for a particular anatomical axis (AP, ML, or LG) and balance region (FBR_{1-5}), a significant difference in experimental group (Y, O_S, or O_M) was detected. *Indicates the particular experimental group and quadrant was significantly different from the other two anatomical planes. #Signifies that for the particular experimental group and anatomical plane the labeled $FBR_{1/3}$ was significantly different from $FBR_{2,4,5}$ in that same experimental group and anatomical plane. †Signifies that for the particular experimental group and anatomical plane the labeled $FBR_{2/4}$ was significantly different from $FBR_{1,3,5}$ in that same experimental group and anatomical plane. ‡Signifies that for the particular experimental group and anatomical plane, FBR_5 was significantly different from FBR_{1-4} in that same experimental group and anatomical plane. More differences were detected but are not listed for simplicity.

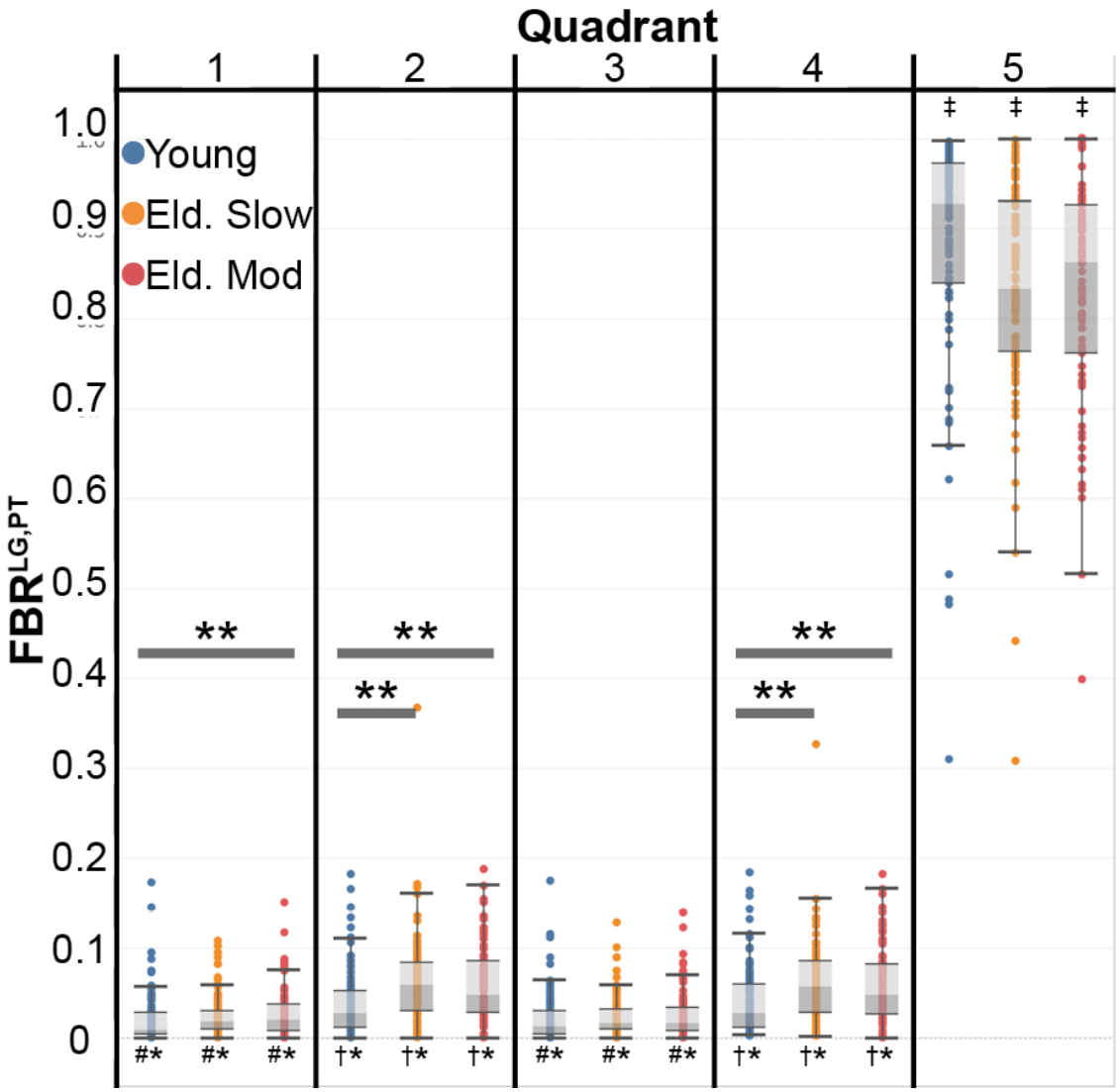

Figure 4.12: $FBR_n^{LG,PT}$ for the LG pelvis-torso comparison. **Indicates for a particular anatomical axis (AP, ML, or LG) and balance region (FBR_{1-5}), a significant difference in experimental group (Y, O_S, or O_M) was detected. *Indicates the particular experimental group and quadrant was significantly different from the other two anatomical planes. #Signifies that for the particular experimental group and anatomical plane the labeled $FBR_{1/3}$ was significantly different from $FBR_{2,4,5}$ in that same experimental group and anatomical plane. †Signifies that for the particular experimental group and anatomical plane the labeled $FBR_{2/4}$ was significantly different from $FBR_{1,3,5}$ in that same experimental group and anatomical plane. ‡Signifies that for the particular experimental group and anatomical plane, FBR_5 was significantly different from FBR_{1-4} in that same experimental group and anatomical plane. More differences were detected but are not listed for simplicity.

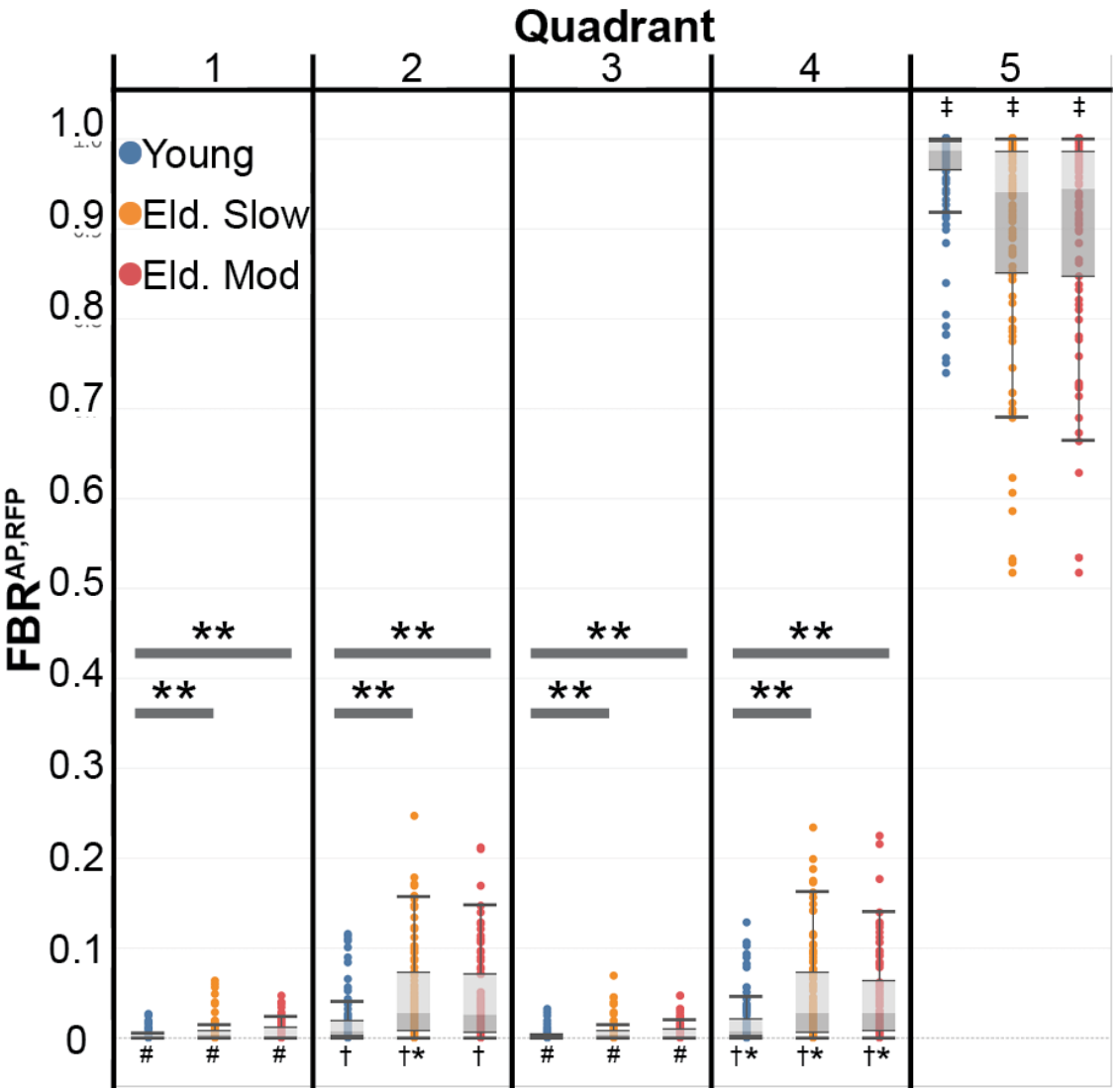

Figure 4.13: $FBR_n^{AP,RFP}$ for the AP right femur-pelvis comparison. **Indicates for a particular anatomical axis (AP, ML, or LG) and balance region (FBR_{1-5}), a significant difference in experimental group (Y, O_S, or O_M) was detected. *Indicates the particular experimental group and quadrant was significantly different from the other two anatomical planes. #Signifies that for the particular experimental group and anatomical plane the labeled $FBR_{1/3}$ was significantly different from $FBR_{2,4,5}$ in that same experimental group and anatomical plane. †Signifies that for the particular experimental group and anatomical plane the labeled $FBR_{2/4}$ was significantly different from $FBR_{1,3,5}$ in that same experimental group and anatomical plane. ‡Signifies that for the particular experimental group and anatomical plane, FBR_5 was significantly different from FBR_{1-4} in that same experimental group and anatomical plane. More differences were detected but are not listed for simplicity.

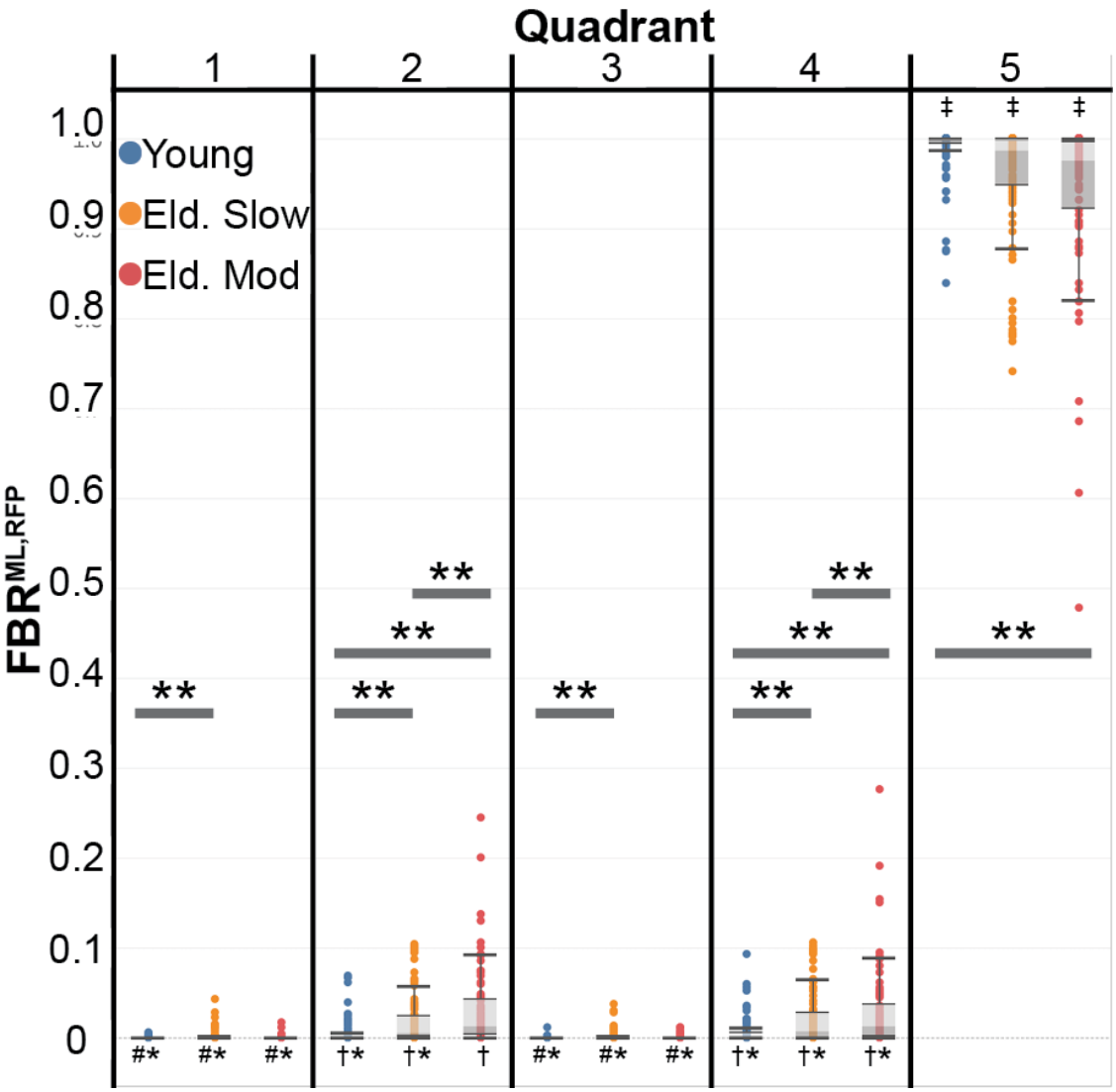

Figure 4.14: $FBR_n^{ML,RFP}$ for the ML right femur-pelvis comparison. **Indicates for a particular anatomical axis (AP, ML, or LG) and balance region (FBR_{1-5}), a significant difference in experimental group (Y, O_S, or O_M) was detected. *Indicates the particular experimental group and quadrant was significantly different from the other two anatomical planes. #Signifies that for the particular experimental group and anatomical plane the labeled $FBR_{1/3}$ was significantly different from $FBR_{2,4,5}$ in that same experimental group and anatomical plane. †Signifies that for the particular experimental group and anatomical plane the labeled $FBR_{2/4}$ was significantly different from $FBR_{1,3,5}$ in that same experimental group and anatomical plane. ‡Signifies that for the particular experimental group and anatomical plane, FBR_5 was significantly different from FBR_{1-4} in that same experimental group and anatomical plane. More differences were detected but are not listed for simplicity.

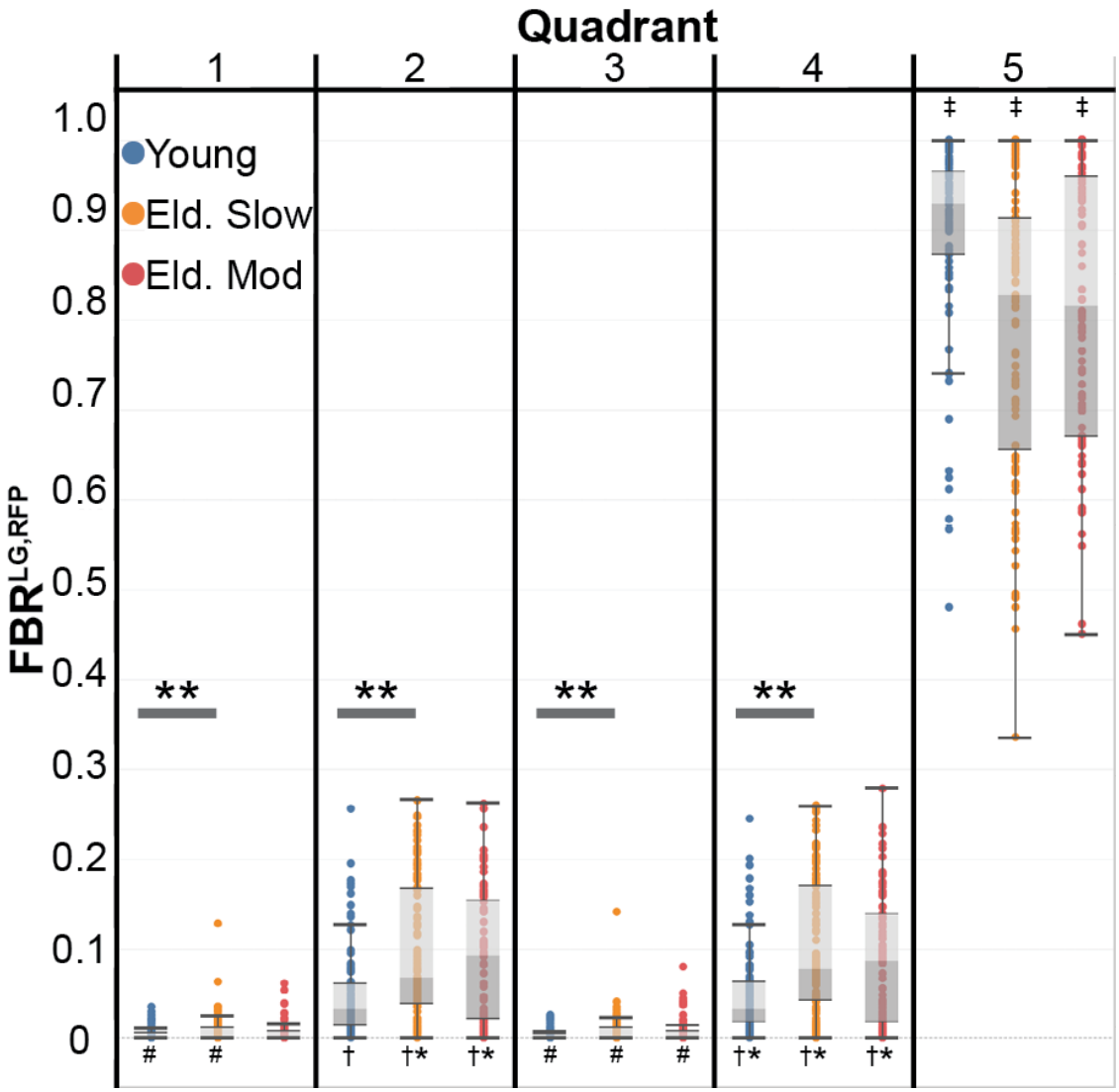

Figure 4.15: $FBR_n^{LG,RFP}$ for the LG right femur-pelvis comparison. **Indicates for a particular anatomical axis (AP, ML, or LG) and balance region (FBR_{1-5}), a significant difference in experimental group (Y, O_S, or O_M) was detected. *Indicates the particular experimental group and quadrant was significantly different from the other two anatomical planes. #Signifies that for the particular experimental group and anatomical plane the labeled $FBR_{1/3}$ was significantly different from $FBR_{2,4,5}$ in that same experimental group and anatomical plane. †Signifies that for the particular experimental group and anatomical plane the labeled $FBR_{2/4}$ was significantly different from $FBR_{1,3,5}$ in that same experimental group and anatomical plane. ‡Signifies that for the particular experimental group and anatomical plane, FBR_5 was significantly different from FBR_{1-4} in that same experimental group and anatomical plane. More differences were detected but are not listed for simplicity.

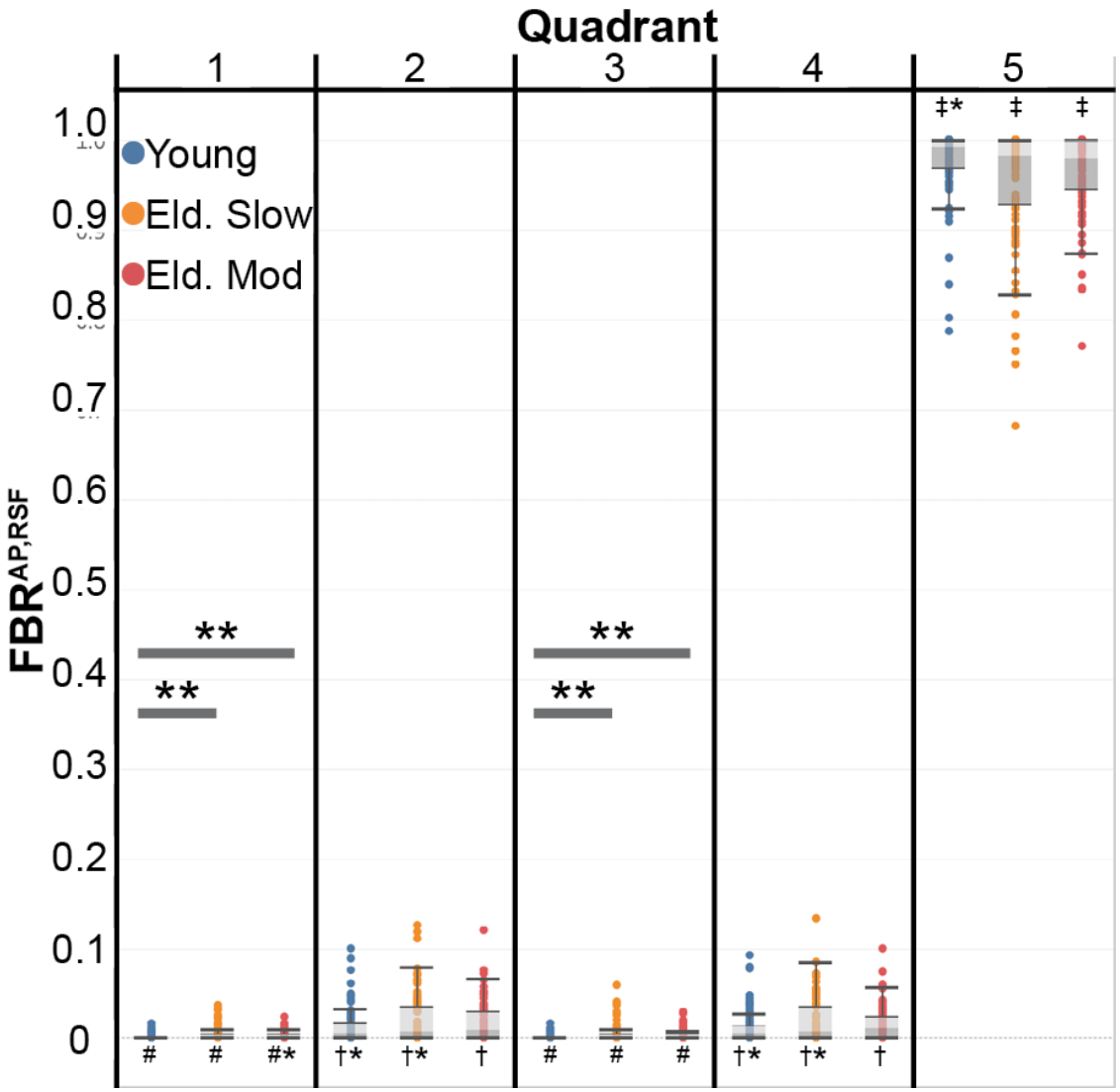

Figure 4.16: $FBR_n^{AP,RSF}$ for the AP right shank-femur comparison. **Indicates for a particular anatomical axis (AP, ML, or LG) and balance region (FBR_{1-5}), a significant difference in experimental group (Y, O_S, or O_M) was detected. *Indicates the particular experimental group and quadrant was significantly different from the other two anatomical planes. #Signifies that for the particular experimental group and anatomical plane the labeled $FBR_{1/3}$ was significantly different from $FBR_{2,4,5}$ in that same experimental group and anatomical plane. †Signifies that for the particular experimental group and anatomical plane the labeled $FBR_{2/4}$ was significantly different from $FBR_{1,3,5}$ in that same experimental group and anatomical plane. ‡Signifies that for the particular experimental group and anatomical plane, FBR_5 was significantly different from FBR_{1-4} in that same experimental group and anatomical plane. More differences were detected but are not listed for simplicity.

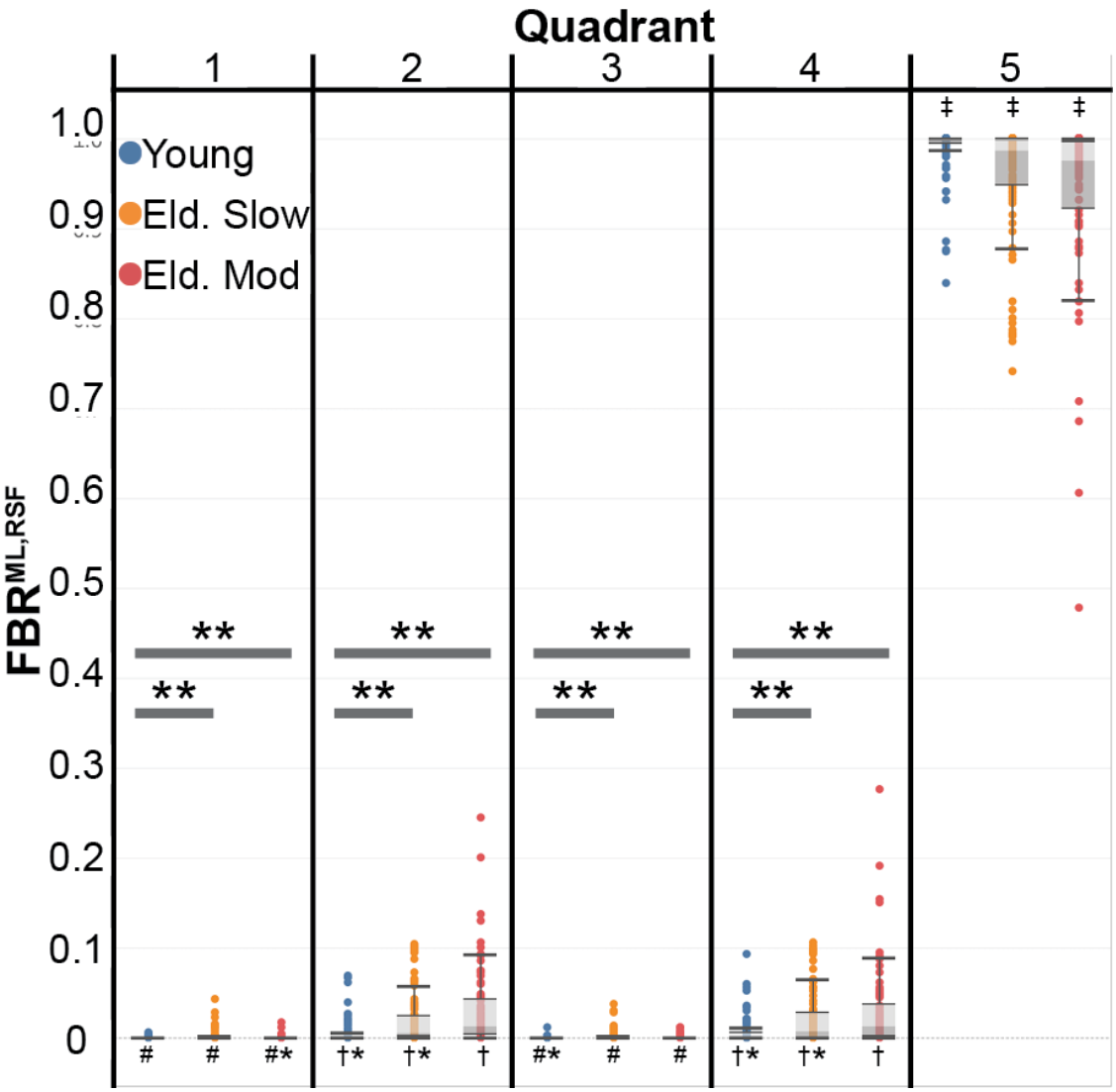

Figure 4.17: $FBR_n^{ML,RSF}$ for the ML right shank-femur comparison. **Indicates for a particular anatomical axis (AP, ML, or LG) and balance region (FBR_{1-5}), a significant difference in experimental group (Y, O_S, or O_M) was detected. *Indicates the particular experimental group and quadrant was significantly different from the other two anatomical planes. #Signifies that for the particular experimental group and anatomical plane the labeled $FBR_{1/3}$ was significantly different from $FBR_{2,4,5}$ in that same experimental group and anatomical plane. †Signifies that for the particular experimental group and anatomical plane the labeled $FBR_{2/4}$ was significantly different from $FBR_{1,3,5}$ in that same experimental group and anatomical plane. ‡Signifies that for the particular experimental group and anatomical plane, FBR_5 was significantly different from FBR_{1-4} in that same experimental group and anatomical plane. More differences were detected but are not listed for simplicity.

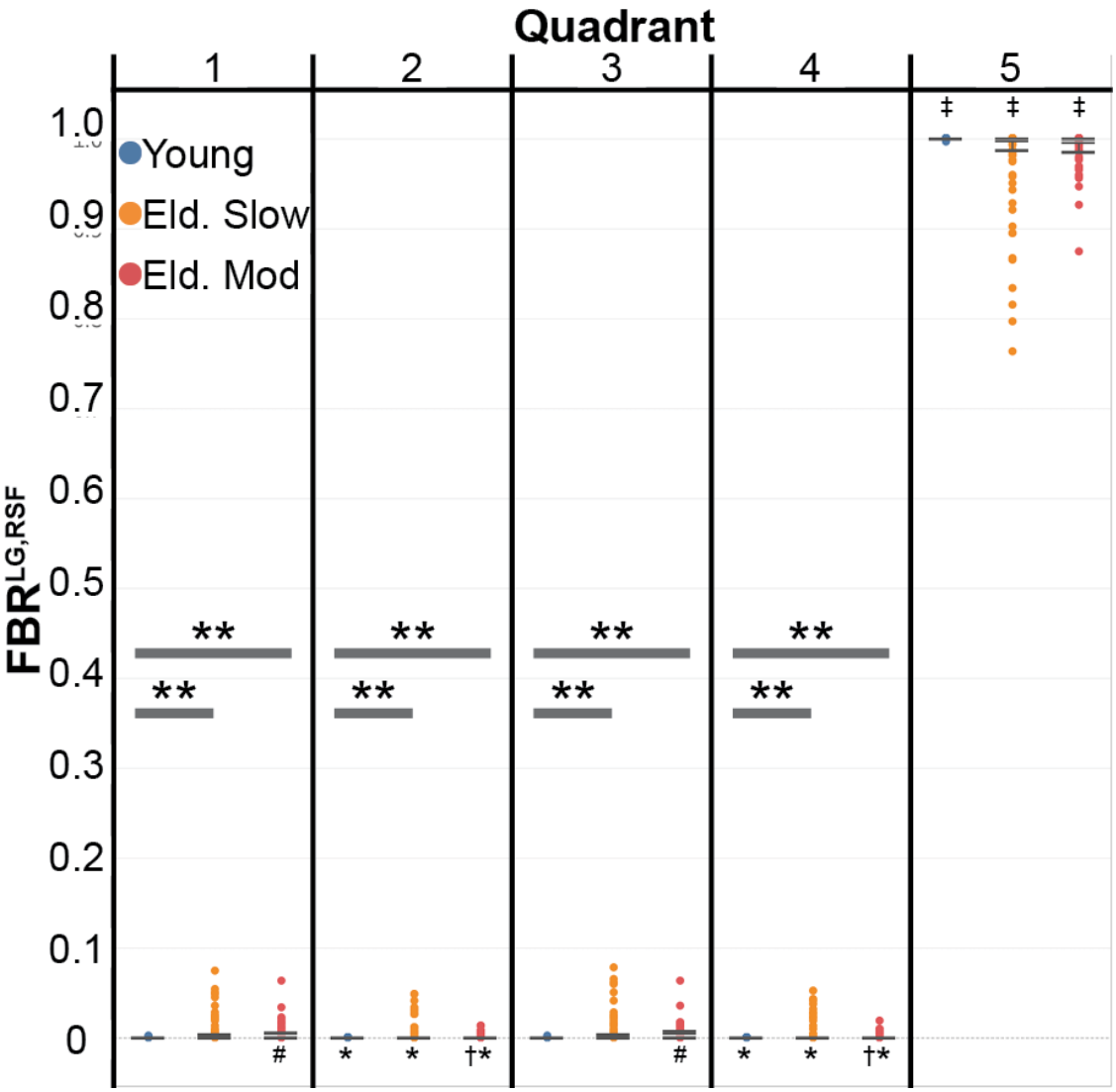

Figure 4.18: $FBR_n^{LG,RSF}$ for the LG right shank-femur comparison. **Indicates for a particular anatomical axis (AP, ML, or LG) and balance region (FBR_{1-5}), a significant difference in experimental group (Y, O_S, or O_M) was detected. *Indicates the particular experimental group and quadrant was significantly different from the other two anatomical planes. #Signifies that for the particular experimental group and anatomical plane the labeled $FBR_{1/3}$ was significantly different from $FBR_{2,4,5}$ in that same experimental group and anatomical plane. †Signifies that for the particular experimental group and anatomical plane the labeled $FBR_{2/4}$ was significantly different from $FBR_{1,3,5}$ in that same experimental group and anatomical plane. ‡Signifies that for the particular experimental group and anatomical plane, FBR_5 was significantly different from FBR_{1-4} in that same experimental group and anatomical plane. More differences were detected but are not listed for simplicity.

4.6.1 The Effect of Age and Gait Speed on Balance

While the text below highlights significant differences in FBR due to age and gait speed, Table 4.19 also contains all these comparisons graphically. For the pelvis-torso comparison (Fig. 4.10-4.12), all anatomical planes (AP, ML, LG) showed the trend $FBR_{2,4}^{O_S,E_f} > FBR_{2,4}^{Y}$ (Effect size, r = 0.17-0.54). There were no differences between the two older age groups in regions 2 and 4 in the AP and LG axes (Fig. 4.10 and 4.11). For the ML axis, $FBR_{2,4}^{O_M} > FBR_{2,4}^{O_S}$ (Fig. 4.11, r = 0.20 and 0.21, respectively). The ML axis also showed a significant difference between Y and O_M in regions 1 and 3 ($FBR_{1,3}^{O_M} > FBR_{1,3}^{Y}$, r = 0.18 and 0.21, respectively). The LG axis displayed one similar trend ($FBR_{1}^{O_M} > FBR_{1}^{Y}$, r = 0.16), but only for balance region 1. For all three axes in the pelvis-torso comparison, there was no significant differences between experimental groups in FBR_5.

For the right femur-pelvis comparison (Fig. **??**), all anatomical planes showed the trend $FBR_{1,2,4}^{O_S} > FBR_{1,2,4}^{Y}$ (r = 0.17-0.73). Anatomical axes AP (Fig. 4.13) and ML (Fig. 4.14) also showed significant differences between Y and O_M in balance regions 2 and 4 ($FBR_{2,4}^{O_M} > FBR_{2,4}^{Y}$, r = 0.31-0.73). The AP axis also showed differences between Y and O_M in balance regions 1 and 3 ($FBR_{1,3}^{O_M} > FBR_{1,3}^{Y}$. Significant differences between older groups only existed in the ML axis and in balance regions 2 and 4 (Fig. 4.14, $FBR_{2,4}^{O_M} > FBR_{2,4}^{O_S}$, r = 0.17 and 0.16, respectively). For all three axes in the right femur-pelvis comparison, there was no differences between experimental groups in FBR_5 with the exception of the ML axis and groups Y and O_M ($FBR_{5}^{Y} > FBR_{5}^{O_M}$, r = 0.15).

For the right shank-femur comparison (Fig. 4.16-4.18), all anatomical planes showed the trend $FBR_{1,3}^{O_S,O_M} > FBR_{1,3}^{Y}$, r = 0.18-0.51). The ML (Fig. 4.17) and LG (Fig. 4.18) also showed the trend $FBR_{2,4}^{O_S,O_M} > FBR_{2,4}^{Y}$, r =

0.17-0.57). There were no significant differences between the two older groups for the right shank-femur comparison. In addition, there was no differences between all experimental groups in FBR_5 in all three axes.

		AP Axis			ML Axis			LG Axis		
	Balance Region	Y vs. E_S	Y vs. E_M	E_S vs. E_M	Y vs. E_S	Y vs. E_M	E_S vs. E_M	Y vs. E_S	Y vs. E_M	E_S vs. E_M
Pelvis-Torso	FBR_1					<			<	
	FBR_2	<<	<		<	<<	<	<<	<<	
	FBR_3					<				
	FBR_4	<	<		<<	<<<	<	<<	<<	
	FBR_5									
R. Femur-Pelvis	FBR_1	<<	<		<			<		
	FBR_2	<<	<<		<<<	<<<	<	<		
	FBR_3	<<	<		<			<		
	FBR_4	<<	<<		<<	<<<	<	<		
	FBR_5					>				
R. Shank-Femur	FBR_1	<	<		<<	<<<		<<	<<	
	FBR_2				<<	<<<		<	<	
	FBR_3	<	<		<<	<<		<<	<<	
	FBR_4				<<<	<<<		<	<	
	FBR_5									

Figure 4.19: Summary of all comparisons and effect sizes pertaining to the effect of age and gait speed on value of FBR. The $<$ and $>$ symbols represent if the first value is greater than or less than the second value, for example, $Y < O_S$. The number of symbols is representative of the effect size for the corresponding post hoc comparison: a) $>$ or $<$ Small effect size, $r < 0.30$, b) $>>$ or $<<$ Moderate effect size, $0.30 < r < 0.50$, and c) $>>>$ or $<<<$ Large effect size, $r > 0.50$.

4.6.2 The Effect of Balance Region on $FBR^{P,UL}$

Post-hoc analysis revealed the general trend that for all three comparisons (pelvis-torso, right femur-pelvis, and right shank-femur), all experimental groups (Y, O_S, and O_M) and anatomical axes (AP, ML, LG) $FBR_5 > FBR_{1-4}$ (r = 0.52 - 2.6). In general as well for all comparisons, experimental groups and anatomical axes, $FBR_{2,4} > FBR_{1,3}$ (r = 0.16-0.63) with no significant differences between FBR_1 and FBR_3 and no significant dif-

ferences between FBR_2 and FBR_4. The exception to this trend was in the right shank-femur comparison in the LG anatomical axis and for experimental groups Y and O_S where there were inconsistent differences between FBR_{1-4}; however, FBR_5 was still greater than and significantly different from FBR_{1-4}.

4.6.3 The Effect of Anatomical Plane on FBR_n^{UL}

When comparing the pelvis-torso, (Fig. 4.10-4.12), for each of the three experimental groups (Y, O_S, and O_M) and balance regions 1-4 (FBR_{1-4}), the three anatomical axes were significantly different following the general trend $FBR^{AP} > FBR^{LG} > FBR^{ML}$ (r = 0.17-1.01). Since the summed value of $FBR_{1-5} = 1$ within each anatomical axis, for each of the three experimental groups in FBR_5 the opposite trend existed, $FBR^{AP} < FBR^{ML,LG}$, but there was no significant differences between FBR^{ML} and FBR^{LG}.

When comparing the right femur-pelvis (Fig. 4.13-4.15), for each of the three experimental groups, $FBR_{1,3}^{AP,LG} > FBR_{1,3}^{ML}$ (r = 0.31-0.51) with no difference between anatomical axes AP and LG. For young and older slow participants, $FBR_{2,4}^{LG} > FBR_{2,4}^{AP} > FBR_{2,4}^{ML}$ (r = 0.36-1.0). For older moderate participants $FBR_4^{LG} > FBR_4^{AP} > FBR_4^{ML}$, however, $FBR_4^{LG} > FBR_4^{AP,ML}$ with no significance differences between AP and ML anatomical axes. For all experimental groups, $FBR_5^{ML} > FBR_5^{LG}$, meanwhile FBR_5^{AP} was not significantly different from either FBR_5^{ML} or FBR_5^{LG}.

When comparing the right shank-femur (Fig. 4.13-4.15), for Y and O_S experimental groups, $FBR_{2,4}^{AP} > FBR_{2,4}^{ML} > FBR_{2,4}^{LG}$ (r = 0.16-0.89); however, for regions 1 and 3 there were no significant differences between anatomical axes. For experimental group O_M, $FBR_{2,4}^{LG} < FBR_{2,4}^{AP,ML}$ (r = 0.63-0.75) with no significant difference between axes AP and ML. When con-

sidering FBR_5, experimental group Y had an effect of anatomical axis with $FBR^{AP} < FBR^{ML,LG}$ (r = 0.15-0.23). $FBR_5^{AP} < FBR_5^{LG}$ (r = 0.15) for experimental group O_S. There were no differences between anatomical axes for FBR_5 within experimental group O_M.

		Young Group			Elderly Slow Group			Elderly Moderate Group		
	Balance Region	AP vs.ML	AP vs.LG	ML vs.LG	AP vs.ML	AP vs.LG	ML vs.LG	AP vs.ML	AP vs.LG	ML vs.LG
Pelvis-Torso	FBR_1	>>>	>>>	<<	>>>	>>>	<<	>>>	>>>	<
	FBR_2	>>>	>>>	<<	>>>	>>>	<<<	>>>	>>	<
	FBR_3	>>>	>>>	<<	>>>	>>>	<<	>>>	>>>	<
	FBR_4	>>>	>>>	<<<	>>>	>>>	<<<	>>>	>>>	<
	FBR_5	<	<		<	<		<	<	
R. Femur-Pelvis	FBR_1	>>		>>	>>>		>>	>>>		>>
	FBR_2	>>>	<<<	<<<	>>	<<	<<<		<<	<<
	FBR_3	>>		>>	>>		>>	>>		>>
	FBR_4	>>>	<<<	<<<	>>	<<	<<<	>	<<	<<<
	FBR_5			>			>			>
R. Shank-Femur	FBR_1		>				>	<		>
	FBR_2	>>>	>>>	>	<	>>>	>>		>>>	>>>
	FBR_3		>				>			>
	FBR_4	>>>	>>>		<	>>>	>>>		>>>	>>>
	FBR_5	<	<			<				

Figure 4.20: Summary of all comparisons and effect sizes pertaining to the effect of anatomical axis on value of FBR. The < and > symbols represent if the first value is greater than or less than the second value, for example, $Y < O_S$. The number of symbols is representative of the effect size for the corresponding post hoc comparison: a) > or < Small effect size, $r < 0.30$, b) >> or << Moderate effect size, $0.30 < r < 0.50$, and c) >>> or <<< Large effect size, $r > 0.50$.

4.7 Discussion

This chapter aimed to develop new methods for evaluating static balance technique. The approach was to develop a new metric, termed the frequency in balance region ($FBR_n^{P,LU}$), that quantified the frequency of time during which body segments deviate from an inverted pendulum model. This

measure was numerically defined in Section 4.3 and then used to evaluated differences in static balance technique in three population: young adults (Y), older slow gait speed adults (O_S), and older moderately gait speed adults (O_M). We explicitly tested the hypotheses that differences existed when:

1. comparing ML sway, AP sway and swept area static balance metrics between younger, older slow and older moderate adults (H1),
2. comparing $FBR_n^{P,LU}$ between younger, older slow and older moderate adults (H2),
3. comparing $FBR_n^{P,LU}$ in each balance region (H3), and
4. comparing $FBR_n^{P,LU}$ in each anatomical direction (H4).

The first hypothesis of this work (H1) aimed to compare the population of participants in this experiment to standard, outcome-based results from the literature. As previously discussed, Priplata et al. [151] only found small differences between younger and older adults when computing swept area. While this experiment observed a small difference, it was only significantly different between O_M and Y, not between O_S and Y. The difference, however, was opposite that observed by Priplata et al. [151] with $Y > O_M$ as oppose to older being greater than young. Since swept area is a product of AP and ML range, the results presented here could be opposite that of Priplata et al. [151] due to O_M participants having a trending lower ML range than younger participants. Melzer et al. [144] compared older faller to non-fallers and only found differences in the ML range with fallers having a significantly greater ML range than non-fallers. While not a direct comparison, O_S has a significantly higher ML range than O_M. Since slower gait speeds are associated with higher rates of falls [124, 125], the present study is consistent with these trends. Swept area using a single marker also makes the inverted pendulum

assumption. Therefore, the limited differences in swept area do not mean the same balance strategy was used. A similar swept area could be obtained with different balance strategies.

Hypothesis 2 of this work aimed to see if our new metric quantifying balance technique ($FBR_n^{P,LU}$) was sensitive to balance changes that occur as a result of aging and possible balance changes that might be associated with changes in older gait speed. The results presented here support this hypothesis, however, small effect sizes between O_M and O_S groups question the clinical relevance of differences due to gait speed. In general, older participants had a greater task percentage in FBR_{1-4} compared to the younger individuals. In other words, older participants spent a greater task percentage deviating from an inverted pendulum than younger participants. These age differences primarily existed for the AP axis (femur-pelvis and pelvis-torso) and ML axis (shank-femur and femur-pelvis) as seen in Table 4.19. The gluteus medius, a hip abductor, plays an important role in ML stability, especially with increasing walking speeds [122]. Tirosh et al. [166] found decreased recruitment in the gluteus medius in older adults, which could lead to decreased stability during walking compared to younger adults. Decreased gluteus medius recruitment was also observed when Lim et al. [167] controlled for gait speed thereby contributed less to ML stability. Decreased gluteus medius recruitment or strength could be contributing to the results seen here where older adults pelvis tended to rotated more in the ML axis relative to the femur as seen in Fig. 4.14 and Table 4.20. This study did not directly measure muscle strength and it is therefore difficult to conclude if the differences observed due to aging are in fact due to weakened muscle groups. Despite small effect sizes, $FBR^{ML,RFP}$ differences between O_S and O_M groups could also be early evidence of greater weakening in hip mus-

cles, such as the gluteus medius, in slower walkers, but it is uncertain if this difference is clinically relevant. Finally, greater time spent in $FBR_{2,4}$ when comparing the pelvis-torso and femur-pelvis could be representative of decreased trunk stability leading to more torso motion relative to the pelvis and more pelvis motion relative to the femur. Decreased trunk stability is also correlated with balance control [168].

Continuing to assess H2, large effects sizes and difference between young and older participants were observed when comparing the shank-femur in the ML axis. Ankle ROM and power tend to decrease as a result of aging [169, 159, 170]. Therefore, it is possible that trends observed when comparing shank-femur are due to upper segments and joints (i.e. knee, hip, and core) compensating for lack of ankle motion and power. Additionally, knee proprioception decreases with aging [171], which could contribute to more knee motion during static balance. The knee joint is primarily a hinge joint moving along its AP axis. Most of the shank-femur trends, which are indicative of knee motion, are observed off-axis (ML and LG) which could be due in part to decreased overall knee stability, increasing varus-valgus motion.

The data here also supported Hypothesis 3 that different percentages of time were spent in each balance region, with $FBR_5 > FBR_{1-4}$ in nearly all axes (AP, ML, and LG), segment comparisons (PT, RFP, and RSF), and experimental group (Y, O_S, and O_M). This data also supported $FBR_{2,4} > FBR_{1,3}$ for a majority of axes, segments, and experimental groups. As shown in Fig. 4.5, $FBR_{2/4}$ correspond to a balance strategy in which the upper segment rotates with a larger magnitude in the opposite direction of the lower segment, consistent with observations made by Aramaki et al. [160]. Unlike Aramaki et al. [160], this work is able to decouple the relative angular velocity of upper segments into the AP, ML, and LG axes. Additionally, Aramaki

et al. [160] only quantified relative motion between the head and hips. Here, we are able to decompose pelvis from torso motion, femur from pelvis motion, and shank from femur motion. The additional decomposition of balance strategy into multiple axes allows for a more comprehensive understanding of balance strategy. As shown in Sections 4.4.1-4.4.3, different participants used strategies relying more on the torso, while others used strategies involving all joint. Additionally, we find differences between older gait speed groups, specifically in the ML direction that were not present in the AP direction, which could be attributed to weakness in certain ML stabilizing muscle groups. The ability to decompose balance technique into the three rotation axes could lead to more informed strengthening exercises.

Finally, the data supports H4 that $FBR_n^{P,LU}$ does change across anatomical axis, as highlighted in Table 4.20. The axis with the highest percentage of time in FBR_{1-4} was not consistent between segment comparisons. For example, the AP axis had a greater percentage of the task in FBR_{1-4} than ML and LG when comparing pelvis-torso, while the LG axis had a greater percentage of the task in FBR_{1-4} than AP and ML when comparing femur-pelvis. For each segment comparison, the axis with the highest percentage of time spent in FBR_{1-4} could be the most vulnerable to muscle weakening or injury. In the case of the AP axis for the pelvis torso, for example, if participants have more weakening of the core or back muscles, it is possible that the time spent in FBR_{1-4}^{AP} could increase and make them more vulnerable to loss of balance control. Results indicating more time spent in FBR_{1-4}^{AP} could inform PTs and OTs what muscle groups to generally prescribe patients to strengthen who might be at risk of loosing balance. From the examples presented in this paragraph, that would mean increasing core and back strength to maintain stability in the spine and gluteus strengtheners for the hips, as

also discussed previously. It is also important to note that when comparing the shank-femur, younger adults spent more time with reciprocal double pendulum behavior ($FBR_{2,4}$) in the AP axis than ML. Meanwhile, O_M there was no difference between the AP and ML plane, while O_S spent less time in AP than ML although the effect size was small. Trends of the shank-femur $FBR_{2,4}^{AP} < FBR_{2,4}^{ML}$ could be further evidence of less ML stability in the O_S as we start to see these participants spend more percentages of the task with relative motion between segments in the ML direction.

This work operated under the assumption that a simple inverted pendulum model (Section 4.2) was not sufficient to appropriately quantify static balance technique. Previous literature using younger populations shows that body segments above the ankle joints are fairly rigid, with a linear relationship in marker displacement as a function of height from the ankle joint [155]. Previous work also uses double pendulum models by adding a joint about the hips [160, 162]. Only Kim et al. [163] explored other joints beyond the hips by looking at double pendulum behavior about the knee joint. Little other work explores other joints despite evidence showing some knee, hip, and torso flexion exists in the very work aimed at validating the inverted pendulum model [155]. On average young and older participants spent 27% and 35%, respectively, of task time deviating from an inverted pendulum in the AP axis. Our work demonstrates that there are instances of time where assuming inverted pendulum behavior is not appropriate. Assessing the behavior of multiple joints and axes provides a comprehensive picture of a participant's balance strategy that could inform on certain muscle weakness and compensatory strategies that would be missed using a single pendulum model. Aramaki et al. [160] also agreed the usefulness of a double pendulum, showing that the upper torso tended to move in the opposite direction as the lower leg segment,

but there were times where these segments also moved in the same direction. The data presented here shows a general $FBR_{2,4} > FBR_{1,3}$, where time in $FBR_{2,4}$ is time where the upper segment is moving in the opposite direction as the lower segment. Our results, however, extend upon that of Aramaki et al. [160] because of our decomposition into multiple axes and joints. Additionally, Accornero et al. [162] found that there existed rotational motion about the hips. Here we find that more time spent FBR_{1-4} in the LG axis than ML axis when comparing the pelvis and torso, indicative of longitudinal twisting of the upper body relative to the hips. When comparing the femur to pelvis, we fine more time spent in $FBR_{2,4}$ in the LG axis compared to both the AP and ML axes. Both findings in the pelvis-torso and femur-pelvis agree with findings by Accornero et al. [162] illustrating rotation at the hips during static balance tasks, but a balance description uses FBR is able to see how other segments, specifically the torso and femur, are able to compensate for this hip motion.

Manchester et al. [159] first described differences between young and older balance strategies, finding that older adults tended to use more of a hip-based strategy as compared to ankle-based for younger adults in the AP plane. These results are supported here as we see greater percentage of task being spent outside of FBR_5 when comparing the femur-pelvis in both the AP and ML axes, and in the ML axis when comparing the pelvis-torso and shank-femur as well. A greater percentage of the task in FBR_{1-4} when comparing the femur-pelvis indicates that the pelvis is moving relative to the knee and ankle, supporting a hip-based strategy compared to an ankle-based strategy. Additionally, as previously stated, increased time in FBR_{1-4} when comparing the shank-femur could equally be due to decreased tibial angular velocity (that could be caused by ankle flexion/extension or inversion/eversion) as it

is indicative of more femur relative angular velocity (that could come from knee flexion/extension). Accornero et al. [162] also assessed changes in balance between younger and older adults, describing older participants as more rigid and less flexible than younger adults. Accornero et al. [162] used simplified double pendulum model and a series of metrics that make it difficult to infer actual balance strategy because of some joints that are left out, such as the torso. It is possible that a double pendulum model that does not appropriately decouple certain joints could appear similar to patterns expected during a single pendulum model, similar to the findings of Gage et al. [155]. As we do here, decoupling more joints provides a comprehensive assessment of balance technique that is valuable for individuals and clinical populations by revealing some potential muscle weakness.

Hypothesis 2 of this work aimed to better disambiguate older adults with slow versus moderate gait speeds using the SBT task and static balance technique. While this work showed some differences between these two older groups, the effect sizes were small and it is difficult to conclude whether these differences are clinically relevant or warrant clinical intervention. The clinical relevance of the observed small effects sizing is likely due to static balance not sufficiently encompassing all mechanisms that are involved in human gait. Gait and locomotion are integrated tasks of which static balance plays a role. However, dynamic balance and higher order aspects of proprioception, vision, cognition, strength, and cardiopulmonary function, also play a large role in locomotion, part of the reason it is still very difficult to disambiguate slow from fast older walkers. While FBR provides insight into static balance strategy and potential muscle weaknesses, it is not currently sensitive to other measures, such as gait speed. Other features likely play a more significant role in gait speed decrements in older adults. Analysis of a series of tasks and their

corresponding technique, similar to the SPPB, might be more appropriate than one simple static balance test. Additionally, one single deficit might not be the culprit for all slow older walkers; the variability within the population is multi-factorial. However, FBR was sensitive to general age-related changes in balance technique. As stated in Section 1.1, OTs typically uses multiple motion features to assess a patient's performance when completing a task. If an older adult entered a clinic, they would likely assess features beyond balance, such as motor coordination. Future work will include analysis that uses multiple technique-based metrics, such as the coordination measures used in Chapters 2 and 3.

This work focused entirely on a marker-based analysis with insight into future analysis using wearable sensors. Future work will explore the ability to collect FBR using a network of IMUs as this would make it easier to collect these data in clinical environments. Accurate alignment of the IMU reference frame with the corresponding body segment reference frames is still a challenge [67, 69]. Inappropriate alignment could lead to angular velocity cross talk between axes, especially those with small value, such as ML and LG of the knee axis. Alignment errors are not limited to the IMUs as small misalignment or movement of the reflective motion capture marker location relative to appropriate anatomical land marks could lead to similar errors in this analysis.

4.8 Conclusions

Static balance is assessed and quantified using outcome-based measures that do not inform on underlying kinematic and motor control techniques. This work developed a metrics for static balance, $FBR_n^{P,UL}$, and used it to evaluate changes in balance strategy due to aging and changes in gait speed. Anal-

ysis showed that this new measure was able to quantify aspects of balance strategy and highlight differences in technique between younger and older adults. While this metric was not sensitive to older participant gait speed, locomotion is an integrative task that might not be thoroughly explained by one measure of static balance measure. This novel measure does allow for potential analysis of other clinical population and could provide the sensitivity to better assess disorders more directly related to balance and postural control.

Chapter 5

Conclusions and Future Work

The goal of this work was to develop quantified, motion-based measures for decisions that are often made qualitatively focusing specifically on challenges faced by the domains of rehabilitation and aerospace medicine. Based on observations of OTs (Section 1.1) and observations of MKIII suit fit checks (Section 3.1.2), we set out to address the following research questions in both our domains of interest:

1. Can we provide information on ***how*** motions are performed not just the outcomes of the motions being performed?
2. Are these metrics sensitive enough to detect operationally relevant differences that might influence decision making?

In this thesis, these research questions were addressed in the following three Specific Aims:

1. **Develop and determine whether a new metric for coordination can detect operationally relevant differences in motor control**
2. **Adaptation and validation of this new measure for coordination to the field of bioastronautics, specifically detecting operationally relevant changes in suit fit**

3. **Develop and determine how differences in balance technique can detect operationally relevant differences in postural control**

The first aim was addressed in Chapter 2 with the description and development of a new, more intuitive measure for joint coordination called the relative coordination metrics (ρ) and assessed how it could detect coordination differences during a grasping task. This coordination measure was then adapted to tackle the problems associated with dynamic spacesuit fit in Chapter 3. Finally, Chapter 4 introduced a new metric for quantifying balance technique (FBR) and used it to evaluate static balance strategy differences between older and younger adults.

5.1 Summary of Results

This section summarizes the main results from each of the chapters of this thesis. Section 5.2 presents major contributions to the literature.

5.1.1 A Method for Quantifying Coordination during Non-Cyclic Motions

Chapter 2 introduced existing methods used to quantify joint coordination. These existing measures, however, made it difficult to infer the underlying joint motion profiles. The Relative Coordination Metric (ρ, Eq. 2.7 and Eq. 2.8) is velocity-based and has fewer mathematical transformations, making it easier to relate to the underlying joint motions. ρ is a time-series metric and a composite metric ($\hat{t}_{\pm Z_n}$) was defined to provide summary coordination measures. Using ρ to evaluate the coordination patterns of a grasping task in a healthy population, we demonstrate that ρ is sensitive to differences in strategy between planar reaching tasks with slight differences, such as path

length or grasping different objects (pen and cup). We also show and discuss how the interpretation of ρ can be affected by the implemented normalization scheme. Similar to measures of gait, normative data will be required to interpret other task strategies.

5.1.2 Objective Means of Quantifying Spacesuit Fit

Chapter 3 considered spacesuit fit. The suit fit process was evaluated through a similar cognitive task analysis discussed in Section 1.1.1 to inform the types of quantitative metrics that could support operational decision-making. We defined two areas of fit: static and dynamic fit (Fig. 3.2). We then performed an experiment to determine how changes in static fit, specifically padding between the hips and suit hip brief, would affect dynamic fit. To quantify dynamic fit, ρ from Chapter 2 was repurposed to quantify the relative motion between the human and the suit (ρ_{HS}, Eq. 3.2). A pilot study showed ($n = 3$), the data showed that the effect of padding on gait parameters and dynamic was mixed and subject-specific. Since each participant was wearing a different configuration of the MKIII spacesuit, there was some evidence that the length of the leg compared to the human leg length and boot fit contributed more to changes in ρ_{HS} and dynamic fit than the padding we placed between the human and suit hip. This experiment did not attempt to assess "goodness" of fit, simply the sensitivity of new candidate metrics to changes in performance due to components of fit. As fit is a function of multiple factors, it is necessary to have multiple metrics to quantify this complex term. Regardless, this work was some of the first to decouple human motion and suit motion to understand how the human moved within the suit. It was also the first to define terms such as static and dynamic fit.

5.1.3 Technique-based Measures for the Standing Balance Test

Chapter 4 of this thesis considered quantifying balance technique. Static balance is assessed and quantified using outcome-based measures that do not inform on underlying kinematic and motor control techniques, such as the inverted pendulum model that considers all joints to be rigid except the ankle joint. This work developed a metric for static balance, Frequency in Balance Region or $FBR_n^{P,UL}$ that provides an understanding of the relative motion between body segments. While walking is known to slow due to the aging process, evidence shows that slower gait speeds are correlated with higher mortality. This work therefore used $FBR_n^{P,UL}$ to evaluate changes in static balance strategy due to aging and changes in gait speed. This new measure was able to quantify aspects of balance strategy and highlight differences in technique between younger and older adults. While this metric was not sensitive to older participant gait speed, locomotion is an integrative task that might not be thoroughly explained by one measure of static balance.

5.2 Contributions to Literature

This thesis makes several contributions to the existing literature on human biomechanics, rehabilitation, and, aerospace medicine:

1. We define a new metric for coordination that is velocity-based, has the ability to compare 2 or more joint DoF, can be applied to cyclic and non-repetitive tasks, and is easier to relate to the underlying kinematics.
2. We provide recommendations for the appropriate normalization of ρ and $\hat{t}_{\pm Z_n}$ for upper extremity planar tasks.
3. We provide a comprehensive definition and categorization of spacesuit fit: static and dynamic fit. These definitions can be used to better

quantify and understand the problems associated with fit as well as other human-machine systems such as exoskeletons.

4. We defined a new measure for dynamic spacesuit fit (ρ_{HS}) that can be used to measure the relative motion between humans and spacesuits using small and easy-to-use IMUs.
5. We demonstrated that in the Mark III spacesuit aspects of static fit, such as boot sizing and leg length, have a higher impact on dynamic fit than indexing that can be used to modify static fit.
6. We defined a new metric for balance that quantifies multi-axis static balance technique by measuring deviations from an inverted pendulum model of multiple body segments.
7. We demonstrated differences in multi-axis balance technique between older and younger adults, specifically that older adults in the medio-lateral direction, spent more time behaving like multi-segment inverted pendulums compared to younger adults.

5.3 Applications and Future Work

This thesis sits at the intersection of several fields with many open research questions. The three chapters and specific aims of this thesis only scratch the surface of the many open ended problems associated with the needs of rehabilitation, tele-rehabilitation, and spacesuit fit. For example, this thesis only focused on quantifying two human motion features: coordination and balance. However, work by Stirling and McLean [2] described a much larger list of motion parameters need to be addressed for clinicians to have all the information required for defining a plan-of-care. We now present some of the closely-related areas that we did not address in this thesis, and some

research and development directions worth additional investigation based on the results of this work.

5.3.1 Computing Coordination Patterns for a Diverse Set of Tasks

In Chapter 2 of this thesis, we derived and presented a new metric for coordination termed the Relative Coordination Metric (ρ_{12}, Eq. 2.7). Additionally, we used this metric to quantify and assess upper extremity coordination of four variations to a reaching and grasping task confined to a table. As discussed in Chapter 1, rehabilitation is a heterogeneous clinical practice that is personalized to the patient and their respective pathology. If the goal is to use metrics like these to help influence decision-making, there is also a need to understand the motor control patterns of healthy individuals for a variety of ADLs, such as over head reaching, two handed carrying, and more. One way such way of quickly understanding healthy motor patterns would be to take advantage of large databases, such as the Carnegie Mellon Motion Database [172]. This database provides a comprehensive and diverse set of healthy patient motion profiles that could be used to create a series of references for clinicians. While ρ_{12} is more intuitive than existing coordination metrics, a standard set of nominal ρ_{12} would facilitate the use of the metric in clinical settings by providing examples to clinicians and facilitating learning. Since many physical medicine physicians are taught to visually assess their patients, a database of nominal measures could be used as a resource to aid translatability and usability in clinical environments. This suggestion is similar to current clinical practice in gait labs. Currently available databases might not successfully capture all the motion variability that exists within the population. Available databases need to be extended to have additional participants to examine the natural variance. More work is needed to un-

derstand that natural variance that exists within the population to establish guidelines for operationally relevant changes in motor control that might require clinical intervention.

5.3.2 Longitudinal Progression of Patient Progression

One of the goals of tele-rehabilitation (Section 1.1.1) is to disambiguate patient progression in between visits. In between clinical visits it is unclear if a patient performs their therapy tasks appropriately, if at all, while at home. Future, longitudinal studies could explore integrating sensors into patient homes. These sensors could collect data to help OTs better understand progression at home and help influence patient plan-of-care decisions. Collecting data in both the clinic and home environment could also help quantify the variability found in data collected in the home environment and associated with patients putting on sensors themselves compared to a researcher or clinician.

Additionally, early detection of musculoskeletal disease can prompt early intervention that improves outcomes and quality of life. These improved outcomes have specifically been studied, for example, in Parkinson's [173], psoriatic arthritis [174], and dismobility [123]. Early diagnosis of some of these diseases, however, can be difficult. In the case of Parkinson's, as much as 60% of neurons are often degenerated before neurologists can make a diagnosis based on the established clinical criteria [173]. Advanced motion motoring could be used to track patients more longitudinally and establish new diagnostic criteria. It is possible that the rise of more advanced and portable wearable sensors could allow for more sensitive measures that detect operationally relevant changes in motor control prior to it being visible to the naked eye. Future work could explore longitudinal motion motoring of

patients with various musculoskeletal diseases to help develop techniques and metrics that detect these diseases even earlier. Using genetic testing, high-risk patients could also be monitored over long periods of time to quantify some of the earliest signs of these debilitating diseases. Home motoring of high-risk patients has the potential to detect instances of poor motor performance that might not be seen in the clinic. For example, higher rates of tripping categorize a patient as high-risk for falling, but sometimes the patient might not remember this and report it to their clinician [175]. Therefore, a system that is able to detect these relevant changes in motion performance while the patient is away from the clinic could also help with early diagnosis and intervention.

5.3.3 Development Goal-based Performance Metrics

As stated in Section 5.3.1, understanding the motors patterns of healthy individuals also provides a template that could be used for potential patient goals setting. Figure 1.1 highlights potential tele-rehabilitation system implementations. Vocal and visual cuing is a vital piece of feedback for patients as they go through any form of rehabilitation [2]. If these metrics were used in a tele-rehabilitation setting, a database of goal motion profiles could be used to train patients at home. In telemedicine, providing patients with visual feedback and goals while they are home is known to improve motivation and compliance with the home plan-of-care, something critical to any rehabilitative program [176]. One way we could create goal-based metrics is quantifying the coordination between a desired and undesired motor pattern. In other words, similar to how in Chapter 3 we quantified the coordination between the human and suit (Eq. 3.2), we compute the relative coordination between the desired coordination pattern of a joint compared to what the

patient is doing at home. Comparing patient coordination to desired coordination patterns provides patients with a goal. This type of real-time feedback and goal setting could replace the vocal, tactile, and visual cues provided by the clinician. Future work could assess the feasibility of such a metric and its usefulness in a clinical and tele-rehabilitation settings.

5.3.4 Comprehensive Suit Fit Assessments

Figure 3.1 highlights the many decisions made when fitting a human to a spacesuit. Chapter 3 of this thesis quantified two aspects of dynamic fit, leaving many more to be explored. For example, in Fig. 3.1b, shoulder strap tension is frequently reevaluated during the fit check process. Future work could explore nominal shoulder strap tensions based on different astronaut anthropometry.

In order to more comprehensively understand what sizing components of the spacesuit have the largest effect on performance, a comprehensive large scale study in which participants wear and perform tasks with different suit sizing configurations is necessary. Our study varied aspects of static fit through the addition of padding and measured changes in dynamic fit. We concluded that certain boot designs and leg lengths might have a greater effect on dynamic fit than the padding added. Therefore, future work should explore varying other aspects of the suit configuration and evaluating their effects on task performance and fit metrics. Our work here demonstrates that the spacing between the human and suit does not have a large effect on performance and fit, at least in the hip region we assessed and within the range we saw in this experiment ($\leq 0.75in$, Table 3.1). This knowledge gives suit design engineers flexibility when constructing future generations of the spacesuit. A larger comprehensive study allows engineers to decide what

sizing changes would result in operationally relevant changes in performance. In other words, we could better understand how many different sizes of the spacesuit we would need for our astronauts. A larger study with more participants would also begin to capture more of the variability that exists in the population as it relates to spacesuit sizing. Finally, it is important that any future suit fit experiments collect more comprehensive and thorough subjective feedback from participants so we can begin to understand how these more objective fit measures relate to qualitative preferences.

5.3.5 Suit Fit in Operationally Relevant Environments

Recently, the first all female EVA was canceled due to operational constraints and suit size availability [177]. Astronaut Anne McClain was replaced due to the unavailability of a medium sized EMU torso. In microgravity, astronauts can grow $1 - 3in$ due to the lack of gravity allowing for spinal elongation. McClain trained in both a medium and large sized upper torso on Earth to prepare for this possibility, but after performing one spacewalk in the large upper torso while aboard to the ISS, realized she still preferred the medium sized suit. Due to time constraints, it was easier for NASA to switch astronauts for the place all-female spacewalk than reconfigure the EMU spacesuit. This resulted in a PR nightmare for NASA but also sheds light on how important it is to understand suit fit more than ever, especially understanding how fit might change in non-1G environments. Future work should explore suit fit in more operationally relevant environments where possible. For example, as NASA prepares for return missions to the moon, they could test the sizes and performance of their next-gen planetary suits on parabolic flights that are able to mimic lower gravitational environments. The drawback of parabolic flight is that the periods of time in lower gravity on not long enough to

evaluate tasks over relevant time periods. For longer time scales, the Active Response Gravity Offload System (ARGOS) could be used to mimic lower gravity fields, but the human still experiences Earth gravity inside the suit, leading to similar pressures experiences by the astronaut in the direction of gravity. While not perfect analogs, parabolic flight and ARGOS would provide a more comprehensive understanding of suit fit in a gravitational environment more relevant to the one where astronauts will actually operate.

5.3.6 Assessing Balance Technique of Other Patient Populations

Similar to the recommendations and future work presented in Section 5.3.2, our new measure for balance could be used to assess postural differences associated with other clinical balance disordered. FBR could be applied to better understand the underlying balance technique associated with pathologies with more direct effects on static balance, such as muscular dystrophy, cerebral palsy, vestibular disorders, and multiple sclerosis. Future work could also explore the progression of these balance disorder over time to help clinicians compile new standards for early detection and diagnosis of underlying disease.

5.4 Concluding Remarks

This thesis took a first step in making complex motion data easier to digest for people who need it to make decisions relevant to their field. We did not explicitly set out to build a tele-rehabilitation system or redesign the spacesuit. The design of a spacesuit or the development of tele-rehabilitation tools require the fusing multiple streams of data. Within this thesis, we designed and evaluated metrics that are essential for accomplishing these larger goals

of developing tele-rehabilitation systems or building better spacesuits. Human biomechanics necessitates a complex recruitment of our neurological and musculoskeletal system. Subject matter experts, such as OTs and suit engineers, fuse many streams of data together. Looking at every data stream available to them can be an overwhelming tasks, which is why biomechanical human performance metrics for decision-making, like the ones created in this thesis, could reduce the workload and enable improved decision making of subject matter experts.

Bibliography

[1] R. A. Fineman, T. M. McGrath, D. G. Kelty-Stephen, A. F. J. Abercromby, and L. A. Stirling, "Objective Metrics Quantifying Fit and Performance in Spacesuit Assemblies," *Aerospace Medicine and Human Performance*, vol. 89, pp. 985–995, nov 2018.

[2] L. Stirling and J. MacLean, "Roadmap for the Development of at-Home Telemonitoring Systems to Augment Occupational Therapy," *IEEE transactions on Human-Machine Systems*, vol. 46, no. 4, pp. 1–12, 2016.

[3] H. Beyer and K. Holtzblatt, *Contextual Design: Defining Consumer-Centered Systems*. 1999.

[4] K. Holtzblatt and S. Jones, "Contextual inquiry: A participatory technique in system design," in *Participatory Design: Principals and Practices* (D. Schuler and Namioka, A., eds.), pp. 177–210, CRC Press, 1993.

[5] American Academy of Physical Medicine and Rehabilitation, "What is the Difference Between Physical Therapy and Physiatry," 2019.

[6] C. Ballinger, A. Ashburn, J. Low, and P. Roderick, "Unpacking the black box of therapy a pilot study to describe occupational therapy and physiotherapy interventions for people with stroke," *Clinical Rehabilitation*, vol. 13, pp. 301–309, aug 1999.

[7] P. Langhorne, J. Bernhardt, and G. Kwakkel, "Stroke rehabilitation," *The Lancet*, vol. 377, pp. 1693–1702, may 2011.

[8] E. M. Steultjens, J. Dekker, L. M. Bouter, J. C. van de Nes, E. H. Cup, and C. H. van den Ende, "Occupational Therapy for Stroke Patients," *Stroke*, vol. 34, pp. 676–687, mar 2003.

[9] F. Clark, "Occupational Therapy for Independent-Living Older Adults," *JAMA*, vol. 278, p. 1321, oct 1997.

[10] VA/DOD, "VA/DoD Clinical Practice Guideline for Rehabilitation of Lower Limb Amputation," tech. rep., Veterans Affiars and The Department of Defense, Washington DC, 2007.

[11] J. Case-Smith, "Outcomes in Hand Rehabilitation Using Occupational Therapy Services," *American Journal of Occupational Therapy*, vol. 57, pp. 499–506, sep 2003.

[12] American Occupational Therapy Association, "Occupational Therapy Practice Framework: Domain and Process (3rd Edition)," *American Journal of Occupational Therapy*, vol. 68, p. S1, sep 2017.

[13] S. Ashford, M. Slade, F. Malaprade, and L. Turner-Stokes, "Evaluation of functional outcome measures for the hemiparetic upper limb: A systematic review," *Journal of Rehabilitation Medicine*, vol. 40, no. 10, pp. 787–795, 2008.

[14] L. Resnik and M. Borgia, "Reliability of Outcome Measures for People With Lower-Limb Amputations: Distinguishing True Change From Statistical Error," *Physical Therapy*, vol. 91, pp. 555–565, apr 2011.

[15] I.-m. Velstra, C. S. Ballert, and A. Cieza, "A Systematic Literature Review of Outcome Measures for Upper Extremity Function Using the International Classification of Functioning, Disability, and Health as Reference," *PM&R*, vol. 3, pp. 846–860, sep 2011.

[16] M. de Kraker, R. Selles, T. Schreuders, H. Stam, and S. Hovius, "Palmar Abduction: Reliability of 6 Measurement Methods in Healthy Adults," *The Journal of Hand Surgery*, vol. 34, pp. 523–530, mar 2009.

[17] V. M. Pomeroy, A. Pramanik, L. Sykes, J. Richards, and E. Hill, "Agreement between physiotherapists on quality of movement rated via videotape," *Clinical Rehabilitation*, vol. 17, pp. 264–272, may 2003.

[18] P. L. Hudak, P. C. Amadio, and C. Bombardier, "Development of an upper extremity outcome measure: the DASH (disabilities of the

arm, shoulder and hand) [corrected]. The Upper Extremity Collaborative Group (UECG)," *American journal of industrial medicine*, vol. 29, no. 6, pp. 602–8, 1996.

[19] V. Mathiowetz, K. Weber, N. Kashman, and G. Volland, "Adult Norms for the Nine Hole Peg Test of Finger Dexterity," *The Occupational Therapy Journal of Research*, vol. 5, pp. 24–38, jan 1985.

[20] S. Shah, F. Vanclay, and B. Cooper, "Improving the sensitivity of the Barthel Index for stroke rehabilitation," *Journal of Clinical Epidemiology*, vol. 42, pp. 703–709, jan 1989.

[21] J. Sanford, J. Moreland, L. R. Swanson, P. W. Stratford, and C. Gowland, "Reliability of the Fugl-Meyer Assessment for Testing Motor Performance in Patients Following Stroke," *Physical Therapy*, vol. 73, pp. 447–454, jul 1993.

[22] L. Palmer and M. Epler, *Fundamentals of musculoskeletal assessment techniques*. Philadelphia: Lippincott Williams & Wilkins, 2 ed., 1998.

[23] S. L. Wolf, P. A. Catlin, M. Ellis, A. L. Archer, B. Morgan, and A. Piacentino, "Assessing Wolf motor function test as outcome measure for research in patients after stroke.," *Stroke*, vol. 32, pp. 1635–9, jul 2001.

[24] V. Mathiowetz, G. Volland, N. Kashman, and K. Weber, "Adult Norms for the Box and Block Test of Manual Dexterity," *American Journal of Occupational Therapy*, vol. 39, pp. 386–391, jun 1985.

[25] P. A. Heidenreich, J. G. Trogdon, O. A. Khavjou, J. Butler, K. Dracup, M. D. Ezekowitz, E. A. Finkelstein, Y. Hong, S. C. Johnston, A. Khera, D. M. Lloyd-Jones, S. A. Nelson, G. Nichol, D. Orenstein, P. W. F. Wilson, and Y. J. Woo, "Forecasting the future of cardiovascular disease in the United States: A policy statement from the American Heart Association," *Circulation*, vol. 123, no. 8, pp. 933–944, 2011.

[26] H. C. Noel, D. C. Vogel, J. J. Erdos, D. Cornwall, and F. Levin, "Home telehealth reduces healthcare costs.," *Telemedicine journal and e-health*

: *the official journal of the American Telemedicine Association*, vol. 10, no. 2, pp. 170–83, 2004.

[27] C. L. Turvey, D. Willyard, D. H. Hickman, D. M. Klein, and O. Kukoyi, "Telehealth screen for depression in a chronic illness care management program," *Telemedicine journal and e-health : the official journal of the American Telemedicine Association*, vol. 13, no. 1, pp. 51–56, 2007.

[28] E. M. Hunkeler, J. F. Meresman, W. a. Hargreaves, B. Fireman, W. H. Berman, a. J. Kirsch, J. Groebe, S. W. Hurt, P. Braden, M. Getzell, P. a. Feigenbaum, T. Peng, and M. Salzer, "Efficacy of nurse telehealth care and peer support in augmenting treatment of depression in primary care.," *Archives of family medicine*, vol. 9, no. 8, pp. 700–708, 2000.

[29] S. M. Landow, A. Mateus, K. Korgavkar, D. Nightingale, and M. A. Weinstock, "Teledermatology: Key factors associated with reducing face-to-face dermatology visits," *Journal of the American Academy of Dermatology*, vol. 71, no. 3, pp. 570–576, 2014.

[30] T. G. Russell, "Physical rehabilitation using telemedicine.," *Journal of telemedicine and telecare*, vol. 13, no. 5, pp. 217–220, 2007.

[31] M. K. O. Malley, S. Member, S. N. Purkayastha, N. Howie, and M. D. Byrne, "Technical Correspondence Motion-Based Performance Metrics," vol. 44, no. 1, pp. 139–145, 2014.

[32] C. D. Wickens, "Situation Awareness and Workload," *American Psychological Society*, no. c, pp. 128–133, 2002.

[33] W. B. Rouse and N. M. Morris, "On looking into the black box: Prospects and limits in the search for mental models," *Psychological Bulletin*, vol. 100, no. 3, pp. 349–363, 1986.

[34] D. Schroeder, F. Korsakov, C. M. P. Knipe, L. Thorson, A. M. Ellingson, D. Nuckley, J. Carlis, and D. F. Keefe, "Trend-centric motion visualization: Designing and applying a new strategy for analyzing scientific motion collections," *IEEE Transactions on Visualization and Computer Graphics*, vol. 20, no. 12, pp. 2644–2653, 2014.

[35] P. Gregory, J. Alexander, and J. Satinsky, "Clinical Telerehabilitation: Applications for Physiatrists," *PM and R*, vol. 3, no. 7, pp. 647–656, 2011.

[36] D. Kairy, P. Lehoux, C. Vincent, and M. Visintin, "A systematic review of clinical outcomes, clinical process, healthcare utilization and costs associated with telerehabilitation.," *Disability and rehabilitation*, vol. 31, no. 6, pp. 427–447, 2009.

[37] A. A. Rizzo, D. Strickland, and S. Bouchard, "The Challenge of Using Virtual Reality in Telerehabilitation," *Telemedicine Journal and e-Health*, vol. 10, pp. 184–195, jun 2004.

[38] P. O. Riley, G. Paolini, U. Della Croce, K. W. Paylo, and D. C. Kerrigan, "A kinematic and kinetic comparison of overground and treadmill walking in healthy subjects," *Gait & Posture*, vol. 26, pp. 17–24, jun 2007.

[39] M. K. Holden, T. A. Dyar, and L. Dayan-Cimadoro, "Telerehabilitation Using a Virtual Environment Improves Upper Extremity Function in Patients With Stroke," *IEEE Transactions on Neural Systems and Rehabilitation Engineering*, vol. 15, pp. 36–42, mar 2007.

[40] B. C. Huijgen, M. M. Vollenbroek-Hutten, M. Zampolini, E. Opisso, M. Bernabeu, J. Van Nieuwenhoven, S. Ilsbroukx, R. Magni, C. Giacomozzi, V. Marcellari, S. S. Marchese, and H. J. Hermens, "Feasibility of a home-based telerehabilitation system compared to usual care: arm/hand function in patients with stroke, traumatic brain injury and multiple sclerosis," *Journal of Telemedicine and Telecare*, vol. 14, pp. 249–256, jul 2008.

[41] J. Langan, K. DeLave, L. Phillips, P. Pangilinan, and S. Brown, "Home-based telerehabilitation shows improved upper limb function in adults with chronic stroke: A pilot study," *Journal of Rehabilitation Medicine*, vol. 45, no. 2, pp. 217–220, 2013.

[42] B. O'Brien, J. Thode, I. Anderson, E. Calius, E. Haemmerle, and S. Xie, "Integrated extension sensor based on resistance and voltage measure-

ment for a dielectric elastomer," vol. 652415, no. April 2007, p. 652415, 2007.

[43] Human Factors and Medical Panel, "Cognitive Task Analysis," tech. rep., 2000.

[44] J. Schraagen, S. Chipman, and V. Shalin, *Cognitive Task Analysis*. Psychology Press, 2000.

[45] J. M. Tappan, D. J. Pitman, M. L. Cummings, and D. Miglianico, "Display Requirements for an Interactive Rail Scheduling Display," pp. 352–361, 2011.

[46] M. R. Endsley, "Toward a Theory of Situation Awareness in Dynamic Systems," *Human Factors: The Journal of the Human Factors and Ergonomics Society*, vol. 37, pp. 32–64, mar 1995.

[47] R. A. Fineman and L. A. Stirling, "Quantification and visualization of coordination during non-cyclic upper extremity motion," *Journal of Biomechanics*, vol. 63, pp. 82–91, 2017.

[48] P. F. Lamb and M. Stöckl, "On the use of continuous relative phase: Review of current approaches and outline for a new standard," *Clinical Biomechanics*, vol. 29, no. 5, pp. 484–493, 2014.

[49] I. Abramov, N. Moiseyev, and A. Stoklitsky, "Concept of space suit enclosure for planetary exploration," *SAE Conference*, 2001.

[50] M. Gernhard, J. Jones, R. Scheuring, A. F. J. Abercromby, J. Tuxhorn, and J. Norcross, "Risk of Compromised EVA performance and crew health due to inadequate EVA suit systems," in *Human Health and Performance Risks in Space Exploration Missions* (J. McMurphee and J. Charles, eds.), Houston, TX: NASA SSP-2009-3405, 2009.

[51] A. Ross, L. Aitchison, R. Rhodes, E.-b. Mobility, E.-v. M. Unit, E. P. Garment, and E.-v. Activity, "Advanced Extra-vehicular Activity Pressure Garment Requirements Development," *45th International Conference on Environmental Systems*, no. July, 2015.

[52] C. E. Carr and D. J. Newman, "Space suit bioenergetics: Framework and analysis of unsuited and suited activity," *Aviation Space and Environmental Medicine*, vol. 78, no. 11, pp. 1013–1022, 2007.

[53] C. R. Cullinane, R. A. Rhodes, and L. A. Stirling, "Mobility and Agility During Locomotion in the Mark III Space Suit," *Aerospace Medicine and Human Performance*, vol. 88, no. 6, pp. 589–596, 2017.

[54] L. Stirling, H. C. Siu, E. Jones, and K. Duda, "Human Factors Considerations for Enabling Functional Use of Exosystems in Operational Environments," *IEEE Systems Journal*, vol. 13, pp. 1072–1083, mar 2019.

[55] A. F. J. Abercromby, J. S. Cupples, S. Rajulu, J. A. Buffington, J. R. Norcross, S. P. Chappell, W. Science, and E. Group, "Integrated Extravehicular Activity Human Research Plan: 2016," no. July, 2016.

[56] E. Benson and S. Rajulu, "Complexity of Sizing for Space Suit Applications," *Apollo The International Magazine Of Art And Antiques*, pp. 599–607, 2009.

[57] Peng Cheng and B. Oelmann, "Joint-Angle Measurement Using Accelerometers and GyroscopesA Survey," *IEEE Transactions on Instrumentation and Measurement*, vol. 59, pp. 404–414, feb 2010.

[58] M. Mihelj, "Inverse Kinematics of Human Arm Based on Multisensor Data Integration," *Journal of Intelligent and Robotic Systems*, vol. 47, pp. 139–153, oct 2006.

[59] A. Murgia, V. Kerkhofs, H. Savelberg, and K. Meijer, "A portable device for the clinical assessment of upper limb motion and muscle synergies," in *2010 Annual International Conference of the IEEE Engineering in Medicine and Biology*, pp. 931–934, IEEE, aug 2010.

[60] R. E. Mayagoitia, A. V. Nene, and P. H. Veltink, "Accelerometer and rate gyroscope measurement of kinematics: An inexpensive alternative to optical motion analysis systems," *Journal of Biomechanics*, vol. 35, no. 4, pp. 537–542, 2002.

[61] M. Vanegas and L. Stirling, "Characterization of inertial measurement unit placement on the human body upon repeated donnings," *2015 IEEE 12th International Conference on Wearable and Implantable Body Sensor Networks, BSN 2015*, 2015.

[62] A. G. Cutti, A. Ferrari, P. Garofalo, M. Raggi, A. Cappello, and A. Ferrari, "'Outwalk': A protocol for clinical gait analysis based on inertial and magnetic sensors," *Medical and Biological Engineering and Computing*, vol. 48, no. 1, pp. 17–25, 2010.

[63] J. Favre, B. M. Jolles, R. Aissaoui, and K. Aminian, "Ambulatory measurement of 3D knee joint angle," *Journal of Biomechanics*, vol. 41, no. 5, pp. 1029–1035, 2008.

[64] J. Favre, R. Aissaoui, B. M. Jolles, J. A. de Guise, and K. Aminian, "Functional calibration procedure for 3D knee joint angle description using inertial sensors," *Journal of Biomechanics*, vol. 42, no. 14, pp. 2330–2335, 2009.

[65] R. V. Vitali, S. M. Cain, R. S. McGinnis, A. M. Zaferiou, L. V. Ojeda, S. P. Davidson, and N. C. Perkins, "Method for estimating three-dimensional knee rotations using two inertial measurement units: Validation with a coordinate measurement machine," *Sensors (Switzerland)*, vol. 17, no. 9, 2017.

[66] T. Seel and T. Schauer, "Joint Axis and Position Estimation from Inertial Measurement Data by Exploiting Kinematic Constraints," pp. 0–4, 2012.

[67] T. Seel, J. Raisch, and T. Schauer, "IMU-based joint angle measurement for gait analysis.," *Sensors (Basel, Switzerland)*, vol. 14, pp. 6891–909, 2014.

[68] P. Muller, M.-A. Begin, T. Schauer, and T. Seel, "Alignment-Free, Self-Calibrating Elbow Angles Measurement using Inertial Sensors," *IEEE Journal of Biomedical and Health Informatics*, vol. 21, no. 2, pp. 1–1, 2016.

[69] T. McGrath, R. Fineman, and L. Stirling, "An Auto-Calibrating Knee Flexion-Extension Axis Estimator Using Principal Component Analysis with Inertial Sensors," *Sensors*, vol. 18, pp. 1–17, jun 2018.

[70] C. U. Eke, S. M. Cain, and L. A. Stirling, "Strategy quantification using body worn inertial sensors in a reactive agility task," *Journal of Biomechanics*, vol. 64, pp. 219–225, 2017.

[71] A. M. Zaferiou, L. Ojeda, S. M. Cain, R. V. Vitali, S. P. Davidson, L. Stirling, and N. C. Perkins, "Quantifying performance on an outdoor agility drill using foot-mounted inertial measurement units," *PLOS ONE*, vol. 12, p. e0188184, nov 2017.

[72] S. M. Cain, R. S. McGinnis, S. P. Davidson, R. V. Vitali, N. C. Perkins, and S. G. McLean, "Quantifying performance and effects of load carriage during a challenging balancing task using an array of wireless inertial sensors," *Gait and Posture*, vol. 43, pp. 65–69, 2016.

[73] L. Ojeda, A. Zaferiou, S. Cain, R. Vitali, S. Davidson, L. Stirling, and N. Perkins, "Estimating Stair Running Performance Using Inertial Sensors," *Sensors*, vol. 17, p. 2647, nov 2017.

[74] J. Howcroft, J. Kofman, E. D. Lemaire, M. O'Sullivan, and N. Baddour, "Review of fall risk assessment in geriatric populations using inertial sensors," *Journal of NeuroEngineering and Rehabilitation*, vol. 10, no. 1, p. 91, 2013.

[75] N. A. Bernstein, *The co-ordination and regulation of movements: Conclusions towards the Study of Motor Co-ordination*. Oxford: Pergamon Press, 1967.

[76] M. T. Turvey, "Coordination.," *The American psychologist*, vol. 45, no. 8, pp. 938–953, 1990.

[77] L. Stirling and J. MacLean, "Roadmap for the Development of at-Home Telemonitoring Systems to Augment Occupational Therapy," *IEEE transactions on Human-Machine Systems*, vol. 46, no. 4, pp. 1–12, 2016.

[78] R. V. Vitali, S. M. Cain, S. P. Davidson, and N. C. Perkins, "Human crawling performance and technique revealed by inertial measurement units," *Journal of Biomechanics*, vol. 84, pp. 121–128, 2019.

[79] G. Wu, S. Siegler, P. Allard, C. Kirtley, A. Leardini, D. Rosenbaum, M. Whittle, D. D. D'Lima, L. Cristofolini, H. Witte, O. Schmid, and I. Stokes, "ISB recommendation on definitions of joint coordinate system of various joints for the reporting of human joint motionpart I: ankle, hip, and spine," *Journal of Biomechanics*, vol. 35, no. 4, pp. 543–548, 2002.

[80] S. L. Chiu, C. C. Chang, J. T. Dennerlein, and X. Xu, "Age-related differences in inter-joint coordination during stair walking transitions," *Gait and Posture*, vol. 42, no. 2, pp. 152–157, 2015.

[81] B. C. Heiderscheit, J. Hamill, and R. E. A. van Emmerik, "Variability of stride characteristics and joint coordination among individuals with unilateral patellofemoral pain," *Journal of Applied Biomechanics*, vol. 18, pp. 110–121, 2002.

[82] J. Hamill, R. E. A. van Emmerik, B. C. Heiderscheit, and L. Li, "A dynamical systems approach to lower extremity running injuries," *Clinical Biomechanics*, vol. 14, no. 5, pp. 297–308, 1999.

[83] C. Schnitzler, L. Seifert, V. Ernwein, and D. Chollet, "Arm coordination adaptations assessment in swimming," *International Journal of Sports Medicine*, vol. 29, no. 6, pp. 480–486, 2008.

[84] M. Varlet and M. J. Richardson, "Computation of continuous relative phase and modulation of frequency of human movement," *Journal of Biomechanics*, vol. 44, no. 6, pp. 1200–1204, 2011.

[85] M. J. Kurz and N. Stergiou, "Effect of normalization and phase angle calculations on continuous relative phase," *Journal of Biomechanics*, vol. 35, no. 3, pp. 369–374, 2002.

[86] R. Robins, J. Wheat, G. Irwin, and R. Bartlett, "The Effect of Shooting Distance on Movement Variability in Basketball," *Journal of Human Movement Studies*, vol. 50, no. 4, pp. 217–238, 2006.

[87] J. P. Scholz and J. A. S. Kelso, "A Quantitative Approach to Understanding the Formation and Change of Coordinated Movement Patterns," *Journal of Motor Behavior*, vol. 21, pp. 122–144, jun 1989.

[88] R. H. Miller, R. Chang, J. L. Baird, R. E. Van Emmerik, and J. Hamill, "Variability in kinematic coupling assessed by vector coding and continuous relative phase," *J Biomech*, vol. 43, no. 13, pp. 2554–2560, 2010.

[89] B. T. Peters, J. M. Haddad, B. C. Heiderscheit, R. E. a. Van Emmerik, and J. Hamill, "Limitations in the use and interpretation of continuous relative phase.," *Journal of biomechanics*, vol. 36, no. 2, pp. 271–274, 2003.

[90] U. H. Buzzi, N. Stergiou, M. J. Kurz, P. A. Hageman, and J. Heidel, "Nonlinear dynamics indicates aging affects variability during gait," *Clinical Biomechanics*, vol. 18, pp. 435–443, jun 2003.

[91] G. Wu and P. R. Cavanagh, "ISB Recommendations in the Reporting for Standardization of Kinematic Data," *Journal of Biomechanics*, vol. 28, no. 10, pp. 1257–1261, 1995.

[92] G. Wu, F. C. Van Der Helm, H. E. Veeger, M. Makhsous, P. Van Roy, C. Anglin, J. Nagels, A. R. Karduna, K. McQuade, X. Wang, F. W. Werner, and B. Buchholz, "ISB recommendation on definitions of joint coordinate systems of various joints for the reporting of human joint motion - Part II: Shoulder, elbow, wrist and hand," *Journal of Biomechanics*, vol. 38, no. 5, pp. 981–992, 2005.

[93] N. Beckers, R. Fineman, and L. Stirling, "Anticipatory signals in kinematics and muscle activity during functional grasp and release," in *2015 IEEE 12th International Conference on Wearable and Implantable Body Sensor Networks, BSN 2015*, 2015.

[94] I. Olivier, L. Hay, C. Bard, and M. Fleury, "Age-related differences in the reaching and grasping coordination in children: Unimanual and bimanual tasks," *Experimental Brain Research*, vol. 179, no. 1, pp. 17–27, 2007.

[95] J. F. Soechting and F. Lacquaniti, "Invariant characteristics of a pointing movement in man," *Journal of Neuroscience*, vol. 1, no. 7, pp. 710–20, 1981.

[96] F. Lacquaniti and J. F. Soechting, "Coordination of arm and wrist motion during a reaching task.," *The Journal of neuroscience : the official journal of the Society for Neuroscience*, vol. 2, no. 4, pp. 399–408, 1982.

[97] S. L. Delp, F. C. Anderson, A. S. Arnold, P. Loan, A. Habib, C. T. John, E. Guendelman, and D. G. Thelen, "OpenSim: Open source to create and analyze dynamic simulations of movement," *IEEE transactions on bio-medical engineering*, vol. 54, no. 11, pp. 1940–1950, 2007.

[98] K. R. S. Holzbaur, W. M. Murray, and S. L. Delp, "A model of the upper extremity for simulating musculoskeletal surgery and analyzing neuromuscular control," *Annals of Biomedical Engineering*, vol. 33, no. 6, pp. 829–840, 2005.

[99] W. D. Schot, E. Brenner, and J. B. J. Smeets, "Robust movement segmentation by combining multiple sources of information," *Journal of Neuroscience Methods*, vol. 187, pp. 147–155, mar 2010.

[100] Y. Benjamini and Y. Hochberg, "Controlling the false discovery rate: a practical and powerful approach to multiple testing," 1995.

[101] M. Dwass, "Modified Randomization Tests for Nonparametric Hypotheses," *The Annals of Mathematical Statistics*, vol. 28, no. 1, pp. 181–187, 1957.

[102] L. Ricci, F. Taffoni, and D. Formica, "On the orientation error of IMU: Investigating static and dynamic accuracy targeting human motion," *PLoS ONE*, vol. 11, no. 9, pp. 1–15, 2016.

[103] A. C. H. Geurts, M. De Haart, I. J. W. Van Nes, and J. Duysens, "A review of standing balance recovery from stroke," *Gait and Posture*, vol. 22, no. 3, pp. 267–281, 2005.

[104] N. S. Ward, "Compensatory mechanisms in the aging motor system," *Ageing Research Reviews*, vol. 5, no. 3, pp. 239–254, 2006.

[105] F. Meyen, B. Holschuh, R. Kobrick, S. Jacobs, and D. Newman, "Robotic Joint Torque Testing: A Critical Tool in the Development of Pressure Suit Mobility Elements," in *41st International Conference on Environmental Systems*, (Reston, Virigina), American Institute of Aeronautics and Astronautics, jul 2011.

[106] M. Di Capua and D. L. Akin, "Body Pose Measurement System: System Validation and Range of Motion/Kinematic Analysis of Three Pressure Suits," in *43rd International Conference on Environmental Systems*, (Reston, Virginia), pp. 1–31, American Institute of Aeronautics and Astronautics, jul 2013.

[107] P. J. Bertrand, A. Anderson, A. Hilbert, and D. Newman, "Feasibility of Spacesuit Kinematics and Human-Suit Interactions," *44th International Conference on Environmental Systems*, no. July, 2014.

[108] A. P. Anderson and D. J. Newman, "Pressure sensing for in-suit measurement of space suited biomechanics," *Acta Astronautica*, vol. 115, pp. 218–225, oct 2015.

[109] H. Kim, "Virtual Fit Check: Parametric Human Body and Suit Models," in *Extravehicular Activity Technology Workshop*, (Houston, TX), 2017.

[110] L. Stirling, P. Arezes, and A. Anderson, "Implications of Space suit Injury Risk for Developing Computational Performance Models," vol. 90, no. 6, pp. 1–14, 2019.

[111] B. Mariani, H. Rouhani, X. Crevoisier, and K. Aminian, "Quantitative estimation of foot-flat and stance phase of gait using foot-worn inertial sensors," *Gait and Posture*, vol. 37, no. 2, pp. 229–234, 2013.

[112] J. R. Rebula, L. V. Ojeda, P. G. Adamczyk, and A. D. Kuo, "Measurement of foot placement and its variability with inertial sensors," *Gait and Posture*, vol. 38, no. 4, pp. 974–980, 2013.

[113] P. B. Davenport, "Rotations about nonorthogonal axes.," *AIAA Journal*, vol. 11, pp. 853–857, jun 1973.

[114] J. Cohen, *Statistical Power Analysis for the Behavioral Sciences*. New York, NY: Lawrence Erlbaum Associates, 1988.

[115] M. Babyak, "What You See May Not be What You Get: A Brief Introduction to Overfitting in Regression Type Models," *Psychosomatic Medicine*, vol. 66, no. 3, pp. 411–421, 2004.

[116] F. Harrel, K. Lee, and D. Mark, "Multivariable prognostic models: issues in developing models, evaluating assumptions and adequacy, and measureing and reducing errors," *Statistics in Medicine*, vol. 15, pp. 361–87, 1996.

[117] S. Finlay, *Predictive Analysis, data mining, and big data: Myths, Misconceptions and Methods*. New York, NY: Palgrave Macmillan, 2014.

[118] K. H. Yuan and K. Hayashi, "Bootstrap approach to inference and power analysis based on three test statistics for covariance structure models," *British Journal of Mathematical and Statistical Psychology*, 2003.

[119] J. R. Brinkmann and J. Perry, "Rate and range of knee motion during ambulation in healthy and arthritic subjects," *Physical Therapy*, vol. 65, no. 7, pp. 1055–1060, 1985.

[120] M. Kadaba, H. Ramakrishnan, M. Wootten, J. Gainey, G. Gorton, and G. Cochran, "Repeatability of Kinematic, Kinetic, and Electromyographic Data in Normal Adult Gait," *Journal of Orthopaedic Research*, vol. 7, no. 6, pp. 849–860, 1989.

[121] M. LaFiandra, R. C. Wagenaar, K. G. Holt, and J. P. Obusek, "How do load carriage and walking speed influence trunk coordination and stride parameters?," *Journal of Biomechanics*, vol. 36, no. 1, pp. 87–95, 2003.

[122] C. T. John, A. Seth, M. H. Schwartz, and S. L. Delp, "Contributions of muscles to mediolateral ground reaction force over a range of walking speeds," *Journal of Biomechanics*, vol. 45, no. 14, pp. 2438–2443, 2012.

[123] S. E. Hardy, S. Perera, Y. F. Roumani, J. M. Chandler, and S. A. Studenski, "Improvement in usual gait speed predicts better survival in older adults," *Journal of the American Geriatrics Society*, vol. 55, no. 11, pp. 1727–1734, 2007.

[124] V. Castranova, B. Asgharian, P. Sayre, W. Virginia, and N. Carolina, "A Diagnosis of DismobilityGiving Mobility Clinical Visibility: A Mobility Working Group Recommendation," vol. 311, no. 20, pp. 1922–2013, 2016.

[125] S. Studenski, S. Perera, K. Patel, C. Rosano, K. Faulkner, M. Inzitari, J. Brach, J. Chandler, P. Cawthon, E. B. Connor, M. Nevitt, M. Visser, S. Kritchevsky, S. Badinelli, T. Harris, A. B. Newman, J. Cauley, L. Ferrucci, and J. Guralnik, "Gait speed and survival in older adults," *JAMA : the journal of the American Medical Association*, vol. 305, no. 1, pp. 50–58, 2011.

[126] B. Salzman, "Gait and balance disorders in older adults.," *American family physician*, vol. 82, no. 1, pp. 61–8, 2010.

[127] A. NB, "Gait disorders in older adults.," *Clinical Geriatrics*, vol. 7, no. 3, pp. 73–81, 1999.

[128] D. A. Sterling, J. A. O. Connor, and J. Bonadies, "Geriatric Falls: Injury Severity Is High and Disproportionate to Mechanism.," *Journal of Trama*, no. January, pp. 116–119, 2001.

[129] S. M. Bruijn, J. H. van Dieën, O. G. Meijer, and P. J. Beek, "Is slow walking more stable?," *Journal of Biomechanics*, vol. 42, no. 10, pp. 1506–1512, 2009.

[130] H. G. Kang and J. B. Dingwell, "Effects of walking speed, strength and range of motion on gait stability in healthy older adults," *Journal of Biomechanics*, vol. 41, no. 14, pp. 2899–2905, 2008.

[131] D. A. Winter, A. E. Patla, J. S. Frank, and S. E. Walt, "Biomechanical walking pattern changes in the fit and healthy elderly," *Physical Therapy*, vol. 70, no. 6, pp. 340–347, 1990.

[132] M. E. Cress, K. B. Schechtman, C. D. Mulrow, M. A. Fiatarone, M. B. Gerety, and D. M. Buchner, "Relationship between physical performance and self-perceived physical function," 1995.

[133] S. Y. Tsai, L. Y. Chi, C. H. Lee, and P. Chou, "Health-related quality of life as a predictor of mortality among community-dwelling older persons," *European Journal of Epidemiology*, vol. 22, no. 1, pp. 19–26, 2007.

[134] A. Molzahn, S. M. Skevington, M. Kalfoss, and K. S. Makaroff, "The importance of facets of quality of life to older adults: An international investigation," *Quality of Life Research*, vol. 19, no. 2, pp. 293–298, 2010.

[135] W. J. Rejeski and S. L. Mihalko, "Physical Activity and Quality of Life in Older Adults," *The Journals of Gerontology Series A: Biological Sciences and Medical Sciences*, vol. 56, pp. 23–35, oct 2001.

[136] I. B. Wilson, "Linking Clinical Variables With Health-Related Quality of Life," *JAMA*, vol. 273, p. 59, jan 1995.

[137] S. P. Sayers, J. M. Guralnik, A. B. Newman, J. S. Brach, and R. a. Fielding, "Concordance and discordance between two measures of lower extremity function: 400 meter self-paced walk and SPPB.," *Aging clinical and experimental research*, vol. 18, no. 2, pp. 100–106, 2006.

[138] J. M. Guralnik, L. Ferrucci, E. M. Simonsick, M. E. Salive, and R. B. Wallace, "Lower-Extremity Function in Persons over the Age of 70 Years as a Predictor of Subsequent Disability," *New England Journal of Medicine*, vol. 332, no. 9, pp. 556–562, 1995.

[139] B. Oh, B. Cho, H.-C. Choi, K.-Y. Son, S. M. Park, S. Chun, and S.-I. Cho, "The influence of lower-extremity function in elderly individuals' quality of life (QOL): an analysis of the correlation between

SPPB and EQ-5D.," *Arch Gerontol Geriatr*, vol. 58, no. 2, pp. 278–282, 2018.

[140] T. M. Gill, "Assessment of function and disability in longitudinal studies," *Journal of the American Geriatrics Society*, vol. 58, no. SUPPL. 2, pp. 308–312, 2010.

[141] A. Harnish, W. Dieter, A. Crawford, and T. E. Shubert, "Effects of Evidence-Based Fall Reduction Programing on the Functional Wellness of Older Adults in a Senior Living Community: A Clinical Case Study," *Frontiers in Public Health*, vol. 4, no. December, pp. 1–9, 2016.

[142] R. W. Bohannon, "Reference Values for the Timed Up and Go Test," *Journal of Geriatric Physical Therapy*, vol. 29, no. 2, pp. 64–68, 2006.

[143] R. W. Bohannon, "Comfortable and maximum walking speed of adults aged 20-79 years: Reference values and determinants," *Age and Ageing*, vol. 26, no. 1, pp. 15–19, 1997.

[144] I. Melzer, N. Benjuya, and J. Kaplanski, "Postural stability in the elderly: A comparison between fallers and non-fallers," *Age and Ageing*, vol. 33, no. 6, pp. 602–607, 2004.

[145] M. Chiacchiero, B. Dresely, U. Silva, R. DeLosReyes, and B. Vorik, "The relationship between range of movement, flexibility, and balance in the elderly," *Topics in Geriatric Rehabilitation*, vol. 26, no. 2, pp. 148–155, 2010.

[146] D. A. Winter, "Human blance and posture control during standing and walking," *Gait & posture*, vol. 3, no. 4, pp. 193–214, 1995.

[147] L. D. Bogle Thorbahn, R. a. Newton, and D. Bogle, "Use of the Berg Balance Test to predict falls in elderly persons.," *Physical therapy*, vol. 76, no. 6, pp. 576–83; discussion 584–5, 1996.

[148] R. W. Bohannon, P. a. Larkin, a. C. Cook, J. Gear, and J. Singer, "Decrease in timed balance test scores with aging.," *Physical therapy*, vol. 64, no. 7, pp. 1067–1070, 1984.

[149] J. D. Willson, C. P. Dougherty, M. L. Ireland, and I. M. C. Davis, "Core stability and its relationship to lower extremity function and injury.," *The Journal of the American Academy of Orthopaedic Surgeons*, vol. 13, no. 5, pp. 316–325, 2005.

[150] J. Schlicht, D. N. Camaione, and S. V. Owen, "Effect of Intense Strength Training on Standing Performance in Older Adults," *Journal of Gerontology: Medical Sciences*, vol. 56, no. 5, pp. 281–286, 2001.

[151] A. A. Priplata, J. B. Niemi, J. D. Harry, L. A. Lipsitz, and J. J. Collins, "Vibrating insoles and balance control in elderly people.," *Lancet (London, England)*, vol. 362, no. 9390, pp. 1123–4, 2003.

[152] C. Kinnaird, J. Lee, W. J. Carender, M. Kabeto, B. Martin, and K. H. Sienko, "The effects of attractive vs . repulsive instructional cuing on balance performance," *Journal of NeuroEngineering and Rehabilitation*, pp. 1–5, 2016.

[153] K. H. Sienko, M. D. Balkwill, L. I. E. Oddsson, and C. W. Iii, "The effect of vibrotactile feedback on postural sway during locomotor activities," *Journal of NeuroEngineering and Rehabilitation*, vol. 10, no. 1, p. 1, 2013.

[154] J. J. Collins and C. J. De Luca, "The effects of visual input on open-loop and closed-loop postural control mechanisms," *Experimental Brain Research*, vol. 103, no. 1, pp. 151–163, 1995.

[155] W. H. Gage, D. A. Winter, J. S. Frank, and A. L. Adkin, "Kinematic and kinetic validity of the inverted pendulum model in quiet standing," *Gait and Posture*, vol. 19, no. 2, pp. 124–132, 2004.

[156] A. Hof, M. Gazendam, and W. Sinke, "The condition for dynamic stability," *Journal of Biomechanics*, vol. 38, pp. 1–8, jan 2005.

[157] D. A. Winter, A. Patla, and F. Prince, "Stiffness control of balance during quiet standing," *Gait & Posture*, vol. 5, pp. 154–155, apr 1997.

[158] A. Shumway-Cook and M. Woollacott, *Motor Control: Translating Research into Clinical Practice*. 3 ed., 2007.

[159] D. Manchester, M. Woollacott, N. Zederbauer-Hylton, and O. Marin, "Visual, Vestibular and Somatosensory Contributions to Balance Control in the Older Adult," *Journal of Gerontology*, vol. 44, pp. M118–M127, jul 1989.

[160] Y. Aramaki, D. Nozaki, K. Masani, T. Sato, K. Nakazawa, and H. Yano, "Reciprocal angular acceleration of the ankle and hip joints during quiet standing in humans," *Experimental Brain Research*, vol. 136, pp. 463–473, feb 2001.

[161] P. Crenna, C. Frigo, J. Massion, and A. Pedotti, "Forward and backward axial synergies in man," *Experimental Brain Research*, vol. 65, pp. 538–548, feb 1987.

[162] N. Accornero, M. Capozza, S. Rinalduzzi, and G. W. Manfredi, "Clinical multisegmental posturography: Age-related changes in stance control," *Electroencephalography and Clinical Neurophysiology - Electromyography and Motor Control*, vol. 105, no. 3, pp. 213–219, 1997.

[163] K. J. Kim, V. Agrawal, C. Bennett, I. Gaunaurd, L. Feigenbaum, and R. Gailey, "Measurement of lower limb segmental excursion using inertial sensors during single limb stance," *Journal of Biomechanics*, vol. 71, pp. 151–158, 2018.

[164] L. Stirling and J. MacLean, "Roadmap for the Development of at-Home Telemonitoring Systems to Augment Occupational Therapy," *IEEE transactions on Human-Machine Systems*, vol. 46, no. 4, pp. 1–12, 2016.

[165] G. K. Seidel, D. M. Marchinda, M. Dijkers, and R. W. Soutas-Little, "Hip joint center location from palpable bony landmarks-A cadaver study," *Journal of Biomechanics*, vol. 28, no. 8, pp. 995–998, 1995.

[166] O. Tirosh and W. A. Sparrow, "Age and walking speed effects on muscle recruitment in gait termination," *Gait and Posture*, vol. 21, no. 3, pp. 279–288, 2005.

[167] Y. P. Lim, Y. C. Lin, and M. G. Pandy, "Muscle function during gait is invariant to age when walking speed is controlled," *Gait and Posture*, vol. 38, no. 2, pp. 253–259, 2013.

[168] U. Granacher, A. Gollhofer, T. Hortobágyi, R. W. Kressig, and T. Muehlbauer, "The Importance of Trunk Muscle Strength for Balance, Functional Performance, and Fall Prevention in Seniors: A Systematic Review," *Sports Medicine*, vol. 43, pp. 627–641, jul 2013.

[169] S. K. Bok, T. H. Lee, and S. S. Lee, "The effects of changes of ankle strength and range of motion according to aging on balance," *Annals of Rehabilitation Medicine*, vol. 37, no. 1, pp. 10–16, 2013.

[170] K. A. Boyer, R. T. Johnson, J. J. Banks, C. Jewell, and J. F. Hafer, "Systematic review and meta-analysis of gait mechanics in young and older adults," *Experimental Gerontology*, vol. 95, pp. 63–70, 2017.

[171] Y.-C. Pai, W. Z. Rymer, R. W. Chang, and L. Sharma, "Effect of age and osteoarthritis on knee proprioception," *Arthritis & Rheumatism*, vol. 40, pp. 2260–2265, dec 1997.

[172] C. M. University, "CMU Graphics Lab Motion Capture Database," 2006.

[173] A. Gaenslen and D. Berg, "Early diagnosis of Parkinson's disease," *International Review of Neurobiology*, vol. 90, no. C, pp. 81–92, 2010.

[174] A. P. Anandarajah and C. T. Ritchlin, "The diagnosis and treatment of early psoriatic arthritis," *Nature Reviews Rheumatology*, vol. 5, pp. 634–641, nov 2009.

[175] M. Pijnappels, N. D. Reeves, C. N. Maganaris, and J. H. van Dieën, "Tripping without falling; lower limb strength, a limitation for balance recovery and a target for training in the elderly," *Journal of Electromyography and Kinesiology*, vol. 18, pp. 188–196, apr 2008.

[176] H. Hoaas, H. K. Andreassen, L. A. Lien, A. Hjalmarsen, and P. Zanaboni, "Adherence and factors affecting satisfaction in long-term telerehabilitation for patients with chronic obstructive pulmonary disease: a

mixed methods study," *BMC Medical Informatics and Decision Making*, vol. 16, p. 26, dec 2016.

[177] J. Fortin and K. Zraick, "First All-Female Spacewalk Canceled Because NASA Doesn't Have Two Suits That Fit," mar 2019.

Appendix A

Testing Material and Questionnaires

This appendix contains all testing material and screening questionnaires used in Chapter 4 during the experiment in Section 4.5 of this thesis.

Date: _____ Subject Number: _____

Background Questionnaire

Start Time: _____

Experimenter: I am going to ask you a series of background questions to aid us in our experiment:

1. Age? _____

2. Gender? ☐ Male ☐ Female

3. Are you in pain today? ☐ YES ☐ NO
If YES, how would you rate it on a scale of 0 (no pain) to 10 (agonizing pain)? _____

4. On a scale from 1 (no fatigue) to 10 (extreme fatigue), how would you rate your current level of fatigue? _____

5. Have you consumed any caffine today? ☐ YES ☐ NO
If YES, how many equivalent cups of coffee have you had today? _____

6. Do you exercise? ☐ YES ☐ NO
If YES, please specify the exercise and frequency:

	YES	NO	For Experimenter's Use Only
Cardio			
Strength			

If YES, please specify when was the last time you exercised? _____

7. What is your dominant hand? ☐ Left ☐ Right

8. What is your dominant foot? ☐ Left ☐ Right

Date: _____ Subject Number: _____

Screening Health Questionnaire

Start Time: _____

Experimenter: I am going to ask you a series of questions to screen for any exclusion criteria in this experiment:

1. In the last week, have you experienced:

	YES	NO	For Experimenter's Use Only
Numbness			
Weakness in Lower Extremities			
Shortness of Breath			
Chest Pain/Heart Palpitations			
Dizziness or Loss of Conciousness			

Answering YES to the bolded questions above will exclude the subject from this study.

2. Have you ever been diagnosed with the following conditions:

	YES	NO	For Experimenter's Use Only
High Blood pressure / Heart Problems (Circle One)			
Circulatory / Vascular / Blood Problems			
Stroke			
Lung Problems / Tuberculosis			
Diabetes			
Head Injury / Seizure disorders / Epilepsy			
Neurology Problem (Parkinson's, MS, Neuropathy, etc.)			
Athritis (Rheumatoid, Osteo, Osteoporosis, Osteopenia)			
Orthopedic Problems (fracture, dislocations, etc.)			
Visual / Hearing / Sensory Problems			

Answering YES to the bolded conditions listed above will exclude the subject from this study.

3. Please list any lower extremity surgeries for which you have been hospitalized:

Surgery	Year	Surgery	Year

Any lower extremity surgey within the last 6 months will exclude the subject from this study.

4. Do you take any medication? ☐ YES ☐ NO

Please list any prescription or non-prescription drugs (i.e. herbal supplements, vitamins) you are presently taking:

Medicine and Reason for taking	Medicine and Reason for taking

Any medications with known musculoskeletal side effects will exclude the subject from this study.

5. Do you have a pacemaker/Defibrillator? ☐ YES ☐ NO

Answering YES to the above question will exclude the subject from this study.

Date: _____ Subject Number: _____

6. Do you have any allergies? (i.e. materials, latex, etc.)
If YES, please list any allergies you have: _____

Allergies to any materials found within our device will exclude the subject from this study.

7. Do walk with any assistive devices? (cane, walker, etc.) ☐ YES ☐ NO
If YES, please list what you use: _____

Answering YES to the above question will exclude the subject from this study.

8. Are you between the ages of 18-30 or above the age of 65? ☐ YES ☐ NO

Answering NO to the above question will exclude the subject from this study.

9. Are you fluent in English? ☐ YES ☐ NO

Answering NO to the above question will exclude the subject from this study.

Is this subject eligible for this study? ☐ YES ☐ NO

End Time: _____

Appendix B

Supplemental Figures: Technique-based Measures for the Standing Balance Test

This appendix contains supplemental figures for results and statistical analysis of left-side Frequency in Balance Region (FBR) performed in Chapter 4 during the experiment in Section 4.5.

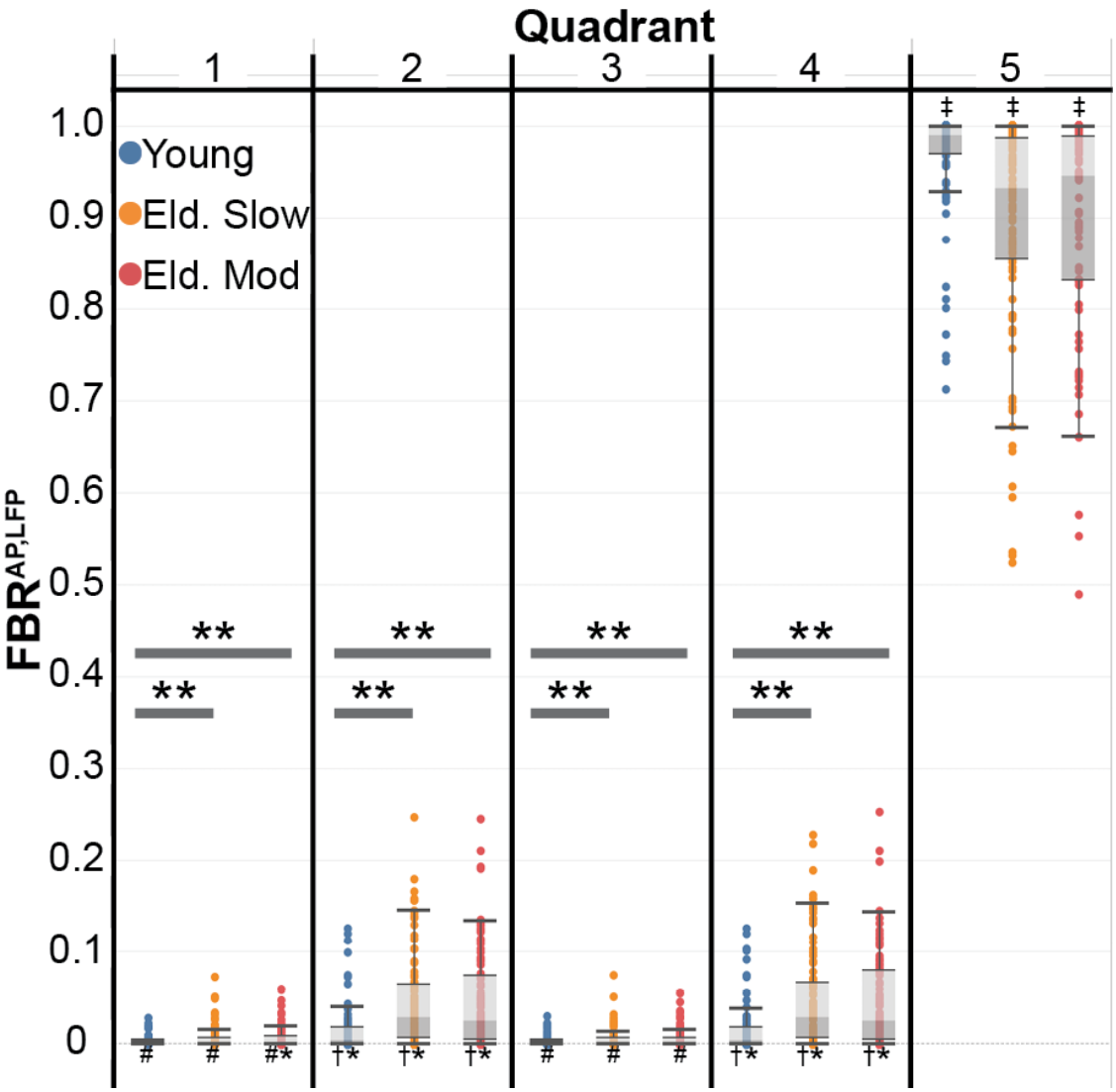

Figure B.1: $FBR_n^{AP,LFP}$ for the AP left femur-pelvis comparison. **Indicates for a particular anatomical axis (AP, ML, or LG) and balance region (FBR_{1-5}), a significant difference in experimental group (Y, O_S, or O_M) was detected. *Indicates the particular experimental group and quadrant was significantly different from the other two anatomical planes. #Signifies that for the particular experimental group and anatomical plane the labeled $FBR_{1/3}$ was significantly different from $FBR_{2,4,5}$ in that same experimental group and anatomical plane. †Signifies that for the particular experimental group and anatomical plane the labeled $FBR_{2/4}$ was significantly different from $FBR_{1,3,5}$ in that same experimental group and anatomical plane. ‡Signifies that for the particular experimental group and anatomical plane, FBR_5 was significantly different from FBR_{1-4} in that same experimental group and anatomical plane. More differences were detected but are not listed for simplicity.

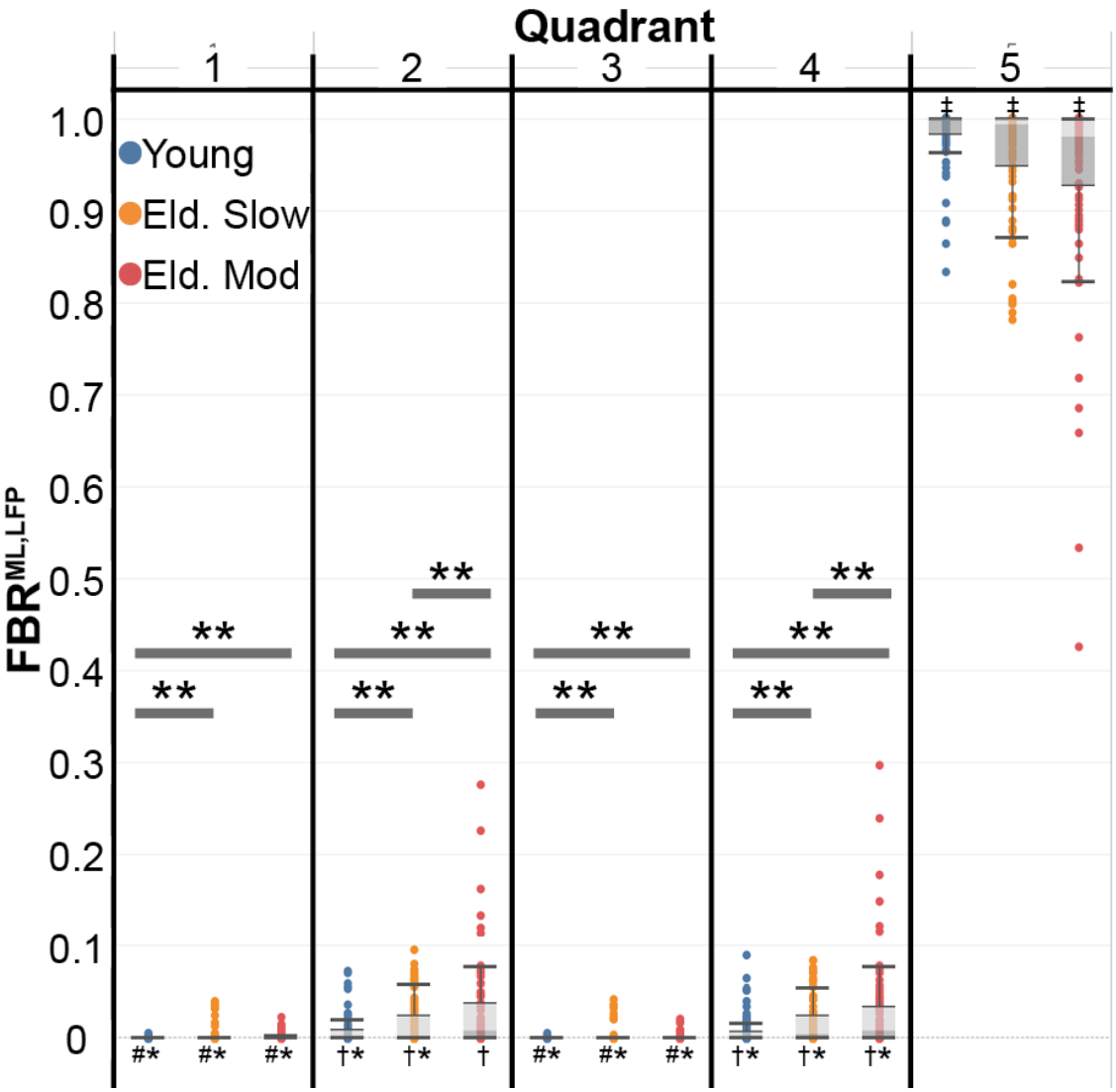

Figure B.2: $FBR_n^{ML,LFP}$ for the ML left femur-pelvis comparison. **Indicates for a particular anatomical axis (AP, ML, or LG) and balance region (FBR_{1-5}), a significant difference in experimental group (Y, O_S, or O_M) was detected. *Indicates the particular experimental group and quadrant was significantly different from the other two anatomical planes. #Signifies that for the particular experimental group and anatomical plane the labeled $FBR_{1/3}$ was significantly different from $FBR_{2,4,5}$ in that same experimental group and anatomical plane. †Signifies that for the particular experimental group and anatomical plane the labeled $FBR_{2/4}$ was significantly different from $FBR_{1,3,5}$ in that same experimental group and anatomical plane. ‡Signifies that for the particular experimental group and anatomical plane, FBR_5 was significantly different from FBR_{1-4} in that same experimental group and anatomical plane. More differences were detected but are not listed for simplicity.

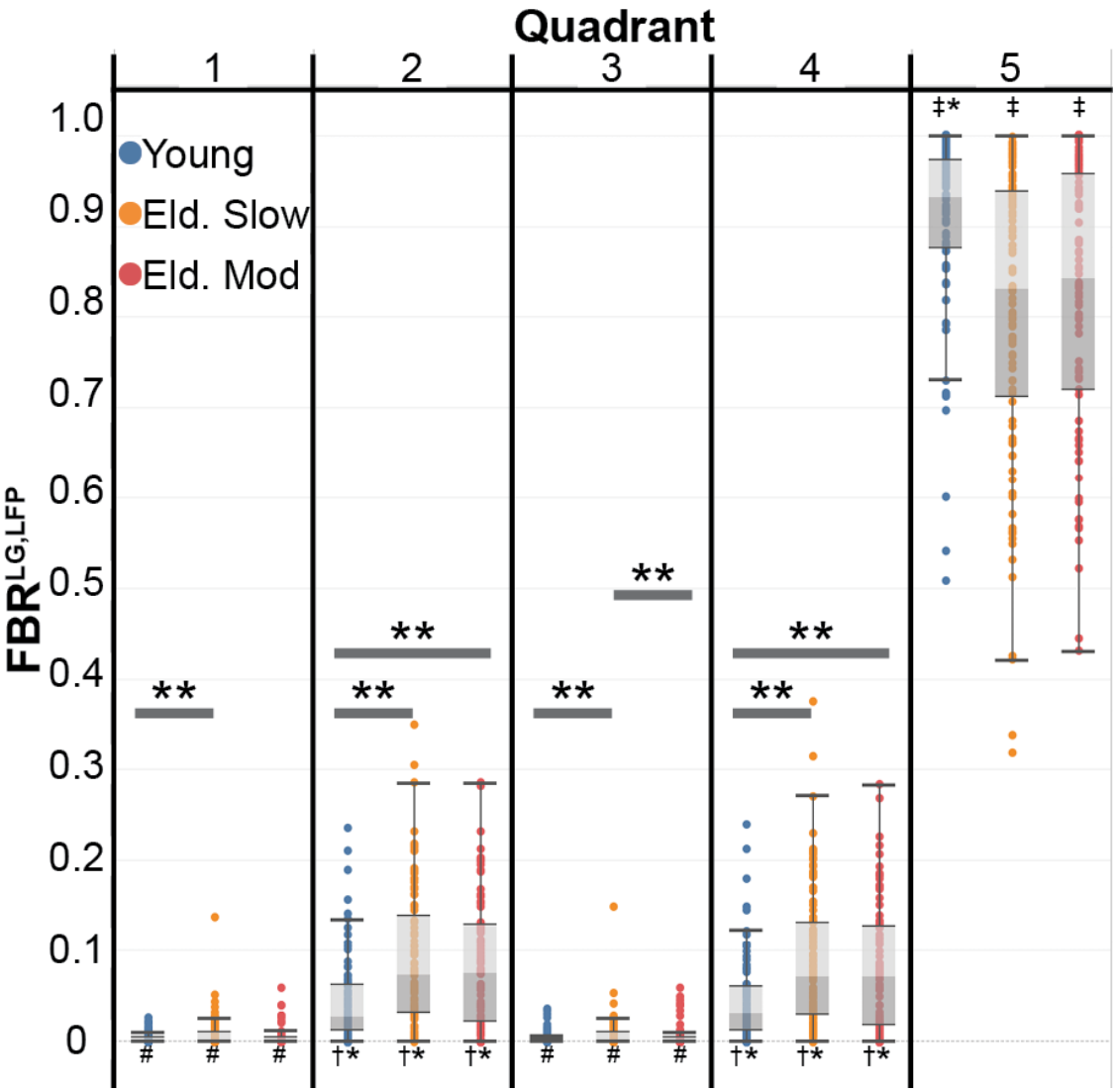

Figure B.3: $FBR_n^{LG,LFP}$ for the LG left femur-pelvis comparison. **Indicates for a particular anatomical axis (AP, ML, or LG) and balance region (FBR_{1-5}), a significant difference in experimental group (Y, O_S, or O_M) was detected. *Indicates the particular experimental group and quadrant was significantly different from the other two anatomical planes. #Signifies that for the particular experimental group and anatomical plane the labeled $FBR_{1/3}$ was significantly different from $FBR_{2,4,5}$ in that same experimental group and anatomical plane. †Signifies that for the particular experimental group and anatomical plane the labeled $FBR_{2/4}$ was significantly different from $FBR_{1,3,5}$ in that same experimental group and anatomical plane. ‡Signifies that for the particular experimental group and anatomical plane, FBR_5 was significantly different from FBR_{1-4} in that same experimental group and anatomical plane. More differences were detected but are not listed for simplicity.

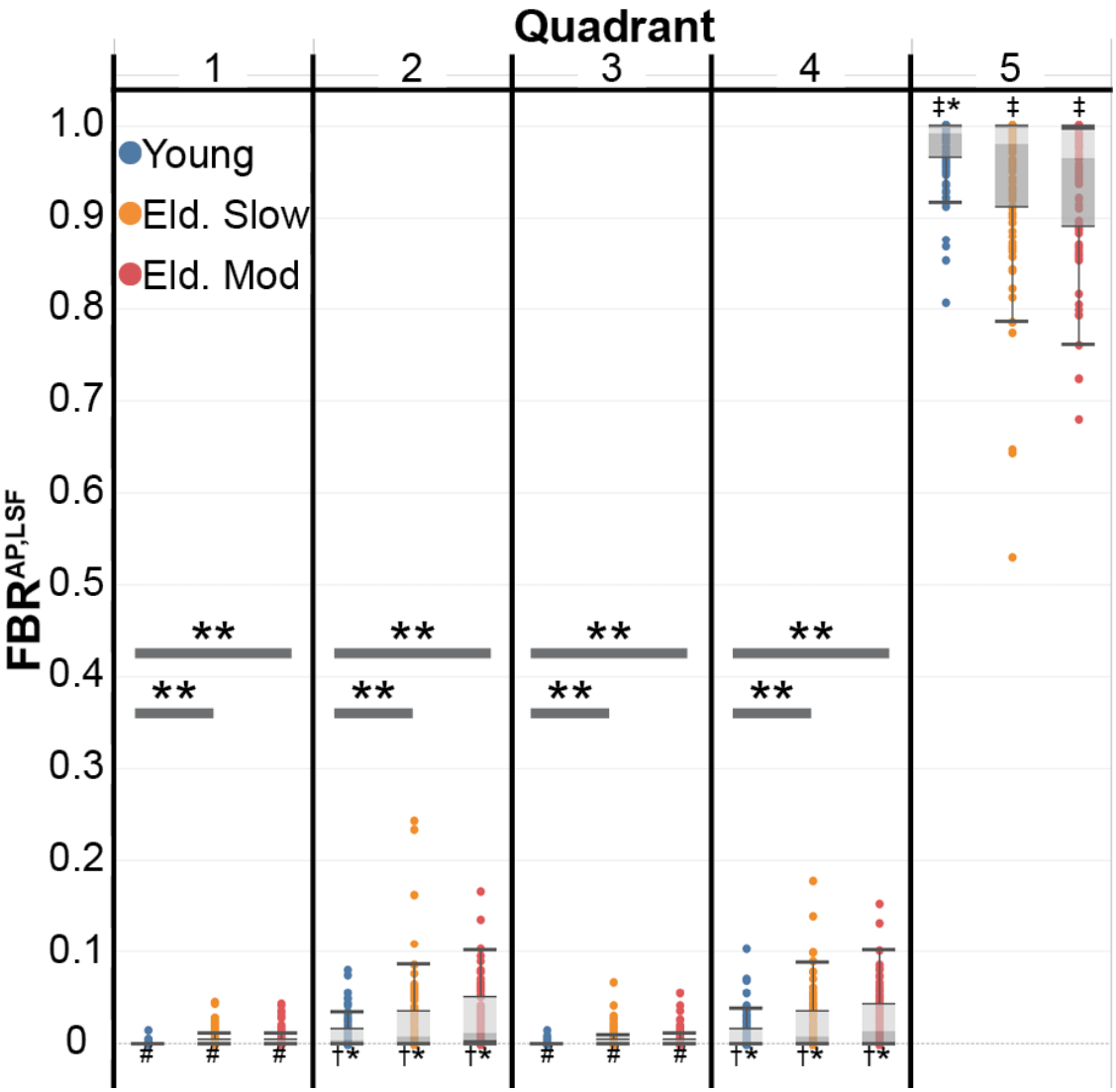

Figure B.4: $FBR_n^{AP,LSF}$ for the AP left shank-femur comparison. **Indicates for a particular anatomical axis (AP, ML, or LG) and balance region (FBR_{1-5}), a significant difference in experimental group (Y, O_S, or O_M) was detected. *Indicates the particular experimental group and quadrant was significantly different from the other two anatomical planes. #Signifies that for the particular experimental group and anatomical plane the labeled $FBR_{1/3}$ was significantly different from $FBR_{2,4,5}$ in that same experimental group and anatomical plane. †Signifies that for the particular experimental group and anatomical plane the labeled $FBR_{2/4}$ was significantly different from $FBR_{1,3,5}$ in that same experimental group and anatomical plane. ‡Signifies that for the particular experimental group and anatomical plane, FBR_5 was significantly different from FBR_{1-4} in that same experimental group and anatomical plane. More differences were detected but are not listed for simplicity.

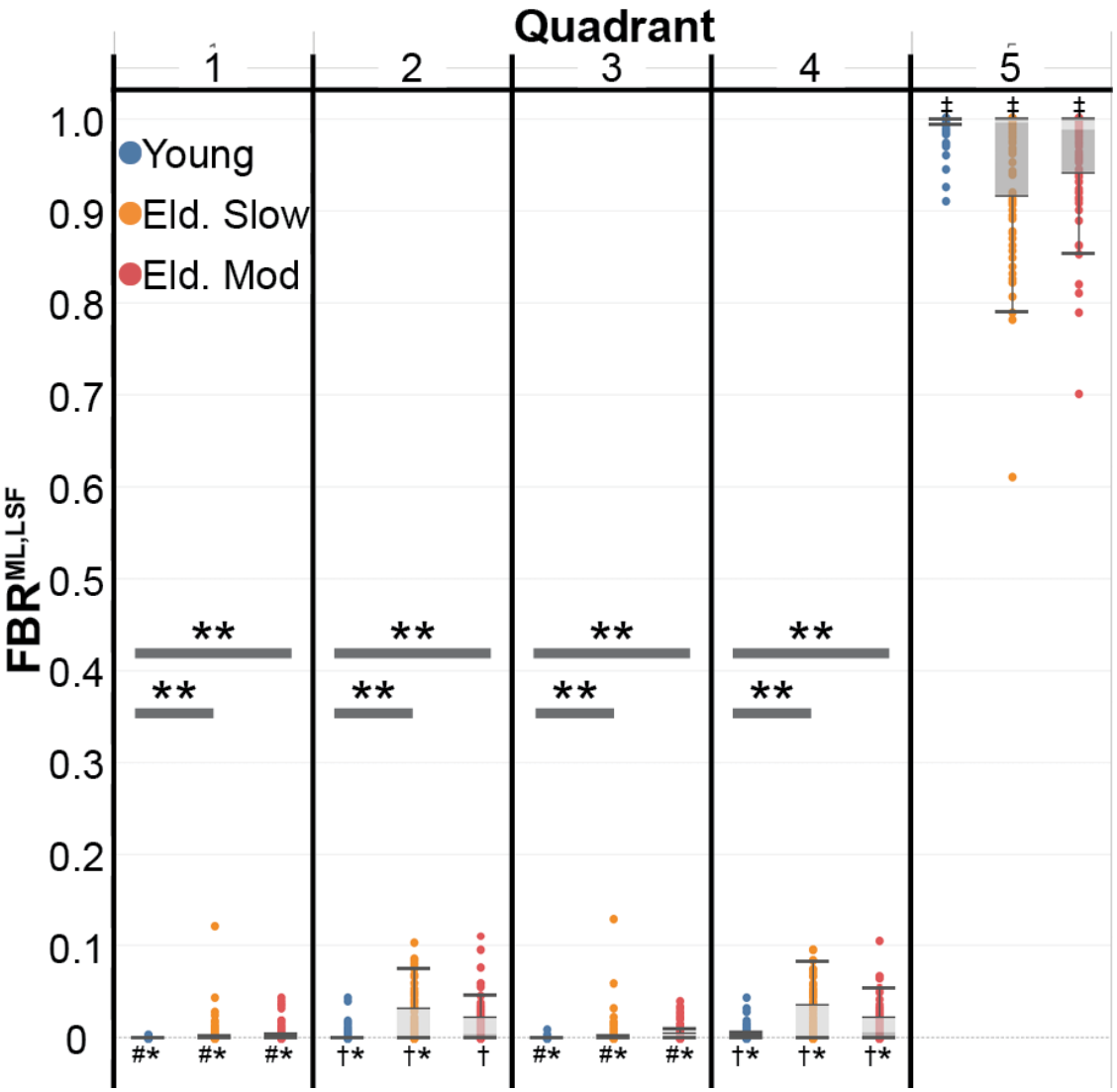

Figure B.5: $FBR_n^{ML,LSF}$ for the ML left shank-femur comparison. **Indicates for a particular anatomical axis (AP, ML, or LG) and balance region (FBR_{1-5}), a significant difference in experimental group (Y, O_S, or O_M) was detected. *Indicates the particular experimental group and quadrant was significantly different from the other two anatomical planes. #Signifies that for the particular experimental group and anatomical plane the labeled $FBR_{1/3}$ was significantly different from $FBR_{2,4,5}$ in that same experimental group and anatomical plane. †Signifies that for the particular experimental group and anatomical plane the labeled $FBR_{2/4}$ was significantly different from $FBR_{1,3,5}$ in that same experimental group and anatomical plane. ‡Signifies that for the particular experimental group and anatomical plane, FBR_5 was significantly different from FBR_{1-4} in that same experimental group and anatomical plane. More differences were detected but are not listed for simplicity.

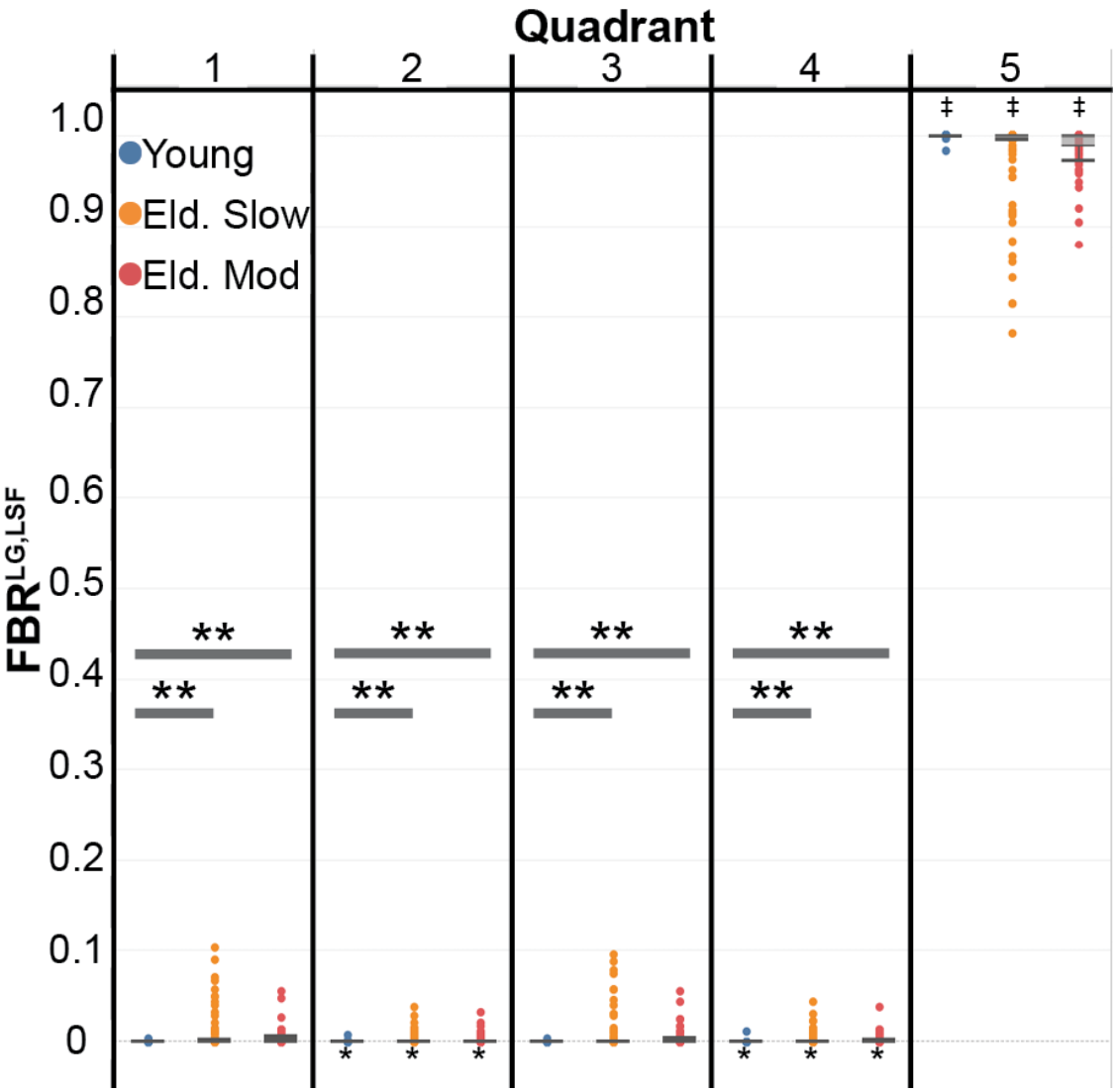

Figure B.6: $FBR_n^{LG,LSF}$ for the LG left shank-femur comparison. **Indicates for a particular anatomical axis (AP, ML, or LG) and balance region (FBR_{1-5}), a significant difference in experimental group (Y, O_S, or O_M) was detected. *Indicates the particular experimental group and quadrant was significantly different from the other two anatomical planes. #Signifies that for the particular experimental group and anatomical plane the labeled $FBR_{1/3}$ was significantly different from $FBR_{2,4,5}$ in that same experimental group and anatomical plane. †Signifies that for the particular experimental group and anatomical plane the labeled $FBR_{2/4}$ was significantly different from $FBR_{1,3,5}$ in that same experimental group and anatomical plane. ‡Signifies that for the particular experimental group and anatomical plane, FBR_5 was significantly different from FBR_{1-4} in that same experimental group and anatomical plane. More differences were detected but are not listed for simplicity.

		AP Axis			ML Axis			LG Axis		
	Balance Region	Y vs. E_S	Y vs. E_M	E_S vs. E_M	Y vs. E_S	Y vs. E_M	E_S vs. E_M	Y vs. E_S	Y vs. E_M	E_S vs. E_M
L. Femur-Pelvis	FBR_1	<<	<		<	<		<		
	FBR_2	<<	<<		<<<	<<<	<	<	<	
	FBR_3	<<	<		<			<		
	FBR_4	<<	<<		<<	<<<	<	<	<	
	FBR_5									
L. Shank-Femur	FBR_1	<	<<		<<	<<		<<	<<	
	FBR_2	<	<		<<	<<<		<	<	
	FBR_3	<	<<		<<	<<		<<	<<	
	FBR_4	<	<		<<	<<<		<	<<	
	FBR_5									

Figure B.7: Summary of all comparisons and effect sizes pertaining to the effect of age and gait speed on value of FBR. The $<$ and $>$ symbols represent if the first value is greater than or less than the second value, for example, $Y < O_S$. The number of symbols is representative of the effect size for the corresponding post hoc comparison: a) $>$ or $<$ Small effect size, $r < 0.30$, b) $>>$ or $<<$ Moderate effect size, $0.30 < r < 0.50$, and c) $>>>$ or $<<<$ Large effect size, $r > 0.50$.

		Young Group			Elderly Slow Group			Elderly Moderate Group		
	Balance Region	AP vs.ML	AP vs.LG	ML vs.LG	AP vs.ML	AP vs.LG	ML vs.LG	AP vs.ML	AP vs.LG	ML vs.LG
L. Femur-Pelvis	FBR_1	>>		>>	>>>		>>	>>>		>>
	FBR_2	>>>	<<<	<<<	>>	<<	<<<	>	<<	<<
	FBR_3	>>		>>	>>		>>	>>		>>
	FBR_4	>>>	<<<	<<<	>>	<<	<<<	>	<<	<<<
	FBR_5			>			>			>
L. Shank-Femur	FBR_1	>	>					<	>	
	FBR_2	>>>	>>>	>	<	>>>	>>	>	>>>	>>>
	FBR_3		>					<		>
	FBR_4	>>>	>>>	>	<	>>>	>>>	>	>>>	>>>
	FBR_5		<			<			<	

Figure B.8: Summary of all comparisons and effect sizes pertaining to the effect of anatomical axis on value of FBR. The $<$ and $>$ symbols represent if the first value is greater than or less than the second value, for example, $Y < O_S$. The number of symbols is representative of the effect size for the corresponding post hoc comparison: a) $>$ or $<$ Small effect size, $r < 0.30$, b) $>>$ or $<<$ Moderate effect size, $0.30 < r < 0.50$, and c) $>>>$ or $<<<$ Large effect size, $r > 0.50$.

List of Figures

1.1 Graphical Representation of Tele-rehabilitation approaches. Technologies that could be used to collect patient data include: wearable sensors, optical cameras, depth sensing cameras. Information could be sent directly to the clinician for evaluation or the system could intelligently provide feedback to the patient in real-time via visual or auditory aids using a screen or virtual reality. 18

1.2 Modified Cognitive Task Analysis methodology developed to generate performance metrics for occupational therapy decision-making aids. 22

1.3 A sample workflow diagram for a physical therapy session containing various activities and patient evaluations borrowed from Stirling and McLean [2] 23

1.4 Existing Spacesuit Assembly Designs. A) The Extravehicular Mobility Unit (EMU) is designed for use in microgravity environment, while B) the Mark III is designed for planetary exploration. C) The Z-2 advanced suit concept is meant for use in both environments. 27

2.1 Sample hip and knee joint angle and angular velocity data from a single step. Joint coordinate systems are defined based on International Society of Biomechanics recommendation [79]. Hip **flexion/extension** is positive when in the anterior plane and negative when in the posterior plane. Hip **adduction** is positive when moving towards the midline and negative when moving away. Hip **rotation** is positive when rotating towards the rotating and negative when moving away. Knee **flexion** is defined as 0° when straight and negative when bent. 37
2.2 Position-Velocity phase space representations of hip flexion axis and knee using data found in Fig. 2.1a and Fig. 2.1b, respectively. The start of the step ($t = 0$) is represented by the red markers that slowly transition to blue markers, representing the end of the step ($t = 1$). 39
2.3 Hip Flexion ϕ_{Hips} and Knee ϕ_{Hips} with corresponding γ^{HK} over a single representative step 41
2.4 Hip Flexion θ_{Hips} and Knee θ_{Knee} with corresponding τ^{HK} over a single representative step 44
2.5 Example data and values of BCM borrowed from Vitali et al. [78] 46
2.6 Simulated Data and Corresponding ρ_{AB} for Independent Segment A motion. Solid black line treats ρ_{AB} as undefined when Segment A and B are not moving, while the dashed black line does not remove noise when both segments are stationary. . . 52
2.7 Simulated Data and Corresponding ρ_{AB} for Independent Segment B motion 54
2.8 Simulated Data and Corresponding ρ_{AB} for Dual Joint motion 55

2.9 Simulated Data and Corresponding ρ_{AB} for Dual Joint motion 57
2.10 Simulated Data and Corresponding ρ_{AB} for Dual Joint motion 59
2.11 Graphical description Frequency in Coordination Zone ($\hat{t}_{\pm Z_n}$) . 61
2.12 Task Description: participants, seated behind a table, moved an object from the distal location to the proximal location on the table and back. Each trial was divided into two trajectories while interacting with each object. Each trajectory included 5 stages: reach, grasp, transport, release, and return. 63
2.13 Time-series Shoulder-Elbow Relative Coordination Metric (ρ_{se}): A time-series representation of the ρ_{se} between the shoulder and elbow using all five normalization schemes presented in Table 2.1. $+\rho_{se}$ is representative of shoulder dominated motion, while $-\rho_{se}$ is representative of elbow dominated motion. Shaded regions represent the locations of grasp (blue) and release (red) ±standard deviation. Shaded regions represent the locations of grasp (blue) and release (red) ±standard deviation. Shaded regions around each normalization scheme represent ±standard error. 68
2.14 Time-series Shoulder-Wrist Relative Coordination Metric (ρ_{sw}): A time-series representation of the ρ_{sw} between the shoulder and wrist using all five normalization schemes presented in Table 2.1. $+\rho_{sw}$ is representative of shoulder dominated motion, while $-\rho_{sw}$ is representative of wrist dominated motion. Shaded regions represent the locations of grasp (blue) and release (red) ±standard deviation. Shaded regions around each normalization scheme represent ±standard error. 69

2.15 Time-series Elbow-Wrist Relative Coordination Metric (ρ_{ew}): A time-series representation of the ρ_{ew} between the elbow and wrist using all five normalization schemes presented in Table 2.1. $+\rho_{sw}$ is representative of elbow dominated motion, while $-\rho_{sw}$ is representative of wrist dominated motion. Shaded regions represent the locations of grasp (blue) and release (red) ±standard deviation. Shaded regions around each normalization scheme represent ±standard error. 70

2.16 ρ by Normalization Scheme and Trajectory Stage during Trajectory 1 when grasping a cup. The five stages tested were A) 50% of reach, B) grasp, C) 50% of transport, D) release, E) 50% of return. *Indicates that the selected ρ norm-stage was significantly different from all other normalization schemes at that stage. #Indicates that the selected ρ norm-stage was significantly different across stages for that normalization scheme. More significant differences were present, but not shown here for simplicity. 72

2.17 ρ by Normalization Scheme and Trajectory Stage during Trajectory 2 when grasping a cup. The five stages tested were A) 50% of reach, B) grasp, C) 50% of transport, D) release, E) 50% of return. *Indicates that the selected ρ norm-stage was significantly different from all other normalization schemes at that stage. #Indicates that the selected ρ norm-stage was significantly different across stages for that normalization scheme. More significant differences were present, but not shown here for simplicity. 73

2.18 ρ by Normalization Scheme and Trajectory Stage during Trajectory 1 when grasping a pen. The five stages tested were A) 50% of reach, B) grasp, C) 50% of transport, D) release, E) 50% of return. *Indicates that the selected ρ norm-stage was significantly different from all other normalization schemes at that stage. #Indicates that the selected ρ norm-stage was significantly different across stages for that normalization scheme. More significant differences were present, but not shown here for simplicity. 74
2.19 ρ by Normalization Scheme and Trajectory Stage during Trajectory 2 when grasping a pen. The five stages tested were A) 50% of reach, B) grasp, C) 50% of transport, D) release, E) 50% of return. *Indicates that the selected ρ norm-stage was significantly different from all other normalization schemes at that stage. #Indicates that the selected ρ norm-stage was significantly different across stages for that normalization scheme. More significant differences were present, but not shown here for simplicity. 75
2.20 Percent Time in Coordination Zone When Grasping Cup by Normalization Scheme. *Indicates that the selected value was significantly different from all other $\hat{t}_{\pm Z_n}$ computed for the cup. #Indicates that the selected value was significantly different from the corresponding $\hat{t}_{\pm Z_n}$ of the pen. More significant differences were present, but not shown here for simplicity. 77

2.21 Percent Time in Coordination Zone When Grasping Cup by Normalization Scheme. *Indicates that the selected value was significantly different from all other $\hat{t}_{\pm Z_n}$ computed for the pen. #Indicates that the selected value was significantly different from the corresponding $\hat{t}_{\pm Z_n}$ of the cup. More significant differences were present, but not shown here for simplicity. 78
2.22 Percent Time in Coordination Zone During Trajectory 1 by Normalization Scheme. *Indicates that the selected value was significantly different from all other $\hat{t}_{\pm Z_n}$ computed for Trajectory 1. #Indicates that the selected value was significantly different for the $\hat{t}_{\pm Z_n}$ of the opposing Trajectory 2. More significant differences were present, but not shown here for simplicity. 79
2.23 Percent Time in Coordination Zone During Trajectory 2 by Normalization Scheme. *Indicates that the selected value was significantly different from all other $\hat{t}_{\pm Z_n}$ computed for Trajectory 2. #Indicates that the selected value was significantly different for the $\hat{t}_{\pm Z_n}$ of the opposing Trajectory 1. More significant differences were present, but not shown here for simplicity. 80

3.1 Cognitive Task Analysis Decision Workflow Diagram MKIII Fit Checks 92
3.2 Schematics highlighting aspects of: a) Static Fit, and b) Dynamic Fit extracted from a CTA of MKIII fit checks (Fig. 3.1) 98
3.3 Locations of padding and inertial measurement unit sensors on humans for Configuration 0 (C0), Configuration 1 (C1), and Configuration 2 (C2). 102

3.4 Time-series representations of ρ^{F}_{HS}[A-C] and ρ^{T}_{HS}[D-F] for each configuration: US (light green), C0 (blue), C1 (red), and C2 (black). Vertical lines represent the gait phases stance (green), heel off (yellow), toe off (orange), and max swing (purple). Solid lines represent means across all 20 steps and shaded regions represent 1 SD. For these plots, time-series were normalized and resampled to be the same length based on the trial with the most samples (250 samples, i.e., $\sim 1.95s$). 112

4.1 Life Expectancy and Disability Rate in Older Adults by Gait Speed (Source: Castranova et al. [124] and Studenski et al. [125]) 127

4.2 Possible Models and Mechanisms to Maintain Static Balance: a) is representative of a single inverted pendulum model where all segments above the ankles are rigid and do not move relative to one another while b) is representative of a double pendulum model in which static balance can be achieved through additional joint motion, such as the hip (shown), knee (not shown, or torso (not shown). 131

4.3 IMU movement trajectories in the horizontal plane (blue solid line, perimeter (red dashed line, and maximum excursions in the ML and AP directions of the (a) thigh and (b) shank during single leg stance (a green dotted line and a black dash-dot line). (c) ROLS excursion diagram. Adapted from Kim et al. [163] . 134

4.4 A multi-segmented inverted pendulum Model for static balance in which the body is divided into seven segments: torso (T), pelvis (p), right femur (RF), left femur (LF), right shank (RS), and left shank (LS). Each segment contains its own reference frame and coordinate system where each axis corresponds with its underlying anatomical axes: anteroposterior (AP), medio-lateral (ML), and longitudinal (LG). 136

4.5 Definition and derivation of Frequency in Balance Region and corresponding balance strategies. Time spent in $FBR_{2,4}^{P,LU}$ is representative of a balance strategy in which the upper segment is rotating faster and in the opposite direction of the lower segment . Time spent in $FBR_{1,3}^{P,LU}$ is representative of a balance strategy where the upper segment is rotating at faster rate and same direction as the lower segment. Time spent in $FBR_{5}^{P,LU}$ is representative of balance strategies in which the upper segment has no relative motion to the lower segment. The above example represents six 30s static balance trails of a single participant comparing the angular velocity of the pelvis with the angular velocity of the torso relative to the pelvis in the AP axis. The corresponding values of FBR for this case are: $FBR_{1}^{AP,PT} = 0.08$, $FBR_{2}^{AP,PT} = 0.13$, $FBR_{3}^{AP,PT} = 0.07$, $FBR_{1}^{AP,PT} = 0.14$, and $FBR_{5}^{AP,PT} = 0.58$. 140

4.6 Individual Balance Strategy for Two Trials of Single Young Participants in AP Plane. Green regions represents time points where the segments behave as rigid, single pendulums. Any other areas represents double-pendulum behaviors with different balance strategies. 143

4.7 Individual Balance Strategy for Two Older Participants in AP Plane. Green regions represents time points where the segments behave as rigid, single pendulums. Any other areas represents double-pendulum behaviors with different balance strategies. 145
4.8 Individual Balance Strategy for One Older Participants in the ML and LG Planes 147
4.9 Motion Capture Marker and IMU Locations: a) Approximate reflective marker and IMU locations on corresponding anatomical landmarks. b) Reflective Markers used to define segments of balance model: Shank (S), Femur (F), pelvis (P), and Torso (T). Markers not used for this balance model present with greater opacity. Solid, filled, black markers represent physical markers while markers with white center were virtually created during data processing. 152

4.10 $FBR_n^{AP,PT}$ for the AP pelvis-torso comparison. **Indicates for a particular anatomical axis (AP, ML, or LG) and balance region (FBR_{1-5}), a significant difference in experimental group (Y, O_S, or O_M) was detected. *Indicates the particular experimental group and quadrant was significantly different from the other two anatomical planes. #Signifies that for the particular experimental group and anatomical plane the labeled $FBR_{1/3}$ was significantly different from $FBR_{2,4,5}$ in that same experimental group and anatomical plane. †Signifies that for the particular experimental group and anatomical plane the labeled $FBR_{2/4}$ was significantly different from $FBR_{1,3,5}$ in that same experimental group and anatomical plane. ‡Signifies that for the particular experimental group and anatomical plane, FBR_5 was significantly different from FBR_{1-4} in that same experimental group and anatomical plane. More differences were detected but are not listed for simplicity. 156

4.11 $FBR_n^{ML,PT}$ for the ML pelvis-torso comparison. **Indicates for a particular anatomical axis (AP, ML, or LG) and balance region (FBR_{1-5}), a significant difference in experimental group (Y, O_S, or O_M) was detected. *Indicates the particular experimental group and quadrant was significantly different from the other two anatomical planes. #Signifies that for the particular experimental group and anatomical plane the labeled $FBR_{1/3}$ was significantly different from $FBR_{2,4,5}$ in that same experimental group and anatomical plane. †Signifies that for the particular experimental group and anatomical plane the labeled $FBR_{2/4}$ was significantly different from $FBR_{1,3,5}$ in that same experimental group and anatomical plane. ‡Signifies that for the particular experimental group and anatomical plane, FBR_5 was significantly different from FBR_{1-4} in that same experimental group and anatomical plane. More differences were detected but are not listed for simplicity. 157

4.12 $FBR_n^{LG,PT}$ for the LG pelvis-torso comparison. **Indicates for a particular anatomical axis (AP, ML, or LG) and balance region (FBR_{1-5}), a significant difference in experimental group (Y, O_S, or O_M) was detected. *Indicates the particular experimental group and quadrant was significantly different from the other two anatomical planes. #Signifies that for the particular experimental group and anatomical plane the labeled $FBR_{1/3}$ was significantly different from $FBR_{2,4,5}$ in that same experimental group and anatomical plane. †Signifies that for the particular experimental group and anatomical plane the labeled $FBR_{2/4}$ was significantly different from $FBR_{1,3,5}$ in that same experimental group and anatomical plane. ‡Signifies that for the particular experimental group and anatomical plane, FBR_5 was significantly different from FBR_{1-4} in that same experimental group and anatomical plane. More differences were detected but are not listed for simplicity. 158

4.13 $FBR_n^{AP,RFP}$ for the AP right femur-pelvis comparison. **Indicates for a particular anatomical axis (AP, ML, or LG) and balance region (FBR_{1-5}), a significant difference in experimental group (Y, O_S, or O_M) was detected. *Indicates the particular experimental group and quadrant was significantly different from the other two anatomical planes. #Signifies that for the particular experimental group and anatomical plane the labeled $FBR_{1/3}$ was significantly different from $FBR_{2,4,5}$ in that same experimental group and anatomical plane. †Signifies that for the particular experimental group and anatomical plane the labeled $FBR_{2/4}$ was significantly different from $FBR_{1,3,5}$ in that same experimental group and anatomical plane. ‡Signifies that for the particular experimental group and anatomical plane, FBR_5 was significantly different from FBR_{1-4} in that same experimental group and anatomical plane. More differences were detected but are not listed for simplicity. 159

4.14 $FBR_n^{ML,RFP}$ for the ML right femur-pelvis comparison. **Indicates for a particular anatomical axis (AP, ML, or LG) and balance region (FBR_{1-5}), a significant difference in experimental group (Y, O_S, or O_M) was detected. *Indicates the particular experimental group and quadrant was significantly different from the other two anatomical planes. #Signifies that for the particular experimental group and anatomical plane the labeled $FBR_{1/3}$ was significantly different from $FBR_{2,4,5}$ in that same experimental group and anatomical plane. †Signifies that for the particular experimental group and anatomical plane the labeled $FBR_{2/4}$ was significantly different from $FBR_{1,3,5}$ in that same experimental group and anatomical plane. ‡Signifies that for the particular experimental group and anatomical plane, FBR_5 was significantly different from FBR_{1-4} in that same experimental group and anatomical plane. More differences were detected but are not listed for simplicity. 160

4.15 $FBR_n^{LG,RFP}$ for the LG right femur-pelvis comparison. **Indicates for a particular anatomical axis (AP, ML, or LG) and balance region (FBR_{1-5}), a significant difference in experimental group (Y, O_S, or O_M) was detected. *Indicates the particular experimental group and quadrant was significantly different from the other two anatomical planes. #Signifies that for the particular experimental group and anatomical plane the labeled $FBR_{1/3}$ was significantly different from $FBR_{2,4,5}$ in that same experimental group and anatomical plane. †Signifies that for the particular experimental group and anatomical plane the labeled $FBR_{2/4}$ was significantly different from $FBR_{1,3,5}$ in that same experimental group and anatomical plane. ‡Signifies that for the particular experimental group and anatomical plane, FBR_5 was significantly different from FBR_{1-4} in that same experimental group and anatomical plane. More differences were detected but are not listed for simplicity. 161

4.16 $FBR_n^{AP,RSF}$ for the AP right shank-femur comparison. **Indicates for a particular anatomical axis (AP, ML, or LG) and balance region (FBR_{1-5}), a significant difference in experimental group (Y, O_S, or O_M) was detected. *Indicates the particular experimental group and quadrant was significantly different from the other two anatomical planes. #Signifies that for the particular experimental group and anatomical plane the labeled $FBR_{1/3}$ was significantly different from $FBR_{2,4,5}$ in that same experimental group and anatomical plane. †Signifies that for the particular experimental group and anatomical plane the labeled $FBR_{2/4}$ was significantly different from $FBR_{1,3,5}$ in that same experimental group and anatomical plane. ‡Signifies that for the particular experimental group and anatomical plane, FBR_5 was significantly different from FBR_{1-4} in that same experimental group and anatomical plane. More differences were detected but are not listed for simplicity. 162

4.17 $FBR_n^{ML,RSF}$ for the ML right shank-femur comparison. **Indicates for a particular anatomical axis (AP, ML, or LG) and balance region (FBR_{1-5}), a significant difference in experimental group (Y, O_S, or O_M) was detected. *Indicates the particular experimental group and quadrant was significantly different from the other two anatomical planes. #Signifies that for the particular experimental group and anatomical plane the labeled $FBR_{1/3}$ was significantly different from $FBR_{2,4,5}$ in that same experimental group and anatomical plane. †Signifies that for the particular experimental group and anatomical plane the labeled $FBR_{2/4}$ was significantly different from $FBR_{1,3,5}$ in that same experimental group and anatomical plane. ‡Signifies that for the particular experimental group and anatomical plane, FBR_5 was significantly different from FBR_{1-4} in that same experimental group and anatomical plane. More differences were detected but are not listed for simplicity. 163

4.18 $FBR_n^{LG,RSF}$ for the LG right shank-femur comparison. **Indicates for a particular anatomical axis (AP, ML, or LG) and balance region (FBR_{1-5}), a significant difference in experimental group (Y, O_S, or O_M) was detected. *Indicates the particular experimental group and quadrant was significantly different from the other two anatomical planes. #Signifies that for the particular experimental group and anatomical plane the labeled $FBR_{1/3}$ was significantly different from $FBR_{2,4,5}$ in that same experimental group and anatomical plane. †Signifies that for the particular experimental group and anatomical plane the labeled $FBR_{2/4}$ was significantly different from $FBR_{1,3,5}$ in that same experimental group and anatomical plane. ‡Signifies that for the particular experimental group and anatomical plane, FBR_5 was significantly different from FBR_{1-4} in that same experimental group and anatomical plane. More differences were detected but are not listed for simplicity. 164

4.19 Summary of all comparisons and effect sizes pertaining to the effect of age and gait speed on value of FBR. The $<$ and $>$ symbols represent if the first value is greater than or less than the second value, for example, $Y < O_S$. The number of symbols is representative of the effect size for the corresponding post hoc comparison: a) $>$ or $<$ Small effect size, $r < 0.30$, b) $>>$ or $<<$ Moderate effect size, $0.30 < r < 0.50$, and c) $>>>$ or $<<<$ Large effect size, $r > 0.50$. 166

4.20 Summary of all comparisons and effect sizes pertaining to the effect of anatomical axis on value of FBR. The $<$ and $>$ symbols represent if the first value is greater than or less than the second value, for example, $Y < O_S$. The number of symbols is representative of the effect size for the corresponding post hoc comparison: a) $>$ or $<$ Small effect size, $r < 0.30$, b) $>>$ or $<<$ Moderate effect size, $0.30 < r < 0.50$, and c) $>>>$ or $<<<$ Large effect size, $r > 0.50$. 168

B.1 $FBR_n^{AP,LFP}$ for the AP left femur-pelvis comparison. **Indicates for a particular anatomical axis (AP, ML, or LG) and balance region (FBR_{1-5}), a significant difference in experimental group (Y, O_S, or O_M) was detected. *Indicates the particular experimental group and quadrant was significantly different from the other two anatomical planes. #Signifies that for the particular experimental group and anatomical plane the labeled $FBR_{1/3}$ was significantly different from $FBR_{2,4,5}$ in that same experimental group and anatomical plane. †Signifies that for the particular experimental group and anatomical plane the labeled $FBR_{2/4}$ was significantly different from $FBR_{1,3,5}$ in that same experimental group and anatomical plane. ‡Signifies that for the particular experimental group and anatomical plane, FBR_5 was significantly different from FBR_{1-4} in that same experimental group and anatomical plane. More differences were detected but are not listed for simplicity. 216

B.2 $FBR_n^{ML,LFP}$ for the ML left femur-pelvis comparison. **Indicates for a particular anatomical axis (AP, ML, or LG) and balance region (FBR_{1-5}), a significant difference in experimental group (Y, O_S, or O_M) was detected. *Indicates the particular experimental group and quadrant was significantly different from the other two anatomical planes. #Signifies that for the particular experimental group and anatomical plane the labeled $FBR_{1/3}$ was significantly different from $FBR_{2,4,5}$ in that same experimental group and anatomical plane. †Signifies that for the particular experimental group and anatomical plane the labeled $FBR_{2/4}$ was significantly different from $FBR_{1,3,5}$ in that same experimental group and anatomical plane. ‡Signifies that for the particular experimental group and anatomical plane, FBR_5 was significantly different from FBR_{1-4} in that same experimental group and anatomical plane. More differences were detected but are not listed for simplicity. 217

B.3 $FBR_n^{LG,LFP}$ for the LG left femur-pelvis comparison. **Indicates for a particular anatomical axis (AP, ML, or LG) and balance region (FBR_{1-5}), a significant difference in experimental group (Y, O_S, or O_M) was detected. *Indicates the particular experimental group and quadrant was significantly different from the other two anatomical planes. #Signifies that for the particular experimental group and anatomical plane the labeled $FBR_{1/3}$ was significantly different from $FBR_{2,4,5}$ in that same experimental group and anatomical plane. †Signifies that for the particular experimental group and anatomical plane the labeled $FBR_{2/4}$ was significantly different from $FBR_{1,3,5}$ in that same experimental group and anatomical plane. ‡Signifies that for the particular experimental group and anatomical plane, FBR_5 was significantly different from FBR_{1-4} in that same experimental group and anatomical plane. More differences were detected but are not listed for simplicity. 218

B.4 $FBR_n^{AP,LSF}$ for the AP left shank-femur comparison. **Indicates for a particular anatomical axis (AP, ML, or LG) and balance region (FBR_{1-5}), a significant difference in experimental group (Y, O_S, or O_M) was detected. *Indicates the particular experimental group and quadrant was significantly different from the other two anatomical planes. #Signifies that for the particular experimental group and anatomical plane the labeled $FBR_{1/3}$ was significantly different from $FBR_{2,4,5}$ in that same experimental group and anatomical plane. †Signifies that for the particular experimental group and anatomical plane the labeled $FBR_{2/4}$ was significantly different from $FBR_{1,3,5}$ in that same experimental group and anatomical plane. ‡Signifies that for the particular experimental group and anatomical plane, FBR_5 was significantly different from FBR_{1-4} in that same experimental group and anatomical plane. More differences were detected but are not listed for simplicity. 219

B.5 $FBR_n^{ML,LSF}$ for the ML left shank-femur comparison. **Indicates for a particular anatomical axis (AP, ML, or LG) and balance region (FBR_{1-5}), a significant difference in experimental group (Y, O_S, or O_M) was detected. *Indicates the particular experimental group and quadrant was significantly different from the other two anatomical planes. #Signifies that for the particular experimental group and anatomical plane the labeled $FBR_{1/3}$ was significantly different from $FBR_{2,4,5}$ in that same experimental group and anatomical plane. †Signifies that for the particular experimental group and anatomical plane the labeled $FBR_{2/4}$ was significantly different from $FBR_{1,3,5}$ in that same experimental group and anatomical plane. ‡Signifies that for the particular experimental group and anatomical plane, FBR_5 was significantly different from FBR_{1-4} in that same experimental group and anatomical plane. More differences were detected but are not listed for simplicity. 220

B.6 $FBR_n^{LG,LSF}$ for the LG left shank-femur comparison. **Indicates for a particular anatomical axis (AP, ML, or LG) and balance region (FBR_{1-5}), a significant difference in experimental group (Y, O_S, or O_M) was detected. *Indicates the particular experimental group and quadrant was significantly different from the other two anatomical planes. #Signifies that for the particular experimental group and anatomical plane the labeled $FBR_{1/3}$ was significantly different from $FBR_{2,4,5}$ in that same experimental group and anatomical plane. †Signifies that for the particular experimental group and anatomical plane the labeled $FBR_{2/4}$ was significantly different from $FBR_{1,3,5}$ in that same experimental group and anatomical plane. ‡Signifies that for the particular experimental group and anatomical plane, FBR_5 was significantly different from FBR_{1-4} in that same experimental group and anatomical plane. More differences were detected but are not listed for simplicity. 221

B.7 Summary of all comparisons and effect sizes pertaining to the effect of age and gait speed on value of FBR. The $<$ and $>$ symbols represent if the first value is greater than or less than the second value, for example, $Y < O_S$. The number of symbols is representative of the effect size for the corresponding post hoc comparison: a) $>$ or $<$ Small effect size, $r < 0.30$, b) $>>$ or $<<$ Moderate effect size, $0.30 < r < 0.50$, and c) $>>>$ or $<<<$ Large effect size, $r > 0.50$. 222

B.8 Summary of all comparisons and effect sizes pertaining to the effect of anatomical axis on value of FBR. The $<$ and $>$ symbols represent if the first value is greater than or less than the second value, for example, $Y < O_S$. The number of symbols is representative of the effect size for the corresponding post hoc comparison: a) $>$ or $<$ Small effect size, $r < 0.30$, b) $>>$ or $<<$ Moderate effect size, $0.30 < r < 0.50$, and c) $>>>$ or $<<<$ Large effect size, $r > 0.50$. 222

List of Tables

1.1 Sample of Common Clinical Outcome Measures. IO=Interactive Objective, IS=Interactive Subject, D=Descriptive 16

1.2 Motion features being quantified for this thesis and their respective situation awareness requirements 25

2.1 Definitions of Normalization Parameters 64

3.1 Subject Data and Testing Order 101

3.2 Knee RoM and Cadence by Subject and Configuration 108

3.3 $\rho^n_{HS}(t)$ Significant Fixed Effect Model Predictions and Coefficients 111

3.4 $\rho^n_{HS}(t)$ Random-Effect Model Predictions for Subject-Configurations 111

4.1 Experimental Group and Participant Demographics 150

4.2 Effect of Experimental Group on Conventional Balance Metrics 155